THE UNIVERSITY
of EDINBURGH

Investigating the Oogenic Potential of Bovine Oogonial Stem Cells

Kelsey Marie Grieve

Thesis submitted for the Degree of Doctor of Philosophy

University of Edinburgh

2017

Declaration

May 2017

I declare that this thesis was composed entirely by myself and that it has not been submitted, in whole or in part, in any previous application for a degree. Except where stated otherwise by reference or acknowledgement in the text, the work presented is entirely my own.

Kelsey Marie Grieve

Abstract

A fixed population of oocytes within primordial follicles, established prior to or just after birth has been firmly believed to support the postnatal mammalian ovary throughout an individual's reproductive lifespan. However, the identification and isolation of cells from adult mammalian ovaries characterised by the expression of both germ and stem cell markers, suggest the presence of mitotically active cells, termed oogonial stem cells (OSCs) that may have the potential to produce new oocytes in the postnatal mammalian ovary. Putative OSCs have been isolated from adult tissues of several mammalian species, including rodents and humans. Upon re-introduction to the ovarian niche, human and rodent OSCs have generated new oocyte like structures which, at least in rodents, have generated functional oocytes capable of fertilisation and subsequent embryonic development to produce healthy offspring.

We hypothesised that OSCs could be isolated from adult bovine ovaries and upon establishment within the appropriate ovarian niche could initiate successful oogenesis.

To investigate this hypothesis, we have utilised fluorescently activated cell sorting (FACS) to isolate putative bovine OSCs (bOSCs) and an ovarian aggregate model, *in vitro* and *in vivo* to explore the oogenic potential of these cells.

Putative bOSCs were successfully isolated by FACS based on the cell surface expression of germ cell marker DDX4 and established in culture. Pluripotency (*LIN28* and *OCT4*) and germ (*IFITM3*, *PRDM1*, *C-KIT* and *DAZL*) cell associated genes were expressed in putative bOSCs established in culture. However, *DDX4* transcripts were not consistently observed throughout bOSC culture.

Aggregation of putative bOSCs with neonatal murine ovarian somatic cells to form chimeric ovarian aggregates, cultured in a hanging drop model for 7 days maintained germ cell phenotype, marked by DAZL expression. A subpopulation of putative bOSCs showed a spherical morphology, an increase in cell size and an association with neighbouring cells. Xenotransplantation of chimeric ovarian aggregates to the kidney capsule of immune deficient mice for 21 days generated multi-laminar follicles and structures with morphological similarities to primordial follicles (termed

pre-primordial follicle-like structures). RNA Scope was unsuccessful in determining the origin of oocytes within chimeric ovarian aggregates. However, oocytes from pre-antral follicles in chimeric ovarian aggregates (n=6; 60.9±3.6μm, mean ± SEM) were significantly (P<0.0001) larger than murine oocytes (n=38; 34.5±1μm, mean ± SEM) aggregated with murine ovarian somatic cells as positive controls, suggesting that these oocytes are undergoing different growth dynamics.

This work has shown that putative bOSCs characterised by the expression of pluripotency and germ cell associated genes are present within adult bovine ovarian tissue and can be isolated using FACS and established in culture. These data also suggest that putative bOSCs may have the potential to undergo oogenesis and illustrate the potential use of these cells as a tool to investigate germ cell differentiation.

Lay Summary

Until recently it was firmly believed that women could not produce new eggs (also known as oocytes) as adults. However, cells with apparent germ line stem cell characteristics (oogonial stem cells (OSC)), have been found in ovaries of women and other mammals. These cells appear capable of producing new oocytes under the right conditions. Supporting cells, known as somatic cells are essential to help create an oocyte which is able to grow and develop, and be successfully fertilised by sperm. Research into OSCs and their supporting cells that may combine to produce new oocytes is essential to assess the potential of these cells in development of fertility treatments.

We have used cow (bovine) oogonial stem cells (bOSCs) as a model to investigate the ability of these specialised cells to create new oocytes. We hypothesised that bOSCs would be able to produce new eggs with the appropriate somatic cell support. bOSCs were removed from adult bovine ovaries using a cell sorting method. bOSCs were initially studied in the laboratory and were unable to produce new oocytes without somatic cell support. Using experimental models where supporting somatic cells from the ovary could be used to aid bOSCs, we found that oocytes and cells like early oocytes were observed. However, we were unable to determine conclusively whether these oocytes were derived from the bOSCs.

Although still early in the experimental stages of research, this study suggests that bOSCs can produce new oocytes when combined with the appropriate somatic cell support. These results also show that the supporting somatic cells are essential to support oogonial stem cells and should be considered in future research. From these results, oogonial stem cells may have the potential to provide new fertility preservation techniques for cancer patients, women suffering from early menopause or infertility.

Acknowledgements

I would like to thank my two supervisors Professor Richard Anderson and Professor Evelyn Telfer, without whom and the funding from the Medical Research Council, this project would never have existed. Without your continued support this project would have been far less enjoyable and considerably more difficult. You have had faith in my capabilities from day one and never doubted that I would eventually finish. You have taught me to appreciate that no result is a negative result and everything has value. I cannot thank you both enough for this opportunity and for giving me the very best start to my scientific career.

Thanks to all the members of both labs too!! To Rosey, Hazel, Karolina, Cheryl and Roseanne from the Anderson lab and Marie, Yvonne and John from the Telfer lab thank you for your support during this project. You have provided brilliant scientific (and non-scientific) discussions over the last (almost) 4 years. I've enjoyed lab meetings with you all, celebrated life events and definitely indulged in my fair share of Marie's cakes. My days won't be the same without you all in them every day. I'd like to give special thanks to Cheryl and Roseanne, my super lab cheerleaders, who picked me up on days when immuno's didn't work, cultures got infected and when my motivation was non-existent. You wiped away my science tears and put a smile back on my face. I couldn't imagine this experience without our 'Sporcle Sessions' and lab lunches on 'curly fry-day'. Not forgetting the lovely research nurses of both labs, Anne, Norma and Joan, although I did not work directly with you, it was always so nice to see you on your trips to the lab.

To everyone else in the CRH and CIP, thanks for the coffee/tea breaks, the lunchtime chats and all of the encouragement during my PhD. I'd particularly like to mention my fellow MSc and PhD buddies, we have been through this crazy adventure together, from our first week of inductions to now. Jess, Ashley, Mike, Bianca, Kasia and Theresia, the past 4 years just wouldn't have been the same without you. I have been welcomed into the CRH family and have made life-long friends. I've enjoyed many CRH socials, karaoke nights and the unforgettable Christmas parties. There are a few people that I would like to mention by name that have been wonderful friends who for them this will not be the last they see of me, so thank you Taj, Lenka, Agi,

Caroline and of course Jess, Ashley, Cheryl and Roseanne (double mentions, you lucky girls!).

I'd also like to thank all of my other fabulous friends who have put up with me cancelling plans in the pursuit of science and listening to me drone on about my scientific failures and achievements. I'm sorry that you haven't seen very much of me over the past year, I can promise you that you'll be seeing much more of me in the future. There are far too many of you to mention you all by name, but you know who you are and thank you!

To my ultimate cheer squad, my family. My wonderful parents, Mum and Dad, you have an unwavering faith in my abilities and fully believe that I can achieve anything before I have even set my mind to it. You have supported me through every exam, essay, dissertation and now thesis. I wouldn't ever be able to thank you enough for everything you have ever done for me, but just know that I fully appreciate it all and love you both very much. I know that you'll try and read this and you may never pass the contents page, but I also know that you'll be almost as proud of it as I am. To my younger brother and sister, Sam and Blythe, you have been a constant support and source of entertainment and have always known exactly what to say to cheer me up. You have kept me grounded and focused on the end goal and have ensured that I don't become too much of a science geek, and for that I will always be grateful.

To Ben, there aren't enough words that I could use to describe how thankful and grateful I am to have you in my life. You have always been more than just a boyfriend and fiancé, you are my best friend. For the past nine months you have been my rock, my ultimate confidante and the one true consistent in my life. You have made me laugh every day and pulled me through the tougher days. I feel so lucky to have your love, support and never ending encouragement. You too have always believed in my abilities, agreed to my crazy ideas without question and helped me chase my dreams. I would also like to thank Ben's family, my soon to be in-laws, who have always shown interest in my science and have always been very supportive. Thank you for all of your love and support.

I am so lucky to have so many wonderful people in my life. Thank you! Thank you! Thank you to you all!!

Publications and Presentations relating to this thesis

Publications

Grieve, K. M., McLaughlin, M., Dunlop, C. E., Telfer, E. E., and Anderson, R. A. (2015). The controversial existence and functional potential of oogonial stem cells. Maturitas *82*, 278-281.

Posters

Grieve, K. M., Deleva, A. I., Dunlop, C. E., Anderson, R. A, Williams, S. A., and Telfer, E. E. Aggregation of bovine oogonial stem cells with mouse somatic cells results in follicle formation. Poster presented at the annual meeting of the Society for Reproduction and Fertility; 2014 September 1-2; Edinburgh, UK. *

Grieve, K. M., Dunlop, C. E., Anderson, R. A., and Telfer, E. E. Exploration of developmental competence of bovine oogonial stem cells *in vitro* using a reaggregation model. Poster presented at Ovarian Club VI; 2015 November 14-15; Barcelona, Spain.

Presentations

Grieve, K. M., Dunlop, C. E., Telfer, E. E., and Anderson, R. A. (2016). Utilising an *in vitro* re-aggregation model to investigate the differentiation of putative bovine oogonial stem cells. Oral presentation at the 49th Annual Meeting of the Society for the Study of Reproduction; 2016 July 16-20; San Diego, USA. **

* Awarded 1st place poster prize

** Awarded USDA-NIFA-AFRI Merit Award

Contents

List of Figures

List of Tables

Abbreviations

Abbreviation	Description
2D	two dimensional
3D	three dimensional
Ab	antibody
ABVD	adriamycin, bleomycin, vinblastine and dacarbazine
AHR	aryl hydrocarbon receptor
AMH	anti-müllerian hormone
ANOVA	analysis of variance
APC	allophycocyanin
ART	artificial reproductive technologies
ATG7	autophagy-related protein 7
ATP	adenosine triphosphate
ATP5B	ATP synthase subunit 5B
b-Gal	b-Galactosidase
BAD	bcl-2-associated death promoter protein
BAX	bcl-2-like protein 4
BCL2	B-cell lymphoma 2
BECN1	beclin-1
bFGF	basic fibroblast growth factor
BMP	bone morphogenetic protein
BMP15	bone morphogenetic protein 15
BMP4	bone morphogenetic protein 4
bOSC	bovine oogonial stem cell
BrdU	5-bromo-2'-deoxyuridine
BSA	bovine serum albumin
C-KIT	tyrosine protein kinase KIT
C. elegans	*Caenorhabditis elegans*
CC3	cleaved caspase 3
CFP	cyan fluorescent protein
cKO	conditional knockout
CMFDA	5-chloromethylfluorescein diacetate
COUP-TFII	COUP transcription factor 2
CTCF	corrected total cell fluorescence
CXCR4	chemokine receptor 4
D. melanogaster	*Drosophila melanogaster*
DAB	3,3′-Diaminobenzidine
DAPI	4',6-diamidino-2-phenylindole
DAZL	deleted in azoospermia-like
DDX4	DEAD-Box Helicase 4 (commonly known as VASA)
DMC1	disrupted meiotic cDNA protein 1

DMEM	Dulbecco's modified eagle medium
DMSO	dimethyl sulfoxide
DNMT3β	DNA methyltransferase 3B
DPPA3	developmental pluripotency associated 3 (commonly known as STELLA)
DSB	double strand DNA break
E	embryonic
EB	embryoid body
EDTA	ethylenediaminetetraacetic acid
EGF	epidermal growth factor
eGFP	enhanced green fluorescent protein
epiLC	epiblast-like cell
ER1	estrogen receptor 1
ER2	estrogen receptor 2
ESC	embryonic stem cell
eYFP	enhanced yellow fluorescent protein
FACS	fluorescence-activated cell sorting
FBS	fetal bovine serum
FBSC	fetal bovine ovarian somatic cells
FGF5	fibroblast growth factor 5
FGSCs	female germline stem cells
FIGα	factor in the germline alpha
FISH	fluorescent in situ hybridisation
FOXL2	forkhead box L2
FST	Follistatin
GATA4	GATA binding protein 4
GDF9	growth differentiation factor 9
GDNF	glial cell-derived neurotrophic factor
GFP	green fluorescent protein
GLP	G9-like protein
GnRH	gonadotropin-releasing hormone
GREL	gonadal ridge epithelial-like
HBSS	Hanks balanced salt solution
hESC	human embryonic stem cell
ICC	immunocytochemistry
IFITM3	interferon-induced transmembrane protein 3
IgG	immunoglobulin G
IHC	immunohistochemistry
IL-6	interleukin 6
iPSC	induced pluripotent stem cell
IVF	*in vitro* fertilisation
KLF4	kruppel-like factor 4

KO	knockout
KSR	knockout serum replacement
LGR5	leucine-rich repeat-containing G-protein coupled receptor 5
LHX8	LIM homeobox protein 8
LIF	leukemia inhibitory factor
LIN28	LIN-28 homologue A
mESC	mouse embryonic stem cell
MLH1	MutL homologue 1
mOSC	mouse oogonial stem cell
NANOG	nanog homeobox protein
NANOS3	nanos C2HC-type zinc finger 3
NBF	natural buffered formalin
NEAA	non-essential Amino Acids
NOBOX	newborn ovary homeobox protein
NR2F2	nuclear receptor subfamily 2 group F member 2
NS	normal serum
OCT4	octamer-binding transcription factor 4
OFP	orange fluorescent protein
OLC	oocyte-like cell
OSC	oogonial stem cell
OSE	ovarian surface epithelium
OSR1	odd-skipped-related protein 1
PBS	phosphate-buffered saline
PECAM1	platelet and endothelial cell adhesion molecule 1
PCNA	proliferating cell nuclear antigen
PCR	polymerase chain reaction
PGC	primordial germ cell
PGCLC	primordial germ cell-like cell
PHA	phytohaemagluttanin
PLZF	promyelocytic leukaemia zinc finger protein
PRDM1	PR domain zinc finger protein 1 (commonly known as Fragilis)
PRDM14	PR domain zinc finger protein 14
PRM2	protamine 2
RA	retinoic acid
RCF	relative centrifugal force
REC8	REC8 meiotic recombination protein
RFP	red fluorescent protein
RSPO1	R-spondin 1
RT-PCR	reverse transcription-polymerase chain reaction
SCID	severe combined immunodeficiency
SDF1	stromal derived factor 1

SEM	standard error of the mean
SMC1β	structural maintenance of chromosome protein 1B
SOHLH1	spermatogenesis and oogenesis specific basic helix-loop-helix 1
SOX17	SRY-box 17
SOX9	SRY-box 9
SRY	sex-determining region Y
SSC	spermatogonial stem cell
SSEA-1	stage-specific embryonic antigen 1
SSEA-4	stage-specific embryonic antigen 4
STAG3	stromal antigen 3
STRA8	stimulated retinoic acid gene 8
SYCP1	synaptonemal complex protein 1
SYCP3	synaptonemal complex protein 3
TCFAP2C	transcription factor AP-2 gamma
TNP1	transition protein 1
TNP2	transition protein 2
UBC	ubiquitin C
WNT	wingless type
WNT3	wingless type 3
WT1	Wilms tumour protein 1
X-Gal	5-bromo-4-chloro-3-indolyl-β-D-galactopyranoside
X. laevis	*Xenopus laevis*
YBX2	Y-box binding protein 2
YFP	yellow fluorescent protein
ZP1	zona pellucida 1
ZP2	zona pellucida 2
ZP3	zona pellucida 3
β-ACTIN	beta-actin
β-Gal	beta-galactosidase

1 Literature Review

1.1 Introduction

The mammalian ovary is a highly dynamic organ which undergoes cyclical changes to produce a meiotic and developmentally competent oocyte(s) each estrous or menstrual cycle. A population of oocytes contained within somatic cells to form ovarian follicles are established just prior to or shortly after birth in mammalian ovaries. The formation of oocytes in the fetal ovary is orchestrated by various extrinsic factors and the temporal switching on and off, of regulatory genes (summarised in Figure 1.1). These controlled processes were believed to generate a fixed population of primordial follicles capable of maintaining fertility throughout an individual's reproductive lifespan without postnatal follicular renewal.

This theory formed a central dogma of ovarian biology for the latter half of the 20th Century. However, evidence in 2004 suggested that a mitotic germ cell may contribute to oocyte and follicle renewal in the postnatal murine ovary (Johnson et al., 2004). These observations renewed interest in mammalian neo-oogenesis. The examination of putative oogonial stem cells and their oogenic potential is essential to better understand ovarian biology, the process of oogenesis and may offer the potential of new artificial reproductive technologies (ART) to assist those unable to conceive naturally.

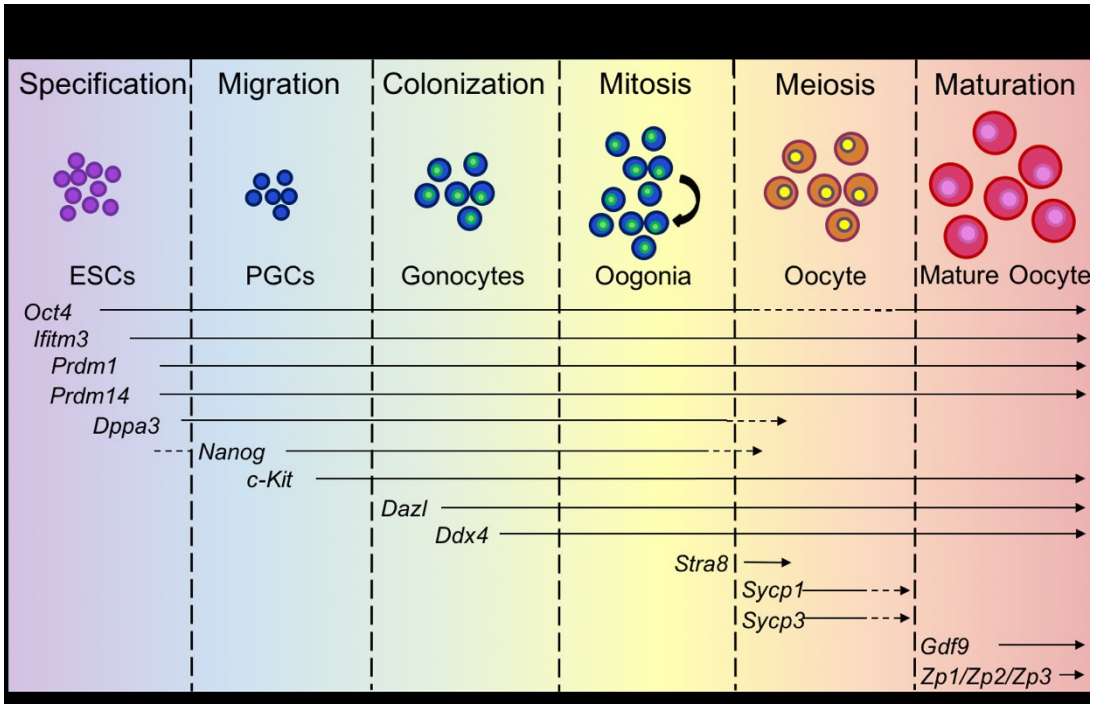

Figure 1.1: Temporal expression of cell markers during oogenesis. Germ cell development is a tightly controlled process, regulated by the temporal expression of essential genes, depicted here, and their corresponding proteins. These markers are used to characterise the stage of germ cell development during oogenesis and artificial gametogenesis. Solid lines represent consistent gene expression and dashed lines represent intermittent gene expression. Figure adapted from Schuh-Huerta and Pera (2011).

1.2 Mammalian prenatal oogenesis

The formation of fetal germ cells takes place within the wider context of the developing embryo where differentiation of a group of specialised totipotent cells, which can give rise to all the tissues of the developing embryo and extra-embryonic tissues, determines germ cell fate to a small proportion of cells. The differentiation of these cells into committed daughter cells is controlled by intrinsic and extrinsic factors, detailed below. Germ cell formation is coordinated in synchronisation with the development of other cell types and tissues. The surrounding soma can influence germ cell fate and is essential to coordinate germ-cell formation, entry into meiosis, maintenance of meiotic arrest, follicle growth and development and the resumption of meiosis. The synergistic communication between developing germ cells and the supporting somatic cells ensures the production of competent oocytes.

1.2.1 Formation of germ cells, migration and colonisation of the developing gonads

The specification of germ cells occurs in the proximal epiblast in the post implantation embryo. Cells expressing Wnt3 are exposed to BMP (Bmp2, Bmp4 and Bmp8b) signalling from the neighbouring extra-embryonic tissues at approximately E5.75 (Lawson et al., 1999; Ying et al., 2000; Ying et al., 2001; Ying and Zhao, 2001). Bmp's act to inhibit somatic cell associated genes (e.g. *Hoxb1 and Hoxa1*), maintain pluripotency genes (e.g. *Oct4*, *Nanog* and *Sox2*) and activate germ cell genes (e.g. *Dppa3*, *Prdm1* and *Prdm14*) through SMAD signalling pathways (Avilion et al., 2003; Chambers et al., 2007; Saitou et al., 2002; Sato et al., 2002; Scholer et al., 1990). All epiblast cells in a developing embryo have the potential to commit to the germline lineage, however approximately 40 PGCs are specified to the germline by E7.5 from a population of *Ifitm3* expressing cells (Saitou et al., 2002; Tanaka and Matsui, 2002), through BMP signal gradients and inhibitory signal gradients (e.g. Cer1, Dkk1 and Lefty1) (Ohinata et al., 2009; Tam and Zhou, 1996). Primordial germ cells are identified by the co-expression of *Ifitm3* and *Dppa3* (Saitou et al., 2002; Sato et al., 2002).

PGC specification is also regulated by *Prdm1*, *Prdm14* and *Tcfap2c* (encodes AP2γ) expression, known as the tripartite transcriptional network (Magnusdottir et al., 2013). Together the expression of these transcription factors coordinate an interdependent transcriptional network to ensure PGC specification (Magnusdottir et al., 2013). Mutations in any of the three key transcription factors (*Prdm1*, *Prdm14* and *Tcfap2c*) causes loss of PGCs or phenotypes more similar to neighbouring somatic cells in mice (Ohinata et al., 2005; Weber et al., 2010; Yamaji et al., 2008). Furthermore, ectopic expression of Prdm1 in an embryonic carcinoma cell line (P19EC) induced expression of PGC genes (*Dppa3*, *Tcfap2c* and *Prdm14*) and maintained expression of *Oct4*. Expression of the tripartite transcriptional network in the cell line further demonstrated the repression of somatic cell genes (Magnusdottir et al., 2013), suggesting that the induction and repression of the appropriate genes for PGC specification is a complex process requiring multiple regulators. In human embryonic stem cells, PGC fate was similarly induced by BMP4 exposure with

upregulation of *PRDM1*, *PRDM14* and *TCFAP2C* (Irie et al., 2015). *SOX17* expression was also increased in human PGC-like cells (PGCLCs) and SOX17 knockdown repressed the expression of *PRDM1* and *TCFAP2C* suggesting that SOX17, which has known roles in the murine endoderm (Kanai-Azuma et al., 2002), is a key regulator of human germ cell fate (Irie et al., 2015). Therefore, BMP signalling is essential for mammalian germ cell specification, however the key regulators which are activated to control PGC fate have similarities and differences between mammalian species.

Following germ cell specification, PGCs migrate to the developing gonads from E7.5-E11.5. Mechanisms underlying the initiation of mammalian PGC migration are yet to be identified, however a strict pathway to the genital ridges is followed by PGCs. Although some get lost in transition, PGCs travel through the posterior primitive streak along the hindgut to the mesoderm where they migrate bilaterally into the gonadal ridges (reviewed by Richardson and Lehmann (2010)). PGC migration is regulated by Kit ligand, expressed by somatic cells and its receptor c-Kit which is expressed on the surface of PGCs. Aberrant PGC migration was observed in $Kit^{-/-}$ mice and cells along the migratory route expressed KIT in a temporal manner to coordinate the migration of PGCs (Gu et al., 2009). Artificial inhibition of Kit ligand in cultured bisected embryos caused a reduction in PGC velocity. Inhibition of c-Kit signalling also resulted in clumping of PGCs (Gu et al., 2009), which may have contributed to decreased cell motility. PGCs interact through long processes during migration forming networks of PGCs undergoing mass migration which may facilitate the migration of the entire population. Cells cease migration in conjunction with the loss of intercellular processes (Gomperts et al., 1994), suggesting that these facilitate the migration of PGCs. The genital ridge also expresses the chemoattractant Sdf1 (stromal derived factor 1) which interacts with PGCs through their expression of the receptor Cxcr4 (chemokine receptor 4) and facilitates their migration to the developing gonads (Ara et al., 2003). Adhesion molecules are also implicated in PGC migration. Disruption of E-cadherin expression in PGCs resulted in failure of PGCs to colonise the genital ridges (Anderson et al., 1999). These results illustrate that several mechanisms and pathways regulate PGC migration to the genital ridges.

As PGCs migrate through the developing embryo they maintain pluripotency and are exposed to various factors which may cause inappropriate differentiation into somatic cell types. PGC specification is protected through cellular mechanisms including epigenetic reprogramming, which is also essential to produce correctly imprinted gametes. In PGCs, Prdm1 binds to maternal chromatin to protect from demethylation (Nakamura et al., 2012) and Prdm14 functions to repress Glp (G9a-like protein) a histone methyl transferase (Yamaji et al., 2008), both serving to preserve the epigenetic imprinting of PGCs. PGC's also undergo global repression of transcription through the de-phosphorylation of RNA Polymerase II (Seki et al., 2007). Together these mechanisms ensure germ cell fate is maintained in PGCs while migrating through various somatic environments in the developing embryo.

PGCs arrive in the sexually ambiguous developing genital ridges from E10.5 (Lawson and Hage, 1994; Molyneaux et al., 2001) and undergo germ cell licensing to reach a sexually competent state. *Dazl* and *Ddx4* expression is associated with post-migratory PGCs and represents their ability to commit to gametogenesis. PGCs in *Dazl*$^{-/-}$ fail to differentiate and retain their PGC phenotype despite the maintenance of Ddx4 expression (Gill et al., 2011), suggesting that *Dazl* and *Ddx4* expression are independent and that Dazl functions as a regulator of germ cell licensing. Germ cell licensing coincides with the arrival of PGCs at the genital ridges which are marked by the expression of Gata4. Prevention of genital ridge formation through genetic knockout models (*Gata4* cKO, *Wt1* KO and *Osr1* KO) inhibits *Dazl* and *Ddx4* expression and consequently, PGCs fail to undergo germ cell licensing and retained a PGC phenotype (Hu et al., 2015). Therefore, the ability of PGCs to become gametogenesis competent cells is dependent on exposure to the genital ridges which induces expression of *Dazl* which acts intrinsically to regulate translation of genes to commit cells to gametogenesis.

PGCs proliferate from specification, throughout migration and continue upon arrival in the gonads resulting in approximately 20,000 in the murine ovary at E13.5 (Byskov, 1986; Lawson and Hage, 1994; Tam and Snow, 1981). Factors including Kit ligand (Dolci et al., 1991; Pesce et al., 1993), fibroblast growth factors (FGFs) including Sdf1 (Kawase et al., 2004; Resnick et al., 1992) and LIF (leukemia

inhibitory factor or interleukin 6 (IL-6); (De Felici and Dolci, 1991; Matsui et al., 1991) have been implicated in PGC proliferation. Although PGCs continue to proliferate in the developing gonads they lose their ability to migrate (De Felici et al., 1992; Gomperts et al., 1994) ensuring that they remain in the correct niche for sex determination and subsequent gametogenesis.

1.2.2 Sex determination

When PGCs arrive in the genital ridges the developing gonads are sexually ambiguous. PGCs are also bipotential with the ability to initiate either oogenesis or spermatogenesis (Adams and McLaren, 2002). The expression of sex-determining region Y (*Sry*) gene in gonadal somatic cells instigates Sertoli cell differentiation and testis formation and in its absence, WNT signalling, *Foxl2* and *Rspo1* expression in XX somatic cells drives the development of ovaries (reviewed by Eggers and Sinclair (2012); summarised in Figure 1.2). *Wnt4* expression in somatic cells is essential for ovarian development as *Wnt4*$^{-/-}$ mice failed to form ovaries and developed structures which expressed enzymes associated with testosterone production (Vainio et al., 1999), indicating the onset of testis formation, although complete sex reversal was not observed. Wnt4 signals through β-catenin pathways to regulate the transcription of downstream targets. *Follistatin* (*Fst*) and *Bmp2* were identified as potential targets of Wnt4, as expression of both genes show downregulation in the absence of Wnt4 in *Wnt4*$^{-/-}$ mice (Yao et al., 2004). WNT4 also acts as a repressor of the male specification pathway through suppression of *Sox9* expression (Kim et al., 2006). However, ectopic overexpression of *Wnt4* in XY embryos did not cause complete sex-reversal but disrupted testis-specific vasculature and inhibited testosterone production (Jordan et al., 2003). Thus, Wnt4 is not the sole factor required to suppress male specification and promote female gonadal differentiation.

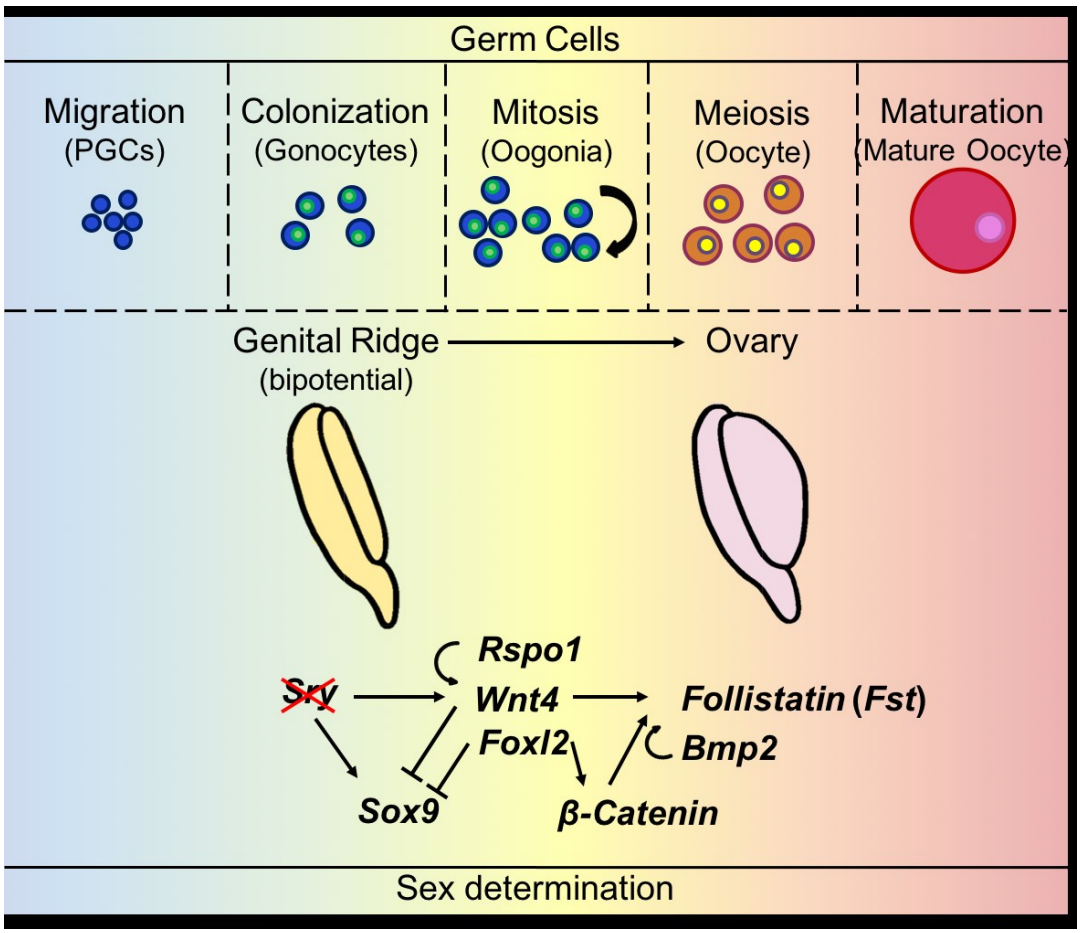

Figure 1.2: Summary of the genes and factors involved in sex determination and the corresponding germ cell developmental stages to form an ovary. In the absence of *Sry* expression the ovarian developmental pathway is initiated marked by the expression of *Wnt4*, *Rspo1* and *Foxl2*, which regulate downstream pathways to induce oogenesis in germ cells.

R-spondin 1 (Rspo1) is a secreted protein which can stabilise β-catenin, a factor in the WNT signalling pathway. Partial sex reversal is observed in *Rspo1*$^{-/-}$ mice (Chassot et al., 2008; Tomizuka et al., 2008) and *RSPO1* null and mutated humans (Parma et al., 2006; Tomaselli et al., 2008), and share a phenotype similar to *Wnt4* null mice. Stabilisation of β-catenin expression in ovarian somatic cells resulted in phenotype rescue (Chassot et al., 2008), which suggests β-catenin acts downstream of RSPO1. *Wnt4*, *Fst* and *Bmp2* were also downregulated in the ovaries of *Rspo1*$^{-/-}$ mice, suggesting Rspo1 is a positive regulator of *Wnt4* expression and therefore indirectly regulates expression of *Fst* and *Bmp2* (Chassot et al., 2008; Tomizuka et al., 2008). β-catenin ectopic over expression in XY embryos causes partial sex reversal and stabilisation of β-catenin, which could interfere with the role of *SRY*,

and has been implicated in human 46 XY disorders of sex development where no apparent mutations in sex-determining genes are identified (Maatouk et al., 2008). Therefore β-catenin is a pro-ovarian signalling molecule in WNT signalling pathways.

Forkhead box L2 protein (Foxl2) is also essential in regulating the development of the mammalian ovary. Foxl2 functions to repress the expression of the pro-testis gene *Sox9*. Elimination of *Foxl2* expression in the embryonic ovary causes a decrease in *Fst* and *Bmp2* expression and results in partial sex reversal (Ottolenghi et al., 2007). These results are similar to those observed in *Wnt4*$^{-/-}$ mice, however, the expression of *Fst* and *Bmp2* did not recover in *Foxl2*$^{-/-}$, which had been reported in *Wnt4*$^{-/-}$ mice, suggesting that Foxl2 is required to maintain the expression of these ovarian genes (Ottolenghi et al., 2007). Foxl2 and Bmp2 demonstrated cooperative upregulation of *Fst* expression in *in vitro* cultures (Kashimada et al., 2011). Furthermore, conditional knockout of *Foxl2* in adult mice caused ovaries to transdifferentiate into testis-like structures with tubular features and Sertoli-like cells, changes which were mediated by the increased expression of *Sox9* (Uhlenhaut et al., 2009). These results illustrate that Foxl2 is essential for both ovarian differentiation and maintenance. Experimental evidence suggests that the role of Foxl2 to supress *Sox9* expression is carried out in cooperation with estrogen receptor 1 and 2 (Er1/Er2) through binding of sequences within the enhancer region of *Sox9* (Bagheri-Fam et al., 2010).

Ovarian development was traditionally viewed as the default gonadal developmental pathway (Jost, 1947), however, the experimental evidence suggests that the ovarian pathway is an active process regulated by the active expression of ovarian genes (*Wnt4*, *Rspo1* and *Foxl2*) and the repression of testis specific genes (*Sox9*).

1.2.3 Entry into meiosis and meiotic arrest

During sex determination, PGCs become oogonia, marked by morphological changes. Oogonia are larger than PGCs and spherical in shape and can be identified by globular mitochondria and expression of Ddx4 (Gondos et al., 1986; Stoop et al., 2005). Oogonia undergo proliferation with incomplete cytokinesis to form germ cell nests interlinked by intercellular bridges (Pepling et al., 1999). Germ cell nests are

surrounded by somatic cells which the dividing oogonia interact with forming ovarian cords (Byskov, 1986).

Oogonia transition from mitotic division and initiate meiosis by entering a pre-meiotic state from approximately E12.5 and enter meiosis at E13.5 in the mouse (Borum, 1961; Menke et al., 2003) and from 11 and 13 weeks gestation, respectively in the human (Baker and Franchi, 1967; Motta et al., 1997), which can be identified by the expression of meiotic genes such as *Sycp3* (Di Carlo et al., 2000). Meiotic initiation occurs in an anterior to posterior wave in a synchronised fashion in the mouse (Menke et al., 2003) and in a slower, more progressive manner in larger mammals including humans, with many oogonia remaining mitotically active as neighbouring follicles form (Anderson et al., 2007).

Entry into meiosis in fetal oogonia is determined by germ cell extrinsic and intrinsic factors (summarised in Figure 1.3). Retinoic acid (RA), the biologically active variant of vitamin A, has been identified as the key germ cell extrinsic regulator in meiotic entry in both the ovary and testis (Anderson et al., 2008; Bowles et al., 2006; Koubova et al., 2014; Koubova et al., 2006). RA derives from the embryonic mesonephros in the mouse (Anderson et al., 2008; Bowles et al., 2006; Koubova et al., 2006) and the ovary in humans (Childs et al., 2011; Le Bouffant et al., 2010). RA accumulates through the downregulation of its metabolizing protein Cyp26b1 under the control of follistatin signalling (Bowles et al., 2006). In germ cells RA signalling activates the expression of *Stra8* and *Rec8* to initiate meiosis (Anderson et al., 2008; Bowles et al., 2006; Koubova et al., 2014; Koubova et al., 2006). Antagonism of RA action decreased the expression of both *Stra8* and *Rec8 in vitro* and caused a decrease in germ cells entering meiosis (Bowles et al., 2006; Koubova et al., 2014). However, *Stra8*$^{-/-}$ mice maintain the expression of *Rec8* (Baltus et al., 2006) and *Rec8*$^{-/-}$ mice maintain the expression of *Stra8* in germ cells (Koubova et al., 2014). Therefore, RA action upon the meiotic genes *Stra8* and *Rec8* is independent of each other. *Stra8*$^{-/-}$ mice are infertile, with no oocytes observed in the adult ovary and embryonic *Stra8*$^{-/-}$ ovaries demonstrated a decrease in *Spo11* and *Dmc1*, which are required to form and repair DNA double-strand breaks (DSBs) essential for meiotic recombination. Furthermore *Stra8*$^{-/-}$ deficient germ cells did not undergo premeiotic

DNA replication (Baltus et al., 2006). Therefore, *Stra8* plays a critical role in premeiotic DNA replication and subsequent entry into meiotic prophase. As such Stra8 has been described as the gatekeeper of germ cell meiosis. In contrast, *Rec8*$^{-/-}$ deficient mice initiate meiosis but errors in chromosome synapsis result in an infertile phenotype (Xu et al., 2005). Thus, Stra8 regulates meiosis at an earlier stage than REC8, however both independently regulate meiosis in response to an extracellular RA signal.

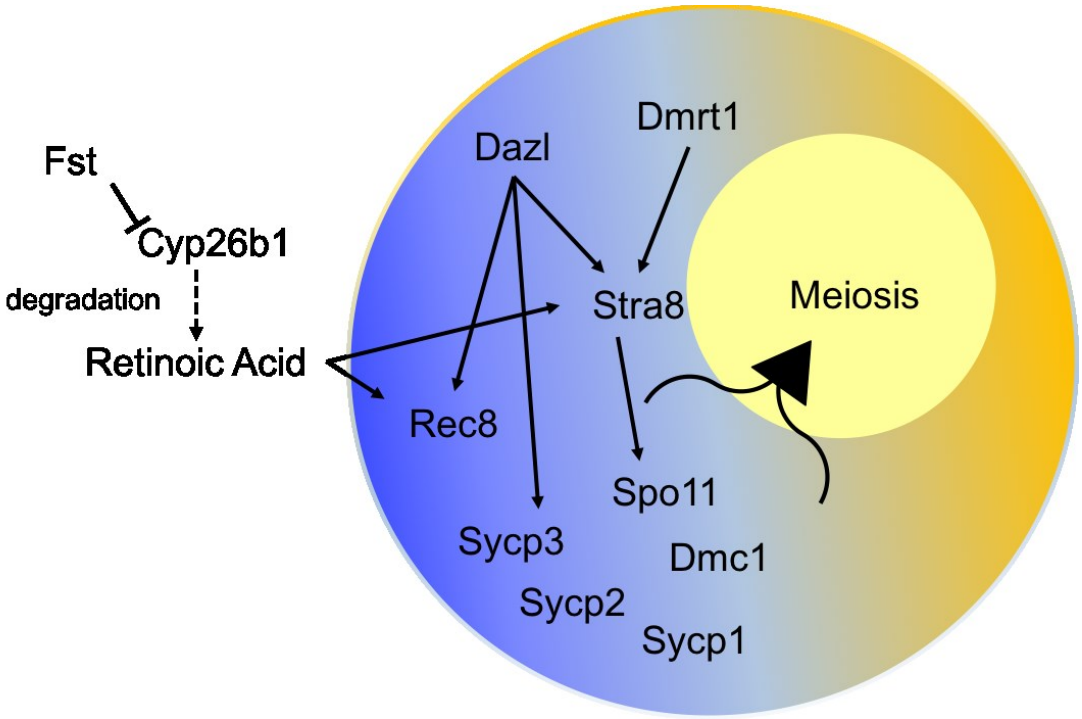

Figure 1.3: Summary of germ cell extrinsic and intrinsic factors which regulate the initiation of meiosis in fetal ovaries. Retinoic acid (RA) accumulates in the extracellular space as a consequence of follistation signal which inhibits the production of CYP26B1 (P450 cytochrome enzyme) responsible for the degradation of RA. RA acts to induce the expression of Stra8 and Rec8 independently, which then act upon downstream targets to induce meiosis. Dazl is an intrinsic meiotic competence factor and works in tandem with RA to initiate meiosis in oogonia.

Dazl expression is crucial to commit PGCs to gametogenesis (Gill et al., 2011), acting as a germ cell intrinsic regulator of meiotic entry (Lin et al., 2008). *Dazl*$^{-/-}$ mice are infertile (Saunders et al., 2003) and *DAZL* mutations are associated with sub-fertility in humans (Reijo et al., 1995). Germ cells in *Dazl*$^{-/-}$ ovaries did not demonstrate chromosome condensation and failed to initiate meiotic recombination and showed decreased expression of several meiotic markers including *Stra8* and its

downstream targets *Spo11* and *Dmc1*, and *Sycp3* and *Rec8*, suggesting that DAZL is a master regulator of germ cell meiosis and acts upstream of *Stra8*, *Sycp3* and *Rec8* (Lin et al., 2008). Experimental evidence suggests that Dazl is a meiotic competence factor and its expression within germ cells and extrinsic RA signalling are both necessary for the initiation of meiosis and work cohesively to ensure meiotic entry in fetal ovarian germ cells.

Following initiation of meiotic prophase I germ cells progress through leptotene (chromosome condensation), zygotene (chromosomal pairing), pachytene (initiation of recombination and arrest in diplotene (chromosomes start to separate but remain attached) (Baillet and Mandon-Pepin, 2012). Once meiosis has initiated, germ cells can no longer proliferate generating a fixed population of oocytes.

1.2.4 Germ cell nest breakdown and primordial follicle formation

Meiosis initiates in germ cells within germ cell nests, which must undergo breakdown to produce oocytes which form primordial follicles with the surrounding pre-granulosa cells. Germ cell nest breakdown is associated with a dramatic decrease in oocyte numbers, with loss of up to 80% of oocytes (Pepling and Spradling, 2001). Three mechanisms of oocyte loss have been proposed to account for such large-scale decline in cell number; apoptosis, autophagy and oocyte expulsion from the ovarian surface epithelium.

Large numbers of oocytes undergo apoptosis, marked by the expression of members of the caspase family which have been observed in the ovaries of different mammalian species including humans (De Felici et al., 2008; Fulton et al., 2005; Ghafari et al., 2007; Jefferson et al., 2006; Lobascio et al., 2007; Pepling and Spradling, 2001). Disruption of caspase 2 caused an increase in the number of primordial follicles in postnatal murine ovaries (Bergeron et al., 1998). Elimination of other members of the apoptotic pathway (reviewed by Hutt (2015)) also causes an increase in primordial follicle numbers, with 3 times the number of primordial follicles observed in *Bax*$^{-/-}$ mice compared to wild type mice (Perez et al., 1999). Pro-apoptotic factor Bax is activated through the actions of the aryl hydrocarbon receptor (AHR) and subsequently binds to Bcl2 allowing formation of an apoptosome in the cytosol of the oocyte (Benedict et al., 2000) and causes activation of caspase 9

resulting in apoptosis (Wei et al., 2001). Bax functions through dimerization with Bad to increase mitochondrial permeability, forming large channels in targeted cells which results in the release of cytochrome c from mitochondria, activating caspases and inducing apoptosis (Cory and Adams, 2002; Wei et al., 2001).

Germ cell nest breakdown is also regulated by extrinsic factors to promote oocyte apoptosis. In the mouse germ cell nest breakdown and primordial follicle formation is initiated postnatally and is at least in part regulated by the elimination of the estrogenic signal fetal ovaries are exposed to in the maternal environment (Chen et al., 2009; Iguchi and Takasugi, 1986; Kezele and Skinner, 2003). Postnatal exposure of estrogen caused increased oocyte survival and resulted in a greater proportion of multi-oocyte follicles (Jefferson et al., 2002), whereas premature removal of estrogen causes early primordial follicle formation in murine ovaries (Chen et al., 2007). Larger mammals undergo germ cell nest breakdown *in utero*, therefore elimination of maternal estrogen cannot account for induction of oocyte apoptosis. However, an estrogen deprived baboon model demonstrated a reduction in the number of primordial follicles (Zachos et al., 2002), indicating a potential role for estrogen signalling in germ cell nest breakdown in larger mammals in addition to rodents. The developing fetal bovine ovary produces an internal supply of estrogen which declines at the onset of primordial follicle formation, suggesting an important role in either germ cell nest breakdown and/or primordial follicle formation in the bovine (Nilsson and Skinner, 2009; Yang and Fortune, 2008).

Signalling pathways activated in pre-granulosa cells have also been implicated in facilitating oocyte apoptosis. Elimination of Notch2 expression in pre-granulosa cells through a *Notch*$^{-/-}$ mouse demonstrated an increase in number of oocytes, but a decrease in fertility associated with multi-oocyte follicles (Xu and Gridley, 2013), due to a decrease in oocyte apoptosis. Perturbation of NOTCH signalling in *in vitro* postnatal ovarian culture also demonstrated failure of germ cell nest breakdown (Trombly et al., 2009). Although exact mechanisms have not been elucidated, it has been hypothesised that somatic cells communicate with oocytes through JAGGED/NOTCH interactions to induce germ cell nest breakdown (Trombly et al., 2009). Follistatin (Fst), is also required for appropriate germ cell nest breakdown.

Females expressing only a single isoform of Fst (Fst-288) had increased numbers of primordial follicles in early postnatal life but demonstrated an accelerated loss of these follicles (Kimura et al., 2011). Germ cell apoptosis was reduced in these mice compared to wild types and the length of germ cell nest breakdown was extended. These results show that germ cell nest breakdown through apoptosis is necessary for healthy primordial follicle formation and suggests that high levels of apoptosis are observed to eliminate sub-standard oocytes.

It has been hypothesised that the purpose of producing 'unnecessary' oocytes is to generate additional nutrients and organelles such as mitochondria which are donated to the surviving oocyte(s) within a germ cell nest by autophagy. This theory has been supported by the observation that apoptosis cannot solely account for the amount of germ cell death (De Felici et al., 2008; Lobascio et al., 2007), furthermore mitochondria have been identified within the cytoplasmic bridges between oogonia (Pepling and Spradling, 2001), suggesting that oogonia share nutrients and organelles. Loss of autophagy genes (*Becn1* or *Atg7*) causes decrease in germ cell numbers in postnatal murine ovaries (Gawriluk et al., 2011), thus autophagy plays a role in maintaining the endowment of oocytes in mammalian ovaries through controlled cell death. Germ cells are also extruded from the ovarian surface epithelial into the peritoneal cavity, for unknown reasons (Motta and Makabe, 1986).

As germ cell nests breakdown, surviving oocytes interact and associate with the surrounding pre-granulosa cells to form primordial follicles. Cytoplasmic bridges between oogonia retract/degrade during this process which is facilitated by proteases (Tingen et al., 2009). Only Foxl2 positive pre-granulosa cells invade germ cell cysts (Pepling et al., 2010). Proliferation of pre-granulosa cells is essential in preparation for primordial follicle assembly and expression patterns suggest Lgr5 expressing cells in the OSE are a potential source of Foxl2 positive pre-granulosa cells (Mork et al., 2012; Rastetter et al., 2014). Oocytes which fail to associate with supporting somatic cells are lost (Byskov, 1986; Pepling and Spradling, 2001). Primordial follicles then become separated from the surrounding mesenchymal stromal cell environment by enclosure in a basement membrane (Rajah et al., 1992). The successful establishment of communication networks between the cell types within a

follicle and between follicles and the surrounding stromal environment is essential to maintain the follicle, and support it through subsequent folliculogenesis.

The ovarian surface epithelium OSE is a modified pelvic mesothelium covering the ovary and is comprised of a single layer of flat-to-cuboidal epithelial cells. It is derived from celomic epithelium in the developing embryo (Auersperg et al., 2001). At approximately 10 weeks of human gestation the fetal OSE undergoes several changes from flat-to-cuboidal simple epithelium and reverts to a monolayer by term. The OSE has been implicated as a potential source of Foxl2 positive pre-granulosa cells (Mork et al., 2012; Rastetter et al., 2014) during murine fetal development and was previously referred to as the 'germinal epithelium', as it was believed that it could give rise to new germ cells (Waldeyer, 1870). More recently it has been suggested as a potential source and niche of mammalian oogonial stem cells (OSCs) postnatally (Bukovsky et al., 2005; Parte et al., 2011; Virant-Klun et al., 2009; Virant-Klun et al., 2008). The oogenic capability of the ovarian surface epithelium has recently been investigated and is discussed further in section 1.4.

1.3 Postnatal oogenesis

In males, germ cell production is maintained in the testis via the ongoing presence of spermatogonial stem cells throughout adult life. In contrast the female ovary appears to have evolved different strategies for oocyte production. Invertebrate and lower vertebrate species, including a number of model organisms such as *Caenorhabditis elegans*, *Drosophila melanogaster* and *Xenopus laevis*, maintain oocyte production from a germ line stem cell population during adult life (Lin, 1997). However, mammalian ovaries with the exception of some prosimian primates (*Loris tardigragus lydekkerianus* (Duke, 1967) and *Nycecticebus coucang*, (David et al., 1974)) and bat species (*Artibeus jamaicensis*, *Glossophaga soricina* and *Sturnira lilium*, (Antonio-Rubio et al., 2013)), were believed to cease oogenesis prior to or just after birth, based on mathematic modelling of follicle growth and atresia (Zuckerman, 1951).

1.3.1 Postnatal oogenesis in invertebrates and lower vertebrates

Germ line stem cells are a common feature of ovaries in invertebrate and lower vertebrate species. Female germline stem cells (FGSCs) must maintain a population of undifferentiated stem cells and give rise to oocytes during the reproductive lifespan of the organism. Two gametogenic strategies have evolved to maintain these processes in species with FGSCs (Lin, 1997):

1. Individual stem cells through asymmetric divisions that produce a daughter stem cell and a differentiated daughter cell (e.g. *Drosophila melanogaster* and *Xenopus laevis*).

2. Collective behaviour of mitotic cells in the gonad maintains a steady source of the germline without individual germ cells undergoing asymmetric division (e.g. *Caenorhabditis elegans*).

Drosophila ovaries contain approximately 18 ovarioles which are responsible for oocyte production. Within each ovariole is a structure known as the germarium which hosts the terminal filament, a somatic structure which is anterior to cap cells which adhere to the germline stem cells. As germline stem cells divide, one daughter cell is maintained within the niche and retains a germline stem cell phenotype, in

contrast the other daughter cell (termed a cystoblast) is displaced from the niche and becomes committed to oocyte differentiation. The cystoblast then undergoes several rounds of mitosis supported by escort cells to form a cyst comprising of 16 cells (cystocyte) which transitions into the next chamber of the germerium. Supported by follicle cells, cystocytes form egg chambers within which the cystocyte cells differentiate into one meiotic oocyte and 15 nurse cells (overview of *Drosophila* oogenesis provided in Bastock and St Johnston (2008); Marca and Somers (2014); Roth (2001)). Similar observations have been seen in *Xenopus laevis* where premeiotic interphase to late pachytene oocytes are found in nests of 16 interconnected cells (Coggins, 1973), which are presumed to be as a consequence of 4 sequential mitotic divisions of a single oogonium.

In contrast, the hermaphrodite *C. elegans* produces oocytes form a population of germline stem cells with a shared common cytoplasm located within the proliferative zone at the distal tip of the organism. Mitotic proliferation of FGSCs in *C. elegans* is under the regulation of the distal tip cell, which if ablated results in meiotic initiation in all proliferating FGSCs (Kimble and White, 1981). As FGSCs move through the proliferation zone into the transition zone their mitotic ability is reduced and they initiate meiosis to form oocytes (overview in Lin (1997)). Other invertebrates such as *Hydra oligactis* and *Hydra magnipapillata* are believed to produce oocytes in a similar fashion.

Despite differences between the mechanisms in which invertebrate and lower vertebrate species maintain oogenesis throughout reproductive life and the processes share commonality in maintaining a germline stem cell. FGSCs also appear to maintain their undifferentiated state as a consequence of the niche within which they are located and differentiation of daughter cells is due to their displacement from the niche.

1.3.2 Postnatal oogenesis in mammals

Prior to the mathematical modelling of ovarian dynamics undertaken by Baron Solomon Zuckerman in 1951 (Zuckerman, 1951), the ability of mammalian ovaries to undergo neo-oogenesis was disputed. Evidence both for and against mammalian neo-oogenesis was presented from the late 19th century to the mid 20th century.

Waldeyer (1870) proposed that oocytes originate from the germinal epithelium after birth and several descriptive studies of mammalian ovaries from different species suggested that oogenesis was not restricted to prenatal life (Allen, 1923; Evans and Swezy, 1931; Kingery, 1917; Sneider, 1940). Two germ cell proliferative phases were observed in the murine ovary, the first during fetal development and the second after birth which ceased just prior to sexual maturity. Oocytes produced prior to birth appeared to degenerate and did not contribute to the population of oocytes ovulated (Kingery, 1917). Similar observations have been observed recently in murine ovaries, where oocytes established prenatally do not contribute to ovulation whereas oocytes established in primordial follicles in early postnatal life support ovulation (Mork et al., 2012). Furthermore, oogenesis was observed to be cyclical in post-natal rat ovaries, with increased numbers of new oocytes derived from the germinal epithelium, approximately every 10 days (Sneider, 1940). New oocyte formation was thought to compensate for loss of degenerating follicles in postnatal rodent ovaries to maintain constant oocyte numbers in young adult ovaries (Allen, 1923).

The assessment of oocyte numbers in mammalian ovaries predicted that pre-natal oogenesis was sufficient to support ovarian development through to ovarian quiescence (Zuckerman, 1951). The author noted their observations applied to all mammalian ovaries examined with the exception of lemurs. Since, histological analysis of ovaries from several other species has identified mitotically active germ cells in postnatal ovaries (David et al., 1974; Duke, 1967). Non-follicular germ cell nests in the ovarian cortex of the adult slender loris (*Loris tardigradus lydekkerianus*) demonstrated mitotic activity and were observed to contribute to the population of primordial follicles, however it is unknown whether these cells contributed to the ovulatory population (David et al., 1974). Ovaries of several bat species (*Artibeus jamaicensis*, *Glossophaga soricina* and *Sturnira lilium*) also contain mitotically active cortical germ cells (Antonio-Rubio et al., 2013).

The physiological contribution of mitotically active germ cells within mammalian ovaries remains unknown, however some experimental evidence is suggestive of active oogenesis in the postnatal mammalian ovary. Cell depth lineage analysis of oocytes in mice showed increased oocyte depth with age, thus oocytes ovulated later

in life had undergone more mitotic divisions than their younger counterparts. Oocyte depth was further increased in ovaries of mice following unilateral ovariectomy, suggesting post-natal renewal of oocytes to compensate for ovarian loss (Reizel et al., 2012). In human patients treated with adriamycin, bleomycin, vinblastine and dacarbazine (ABVD) combined chemotherapy treatment, a greater follicle density was observed when compared to age matched control healthy women (McLaughlin et al., 2017). These results suggest that ABVD treatment caused the formation of new oocytes/follicles in this patient group, although the underlying mechanism for this is yet to be elucidated. Together these results indicate that germ cell renewal may be possible in post-natal mammalian ovaries under certain physiological or pathophysiological conditions.

Investigations into the rates of oocyte atresia in the murine ovary revealed inconsistencies between the levels of cell death and the reproductive lifespan (Johnson et al., 2004). It was postulated that post-natal follicular renewal was necessary to maintain ovulation throughout the murine reproductive life span. The generation of new oocytes in the post-natal mammalian ovary would require the presence of a progenitor germline stem cell, similar to those observed in invertebrate and lower vertebrate species. The lack of a candidate progenitor cell within postnatal mammalian ovaries suggested that neo-oogenesis was not plausible.

1.4 Mammalian oogonial stem cells (OSCs)

Following the establishment of the follicle reserve in the fetal mammalian ovary, this reserve undergoes depletion in early postnatal life. The depletion of primordial follicles can be attributed to their initiation of growth, oocyte apoptosis, follicular atresia and also their expulsion from the ovary into the peritoneal cavity (Motta and Makabe, 1986). However, several studies have demonstrated consistent numbers of primordial follicles over the first several weeks and months in murine ovaries (Johnson et al., 2004; Kerr et al., 2006). Furthermore, fetal and neonatal ovaries transplanted to recipient mice did not show significant reduction in the mean number of primordial follicles from 2-8 weeks after transplantation (Cox et al., 2000). The lack of follicle depletion in the postnatal murine ovary identified in these studies was not found to be associated with a reduction in oocyte apoptosis (Johnson et al., 2004) and or decrease in recruitment to the growing population (Cox et al., 2000; Kerr et al., 2006). These observations are suggestive of follicular renewal to compensate for follicular loss to maintain primordial follicle numbers within the juvenile and early adult ovary. However, the lack of a candidate progenitor cell within mammalian ovaries to support the continual renewal of germ cells suggested that this was perhaps unlikely in postnatal mammalian ovaries.

However, the identification of a mitotically active germ cell marked by the co-expression of Ddx4 and BrdU in adult murine ovaries is indeed supportive of a population of putative female germline stem cells (Johnson et al., 2004). This work contradicted one of the central dogmas of ovarian biology and instigated a wealth of research into putative oogonial stem cells.

1.4.1 Work to date with mammalian oogonial stem cells: for and against their existence and oogeneic capability

Work on mitotically active germ cells in mammalian ovaries, often described as female germline stem cells (FGSCs) or oogonial stem cells (OSCs), over the last decade or so has generated inconsistent results, with evidence for and against their existence and their functional capabilities to produce new oocytes. Johnson and colleagues work in 2004 initially elicited criticisms (Albertini, 2004; Gosden, 2004; Telfer, 2004), which identified several flaws in the methodology undertaken in the

study and provided alternative explanations to the results observed. The mitotic germ cells identified in the surface epithelium were suggested to be germ cells extruding from the ovary into the peritoneal cavity (Gosden, 2004), a phenomenon previously identified in early postnatal life (Motta and Makabe, 1986). Furthermore, the chimeric follicles observed following ovarian transplantation were interpreted as a result of cellular 're-shuffling' following the procedure (Gosden, 2004). However, the expression of early meiotic genes (*Sycp3*, *Spo11* and *Dmc1*) and proteins (Sycp3) not associated with oocytes held in meiotic arrest indicate new germ cell formation in the adult murine ovary (Johnson et al., 2004).

In contrast, gene expression analysis of adult human ovaries showed no expression of early meiotic markers (*SYCP1*, *SPO11* and *PRDM9*) (Liu et al., 2007) and SYCP3 staining was absent from both adult human and monkey ovaries of different ages (Liu et al., 2007; Yuan et al., 2013). Analysis of human ovaries from fetal development through to early adulthood (5 weeks post conception - 32 years old), showed that the expression SSEA-4, a pluripotency associated protein was restricted to pre-natal and early post-natal life (up to 2 years of age) (Byskov et al., 2011). Furthermore, proliferating cell nuclear antigen (Pcna), which is essential for DNA replication and mitosis, was not found to co-localise with germ cells in the post-natal murine ovary (Tan and Fleming, 2004). Taken together these results suggest that the post-natal mammalian ovary does not actively produce new germ cells and is void of mitotically active germ cells or progenitor germ cells. However, it is not inconceivable that mammalian oogonial stem cells may lay dormant within the postnatal ovary and only activate under the correct physiological and/or pathophysiological conditions, which these histological studies may have overlooked. In atrophic mouse ovaries, where histology confirmed complete oocyte depletion, *Dazl* and *Stra8* expression was detected (Niikura et al., 2009), suggesting the presence of germ cells entering meiosis. Stra8 positive cells were identified in the ovarian surface epithelium (OSE) of these ovaries (Niikura et al., 2009). In the ovaries of infertile and post-menopausal women, cytokeratin staining indicated putative stem cells in the OSE (Virant-Klun et al., 2008). These results suggest the OSE as a source of putative OSCs and indicates that putative OSCs may only function under particular circumstances.

Cultures of ovarian surface epithelial cells from the postnatal ovaries of rabbit, sheep, monkey and human developed oocyte-like cells (OLCs) (Bukovsky et al., 2005; Parte et al., 2011; Virant-Klun et al., 2009; Virant-Klun et al., 2008). These cells resembled oocytes, sharing a spherical morphology and were large cells (up to 200μm) in all species studied. As rabbit, sheep, monkey and human OLCs became larger they appeared to develop a zona pellucida-like structure (Bukovsky et al., 2005; Parte et al., 2011; Virant-Klun et al., 2009; Virant-Klun et al., 2008) and human OLCs appeared to associate with other cells to form follicle-like structures (Bukovsky et al., 2005). Human and sheep OLCs were found to express markers associated with germ cells and oocytes (*OCT4*, *C-KIT*, *DDX4*, *DAZL*, *GDF9*, *ZP2* and *ZP4*), however meiotic markers were not observed in OLCs of either species (*SYCP3*) (Parte et al., 2011; Virant-Klun et al., 2009; Virant-Klun et al., 2008), suggesting abnormal oocyte development. Extended culture of rabbit, sheep, monkey and human OLCs derived from OSE cells generated were observed to extrude polar body like structures and embryo-like structures were observed in sheep and human cultures. This data suggests that sheep and human OLCs had undergone parthenogenetic activation, however only morphological information on these structures was provided, although multiple cells within the structures was confirmed by DNA staining (Parte et al., 2011; Virant-Klun et al., 2009). These data show that cells from the ovarian surface epithelium of several mammalian species have spontaneously generated oocyte-like cells during *in vitro* culture and may indicate the presence of a progenitor germline stem cell contained within these cell populations.

Isolation of putative oogonial stem cells from the postnatal ovaries of rodents and humans was successfully achieved using magnetic and fluorescent based cell sorting technologies utilising the cell surface expression of germ cell associated markers (Ddx4/DDX4 and Ifitm3 (commonly known as Fragilis)) (Imudia et al., 2013; Park et al., 2013; White et al., 2012; Zhou et al., 2014; Zou et al., 2009) and GFP expression driven by the *Oct4* promoter (Pacchiarotti et al., 2010). Putative OSCs consistently expressed germ cell (*Dazl*/*DAZL*, *Ddx4/DDX4*, *Prdm1/PRDM1*, *Ifitm3/IFITM3* and *Dppa3/DPPA3*) and pluripotency (*Oct4/OCT4*, *Nanog/NANOG* and *Lin28/LIN28*) associated genes in culture (Imudia et al., 2013; Park et al., 2013;

White et al., 2012; Zhou et al., 2014; Zou et al., 2009). Crucially putative OSCs did not express oocyte associated genes (*Gdf9/GDF9*, *Zp3/ZP3* and *Nobox/NOBOX*) (White et al., 2012), suggesting that these cells are a distinct population of germ cells within the ovary. Cells exhibited high telomerase activity and positively stained for alkaline phosphatase staining (Zou et al., 2009), characteristics associated with stem cells, further indicating that these are germline stem cells. Putative OSCs were estimated to constitute approximately 0.014% ± 0.002% cells in murine ovaries (White et al., 2012) and cells expressing GFP under the control of the Oct4 promoter were found to make up 0.05% of the adult murine ovary (Pacchiarotti et al., 2010). Therefore, putative oogonial stem cells appear to be a unique and small population of cells within the adult mammalian ovary, which can be isolated, cultured long term and maintain their characteristics.

In culture, rodent and human putative OSCs rarely differentiated into OLCs with characteristic features of oocytes including large size (60μm), spherical morphology and zona pellucida-like structures (Pacchiarotti et al., 2010; White et al., 2012; Zhou et al., 2014). Gene expression analysis showed that OLCs expressed oocyte-specific genes, including those associated with the zona pellucida (*Gdf9*/*GDF9*, *Zp1*/*ZP1*, *Zp2*/*ZP2* and *Zp3*/*ZP3*). Rodent OLCs derived from OSCs showed the expression of Sycp3 (Pacchiarotti et al., 2010; Zhou et al., 2014), furthermore, human OLCs co-expressed meiotic markers LHX8 and YBX2 with DDX4 (White et al., 2012), suggesting that these cells have initiated meiosis. Ploidy analysis of human OSC cultures showed the presence of haploid cells, illustrating that a population of cells had completed meiosis (White et al., 2012). These results reflect abnormal meiotic progress, as oocytes do not fully reach haploid status *in situ* as meiosis does not resume until fertilisation, when the cell will contain a maternal and paternal set of DNA to form a zygote. The absence of somatic cell support for spontaneous OLC differentiation *in vitro* may explain the abnormalities observed. In some cases OLCs appeared in association with other smaller cells and when cultured with granulosa cells generated follicle-like structures (Pacchiarotti et al., 2010), suggesting that somatic cell support may assist OLC development. The functional potential of *in vitro* derived OLCs to undergo successful fertilisation has not been reported. The meiotic and developmental competence of OLCs derived from OSCs is essential to

determine whether these cells are oocytes. Thus, further research is essential to investigate the full potential of OLCs.

Introduction of fluorescently labelled rodent OSCs into healthy and sterile recipient ovaries resulted in the formation of GFP expressing oocytes identified within GFP negative follicles (White et al., 2012; Zhou et al., 2014; Zou et al., 2009). The introduction of OSCs into chemotherapy ablated ovaries also rescued endogenous early stage oocytes when compared to control chemotherapy ablated ovaries (Zou et al., 2009). These results suggest that putative OSCs can form oocytes within an ovarian niche, but may also indicate a potential function in ovarian repair. GFP positive oocytes were retrieved following superovulation, which were capable of fertilisation and subsequent embryonic development using IVF (White et al., 2012). Furthermore, GFP oocytes contributed to *in vivo* ovulation and achieved successful fertilisation following natural matings (Zhou et al., 2014; Zou et al., 2009), showing their ability to contribute to oogenesis *in vivo*. It has been suggested that the characteristics associated with putative OSCs and their oogenic capabilities are an artefact of *in vitro* culture (Dunlop et al., 2013), however similar gene expression characteristics have been observed in freshly isolated putative OSCs (Imudia et al., 2013), which would suggest that these cells may have these qualities *in situ*.

The use of genetic mouse models has allowed investigations to determine whether putative OSCs contribute to *in vivo* oogenesis. Lineage-tracing using tamoxifen induced YFP expression showed the absence of adjacent YFP and Ddx4 expressing cells in clusters, suggesting that postnatal ovaries do not undergo germ cell divisions (Lei and Spradling, 2013), whereas tamoxifen exposure at E10.5 generated adjacent lineage marked germ cells in the adult ovary as a consequence of mitotic divisions. All YFP and Ddx4 positive cells were found to be oocytes, thus no other germ cells were identified. Tamoxifen exposure by injection into the ovary caused a localised response only labelling a small proportion of cells; given that putative OSCs are thought to make up an extremely small number of cells within the postnatal ovary it is conceivable that putative OSCs were not labelled. An alternative approach, utilised the expression of three reporter fluorescent proteins (RFP, OFP and CFP) under the *Ddx4* promoter, were utilised to identify potential putative OSCs. Culture of ovarian

cells from these mice showed RFP positive cells unable to undergo mitosis (Zhang et al., 2012), however their morphology would indicate that these cells are oocytes, therefore would not be able to undergo mitosis. The authors concluded that no mitotically active germ cells are present in the postnatal murine ovary. This model has great potential and use for investigating putative OSCs however the authors failed to describe cells expressing OFP or CFP and their potential. Given that any of the fluorescent colours could be expressed under the control of *Ddx4*, this appears like an important oversight and could exclude potential putative OSCs from investigation. These results suggest that postnatal mammalian ovaries do not undergo neo-oogenesis and therefore do not possess putative OSCs. This further indicates that the potential of putative OSCs isolated from postnatal mammalian ovaries to develop into oocytes previously described may be a consequence of *in vitro* culture.

Alternative sources for germline progenitor cells were also investigated. The haemapoietic system was indicated as a source for new postnatal germ cell production when bone marrow and/or peripheral blood transplantation rescued oocyte production in sterile mice (Johnson et al., 2005). However, subsequent parabiosis studies which achieved high levels of haematopoietic chimerism, have illustrated in healthy and sterile mice that bone marrow derived cells do not contribute to oocyte production in the postnatal murine ovary (Eggan et al., 2006). Furthermore, investigators failed to test the functional potential of oocytes thought to be derived from haemapoietic cells (Telfer et al., 2005), thus it is unlikely that the haemapoietic system contributes to oogenesis *in vivo*, but may reflect the permissive nature of haemapoietic stem cells.

The evidence suggests that putative mammalian oogonial stem cells can be isolated from postnatal ovaries and following *in vitro* culture and introduction into an appropriate ovarian niche can undergo oogenesis to form oocytes capable of fertilisation, embryonic development (White et al., 2012) and can produce healthy fertile offspring (Zhou et al., 2014; Zou et al., 2009). However, the physiological contribution of these cells is yet to be determined. Current evidence using genetic models (Zhang et al., 2012), lineage tracing (Lei and Spradling, 2013), follicular counts (Johnson et al., 2004; Kerr et al., 2006) and cell depth analysis (Reizel et al.,

2012) is contradictory. Thus, it is difficult to interpret the role, if any, of putative oogonial stem cells *in vivo* and further investigations are essential to elucidate their potential.

1.4.2 Controversy surrounding the existence of oogonial stem cells in mammalian ovaries

Several groups have reported the isolation of putative OSCs from adult mammalian ovaries (Imudia et al., 2013; Park et al., 2013; White et al., 2012; Zhou et al., 2014; Zou et al., 2009). Following *in vitro* culture these cells have demonstrated the potential to generate new oocytes that are meiotically and developmentally competent and have resulted in healthy fertile offspring (Zhou et al., 2014; Zou et al., 2009). However, controversy surrounding the existence of mammalian oogonial stem cells and their oogenic capacity continues.

It has been suggested that the ability of these cells to undergo successful oogenesis is acquired as a consequence of *in vitro* culture (Dunlop et al., 2013). Pluripotency maintenance factors, such as LIF (leukaemia inhibitory factor, reviewed by Onishi and Zandstra (2015)) can be added to cell cultures to ensure pluripotent cells maintain their phenotype and have been utilised in putative OSC cultures. The effect of *in vitro* culture on putative OSCs has not been elucidated, furthermore, the *in vivo* potential of putative OSCs has not been determined. Thus, it is currently unclear whether putative OSCs are artificially transformed *in vitro*, causing changes that enable oogenesis, however gene expression analysis of freshly isolated murine OSCs shared similar expression patterns to those in culture, suggesting maintenance of cell characteristics rather than alteration (Niikura et al., 2009).

Putative OSCs have been isolated from adult mammalian ovaries based on the cell surface expression of Ddx4/DDX4 or Ifitm3 (White et al., 2012; Zhou et al., 2014; Zou et al., 2009). Ifitm3 is a transmembrane cell surface protein associated with a role in the immune system. In contrast Ddx4 is a germ cell associated RNA helicase, with a cytoplasmic location. Therefore, its use as a cell-surface epitope to isolate putative OSCs has been controversial. Computational analysis has generated conflicting data regarding the possibility of a transmembrane variant of Ddx4 with data for (White et al., 2012; Zou et al., 2009) and against this theory (Zarate-Garcia

et al., 2016). Isolation of viable putative oogonial stem cells relies on their identification using a C-terminus antibody. The use of a N-terminus antibody failed to yield cells, however could recognise putative OSCs once permeablised (White et al., 2012). Cell surface expression of Ddx4 has also been identified in a population of cells within the adult pig testes (Kakiuchi et al., 2014). Furthermore, Ddx4 cell surface expression can be induced in cell populations following plasmid transfection (Kakiuchi et al., 2014). These results suggest that Ddx4 is capable of cell-surface expression and that the use of a C-terminus antibody confounds specificity to this variant. However, it has also been suggested that antibody cross-reactivity may underlie the results observed and the antibody does not identify true Ddx4 cell surface expression (Hernandez et al., 2015).

The ovarian quiescence observed after the menopause is based upon the depletion of ovarian follicles, resulting in age related infertility. However, the presence of putative oogonial stem cells in adult mammalian ovaries and the suggestion that these cells can contribute to oogenesis in postnatal life reignites the question of how the menopause can occur. Should neo-oogenesis occur in the mammalian ovary, how does the ovary deplete its stocks of follicles? This question has been a primary argument against the existence of putative mammalian oogonial stem cells (Horan and Williams, 2017). Stem cells are a specialised cell with the capabilities of self-renewal and differentiation, these abilities are maintained by the stem cell niche. Elimination of the stem cell niche causes differentiation of all female germline stem cells in the ovary of *C.elegans* (Kimble and White, 1981). Furthermore, displacement of FGSCs from the stem cell niche causes the initiation of oogenesis in lower vertebrate and invertebrate species (Lin, 1997). These results illustrate that the stem cell niche plays an essential role in determining cell fate. Thus, should OSCs contribute to oogenesis in the adult mammalian ovary, failure of their niche may ultimately result in the depletion of ovarian follicles. Transplantation of aged murine ovaries into young recipients caused an increase in the number of follicles observed in the aged tissue, suggesting that systemic factors may play a role in maintaining ovarian function (Niikura et al., 2009). In addition, parabiosis of old and young mice showed comparable numbers of immature follicles in ovaries of both age groups, in contrast young ovaries xeno-grafted into aged recipients showed a 50% reduction in

immature follicles when compared with those xeno-grafted into young hosts (Niikura et al., 2009). These results indicate that age-related systemic changes may affect the potential physiological role of putative OSCs in the mammalian ovary.

Oogonial stem cells are a recent discovery in ovarian biology, and significant questions regarding their existence and physiological role remain to be answered. However, they provide an interesting avenue for further research in ovarian biology, oogenesis and have the potential for major clinical applications in reproductive technologies, thus should be investigated in greater detail.

1.5 Artificial gametogenesis

The process of mammalian oogenesis *in vivo* is a tightly regulated process requiring the transient switching on and off, of regulatory genes and molecular processes. Due to the difficult nature of studying oogenesis in the developing embryo, our knowledge of the underlying mechanisms is limited. Replication of oogenesis *in vitro* from precursor cells would provide insights into the basic biology of oogenesis, folliculogenesis and meiosis. This avenue of research may also offer potential for new artificial reproductive technologies (ART), where there is increasing demand for novel therapies involving the generation of artificial gametes for same sex couples and patients lacking functional germ cells (Hendriks et al., 2016).

Stem cells are undifferentiated or differentiation limited, self-renewing cells within a distinct niche. These cells are responsible for renewal and regeneration within tissues with the potential to generate different daughter cell types. Pluripotent stem cells have the capacity to differentiate into all the cells of the developing mammalian embryo, thus have the potential to generate germ cells. In tetraploid complementation assays embryonic stem cells (ESCs) and induced pluripotent stem cells (iPSCs) have both successfully contributed to the germ cell lineage, illustrating their ability to successfully undergo gametogenesis (Boland et al., 2009; Zhao et al., 2010).

1.5.1 Oogenesis using embryonic stem cells (ESCs)

Embryonic stem cells are pluripotent stem cells derived from the inner cell mass of a developing blastocyst (Evans and Kaufman, 1981). They have successfully been cultured *in vitro* where they have shown the ability to differentiate into numerous cell types, including hematopoietic, endothelial, muscle and neuronal cells (Keller, 1995). Thus, ESCs are candidate progenitor cells for *in vitro* artificial oogenesis.

In the absence of feeder cells and leukaemia inhibitory factor (LIF), a growth factor known to facilitate the maintenance of pluripotency *in vitro* (Onishi and Zandstra, 2015), murine embryonic stem cells (mESCs) appear to initiate germ cell differentiation (Hubner et al., 2003; Lacham-Kaplan et al., 2006; Novak et al., 2006; Qing et al., 2007; Salvador et al., 2008). mESCs formed large colonies resembling germ cell clusters (Novak et al., 2006) or embryoid bodies (Lacham-Kaplan et al.,

2006; Qing et al., 2007; Salvador et al., 2008), when removed from a pluripotency maintaining environment. These structures expressed germ cell associated genes including *Oct4*, *Ddx4*, *cKit*, *Dppa3* and *Dazl* (Hubner et al., 2003; Lacham-Kaplan et al., 2006; Novak et al., 2006; Qing et al., 2007; Salvador et al., 2008), suggesting the active differentiation of mESCs into germ cells under these circumstances.

OCT4 expression is associated with pluripotency in stem cells, however in the developing embryo, OCT4 expression becomes restricted to the germ line. Germ cell specific *Oct4-GFP* was expressed in 25% and 40% of mESCs after 7 and 8 days in feeder free and LIF free culture to induce differentiation, respectively (Hubner et al., 2003), illustrating their entry into germ cell lineage. *c-Kit* expression, associated with migratory primordial germ cells was also reported in a subpopulation of these (Hubner et al., 2003), and had been observed as early as 48 hours after the initiation of differentiation (Lacham-Kaplan et al., 2006). *Ddx4* expression is switched on in post-migratory germ cells and its expression continues throughout oogenesis and has been identified in differentiating mESCs (Hubner et al., 2003; Lacham-Kaplan et al., 2006). During differentiation of mESCs, using these germ cell markers (*Oct4*, *c-Kit* and *Ddx4*), 3 populations of germ cells were identified associated with various stages of germ cell development (pre-/migratory primordial germ cells, early post-migratory germ cells and post-migratory germ cells prior to meiotic prophase 1) (Hubner et al., 2003). Meiotic markers (Dmc1 and Sycp3), were absent from these cells, illustrating their pre-meiotic status. Further culture of cell aggregates produced follicle-like structures, with large central cells (>40μm), resembling oocytes, and were GFP positive in accordance with *Oct4* re-expression in meiotically arrested oocytes (Hubner et al., 2003).

OLCs derived from mESCs have been described based on morphological characteristics (large spherical cells) and expression of oocyte-specific genes (*Gdf9*, *Zp1*, *Zp2* and *Zp3*) (Hubner et al., 2003; Lacham-Kaplan et al., 2006; Novak et al., 2006; Qing et al., 2007; Salvador et al., 2008). Zona pellucida genes were often expressed in OLCs, but zona pellucida structures were frequently absent from the surface of these cells (Lacham-Kaplan et al., 2006; Qing et al., 2007), and where present (Hubner et al., 2003; Salvador et al., 2008) were often fragile, believed to be

due to the failed expression of one or more zona pellucid proteins (Hubner et al., 2003). Furthermore, the expression of meiotic marker SYCP3 was reported in OLCs (Hubner et al., 2003; Novak et al., 2006), suggesting entry in meiosis. However, investigations into the meiotic potential of OLCs derived from murine ESCs have produced conflicting results. Observations of polar body-like structures further indicates entry into and progression through meiosis of OLCs (Hubner et al., 2003; Salvador et al., 2008). In contrast, fluorescent in situ hybridisation (FISH) of OLCs detected 2 signals for murine chromosome 1 which did not co-localise with Sycp3 signal (Novak et al., 2006). This observation suggests that despite Sycp3 expression, ESC derived OLCs have failed to enter meiosis. This was further supported by a lack of expression of other meiotic associated proteins (including Sycp1, Sycp2, Rec8, Stag3 and Smc1-β) in OLCs (Novak et al., 2006).

During *in vivo* oogenesis, cells transition through several different described cell stages including epiblast cells, primordial germ cells and oogonia from undifferentiated embryonic stem cells, prior to the formation of oocytes. *In situ* these processes are regulated and mediated by the surrounding somatic cells (Wear et al., 2016). The spontaneous differentiation of mESCs reported in the absence of feeder cells and pluripotency maintenance factors did not consistently appear to replicate the transition of cells through each stage of germ cell differentiation. eGFP expression under the regulation of *Gdf9* was detected in large spherical cells within 24 hours of mESC differentiation culture (Salvador et al., 2008). This rapid differentiation of pluripotent stem cells to germ cells *in vitro* may reflect abnormalities in germ cell differentiation in the absence of the appropriate somatic cell support. OLC formation was often reported in conjunction with the presence of follicle-like structures (Hubner et al., 2003; Lacham-Kaplan et al., 2006; Novak et al., 2006), suggesting that somatic cells co-differentiate from pluripotent cells to support germ cell differentiation. Co-culture of differentiating mESCs with neonatal ovarian granulosa cells generated follicle-like structures, with OLCs expressing oocyte associated genes (*Gdf9*, *Figα*, *Zp1*, *Zp2* and *Zp3*) derived from mESCs. In contrast, culture with granulosa cell conditioned medium showed no expression of oocyte associated genes (Qing et al., 2007), suggesting that cell-cell interactions are also important in this process.

Taken together these results suggest that while mESCs appear to initiate differentiation into cells similar to oocytes *in vitro*, these cells do not have the capacity of fully functional oocytes and may reflect abnormal germ cell formation under these conditions. They also indicate that somatic cells are a necessary component for successful germ cell differentiation. Tighter regulation of this process and step-wise co-ordination of the differentiation of pluripotent stem cells may produce functional artificial gametes.

Reconstitution of the mouse germ cell specification pathway *in vitro* via extrinsic manipulation using growth factors to activate cellular pathways in pluripotent stem cells to initiate germ cell differentiation in a step wise manner may better replicate the process of oogenesis. Primordial germ cells are derived from the epiblast cells of the developing embryo. A cocktail of supplements, consisting of Activin A, bFGF and knockout serum replacement (KSR), has been shown to support the differentiation of male and female murine embryonic stem cells into cells resembling epiblasts (Hayashi et al., 2012; Hayashi et al., 2011; Hayashi and Saitou, 2013). These cells shared morphological features and genetic characteristics with epiblasts, demonstrated by the downregulation of genes associated with ESCs (e.g. *Prdm14*) and upregulation of genes associated with epiblast cells (e.g. *Wnt3*, *Fgf5* and *Dnmt3b*) (Hayashi et al., 2012; Hayashi et al., 2011; Hayashi and Saitou, 2013). Furthermore, genes associated with cells of the endoderm were downregulated (*Gata4*, *Gata6* and *Sox17*) (Hayashi et al., 2012; Hayashi et al., 2011; Hayashi and Saitou, 2013). These cells were subsequently termed epiblast-like cells (EpiLCs).

BMP4 is known to co-ordinate PGC differentiation from epiblasts *in vivo* (Lawson et al., 1999), and in response to Bmp4, floating EpiLCs differentiated into primordial germ cell-like cells (PGCLCs) expressing *Prdm1*, *Dppa3* and *Nanos3* (Hayashi et al., 2012; Hayashi et al., 2011; Hayashi and Saitou, 2013). BMP4 has also induced a primordial germ cell-like phenotype in ESCs in a dose dependent manner, which could be inhibited by NOGGIN, a Bmp4 antagonist (Wei et al., 2008). These results could be replicated by addition of Wnt3A, a mesoderm promoting factor (Wei et al., 2008) and provide evidence to suggest that extrinsic factors are pivotal to facilitate derivation of PGCs *in vitro*.

To test the ability of PGCLCs to generate functional oocytes, XX PGCLCs were FACS isolated based on the cell surface expression of Ssea-1 and Integrin-β3 and subsequently aggregated with fetal (E12.5) ovarian somatic cells to form reconstituted ovaries (Hayashi et al., 2012; Hayashi and Saitou, 2013). PGCLCs within cultured reconstituted ovaries showed imprinting patterns and X chromosome activation similar to PGCs in E12.5 murine ovaries, suggesting that PGCLCs have calibrated with the ovarian somatic cell environment, to coordinate their development appropriately with the surrounding soma. Sycp3 staining suggested that PGCLCs in cultured reconstituted ovaries were in the zygotene stage of meiotic prophase 1, indicating their potential meiotic capacity (Hayashi et al., 2012; Hayashi and Saitou, 2013). However, no further development was reported *in vitro*. In contrast, xeno-transplanted reconstituted ovaries contained multi-laminar follicles containing PGCLC derived OLCs. Oocytes retrieved from reconstituted ovaries could successfully undergo fertilisation and embryo transfer to foster mothers resulted in the birth of live healthy offspring (Hayashi et al., 2012; Hayashi and Saitou, 2013). However, abnormalities were observed in oocytes derived from PGCLCs at an increased rate compared to wild type oocytes. These abnormalities included increased proportion of denuded oocytes upon retrieval and oocytes with elliptical shape. Approximately half of zygotes derived from PGCLC oocytes also exhibited 3 pro-nuclei following fertilisation, speculated to be as a result of failure to extrude a 2nd polar body (Hayashi et al., 2012). Thus, while functional oocytes can be derived from murine embryonic stem cells, these results also suggest that the process of ESC differentiation into oocytes has not fully recapitulated *in vivo* processes resulting in a proportion of abnormal oocytes. Furthermore, the use of an *in vivo* model to support the differentiation of ESCs beyond the PGCLC stage provides little insight into the mechanisms and processes required to facilitate oogenesis, but does reveal that the somatic cells are pivotal in facilitating this process.

Functional oocytes have not been differentiated from embryonic stem cells of any other species to date, however, oocyte-like cells have been reported in buffalo ESCs and human ESCs (Aflatoonian et al., 2009; Shah et al., 2015; Xuemei et al., 2013).

Genes associated with primordial germ cell formation (*DAZL*, *VASA* and *PLZF*) meiosis (*SYCP3*, *MLH1*, *TNP1/2* and *PRM2*) and oocytes (*GDF9*, *ZP2* and *ZP3*) were observed in buffalo EBs derived from ESCs (Shah et al., 2015), and a similar pattern of protein expression was also observed. The expression of these markers was facilitated by the addition of BMP4 to cultures, which has previously been implicated in PGC formation during fetal development (Lawson et al., 1999) and could be inhibited by NOGGIN, a BMP4 antagonist. Thus suggesting that BMP4 promotes the differentiation of buffalo ESCs into germ cells. Large (30-50μm) oocyte-like cells were observed in cultures which stained positive for the presence of a zona pellucida. These cells appeared to extrude a polar body during semi-attached development and appeared to undergo parthenogenetic activation to form structures resembling 2-cell, 4-cell and 8-cell embryos during attached development (Shah et al., 2015). These results have not investigated the potential of buffalo OLCs to undergo successful fertilisation but do show evidence of the cells developmental ability through parthenogenetic activation, however this paper has since been retracted due to concerns over control images.

Embryoid bodies derived in non-adherent human ESC cultures, showed an increase in germ cell marker expression, including *C-KIT*, *VASA* and *DAZL* (Aflatoonian et al., 2009; Xuemei et al., 2013). This was observed in conjunction with a decrease in expression of pluripotency associated genes (*OCT4* and *SSEA3*). Retinoic acid (RA), a metabolite of vitamin A, has been shown to be a determining regulator in germ cell specification in the developing ovary (Bowles et al., 2006). When added to human embryoid body cultures, RA caused an increase in germ cell marker expression (Aflatoonian et al., 2009; Xuemei et al., 2013), suggesting that RA may promote the initiation of germ cell development in an artificial environment. Co-culture of hESCs with human fetal gonadal cells increased the proportion of induced-primordial germ cells, marked by the enrichment of *PRMD1*, *DPPA3* and *DAZL*, which could be isolated by the cell-surface co-expression of SSEA-1/KIT/VASA (Park et al., 2009). These results suggest that extrinsic factors provided by the fetal gonadal somatic environment may be required to propagate germ cell differentiation *in vitro*. Work on murine ESCs showed that PGCLCs could be identified and isolated from EBs using FACS based on cell surface expression of Ssea-1 and c-Kit (Hayashi et al., 2012).

Using similar protocols, 0.5-1% of cells in human embryoid bodies were positive for both markers, suggesting that these cells were human PGCLCs (Aflatoonian et al., 2009). Further culture of these cells resulted in large cells with morphological resemblance to oocytes, however immunohistochemical analysis was not possible on these cells, thus it is difficult to ascertain whether these oocyte-like cells also exhibit other features associated with oocytes. However, gene expression analysis of differentiating hESCs showed expression of oocyte specific markers (*GDF9* and *ZP1*) and meiotic markers (*SYCP3*) (Aflatoonian et al., 2009; Xuemei et al., 2013). These results show that oocyte-like cells, determined by morphological assessment and gene expression analysis, have been generated from human embryonic stem cells. However, full analysis of human OLCs is yet to be undertaken. It is unclear whether these cells possess other features of oocytes, such as an intact zona pellucida, and the meiotic and developmental competence of these cells has not been established. To fully explore the potential of these cells would require investigations into the ability of human OLCs to achieve fertilisation and subsequent embryonic development. The creation and destruction of viable human embryos to generate artificial oocytes, raises prominent ethical questions. Somatic-cell nuclear transfer of ESCs would provide infertile individuals with genetic gametes however do not circumvent the ethical issues surrounding the use of ESCs. Thus, alternative cell sources should be used to investigate artificial oogenesis.

1.5.2 Oogenesis using reprogrammed cells (e.g. induced pluripotent stem cells; iPSCs)

Differentiated cells can regain pluripotency under the expression of 4 crucial pluripotency associated genes Oct3/4, Klf4, Sox2 and c-Myc. Induced pluripotent stem cells (iPSCs) have been generated in rodents and humans (Takahashi et al., 2007; Takahashi and Yamanaka, 2006). iPSCs do not raise the same ethical concerns as ESCs and may provide a better clinical precursor cell for artificial gametogenesis. In tetraploid complementation assays murine iPSCs have demonstrated their potential to generate functional germ cells (Boland et al., 2009; Zhao et al., 2010).

Murine iPSCs could be induced to generate EpiLCs and PGCLCs *in vitro* using methods previously employed for ESCs (Hayashi et al., 2012; Hayashi et al., 2011;

Hayashi and Saitou, 2013). When introduced into an ovarian niche iPSC derived PGCLCs formed OLCs *in vitro* and functional oocytes capable of fertilisation to produce healthy offspring when reconstituted ovaries were transplanted *in vivo* (Hayashi et al., 2012; Hayashi et al., 2011; Hayashi and Saitou, 2013). These results suggest that like ESCs, iPSCs can function to produce meiotically and developmentally competent oocytes.

Less success has been achieved with human iPSCs. Co-culture with human fetal gonadal stromal cells caused the induction of primordial germ cell-like cell fate in XY human iPSCs (Park et al., 2009). Induced primordial germ cells from human iPSCs were identified based upon the combined expression of cell surface markers SSEA-1/KIT/VASA, characteristic markers of primordial germ cells. These results indicate that germ cell differentiation can be initiated from human iPSCs, although further work into female (XX) iPSCs is still required. Assessment of the epigenetic status of these cells showed abnormal imprinting erasure compared to control PGCs and hESC derived PGCs (Park et al., 2009), suggesting that PGCLCs derived from human iPSCs may be epigenetically compromised. Artificial oocytes or OLCs from human iPSCs have not yet been reported, thus more investigations are required to elucidate whether iPSCs provide an alternative precursor cell to generate oocytes as a method for assisted reproductive technologies. Further knowledge of their epigenetic stability, tumorigenicity and subsequent safety of any future offspring must be well assessed before their use in clinical practice.

The cell plasticity model suggests that cells possess the ability to cross traditional lineage barriers previously defined by the hierarchical stem cell differentiation model (Estrov, 2009). Trans-differentiation (conversion of a differentiated cell of one lineage to a differentiated cell of another lineage without reinstating pluripotency) of somatic cells *in vitro* into germ cells may also provide a pathway to artificial gametogenesis. Murine skin derived stem cells (SDSCs) collected from neonates formed aggregates in culture which contained Ssea-1 positive cells which upon isolation were found to express germ cell associated proteins Dppa3, Dazl and Ddx4, and had imprinting patterns characteristic of PGCs (Sun et al., 2015). Addition of Activin A to cultures caused an increase in expression of genes associated with

epiblasts (*Dnmt3a*, *Dnmt3b* and *Wnt3*) and subsequently caused an increase in PGCLC formation, in a dose-dependent manner (Sun et al., 2015). These results suggest that Activin A promotes PGCLC formation through the formation of EpiLCs which then initiate germ cell differentiation. Murine skin derived stem cells also generated oocyte-like cells following aggregate formation (Dyce et al., 2011). OLCs were large (30-40μm), expressed germ cell (*Oct4*, *Vasa*, and *Dazl*), oocyte-specific (*Gdf9b*, *ZP1* and *ZP2*) and meiosis specific genes (*Scp3* and *Dmc1*) and were coated in a zona pellucida-like structure, suggesting these cells had become oocytes. Transplantation of SDSC aggregates to ovariectomised recipient immune-deficient mice generated oocyte-like cells developing within follicles, including antral follicles (Dyce et al., 2011), further suggesting that skin stem cells can differentiate into new oocytes, however, the fertilisation potential of these new oocyte-like cells was not described. In the presence of follicular fluid, fetal porcine skin stem cells initiated germ cell development (Dyce et al., 2006). Following aggregate formation, OCT4 positive OLCs were observed within cultures surrounded by cells expressing P450 aromatase, suggesting these structures are follicles. OLCs showed parthenogenetic activation and blastocyst-like structures were detected. However, OLCs failed to undergo successful fertilisation following *in vitro* fertilisation (Dyce et al., 2006), suggesting that OLCs generated from skin cells are abnormal.

Human fetal skin derived stem cells have also formed aggregates in culture which have shown increased expression of *DAZL*, *VASA* and *SyCP3* over time. SYCP3 staining was punctate and elongated suggesting that these cells had entered into meiosis (Ge et al., 2015). A small proportion of cells were also found to be haploid by FACS and FISH analysis, suggesting completion of meiosis in these cells. The presence of haploid cells in these cultures suggests abnormal oocyte development as oocytes fail to achieve haploid status *in situ*, as a consequence of meiotic completion following successful fertilisation. The derivation of OLCs from skin derived stem cells in several species suggests that cells from somatic lineages can transdifferentiate into the germ cell lineage, however abnormalities with epigenetic reprogramming and meiosis suggest that the underlying mechanisms coordinating this process are currently insufficient to generate healthy oocytes.

Oocyte-like cells were also identified in rat pancreatic stem cell cultures. These were observed in association with smaller cells forming follicle-like structures. Oocyte-like cells expressed germ cell (OCT4 and VASA), oocyte (GDF9) and meiotic associated proteins (Sycp3 and Dmc1) (Danner et al., 2007). However, no further analysis was conducted on the meiotic potential of these cells to elucidate their germ cell potential.

Human amniotic fluid stem cells have also generated oocyte-like cells following embryoid body formation (Yu et al., 2014) or exposure to follicular fluid (Cheng et al., 2012). These cells expressed oocyte specific genes (*BMP15*, *GDF9* and *ZP2*) and meiotic genes (*SCP3* and *DMC1*) (Cheng et al., 2012; Yu et al., 2014) and were found in association with smaller cells to form follicle-like structures (Yu et al., 2014). Markers of estrogen biosynthesis were detected, suggesting that somatic cells have co-differentiated to support OLCs and these cells have the potential to produce ovarian steroids (Yu et al., 2014). Haploid cells were detected in differentiating amniotic fluid stem cells (Yu et al., 2014) and embryo-like structures were observed, suggesting parthenogenetic activation (Cheng et al., 2012). These results suggest that human amniotic fluid stem cells can generate OLCs *in vitro*, however the evidence suggests that these cells have undergone abnormal differentiation.

Cells of several different lineages and species have shown potential to generate germ cells using both *in vitro* and *in vivo* methodologies. Evidence of successful oogenesis from murine pluripotent cells provides the first indication that gametogenesis can be artificially recapitulated, although this still requires an *in vivo* period. Differentiation using human cells has been limited thus far, and greater understanding of the underlying mechanisms and more extensive analysis into the functionality of human OLCs is necessary prior to their use in a clinical setting. All avenues of research have identified the importance of the ovarian microenvironment, including paracrine factors and cell-cell interactions, as a regulator in germ cell differentiation, such that in many cases, ovarian somatic cells co-differentiate in conjunction with oocyte-like cells from precursor populations. Thus, the application of artificial gametogenesis as a tool to investigate the mechanisms and pathways underlying oogenesis may reveal greater insight into these processes *in vivo*.

1.6 Models and systems used for the study of oogenesis and folliculogenesis

Various models and methodologies have been employed to expand our understanding of ovarian biology and in particular the processes that underlie oogenesis and folliculogenesis. Genetic rodent models have revealed roles for particular factors and signalling pathways in various aspects of folliculogenesis and identified the importance of these in regulating the production of a developmentally and meiotically competent oocyte. The recapitulation of oogenesis and folliculogenesis *in vitro* and *in vivo* allows for the manipulation of these processes to further enhance our understanding of the mammalian ovary.

1.6.1 In vitro follicle culture systems

Ovarian follicles comprise of an oocyte and supporting somatic granulosa cells and theca cells. It is well established that these cell-cell interactions are essential to coordinate oocyte and follicle growth *in vivo*. Thus, successful *in vitro* systems are likely to be able to maintain these interactions. Furthermore, the requirements of growing follicles are complex and change with advancing developmental stages. Various extrinsic factors are required to support growing follicles and alterations in medium content throughout culture, therefore multi-step culture systems have been developed to support the changing requirements of growing follicles (Cortvrindt et al., 1996; Eppig and O'Brien, 1996; Lenie et al., 2004; McLaughlin and Telfer, 2010; O'Brien et al., 2003; Telfer et al., 2008). Multi-step culture systems may utilise one or more culture technique such as whole tissue culture followed by individual follicle culture and will also supplement media appropriately for the follicle requirements.

Two-dimensional (2D) attachment cultures of ovarian tissue and follicles have had success in producing functional oocytes capable of undergoing meiosis and fertilisation (Cortvrindt et al., 1996; Eppig and O'Brien, 1996; Lenie et al., 2004; O'Brien et al., 2003). Within a 2D culture system follicles undergo structural remodelling, with follicle cells flattening out, which allows better oxygenation and nutrient supply to all cells within the structure, although it has been shown that interactions between the oocyte, granulosa cells and theca cells are maintained (Lenie et al., 2004), 2D systems also demonstrate partial expulsion of the oocyte

from the follicle structure as a consequence of basal membrane rupture (Cortvrindt et al., 1996).

In contrast 3D culture techniques maintain tissue architecture, which is particularly important in follicle development. Interference with cell-cell interactions within a follicle has caused disrupted folliculogenesis in mice. Gap junctions between granulosa cells and oocytes are mediated by the expression of connexin 43 and connexin 37 respectively. Elimination of either of these connexins in mice causes aberrant folliculogenesis through disruption of the bidirectional communication between oocyte and granulosa cells (Ackert et al., 2001; Simon et al., 1997). Therefore, use of 3D culture systems may better support folliculogenesis through maintenance of follicle structure.

3D culture techniques to investigate folliculogenesis have utilised whole tissue, suspension or encapsulation methods. Whole ovary tissue and ovarian cortical culture have been utilised to support the activation of primordial follicles *in vitro* (Eppig and O'Brien, 1996; McLaughlin and Telfer, 2010; O'Brien et al., 2003; Telfer et al., 2008), however development beyond pre-antral stages is not supported (O'Brien et al., 2003). Porous membranes have been utilised in whole tissue culture which allow better oxygenation, nutrient supply and waste removal to provide better experimental outcomes (Morgan et al., 2015).

Suspension techniques, such as hanging drops, rotating vessels and low attachment culture plates, promote maintenance of follicle structure in a scaffold free system with direct access to nutrients and factors within the medium. Gentle orbital movements in rotating vessels prevent cell adhesion to the surface of the culture surface. Their use in 3D follicle culture successfully prevented adhesion (Heise et al., 2005; Rowghani et al., 2004), but the rotation rate required to inhibit adhesion appeared to cause follicle degeneration (Rowghani et al., 2004). In contrast, follicles suspended within micro-drops of medium achieved oocytes capable of fertilisation and subsequent embryonic development, demonstrating their meiotic and developmental competence (Bishonga et al., 2001). Inversion of micro-drop cultures, also known as a hanging drop, have successfully maintained individual follicles and further promoted follicle growth and increased estradiol production in comparison to

conventional micro-drop cultures (Wycherley et al., 2004). Metaphase II oocytes have been achieved from hanging drop cultures of murine secondary follicles (Choi et al., 2013) and human spermatogenesis has been supported for up to 14 days in hanging drop cultures (Jorgensen et al., 2014), therefore hanging drop cultures have been successfully used to support gametogenesis *in vitro*.

Encapsulation techniques utilise hydrogels or synthetic polymers to provide a 3D scaffold for tissue culture. They support the transfer of oxygen, nutrients and waste products between the medium and tissue. Hydrogels such as collagen, fibrin and alginate are preferentially used in tissue culture due to their biocompatibility and ability to support dynamic remodelling of growing cells which is essential for follicle growth (Butcher and Nerem, 2004; Eyrich et al., 2007; Heise et al., 2005). Alginate hydrogels have successfully served as a 3D scaffold for individual follicle development (Amorim et al., 2009; Camboni et al., 2013; Hornick et al., 2013) and ovarian tissue in culture (Laronda et al., 2014). Various concentrations of alginate can be utilised to provide either a firmer or less rigid structure dependent on the culture requirements. More rigid alginate hydrogels have been shown to better support early follicle development whereas larger follicles require more flexibility to support dynamic follicle growth (Hornick et al., 2013). However, transfer of larger molecules to encapsulated tissue may be hindered in more concentrated alginate hydrogels (Heise et al., 2005).

Although 3D culture techniques have been utilised successfully to support follicle and oocyte development, tissue necrosis is often associated with long term culture and cell viability has been shown to decrease after 5 days in culture (reviewed by Edmondson et al. (2014)).

1.6.2 Xeno-graft models for follicle growth

Xeno-transplant models eliminate many of the problems associated with *in vitro* culture systems. Through the development of vasculature to transplanted tissue, a constant nutrient supply and waste disposal system is established (Edmondson et al., 2014). The development of immune deficient rodents has provided the opportunity to investigate oogenesis and folliculogenesis of different species *in vivo* (Aubard, 2003). Two locations are most commonly used for ovarian xeno-transplant models,

the kidney and the ovarian bursa. The kidney has previously been used due to its rich vasculature, which facilitates the vascularisation of transplants which is estimated to occur within 48 hours of transplant (Dissen et al., 1994), furthermore its capsule and location within the body protects any transplanted tissue from potential interference. The ovarian bursa has also been used for similar reasons in addition to placing transplanted tissue into a physiologically relevant location.

Ovarian cortical tissue from cats (Gosden et al., 1994), ewes (Gosden et al., 1994), cows (Hernandez-Fonseca et al., 2005), elephants (Gunasena et al., 1998) and humans (Gook et al., 2001; Oktay et al., 1998) amongst other species, has been successfully xeno-grafted to the kidney capsule of immune deficient rodents. The host's hormonal and systemic environments appear to support the initiation of follicle growth and development beyond pre-antral stages. In the absence of a functional hypothalamic-pituitary-gonadal axis, human follicles could not progress past two layers of granulosa cells, however treatment of recipient mice with FSH supported progression to antral development (Oktay et al., 1998). Marmoset ovarian tissue transplanted to nude mice was able to produce estrogen which was capable of inducing alterations within host vaginal cells, observed by vaginal smears (Candy et al., 1995). These results suggest that xeno-grafted ovarian tissues establish a cross-talk with the host tissues. Castrated male mice have also been utilised as recipients for ovarian tissue transplantation. Bovine ovarian tissue initiated follicular growth in male mice despite gender and species differences. Oocytes collected from transplanted bovine ovarian tissue have achieved meiotic and developmental competence to successfully fertilise following IVF (Campos-Junior et al., 2016; Senbon et al., 2005).

Despite species differences between donor tissue and recipient, these appear not to be detrimental to the initiation of follicle growth, subsequent follicle development, and crucially do not inhibit oocyte acquirement of meiotic and developmental competence. These data suggest that xeno-graft models provide an opportunity to study oogenesis and folliculogenesis of any mammalian species within the rodent model, allowing for genetic and chemical manipulation of the tissue environment long term.

1.6.3 Bovine ovarian model

The bovine ovary is of a similar size to the human ovary, is mono-ovulatory and polycyclic, furthermore the length of folliculogenesis and the resulting size of follicles and functional oocytes is similar (Adams and Pierson, 1995). These similarities between human and bovine ovaries has indicated that the bovine ovary is a good model for the human ovary and human folliculogenesis (Adams and Pierson, 1995; Campbell et al., 2003; Yapura et al., 2011). Human tissue is often scarce and difficult to source, this is particularly prevalent with ovarian tissue, which is often collected from patients undergoing hysterectomy, gender reassignment surgery or cancer treatment, meaning the tissue may be compromised in some way, for example exposure to hormone treatment for gender reassignment. Although a number of research groups now collect ovarian tissue from women undergoing caesarean section surgery, this tissue is also uniquely representative of the ovary during pregnancy rather than at any other physiological state. In contrast, bovine ovarian tissue can be easily collected as a waste product of agricultural enterprise and is reflective of a young, healthy population. Several groups, including our own have utilised bovine ovarian tissue as a model for the human ovary, therefore the use of bovine ovarian tissue as a source of mammalian oogonial stem cells may provide insight into the source and potential of human oogonial stem cells.

1.7 Hypothesis and aims

A population of primordial follicles are established just prior to or shortly after birth in the mammalian ovary, which has been believed to be fixed and as such determined the reproductive life span of an individual. However, a population of putative oogonial stem cells (OSCs) have now been identified in adult mammalian ovaries of several species including rodents and humans. Putative OSCs appear to have undergone oogenesis following isolation from adult ovaries to generate oocyte-like cells (OLCs). Furthermore, rodent OSCs have contributed to the population of ovulatory oocytes and have successfully generated live offspring.

Hypothesis

Putative oogonial stem cells can be isolated from adult bovine ovarian tissue and when combined with somatic cell support can undergo neo-oogenesis and folliculogenesis in a re-aggregation model both *in vitro* and *in vivo*.

Aims

- To isolate, characterise and label bovine oogonial stem cells from adult ovarian cortical tissue.
- To investigate the ability of bovine OSCs to undergo neo-oogenesis and folliculogenesis when combined with somatic cell support both *in vivo* and *in vitro*.
    - To develop an *in vitro* ovarian aggregation culture model to support bOSC differentiation and folliculogenesis.
    - To utilise a xeno-transplant model to examine the oogenic potential of bOSCs when combined with ovarian somatic cells from the same species and other species *in vivo*.

2 General Materials and Methods

2.1 Bovine Tissue

2.1.1 Tissue collection

Adult bovine ovaries were collected by John Binnie from the local abattoir (Longleys Farm, Bridge of Allan, Stirling, FK9 4NE) and transferred at 33-38ºC to the laboratory in HEPES-buffered M199 medium (Life Technologies) supplemented with amphotericin B (2.5µg/ml; Life Technologies), pyruvic acid (25µg/ml), penicillin G (75µg/ml) and streptomycin sulphate (50µg/ml; all chemicals from Sigma-Aldrich). The ovaries were rinsed in 70% ethanol and dissected under laminar flow conditions with a sterile scalpel blade. Fine cortical strips were dissected from the ovaries and placed in holding medium (Leibovitz medium, Life Technologies) supplemented with sodium pyruvate (2mM), glutamine (2mM; both obtained from Life Technologies), BSA (Fraction V, 3mg/ml), penicillin G (75µg/ml) and streptomycin (50µg/ml; All chemicals from Sigma-Aldrich). Tissue pieces were then examined under light microscopy and any damaged, haemorrhaged or excess stromal tissue was excised, prior to further use.

2.1.2 Tissue vitrification

After dissection bovine cortical ovarian fragments were prepared for vitrification as described by Kagawa et al. (2009), with slight modification. The bovine cortical ovarian fragments were initially equilibrated in vitrification medium 1 (Section 2.12) at room temperature for 25 minutes followed by a 15 minutes equilibration in vitrification medium 2 (Section 2.12). The fragments were then placed onto 30mmx0.25mm acupuncture needles (AcuMedic) and submerged in liquid nitrogen. Frozen ovarian cortical strips were transferred to a cryovial (Greiner Bio-one) and placed into a liquid nitrogen tank for long term storage.

2.1.3 Tissue thawing

Prior to use, bovine ovarian cortical tissue fragments were thawed as described by Kagawa et al. (2009). Briefly, ovarian fragments were placed in pre-warmed thaw medium 1 (Section 2.12) for 1 minute followed by a 5 minute incubation in thaw

medium 2 (Section 2.12) at 37ºC. Tissue was then washed twice in holding medium (Section 2.12) for 10 minutes at 37ºC.

2.2 Isolation of bOSCs using fluorescently activated cell sorting (FACS)

Bovine oogonial stem cells were isolated from adult bovine ovarian cortex based upon the expression of germ cell marker DDX4 (Dead-box helicase 4) as described by White et al. (2012) with slight modification (illustrated in Figure 2.1).

2.2.1 Digestion of ovarian tissue

Adult bovine ovarian cortical tissue previously collected from the local abattoir (section 2.1.1) and stored (section 2.1.2), was thawed as described in section 2.1.3. Tissue was then cut into pieces approximately 2x2x1mm in size with sterile scalpels (Swan-Morton) and transferred to sterile gentleMACS C-tubes (Miltenyi Biotec Ltd) with 3ml of pre-warmed collagenase/DNAse solution (600 Units/ml of collagenase type IV and 1 μg/ml DNAse, both supplied by Sigma-Aldrich, in Hanks balanced salt solution (HBSS) without calcium and magnesium, Life Technologies). Tissue was then dissociated using a gentleMACS dissociator (Miltenyi Biotec Ltd) using 3 pre-set programs (1-H_tumor_01.01, 1-H_tumor_02.01 and 1-H_tumor_03.01) with 20 minute incubations placed in a MACSmic Tube Rotator (Miltenyi Biotech Ltd) at 37ºC with humidified air and 5% CO_2 between programs. Once completed, tissue was gently pipetted up and down with a sterile 5ml borocilicate glass pipette (Corning Incorporated) until the majority of tissue was dispersed and filtered through a 100μM cell filter (Sysmex Partec) into a 15ml falcon tube (Corning Incorporated), the filtrate was then made up to 10ml with pre-warmed HBSS and centrifuged at 300RCF for 5minutes. The supernatant was discarded and the cell pellet was gently re-suspended in a total of 10ml pre-warmed HBSS and centrifuged at 300RCF for 5minutes before non-specific blocking (section 2.2.2).

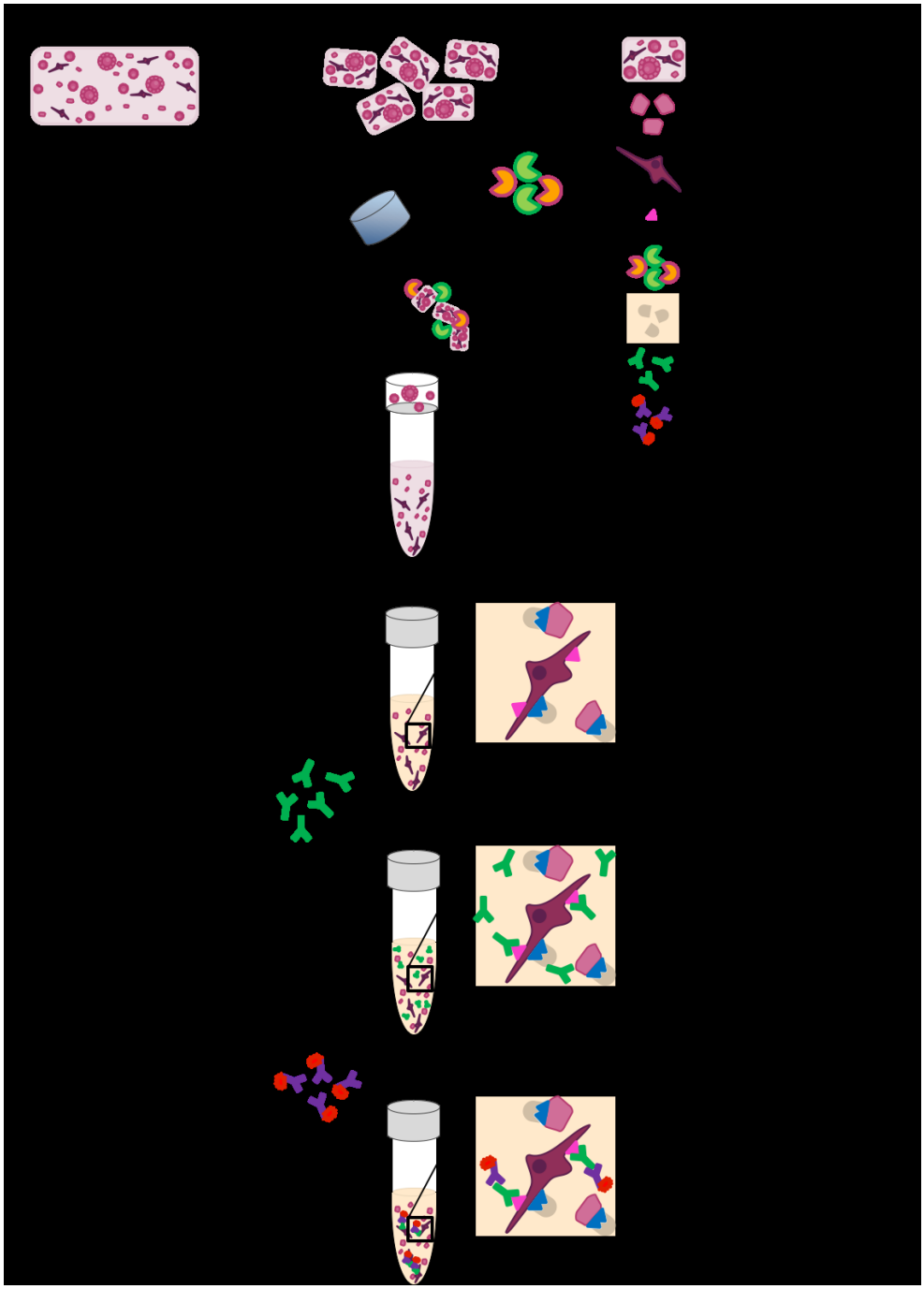

Figure 2.1: A diagrammatic representation of the preparation of bovine tissue for FACS isolation of bOSCs. Adult bovine ovarian cortex was manually dissected into pieces approximately 1x1x2mm in size then enzymatically digested using collagenase IV and DNAse. Following digestion, the disaggregated tissue was filtered through 100uM cell filter to remove large cells and undigested tissue to create a single cell suspension. To prevent non-specific binding of the secondary antibody, a blocking serum was applied to the single cell suspension prior to primary antibody exposure. An anti-DDX4 antibody was used to identify bOSCs in the cell suspension, an APC conjugated goat anti-rabbit secondary antibody was then utilised to amplify this signal.

2.2.2 Non-specific blocking

To prevent non-specific binding of the secondary antibody tissue was blocked with FACS blocking solution (2% goat serum and 2% bovine serum albumin (Sigma-Aldrich) in HBSS without calcium and magnesium) for 20minutes on ice. To establish the parameters of the cell sorting the appropriate negative controls were utilised. 10% of the sample was used as a negative control (primary and secondary antibody omitted) and remained on ice until section 2.2.5, and a further 10% of the sample was used as a secondary antibody only control (primary antibody omitted) and remained on ice until section 2.2.4, see Figure 2.2. The remaining sample was exposed to the primary antibody (section 2.2.3) and utilised for the isolation of bOSCS.

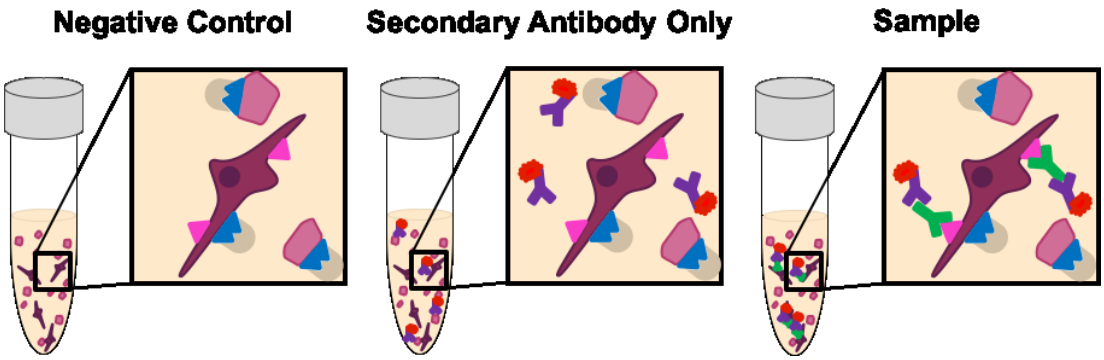

Figure 2.2: Diagram of controls and samples used in FACS to isolate bOSCs. Two controls were used to develop gating strategies to isolate bOSCs using FACS, a negative control (left hand panel) with both primary and secondary antibodies omitted, and a secondary antibody only control (centre panel) with only the primary antibody was omitted. The sample (right hand panel) was exposed to both primary and secondary antibodies to identify bOSCs within adult bovine ovary.

2.2.3 Primary Antibody

After non-specific blocking the sample was made up to 10ml with chilled (4ºC) HBSS and centrifuged at 300RCF. The supernatant was then discarded and the sample was re-suspended in a total of 100µL of Rabbit anti-DDX4 (Abcam, ab13840) diluted 1:10 in FACS blocking solution (as described in section 2.2.2) for 20 minutes on ice. The sample was then washed with 10ml chilled HBSS and centrifuged at 300RCF for 5 minutes. The supernatant was discarded and the sample washed again.

2.2.4 Secondary Antibody

The sample and secondary antibody only control were both washed in chilled HBSS, centrifuged at 300RCF for 5 minutes. The supernatants were then discarded and both samples were re-suspended in a total of 250μL of Goat anti-rabbit IgG conjugated to allophycocynan (APC; Stratech Scientific Limited, 111-136-144-JIR) diluted 1:250 in FACS blocking solution (as described in section 2.2.2) for 20 minutes on ice. The samples were then washed in 10ml chilled HBSS and centrifuged at 300RCF for 5minutes. The supernatants were discarded and the sample and secondary antibody only control washed again.

2.2.5 Fluorescently activated cell sorting

All samples (see Figure 2.2) were washed in 10ml chilled HBSS and centrifuged at 300RCF for 5minutes. The supernatants were discarded and the sample and both controls were re-suspended in 500μL FACS buffer (50μL of FBS in 5ml HBSS). Fluorescently activated cell sorting (FACS) was carried out on a BD FACS Aria II at the Queens Medical Research Institute Flow Cytometry Facility and was conducted by a cytometry specialist, Will Ramsey. Both the negative and secondary antibody only control +/- DAPI (1:1000 dilution, (Sigma-Aldrich), to assess cell viability) were used to determine the gates used, illustrated in Figure 2.2 and Figure 2.3. Cells identified as viable and DDX4 positive were isolated and sorted into OSC media (section 2.12) for propagation in culture (section 2.6.1.1)

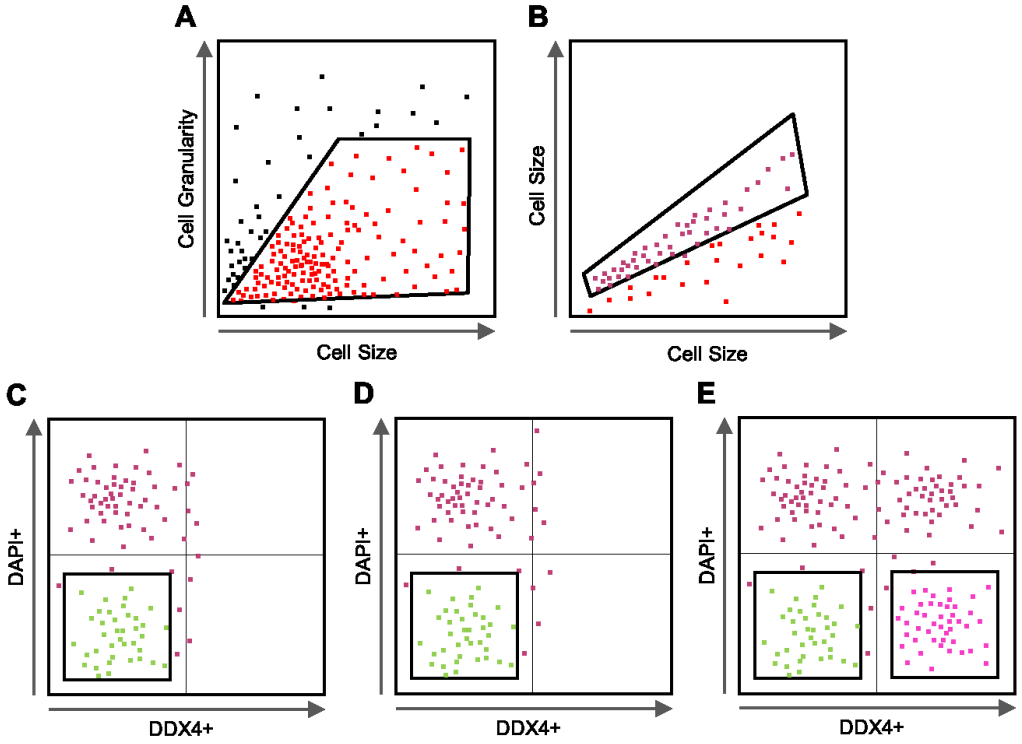

Figure 2.3: FACS gating strategy developed to isolate bOSCs. (A) All events detected by FACS are represented by dots and are initially sorted based on the cell granularity and size, events determined to be cells based on this criteria, are represented in red and then sorted based entirely on size **(B)** to identify single cells shown in purple. **(C, D, E)** Single cells were assessed for viability based on DAPI uptake and DDX4 expression based on APC detection. Cells that appear above the horizontal dotted line on the plots show DAPI uptake and are non-viable, cells to the right of the vertical dotted line show APC expression thus are DDX4 positive. **(C)** Negative control sample, shows viable (green) and non-viable cells all DDX4 negative. **(D)** Secondary antibody only control, illustrates viable (green) and non-viable cells, DDX4 negative, several cells also appear slightly DDX4 positive and these represent background staining and are used to determine collection gates for DDX4 positive cells in the sample to eliminate false positives. **(E)** Sample, illustrates non-viable DDX4 negative and positive cells (purple) and viable DDX4 negative cells (green) and viable DDX4 positive cells (pink). Examples of sorting gates are shown as black outlines on each of the panels and represent the parameters of the gating strategy.

2.3 Derivation of fetal bovine ovarian somatic cells

Fetal bovine ovaries (gestational age 163.5 days) were received from the local abattoir as described in section 2.1.1. Each ovary was placed in a sterile dimple slide with 50µL of Collagenase type IV (10mg/ml in HBSS; Sigma-Aldrich) and pulled apart with 19 gauge needles (Becton Dickenson). Tissue and collagenase mix from

both ovaries were transferred to a 1.5ml tube (Eppendorf UK Ltd) with an additional 400µl of collagenase solution and placed in a thermomixer (Eppendorf UK Ltd) at 37ºC, shaking at 1000rpm for 10 minutes. 50µl of DNAse I (7mg/ml in HBSS, Sigma-Aldrich) was added to the tissue mix and returned to the thermomixer for a further 5minutes shaking at 37ºC. The cell suspension was then centrifuged at 600g for 5minutes and the cell pellet was washed twice with 1ml of HBSS. The cell pellet was then re-suspended in fetal ovarian somatic cell media (section 2.12) and filtered through a 70µm filter (Becton Dickenson), centrifuged at 600g and re-suspended in 1ml media. The cells were split between an appropriate number of wells in a 12 well plate and the volume of each well made up to 1ml with fetal somatic cell media.

The following day, cells were washed twice with pre-warmed PBS (Life Technologies) and new fetal somatic cell media was added (section 2.12). Cells were maintained as described in section 2.6.1.2.

2.4 Murine Tissue

2.4.1 Tissue collection

Neonatal (CD-1, B6SJLF1 or B6;129-Gt(ROSA)26) female mice (postnatal day 0 - 5) were culled by cervical dislocation and ovaries collected for fixation (see section 2.8.1) or disaggregation (see section 2.5.1).

Immune deficient mice (C.B-17/IcrHan Hsd-Prkdc scid), recipients of ovarian aggregates (section 2.5.4) xenotransplanted to the kidney, were culled by lethal exposure to CO_2 and tissues were collected either 7 or 21 days after transplant.

2.5 Ovarian Aggregation Model

We utilised and developed an ovarian aggregation model based on a model previously published by Eppig and Wigglesworth (2000) to investigate the developmental potential of bovine oogonial stem cells, the methodology is described and illustrated (Figure 2.4) below.

2.5.1 Disaggregation of neonatal mouse ovaries

Neonatal (postnatal day 0 - 5; minimum number of 20 ovaries were used to achieve required cell yield) female mice (CD-1, B6SJLF1 or B6;129-Gt(ROSA)26) were culled by cervical dislocation and ovaries were dissected out and transferred to pre-warmed PBS (Life Technologies) supplemented with 1mg/ml BSA (Sigma-Aldrich). Ovaries were then removed from their bursa and added to 2ml pre-warmed trypsin/EDTA/DNAse solution (Trypsin (0.05%) with EDTA (Thermo Fisher Scientific) and 0.02% DNAse I (Sigma-Aldrich) in a 35mm culture dish (Corning Incorporated) for disaggregation. Ovaries were incubated at 37^{o}C with humidified air and 5% CO_2 for 15 minutes. Ovaries were then mechanically dissociated by gentle pipetting up and down and returned to the incubator for a further 5 minutes, twice. The enzymatic digestion was neutralised equal volumes with sterile M199 media supplemented with 1x penicillin-streptomycin, 110µl Sodium Lactate and 10% FBS (all supplements from Sigma-Aldrich) and filtered through 22µm filter (Millipore Ltd). Cell suspension was centrifuged at 450 RCF for 5minutes, supernatant removed and cells re-suspended in 1ml fresh M199 media with supplements as described earlier. Cells were plated in 35mm culture dishes and volumes made up to 3ml in each culture dish. Cells were cultured overnight at 37^{o}C with humidified air and 5% CO_2.

2.5.2 Separation of germ and somatic cells

Germ and somatic cells from neonatal mice were initially separated based on their adhesive potential (Somatic cells will adhere to the base of a culture plate, whereas germ cells will float in the media). Germ cells were aspirated off the somatic cell monolayer and placed in a new 35mm culture dish. The somatic cell monolayer was then washed with 2ml of pre-warmed PBS supplemented with 1mg/ml BSA, twice, to remove any remaining germ cells and cell debris. 2ml of pre-warmed trypsin/EDTA/DNAse was added to the somatic cells for 5minutes at 37^{o}C, then neutralized with equal volumes of M199 with supplements and filtered through a cell filter (size 30µm or 20µm, (Sysmex)). Somatic cells were then centrifuged at 450 RCF for 5minutes, supernatant discarded and cells re-suspended in M199 with

supplements and placed in a new culture dish and returned to 37ºC, with humidified air and 5% CO_2 for 5-6 hours.

Following a second incubation, the murine neonatal ovarian somatic cells were washed with 2 ml pre-warmed PBS, twice. 2ml of pre-warmed trypsin/EDTA/DNAse was added to the somatic cells for 5minutes at 37ºC, then neutralized with equal volumes of M199 with supplements and filtered through a cell filter (size 30μm, 20μm or 10μm, (Sysmex)). Cells were centrifuged at 450 RCF for 5minutes, supernatant discarded and cells re-suspended in an appropriate volume of media for cell counting, prior to aggregation (section 2.5.4).

2.5.3 Culture of neonatal murine somatic cells

Some populations of CD-1 murine neonatal somatic cells were cultured longer term for use in ovarian aggregates. Cells were briefly washed twice with pre-warmed PBS (Life Technologies) and cultured with fetal somatic cell media previously developed for human cells (Bayne et al., 2016), Dulbecco's Modified Eagles Medium (DMEM; without Phenol red) supplemented with 10% Fetal Bovine Serum (FBS), 2mM L-glutamine, 1x MEM Non-Essential Amino Acids (NEAA) and 1x penicillin/streptomycin/amphotericin (all supplements supplied by Life Technologies). Once confluent cells were split using Trypsin (0.05%) with EDTA (Life Technologies) at an appropriate ratio.

2.5.4 Aggregation of ovarian cells

All cell populations used for aggregations were trypsinised, neutralised with equal volumes of media and centrifuged at 450 RCF for 5 minutes and re-suspended in Waymouths media (Life Technologies) with 1xpenicillin-streptomycin (Sigma-Aldrich) and 10% FBS (Life Technologies). Cell populations were manually counted using a haemocytometer. Cells were then combined in the appropriate ratio and combination to create different aggregates (Figure 2.4). Cells were placed into 0.5ml eppendorfs in the desired ratio/concentration and 35μg Phytohaemagluttanin (PHA, Sigma-Aldrich), a natural plant lectin, which promotes mammalian cell agglutination, was added. Between 100,000 – 200,000 cells were used to create aggregates. Cells were mixed by a brief vortex and the centrifuged in a

microcentrifuge at 11,200 RCF for 30 seconds, the 0.5ml eppendorfs were then rotated 180° and cells were centrifuged at 11,200 RCF for 30 seconds a second time. Cell pellets (aggregates) were then transferred with 30µl of Waymouths media with supplements to a hanging drop culture overnight at 37°C with humidified air and 5% CO_2 to encourage cell interaction and adhesion.

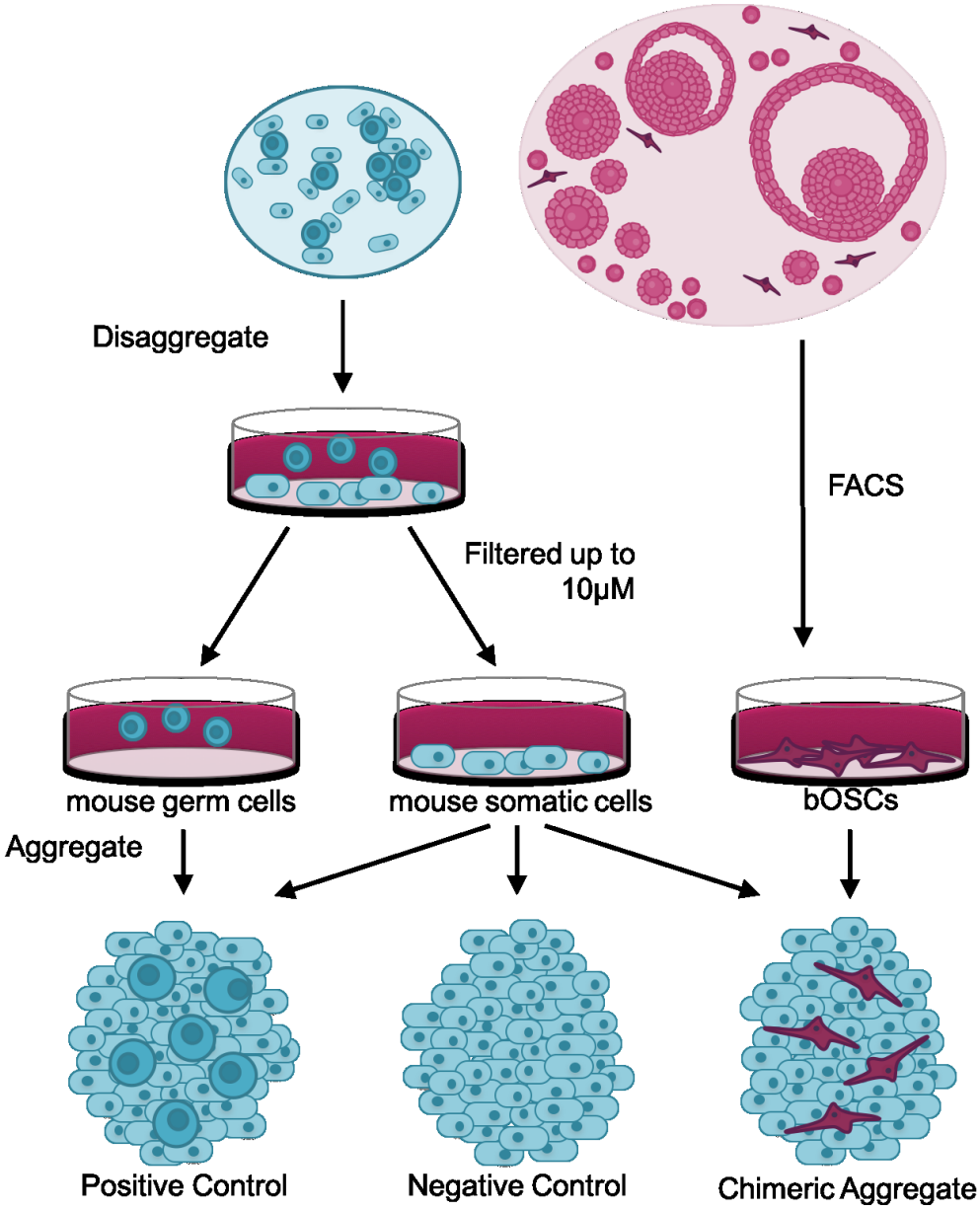

Figure 2.4: Illustration of the ovarian aggregation model. bOSCs were isolated via FACS from adult bovine ovaries and cultured prior to aggregation with other cell populations. Murine neonatal ovaries were collected and enzymatically disaggregated with Trypsin/EDTA, to achieve a single cell suspension, which was cultured overnight in M199 media with supplements. Murine ovarian somatic

cells were then separated from germ cells based on their adhesive potential. Germ cells were washed off the somatic cell monolayer. Somatic cells were also filtered through cell filters (30μM, 20μM or 10μM). Cells were then combined together in the desired numbers/ratios with 35μg PHA and centrifuged prior to an overnight culture in a hanging drop to facilitate adhesion of cells.

2.5.4.1 Positive control ovarian aggregate

Positive control aggregates recombined neonatal murine somatic cell and germ cell populations at varying ratios (Figure 2.4). Positive control aggregates were then either cultured as described in section 2.6.4 or xeno-transplanted as described in section 2.7.1.

2.5.4.2 Negative control ovarian aggregate

To investigate the quality of our separation technique, negative control aggregates were generated, aggregating together mouse neonatal ovarian somatic cells only (Figure 2.4). Negative control aggregates were generated alongside every chimeric aggregate. Negative control aggregates were then either cultured as described in section 2.6.4 or xeno-transplanted as described in section 2.7.1.

2.5.4.3 Chimeric ovarian aggregate

bOSCs isolated (see section 2.2) and cultured (see section2.6.1.1) were aggregated together with neonatal mouse ovarian somatic cells at a ratio of 1:10 respectively (Figure 2.4). Chimeric aggregates were then either cultured as described in section 2.6.4 or xeno-transplanted as described in section 2.7.1.

Chimeric ovarian aggregates were also generated using freshly isolated bOSCs which were frozen (see section 2.6.1.3) until required and thawed before aggregation with neonatal mouse ovarian somatic cells. bOSC viability was assessed using trypan blue (Thermo Fisher Scientific) as a marker of dead cells. An equal volume of 0.4% trypan blue solution was added to 10μl cell suspension. Cells were then loaded onto the haemocytometer and counted. The percentage of viable cells was calculated and the appropriate number of live bOSCs added to neonatal mouse ovarian somatic cells at a ratio of 1:10 respectively. Chimeric ovarian aggregates were then xeno-transplanted as described in section 2.7.1.

2.5.5 Bovine ovarian aggregates

bOSCs were also aggregated with fetal bovine ovarian somatic cells (isolated as described in section 2.3 and cultured as described in section 2.6.1.2) at a ratio of 1:10 respectively. Bovine aggregates were then either cultured as described in section 2.6.4 or xeno-transplanted as described in section 2.7.1.

2.6 Mammalian cell and tissue culture

2.6.1 Cell maintenance

All cell culture was conducted under sterile laminar flow conditions and cells were cultured and maintained at 37ºC with humidified air in 5% CO_2.

2.6.1.1 Culture of bOSCs

Upon isolation from adult ovarian cortex (Section 2.2), bovine oogonial stem cells were placed into pre-warmed OSC medium (Section 2.12) in a single well of a 24 well culture plate (Corning Incorporated). Cells were cultured at 37ºC with humidified air in 5% CO_2 and were refreshed with 100µl of new medium every 48 hours. Once confluent cells were passaged using Trypsin (0.05%) with EDTA (Life Technologies). Trypsin was added to cells for 5 minutes and returned to the incubator to accelerate their detachment. Trypsin was neutralised with pre-warmed OSC medium (Section 2.12) and cells were spun down for 5 minutes at 112 RCF before the supernatant was discarded and the cells were re-suspended in pre-warmed OSC medium (Section 2.12) and split at an appropriate ratio.

2.6.1.2 Culture of FBSCs

Following derivation of the fetal bovine ovarian somatic cells (FBSCs, see section 2.3), cell medium was changed on alternate days. Cells were briefly washed twice with pre-warmed PBS (Life Technologies) and fresh medium (Dulbecco's Modified Eagles Medium (DMEM; without Phenol red) supplemented with 10% Fetal Bovine Serum (FBS), 2mM L-glutamine, 1x MEM Non-Essential Amino Acids (NEAA) and 1x penicillin/streptomycin/amphotericin (all supplements supplied by Life Technologies)). Once confluent cells were split using Trypsin (0.05%) with EDTA (Life Technologies) at an appropriate ratio.

2.6.1.3 Freezing and Storage of cells

To store bOSCs long term, cells were cryopreserved. Following trypsinisation, cells were re-suspended in OSC medium (section 2.12) and centrifuged (112 RCF). The supernatant was discarded and cells were re-suspended in 50% OSC media and 50% cryopreservation media (60% FBS (Life Technologies), 20% DMSO (Sigma) and 20% OSC media) and placed into a cryovial (Sigma). Cryovials were then placed within a Nalgene Mr Frosty (Sigma), filled with isopropyl alcohol and placed in a -80ºC freezer overnight and then transferred to liquid nitrogen for long term storage.

FBSCs were trypsinised and the reaction neutralised with equal volumes of fetal ovarian somatic cell medium (section 2.12). The cell suspension was centrifuged at 450 RCF and cells were re-suspended in 1ml Bambanker (AlphaLaboratories), transferred to a cryovial (Sigma). Cryovials were then placed within a Nalgene Mr Frosty (Sigma), filled with isopropyl alcohol and placed in a -80ºC freezer overnight and then transferred to liquid nitrogen for long term storage. Neonatal murine somatic cells were frozen in the same fashion.

Cells were thawed by heating cryovials to 37ºC in a pre-warmed water bath. The cell suspensions were then centrifuged at the appropriate speed. Cells were then re-suspended in the appropriate medium and placed in a culture dish and cultured at 37ºC in humidified air with 5% CO_2.

2.6.2 Cell labelling

To investigate bOSCs in subsequent experiments, cells were labelled fluorescently for tracking. Several methods were used to label bOSCs and the success of these labelling techniques were assessed using visual assessment of the fluorescent labels (section 2.9.2) and cell growth through assessment of passage frequency.

2.6.2.1 Lentivirus transduction

bOSCs at 50% confluency were transfected with an mCherry lentivirus under the SFFV promotor (Lv-cppt-SFFV-IRES-mCherry-opre; designed by Pamela Brown of the Biomolecular Core) for labelling and subsequent tracking. Lv-cppt-SFFV-IRES-mCherry-opre was added to fresh pre-warmed OSC media at concentrations which represented ratios of either 1:1. 5:1 or 10:1 of virus:bOSCs, respectively then applied

to cells. Polybrene (Sigma-Aldrich) was also added to media at a final concentration of 6μg/ml to facilitate viral transfection of cells. Cells were cultured for 48 hours at 37ºC with humidified air and CO_2. Viral media was then removed, cells washed twice with pre-warmed PBS and replaced with pre-warmed OSC media.

2.6.2.2 Cell tracker dyes

bOSCs were labelled with 5-chloromethylfluorescein diacetate (CMFDA; Thermo Fisher Scientific, C7025) for 30 minutes or 1 hour according to manufacturer's instructions. Briefly, 50μg CMFDA was re-suspended in 50μl DMSO and then added to 15ml OSC medium (section 2.12). 1ml CMFDA labelled OSC media was added to bOSCs for 30 minutes or 1 hour. Medium was then washed off with pre-warmed PBS and then replaced with pre-warmed fresh OSC media. Cells were then visualised as described in section 2.9.2 to visualise CMFDA uptake.

2.6.2.3 Fluorescent Dextrans

Media was aspirated off bOSCs and cells were washed twice with pre-warmed PBS (Life Technologies) and fresh medium with 100μg/ml Rhodamin Dextrans (Thermo Fisher Scientific, D1824; 10,000 MW) was added to the cells. Cells were incubated at 37ºC, with humidified air and 5% CO_2, overnight. Following culture with Rhodamine Dextrans, cell medium was aspirated and cells washed twice with pre-warmed PBS then fresh OSC media added. Cells were visualised as described in section 2.9.2, for rhodamine dextran uptake. If necessary, this process was repeated to achieve a high uptake of dextrans.

2.6.3 Immunostaining of cells

To investigate protein expression and characterise our cells of interest, cells were fixed and immunocytochemistry carried out to identify antigens within the cells.

2.6.3.1 Seeding of Chamber slides

Chamber slides (Thermo Fisher Scientific) were coated with poly-L-lysine (Sigma-Aldrich) for 10 minutes, then washed twice with PBS and left to air dry for 2 hours in a sterile laminar flow hood. Cells were then seeded directly onto chamber slides

and cultured as described in section 2.6.1 until confluent and then fixed (section 2.6.3.2).

2.6.3.2 Cell Fixation

Cells were either fixed using a 50:50 Methanol:Ethanol solution or using NBF, methodology is detailed in each chapter.

For methanol:ethanol fixation, cells in their culture wells or previously seeded on chamber slides were firstly washed with ice cold PBS (Life Technologies) twice, then ice cold methanol:ethanol solution (ratio 50:50) was added to cells, and incubated at -20ºC for 10 minutes. An equal volume of room temperature PBS was then added to the methanol:ethanol solution and aspirated off the cells. Cells were then washed with fresh room temperature PBS twice and an appropriate amount of PBS added to the cells and were then stored at 4ºC. This methodology did not require separate permeabilisation of the cells and proceeded with non-specific blocking (section 2.6.3.3).

Cells fixed with NBF were washed twice with pre-warmed PBS and NBF added to the cells for 10minutes at room temperature. NBF was then removed and cells were washed twice with PBS. Cells fixed with NBF were permeabilised using 0.5% Triton X-100 (Sigma-Aldrich) in PBS for 10 minutes at room temperature, then washed twice with PBS and then an appropriate amount of PBS added to the cells and were then stored at 4ºC.

2.6.3.3 Non-specific blocking

To prevent non-specific blocking of the secondary antibody, cells were blocked with normal serum (NS, serum used was based on the species the secondary antibody was raised in) diluted in PBS (1:4 respectively) with 5% bovine serum albumin (BSA, Sigma-Aldrich), NS/PBS/BSA for 30minutes at room temperature.

When using tyramide as the detection method, the blocking serum was immediately replaced with primary antibody (section 2.6.3.4), however when using a streptavidin conjugated alexaflour, endogenous biotin activity must be blocked. This was done using a streptavidin/biotin blocking kit (Vector Laboratories), according to manufacturer's instructions. Briefly, streptavidin block was diluted 1:4 with PBS and

added to cells for 15minutes at room temperature, then washed with PBS twice and then the biotin block, diluted 1:4 in PBS, was added for 15minutes at room temperature and washed twice in PBS.

2.6.3.4 Primary antibody

Following non-specific blocking, the primary antibody was added to samples diluted in blocking serum (NS/PBS/BSA). Primary antibody concentrations were optimised by titration to find the optimum level of detection lacking non-specific background staining. Table 2.1 below describes the antibodies used and their corresponding dilutions. Primary antibodies were applied to the cells and incubated overnight at 4ºC. Negative controls (primary antibody omitted) were also included.

Table 2.1: Primary antibodies used in immunocytochemistry

Antibody	Dilution	Species	Detection method	Supplier
Tetramethylrhodamine	1:3000	Rabbit	Tyramide	Life Technologies
DDX4	1:300	Rabbit	Streptavidin	Abcam
DAZL	1:800	Mouse	Streptavidin	AbDSerotec
C-KIT	1:100	Rabbit	Streptavidin	DAKO
LIN28	1:500	Rabbit	Streptavidin	Abcam
OCT4	1:250	Mouse	Streptavidin	Santa Cruz
IFITM3	1:500	Rabbit	Streptavidin	Abcam

2.6.3.5 Secondary antibody

Primary antibodies were washed off with two washes of PBS and secondary anitbodies were diluted 1:200 in blocking serum and applied to the cells for 30 minutes at room temperature in a humidity chamber. Secondary antibodies were selected based on their specificity for the primary antibodies and also in accordance with the normal serum used in the blocking step (2.6.3.3). Secondary antibodies are listed in Table 2.2. Chambers on the slides were removed at this stage according to manufacturer's instructions.

Table 2.2: Secondary antibodies used in immunocytochemistry

Antibody	Supplier
Goat anti Rabbit	Vector
Chicken anti Rabbit	Santa Cruz
Chicken anti Mouse	Santa Cruz

2.6.3.6 Visualisation of secondary antibody

Slides were washed in PBS twice for 5minutes to remove any unattached secondary antibody. The secondary antibody is then visualised using either streptavidin or tyramide detection.

For streptavidin detection, alexfluors conjugated to streptavidin (listed in Table 2.3) were diluted 1:200 in PBS and incubated on cells for 1 hour at room temperature in a dark humidity chamber. Slides were then washed twice in PBS for 5minutes in an opaque chamber to prevent fluorescent bleaching.

Table 2.3: Streptavidin conjugated alexafluors for immunocytochemistry

Streptavidin	Supplier
Alexafluor 488	Molecular Probes Inc
Alexafluor 555	Molecular Probes Inc

In contrast, for tyramide detection (Perkin Elmer Incorporated) after washing the peroxidase secondary antibody off with PBS, slides were incubated in tyramide, diluted 1:50 in the prescribed buffer in accordance with the manufacturer's instructions, for 10 minutes in a dark humidity chamber. Slides were then washed in PBS to remove the tyramide, in an opaque chamber to prevent bleaching of the fluorescence.

2.6.3.7 Counterstaining

Nuclei of cells were counterstained with either DAPI (Sigma-Aldrich) or Sytox Green (Molecular Probes Incorporated), to compliment the fluorescent colours used in the immunocytochemistry. Both counterstains were diluted 1:1000 in PBS and added to cells for 10minutes, maintained in the dark and at room temperature.

Following counterstaining, cells were washed with PBS twice and mounted with glass coverslips (CellPath Ltd) using permaflour (Thermo Fisher Scientific). Slides were then maintained at 4^{o}C in the dark until visualisation (section 2.9.4).

2.6.4 *In vitro* culture of ovarian aggregates

Ovarian aggregates generated as described in section 2.5 were cultured using two different methods described below after an initial overnight hanging drop culture to promote cell interaction.

2.6.4.1 Alginate

Ovarian aggregates were transferred from a hanging drop culture to 50µl pre-warmed 1% alginate (Sigma-Aldrich) gel in sterile PBS (Life Technologies) and was dropped into pre-warmed 100µM $CaCl_2$ (VWR) solution for 10minutes, maintained at 37^{o}C to cross-link the alginate. Alginate beads containing ovarian aggregates were then washed twice in pre-warmed Waymouths media with supplements as described earlier (section 2.5.4), the beads were then placed singularly in a well of a 24 well plate (Corning Incorporated) with 1ml of pre-warmed Waymouths media with supplements and incubated at 37^{o}C with humidified and 5% CO_2. 50% of media was replaced with fresh media on alternate days of culture.

2.6.4.2 Hanging drop

Ovarian aggregates were also cultured in a hanging drop continuously for the whole culture period. Aggregates were transferred to fresh medium on alternate days of culture. Briefly, 30µl of pre-warmed Waymouths medium with supplements (Section 2.12) was placed on the internal surface of a 10cm culture plate lid (Corning Incorporated) and aggregates were transferred to the new medium drop using sterile curved forceps. The culture plate lid was then inverted and placed over the culture dish containing sterile PBS (Life Technologies) and incubated at 37^{o}C with humidified air and 5% CO_2.

2.7 Animal Procedures

All animal experiments were conducted under a UK Home Office licence in line with the Animals Scientific Procedure Act (1986).

SCID (C.B.17/IcrHan Hsd-Prkdc) Mice were obtained from Envigo laboratories and CD-1 mice from Charles River laboratories. Mice were allowed a minimum of 6 days to acclimatise to their new environment prior to the start of any experimental work. Mice maintained in a 12 hour light/dark cycle, in a pathogen free environment and SCID mice were housed in individually ventilated cages (IVCs). Food and water were available *ad libitum*.

CD-1 male and female mice were mated and resulting female pups were used for the generation of ovarian aggregates (section 2.4.1).

2.7.1 Xeno-transplant surgery

SCID (C.B.17/IcrHan Hsd-Prkdc) mice underwent bilateral ovariectomy and unilateral kidney xeno-transplantation. SCID mice were anaesthetised with isofluorane (Abbott Laboratory Limited) (5% for induction and 2.5% for maintenance) in oxygen. Once anaesthetised, a patch of hair just below the hump of the back was shaved and the skin then sterilised using surgical scrub (Vetasept). Mice were then provided with a subcutaneous injection of saline around the hind leg and a subcutaneous injection of vetergesic (Abbott Laboratory Limited), at a dose of 0.03mg/ml in 100µl around the neck. A vertical incision along the skin was made in the middle of the back and the ovaries located through the body wall. Skin was held in place using bull dog clamps (R&D Slaughter), and a small incision was made in the body wall directly above the ovary. Using forceps the ovary and ovarian fat pad were removed from the body cavity. Blood circulation to the ovary was clamped by forceps then the ovary and ovarian bursa was removed. Using the ovarian fat pad as a guide the kidney was pulled out of the body cavity with forceps. Sterile PBS was dropped onto the surface of the kidney to keep it hydrated. A tiny incision was made in the kidney capsule using a sterile needle. Using a pulled glass pipette, aggregates were transferred through the hole in the capsule to the surface of the kidney. Aggregates were moved away from the incision to ensure its security when returning the kidney to the body cavity. The kidney and associated tissue is then returned to the body cavity, and the body wall sutured using number 5 polyglactin sutures. The ovary on the opposite side is then also removed following the same procedure. Once the bilateral ovariectomy and unilateral xeno-transplantation was completed, the skin

incision was closed using wound clips (Scientific Laboratory Supplies). Mice were then transferred to individual cages which were maintained at 30ºC while they recovered. Mice were maintained as described in section 2.7 for 21 days until tissue collection.

2.7.2 Tissue collection

7 or 21 days after xeno-transplantation of the tissue, mice were culled by lethal exposure to CO_2 and tissues were collected and fixed in 4% NBF for 6 hrs and then transferred to 70% ethanol prior to embedding in paraffin blocks for histological analysis (section 2.8).

2.8 Histological Techniques

2.8.1 Tissue fixation, embedding and sectioning

All tissues not derived from B6;129-Gt(ROSA)26 mice were fixed in natural buffered formalin (NBF), control adult ovarian tissue (bovine and mouse) were fixed for 24 hours and aggregated ovaries (*in vitro* and *in vivo*) for 6 hours. After fixation, tissues were transferred to 70% ethanol (VWR). *In vitro* cultured ovarian aggregates were then embedded within a 2% agarose gel to allow easy visualisation of the tissue.

Tissues containing cells from B6;129-Gt(ROSA)26 mice were fixed with a 0.2% Glutaraldehyde fixative (0.2% glutaraldehyde and 0.05% 1M $MgCl_2$ in PBS, all reagents sourced from Sigma) for 20 minutes then washed 3 times for 15 minutes each, in a detergent rinse (0.2% 1M $MgCl_2$, 0.01% sodium deoxycholate, 0.02% NP-40 in PBS, all reagents sourced from Sigma). Tissues were then stained with an X-Gal solution (2% (w/v) X-Gal (5-bromo-4-chloro-3-indolyl-β-D-galactopyranaoside), 2% 250mM potassium ferricyanide, 2% 250mM potassium ferrocyanide, 0.2% 1M $MgCl_2$, 0.01% sodium deoxycholate, 0.02% NP-40, 0.02% Tris in PBS, all reagents sourced from Sigma) for 24-48 hours, dependent on tissue size, at 37ºC. Following staining tissues were washed in detergent rinse for 15 minutes, three times, before wax embedding (section 2.8.2).

2.8.2 Tissue embedding and sectioning

Tissue was embedded in wax using an automated Leica TP1050 processor. Tissue embedded in wax blocks were sectioned at 5μM and mounted onto electrostatically charged glass slides (Leica) and maintained at 50^{o}C overnight in a slide oven to ensure tissue adherence to the slide surface.

2.8.3 Dewaxing and tissue rehydration

To assess tissue histology slides were de-waxed by two 5-minute exposures to xylene (VWR), followed by rehydration through decreasing concentrations of ethanol (100%, 100%, 95%, 80% and 70% for 20 seconds each).

2.8.4 Haematoxylin and eosin staining

Tissue histology was analysed by haematoxylin and eosin staining, sections were firstly de-waxed and rehydrated as described in section 2.8.3, followed by a brief wash in running tap water. Tissue was then stained in haematoxylin (CellPath) for 2 minutes, washed in running water, dipped in acid alcohol (CellPath), washed in running water, placed in Scotts Tap Water for 20 seconds, washed in running water and dipped in Eosin (Cell Path) and washed in running water. Excess water was removed from slides prior to dehydration and mounting (section 2.8.5).

Tissues containing B6;129-Gt(ROSA)26 cells were only counterstained with eosin. Sections were dewaxed and rehydrated (section 2.8.3), washed in running tap water and dipped into eosin briefly and washed in running water again prior to dehydration and mounting (section 2.8.5).

2.8.5 Dehydration and mounting

Slides were dehydrated through increasing concentrations of ethanol (70%, 80%, 95%, 100% and 100%) for 20 seconds each and then placed in Xylene twice for 5 minutes. Slides were maintained in Xylene until mounting with glass cover slips (CellPath Limited) using Pertex (Histolab) as an adhesive. Air pockets were pushed away from tissue sections with the application of pressure and were left to dry in a fume hood and subsequently stored in dry storage at room temperature.

2.8.6 Immunofluorescence

To assess tissue antigens slides were dewaxed and rehydrated (section 2.8.3) prior to antigen retrieval. To detect proteins possibly masked by the fixation process, tissues were exposed to pH change and high temperature. Slides were placed in 200ml of 0.01M citrate buffer (pH 6.0) in an instant pot (Amazon) with 1500ml dH_2O and heated to 125^oC, the instant pot was then set to venting and slides were left to cool for 20 minutes then washed and cooled in water 3 times.

2.8.6.1 Non-specific blocking

To prevent non-specific blocking of the primary and secondary antibody, slides were blocked with peroxidase blocking solution (Dako), for 10minutes at room temperature in a humidified chamber. Slides were then washed twice in phosphate-buffered saline (PBS).

To inhibit any non-specific binding of the secondary antibody, slides were incubated in a blocking solution of normal serum (NS) diluted 1:4 in PBS with 5% bovine serum albumin (BSA) (NS/PBS/BSA) for 30 minutes at room temperature in a humidity chamber. The serum chosen was dependent on the species in which the secondary antibody was raised in.

2.8.6.2 Primary antibody

Primary antibodies (listed in table Table 2.4) were diluted in NS/PBS/BSA to an optimum concentration, previously determined by titration on control tissues, which resulted in the maximum level of detection without non-specific staining. Diluted primary antibodies replaced the blocking serum (NS/PBS/BSA) and were incubated on tissue sections overnight at 4^oC in a humidity chamber.

Negative controls (primary antibody omitted) were always used and positive controls were used where applicable and appropriate.

Table 2.4: Primary antibodies used in Immunofluorescence

Antibody	Dilution	Species	Supplier

Cleaved Caspase 3	1:100	Rabbit	Cell Signalling Technology
DAZL	1:800	Mouse	AbDSerotec
β-GAL	1:800	Mouse	Promega
Tetramethylrhodamine	1:3000	Rabbit	Life Technologies

2.8.6.3 Secondary antibody

Following an overnight incubation, the primary antibody was washed off with PBS for 5minutes, twice. The appropriate secondary antibodies (listed in Table 2.5) were selected based on the primary antibody of choice, secondary antibodies are raised against a species-specific sequence on the primary antibody, and diluted 1:200 in blocking serum (NS/PBS/BSA) and applied to slides for 30minutes at room temperature in a humidity chamber.

Table 2.5: Secondary antibodies used in Immunofluorescence

Antibody	Supplier
Chicken anti Rabbit	Santa Cruz
Chicken anti Mouse	Santa Cruz

2.8.6.4 Visualisation of secondary antibody

Alexafluor conjugated secondary antibodies do not require further detection and samples can be counterstained (section 2.8.6.5) after washing off the secondary antibody with PBS, in an opaque chamber to prevent bleaching of the fluorescence.

In contrast, tyramide detection (Perkin Elmer) requires an additional step. After washing the peroxidase secondary antibody off with PBS, slides were incubated in tyramide, diluted 1:50 in the prescribed buffer in accordance with the manufacturer's instructions, for 10 minutes in a dark humidity chamber. Slides were then washed in PBS to remove the tyramide, in an opaque chamber to prevent bleaching of the fluorescence before counterstaining and mounting (section 2.8.6.5).

2.8.6.5 Counterstaining and mounting

Slides were counterstained with DAPI (Sigma-Aldrich) diluted 1:1000 in PBS for 10minutes at room temperature in a dark humidity chamber. Slides were then washed with PBS twice for 5minutes each then mounted with glass coverslips (CellPath Limited) using permafluor (Thermo Fisher Scientific) as an adhesive. Slides were then stored in the dark at 4^{o}C until visualisation (section 2.9.4).

2.8.7 RNA Scope

RNA Scope analysis was carried out by Aquila HistoPlex, University of Edinburgh. Briefly, tissue sections were dewaxed and rehydrated (section 2.8.3) and allowed to air dry for 5 minutes at room temperature. Tissues were then treated with hydrogen peroxidase block for 10 minutes at room temperature and washed in deionised water. Target RNA's were then retrieved by exposure of slides to changes in pH (retrieval buffer, used according to manufacturer's instructions Advanced Cell Diagnostics) and high temperatures (100^{o}C) for 8minutes. Tissue was permeabilised using protease digestion (Protease Plus, Advanced Cell Diagnostics) at 40^{o}C for 15 minutes. Slides were then washed in deionised water and incubated with pre-warmed (40^{o}C) probe (Bt-ATP5b or Mm-UBC) for 30 minutes at 40^{o}C, then washed with buffer for 2 minutes at room temperature. The signal was then amplified using amplification solutions (Advanced Cell Diagnostics); amplification solution 1 was applied for 30 minutes at 40^{o}C, amplification solution 2 for 15 minutes at 40^{o}C, amplification solution 3 for 30 minutes at 40^{o}C, amplification solution 4 for 15 minutes at 40^{o}C, amplification solution 5 for 30 minutes at room temperature and amplification solution 6 for 15 minutes at room temperature. Slides were washed between each amplification with wash buffer twice for 2 minutes at room temperature. DAB was then applied to slides at room temperature for 10 minutes, to detect the signal. Slides were then washed in deionised water and tissue counterstained with Harris haematoxylin for two minutes followed by acid alcohol for 5 seconds, and Scott's tap water for 10 seconds. Slides were then dehydrated and mounted (section 2.8.5). All reagents were sourced from Advanced Cell Diagnostics by Aquila HistoPlex, University of Edinburgh.

2.9 Microscopy

2.9.1 Light microscopy

Tissue histology was imaged with a Provis AX70 (Olympus) or a Zeiss Imager Z1 both fitted with a AxioCam HRc camera (Zeiss) using the Zeiss software which also generated the image scale bars.

2.9.2 Live cell and tissue imaging

Live cell and tissue imaging was conducted using an Axiovert 200 fitted with a AxioCam HRc camera and a Hamamatsu camera for collection of images including fluorescent images. Cells and tissue were maintained at 37ºC with 5% CO_2 throughout live imaging.

2.9.3 Whole tissue microscopy

Whole tissue images were captured using a Leica MZF III with a RS Photometrics camera.

2.9.4 Fluorescent microscopy

Sections were visualised using a Zeiss LSM 780 confocal microscope and scale bars were embedded in the images using Zeiss software.

2.9.5 Image analysis

All image analysis, measurements and cell counting was carried out using ImageJ software.

2.10 cDNA Synthesis and RT-PCR

Bovine Oogonial Stem cells were analysed using conventional polymerase chain reaction (PCR) to assess their gene expression. bOSCs were trypsinised and centrifuged as described above, and re-suspended in 350µL of RLT buffer (Qiagen) and homogenized. RNA was extracted using the RNeasy Micro Kit (Qiagen) with on-column DNase digestion according to manufacturer's instructions. Reverse transcription was performed using Maxima 1st strand cDNA synthesis kit (Life Technologies), with oligo$(dT)_{18}$ and random hexamer primers utilised to prime synthesis of first strand cDNA according to the manufacturer's instructions.

0.5µg of RNA was used in each reaction and negative control samples (RT-) lacking the transcription enzyme were also synthesised to identify contamination in further experiments.

Target-specific PCR was performed using MyTaq HS Red Mix (Bioline) to identify the presence or absence of specific gene transcripts. 1µl of either the RT+ or RT- cDNA reaction was added to RT-PCR reaction mix (Table 2.6) for a total reaction volume of 25µl. Primer pairs and corresponding annealing temperatures and product sizes can be found in Table 2.7 and PCR cycling conditions are detailed in Table 2.8. PCR products were run on agarose gels (1-2.5%, Bioline) with a 100bp ladder (Bioline Reagents Limited) using electrophoresis.

Table 2.6 RT-PCR Reaction Mix

Reagent	Amount Used	Manufacturer
MyTaq HS Red Mix	12.5µl	Bioline
Forward Primer	0.5µl	Integrated DNA Technologies
Reverse Primer	0.5µl	Integrated DNA Technologies
H_2O	10.5µl	Qiagen

Table 2.7 PCR Primer Pairs

Gene Target	Forward Primer	Reverse Primer	Species	Product Size (bp)	Annealing temperatur	Reference
b-ACTIN	CTCTTCCAGCCTT CCTTCCT	GGGCAGTGATC TCTTTCTGC	Bovine	177	52.9 ºC	Lab Designed
OCT4	CGAAGCTGGACA AGGAGAAG	AGAGAACCCCC AGGGTGAG	Ovine	158	52.3 ºC	Gift from Alan McNeilly
LIN28	GGCCGTGGAGTTC ACCTTTA	GTGGCAGTTTG CACTCCTTG	Bovine	194	53.7 ºC	Lab Designed
IFITM3	CACATCCCAGCCC TTGTTCA	TGTTGAACAGG GACCACACG	Bovine	185	54.1 ºC	Lab Designed
PRDM1	CAAATGCCAGAC GTGCAACA	GTGCACAAACT GCGTGAACT	Bovine	191	52.7 ºC	Lab Designed
DDX4	TATATGGGGGAA CCCAGTTG	CATATCCAGCA TGCGATC	Bovine	166	46.9 ºC	Lab Designed
DAZL	GAAGGCAAAATC ATGCCAAACAC	CTTCTGCACAT CCACGTCATTA	Bovine/Human	185	51.2 ºC	Lab Designed
C-KIT	AACACAATGGGA CGGTGGAG	AGGGTGTGAGC ATGGATTTGT	Bovine	112	52.9 ºC	Lab Designed
FOXL2	CCGGCATCTACCA GTACATTATAGC	AGGGTGTGAGC ATGGATTTGT	Bovine	100	52.9 ºC	(Eozenou et al., 2012)
LGR5	AGTTGTTCAGCCT CCGATCT	TGGAAAATGCA TTAGGGTCA	Bovine	81	47.9 ºC	Lab Designed
NR2F2	CGGATCTTCCAAG AGCAAGTG	CACAGGCATCT GAGGTGAACA	Bovine	103	52.5 ºC	Lab Designed

Table 2.8 PCR Cycling Conditions

Action	Temperature (°C)	Time	
Initial denaturation	95	1 minute	
Denaturation	95	15 seconds	Repeat cycle 35 times
Annealing	Primer specific see Table 2.7	30 seconds	
Extension	72	30 seconds	
Final extension	72	10 minutes	

2.11 Statistical Analysis

Statistical analysis was conducted using Graphpad Prism 6 software. One-way ANOVA analysis with post-hoc Tukeys multiple comparisons testing was used where three or more groups were compared when only one variable was present. Where only two groups were present a t-test was used to determine differences between groups.

Corrected total cell fluorescence (CTCF) was calculated using the equation below, to assess the amount of fluorescence in cells. Analysis was conducted using ImageJ and Graphpad Prism 6 software.

$$CTCF = Integrated\ Density - (Cell\ area\ x\ Mean\ background\ fluorescence\ )$$

Mean background fluorescence was calculated based on 5 random background readings within each image.

Data are presented as Mean ± SEM throughout.

2.12 Commonly Used Solutions

Acid Alcohol

Acid alcohol was prepared using 70% ethanol with 1% concentrated hydrochloric acid.

Blocking Serum

Normal serum (Biosera) was diluted 1:4 in PBS with 5% BSA (Sigma-Aldrich)

Citrate Buffer

42.02g Citric acid monohydrate was diluted in 900ml distilled water and brought to pH 6.0 using NaOH.

Fetal ovarian somatic cell medium

Fetal bovine ovarian somatic cells (FBSCs) were cultured in Dulbecco's Modified Eagles Medium (DMEM; without Phenol red) supplemented with 10% Fetal Bovine Serum (FBS), 2mM L-glutamine, 1x MEM Non-Essential Amino Acids (NEAA) and 1x penicillin/streptomycin/amphotericin (all supplements supplied by Life Technologies)

Holding medium

Bovine tissue was held in Leibovitz medium (Life Technologies) supplemented with sodium pyruvate (2 mM), glutamine (2 mM; both obtained from Life Technologies), BSA (Fraction V, 3 mg/ml), penicillin G (75 µg/ml) and streptomycin (50 µg/ml; All chemicals from Sigma-Aldrich).

Oogonial Stem Cell (OSC) Medium

bOSCs were cultured in αMEM (Life Technologies) supplemented with 10% FBS (Life Technologies), 1mM sodium pyruvate (Life Technologies), 1mM non-essential amino acids (Life Technologies), 10^3 units/ml leukemia inhibitory factor (LIF; Millipore), 10 ng/ml recombinant human epidermal growth factor (rhEGF; Life Technologies), 1 ng/ml basic fibroblast growth factor (bFGF; Life Technologies), 40 ng/ml recombinant human glial cell-derived neurotrophic factor (rhGDNF; R & D Systems), 1x-concentrated N-2 supplement (R & D Systems) and 1x-concentrated penicillin-streptomycin-glutamine (Life Technologies), filtered through a 0.22µM filter (Millipore).

Phosphate-Buffered Saline (PBS)

PBS used for immunofluorescence was prepared by adding 1 PBS tablet (Sigma-Aldrich) with 0.01M phosphate buffer, 0.0027M potassium chloride and 0.137M NaCl with a pH of 7.4 to 200ml distilled water.

Scotts Tap Water

2g of sodium bicarbonate and 20g magnesium sulphate 20g were dissolved in 1L of deionised water to make Scotts Tap water.

Thaw medium 1

To thaw cryopreserved ovarian tissue, tissue was placed in holding medium (see above) supplemented with 1M sucrose (Sigma-Aldrich) pre-warmed to 37ºC.

Thaw medium 2

Thawing of cryopreserved ovarian tissue was continued by placing tissue in holding medium (see above) supplemented with 0.5M sucrose (Sigma-Aldrich) pre-warmed to 37ºC.

Vitrification medium 1

Vitrification of ovarian tissue was initiated by incubation in Leibovitz medium (Life Technologies) supplemented with 7.5% Dimethyl sulfoxide (Sigma-Aldrich) and 7.5% Ethylene Glycol (Sigma-Aldrich).

Vitrification medium 2

Vitrification of ovarian tissue was continued by incubation in Leibovitz medium (Life Technologies) supplemented with 20% Dimethyl sulfoxide (Sigma-Aldrich), 20% Ethylene Glycol (Sigma-Aldrich) and 0.5M sucrose (Sigma-Aldrich).

3 Isolation and Characterisation of bovine Oogonial Stem Cells (bOSCs)

3.1 Introduction

A candidate cell within mammalian ovaries capable of self-renewal and differentiation into new oocytes has, until recently, remained unidentified. Alongside numerical data illustrating the disparity between follicle atresia and the murine reproductive lifespan, Johnson et al. (2004) were the first to identify a mitotic germ cell in adult mouse ovaries, illustrated by co-localisation of Dead-box helicase 4 (Ddx4) and BrdU. Together these results suggest that mammalian ovaries contain putative oogonial stem cells capable of supporting neo-oogenesis.

To investigate the characteristics of this cell, its isolation from adult mammalian ovaries has been essential. Since 2004, several groups have used cell sorting techniques (magnetic and fluorescent) to isolate this putative population of oogonial stem cells using germ cell markers such as Ddx4/DDX4 and Ifitm3 (Interferon-induced transmembrane protein 3) (Hernandez et al., 2015; White et al., 2012; Zhou et al., 2014; Zou et al., 2009). Ifitm3 is a cell surface protein, identified as one of the earliest markers of germ cell specification in embryonic stem cells (ESCs) (Saitou et al., 2002; Tanaka and Matsui, 2002). Whereas Ddx4 is an RNA helicase with restricted expression in the germline (Castrillon et al., 2000; Toyooka et al., 2000) marking all germ cells from post-migratory primordial germ cells (PGCs). The use of Ddx4 to identify and isolate OSCs is however controversial as it is understood to have a traditional cytoplasmic location. The nature of magnetic and fluorescently activated cell sorting utilises cell surface proteins to separate different populations of cells. Critics (Hernandez et al., 2015; Pacchiarotti et al., 2010; Zhang et al., 2015) have suggested that due to the traditional cytoplasmic localisation of Ddx4, it is an unsuitable epitope to isolate OSCs from mammalian ovaries. Although computational analysis of the structure of Ddx4 has yielded conflicting evidence to a possible transmembrane domain (White et al., 2012; Zarate-Garcia et al., 2016), cell surface expression of DDX4 has been identified in a population of cells within the adult pig testes (Kakiuchi et al., 2014). Furthermore, Ddx4/DDX4 has been utilised in several studies to isolate OSCs from adult ovaries of different species (Hernandez

et al., 2015; White et al., 2012; Zou et al., 2009), suggesting that Ddx4/DDX4 may have a cell surface location in putative oogonial stem cells. Our lab has previously utilised and amended FACS isolation techniques based on protocols described by White et al. (2012) to isolate OSCs from adult bovine ovaries.

Putative OSCs isolated from rodents, rhesus macaque monkeys and humans are reported to express genes and proteins associated with both germ (e.g. *Dazl/DAZL*, *Ifitm3/IFITM3* and *Prdm1/PRDM1*) and stem (e.g. *Oct4/OCT4*, *Nanog/NANOG* and *Lin28/LIN28*) cells (Pacchiarotti et al., 2010; White et al., 2012; Zhou et al., 2014; Zou et al., 2009). Crucially these cells do not express oocyte specific markers, such as *Zp3/ZP3* and *Gdf9/GDF9* (White et al., 2012), therefore are a distinct population of cells within the mammalian ovary. Further characterisation of these cells has shown high telomerase activity, a characteristic associated with stem cells (Zou et al., 2009). The initial aim of this thesis was to isolate oogonial stem cells (OSCs) from adult bovine ovary and characterise this putative cell population.

To trace oogonial stem cells in subsequent investigations, researchers have used labelling methods such as fluorescent protein expression directed by virus incorporation into the genome (White et al., 2012; Zhou et al., 2014; Zou et al., 2009) and stem cell promoter driven fluorescent protein expression (Pacchiarotti et al., 2010). We aimed to investigate the potential of several different methods of cell labelling to identify which best suited the study of putative bovine oogonial stems cells.

3.2 Materials and Methods

Tissue collection

Adult bovine ovaries were collected and transported to the lab as described in section 2.1.1. Tissue was then vitrified (section 2.1.2) for long term storage until required.

Fluorescently activated cell sorting (FACS) of bovine oogonial stem cells (bOSCs)

Vitrified adult bovine ovarian cortical tissue was thawed (section 2.1.3), then enzymatically and mechanically digested (section 2.2.1) to a single cell suspension. This suspension was then treated with FACS blocking solution (2% goat serum and 2% bovine serum albumin in HBSS without calcium and magnesium) to prevent non-specific binding of the secondary antibody (section 2.2.2). Samples were then exposed to the DDX4 primary antibody (section 2.2.3) followed by the secondary antibody (goat anti-rabbit conjugated with APC; section 2.2.4). Two negative control samples (no antibodies and secondary antibody only) were also utilised. Cells were sorted using a BD FACS Aria machine (BD Bioscience), details of this protocol are outlined in section 2.2.5, and the gating strategy described in Figure 2.3. Cells were placed in culture for propagation and establishment of a colony (section 2.6.1.1)

Fluorescently labelled bOSCs were also analysed for the presence of the fluorescent marker. Cells were trypsinised and re-suspended in 500µL FACS buffer (50µL of FBS in 5ml HBSS) with 0.5µL DAPI to distinguish between live and dead cells. The single cell suspensions were sorted by a BD FACS Aria machine to distinguish between fluorescently labelled and unlabelled bOSCs. Cells were returned to culture after cell sorting (section 2.6.1.1).

Derivation of fetal bovine somatic cells

Fetal bovine somatic cells were derived from fetal bovine ovaries (gestational age 163.5 days) immediately following delivery from the local abattoir (section 2.1.1) as described in section 2.3 and cultured according to section 2.6.1.2. Briefly, ovaries were enzymatically and mechanically digested with Collagenase type IV (10mg/ml in HBSS) and 19 gauge needles. Tissue and collagenase mix were placed in a thermomixer at 37^{o}C, shaking at 112 RCF for 10 minutes. 50µl of DNAse I (7mg/ml

in HBSS) was added to the tissue mix and returned to the thermomixer for a further 5minutes shaking at 37ºC. The cell suspension was then centrifuged at 600g for 5minutes and the cell pellet was washed twice with 1ml of HBSS. Cells were then suspended in fetal ovarian somatic cell media (section 2.12) and filtered through a 70μm filter (Becton Dickenson), centrifuged at 600g and re-suspended in 1ml fetal ovarian somatic cell media and split between an appropriate number of wells in a 12 well plate and the volume of each well made up to 1ml with fetal somatic cell media.

Cells were washed twice with pre-warmed PBS (Life Technologies) and new fetal somatic cell media was added (section 2.12) after overnight culture and maintained as described in section 2.6.1.2.

RNA extraction, cDNA synthesis and RT-PCR

To determine the expression of mRNA transcripts characteristic of germ and pluripotent cells, RT-PCR was performed. RNA extraction, cDNA synthesis and RT-PCR protocols are outlined in section 2.10 and primer pairs detailed in Table 3.1. mRNA transcripts investigated are detailed in the chapter (section 3.3.2).

Table 3.1: PCR primer pairs used to characterise putative bOSCs

Gene Target	Forward Primer	Reverse Primer
β-ACTIN	CTCTTCCAGCCTTCCTTCCT	GGGCAGTGATCTCTTTCTGC
OCT4	CGAAGCTGGACAAGGAGAAG	AGAGAACCCCCAGGGTGAG
LIN28	GGCCGTGGAGTTCACCTTTA	GTGGCAGTTTGCACTCCTTG
IFITM3	CACATCCCAGCCCTTGTTCA	TGTTGAACAGGGACCACACG
PRDM1	CAAATGCCAGACGTGCAACA	GTGCACAAACTGCGTGAACT
DDX4	TATATGGGGGAACCCAGTTG	CATATCCAGCATGCGATC
DAZL	GAAGGCAAAATCATGCCAAACAC	CTTCTGCACATCCACGTCATTA
C-KIT	AACACAATGGGACGGTGGAG	AGGGTGTGAGCATGGATTTGT

Immunocytochemistry

Expression of proteins (details in Table 3.2) within bOSCs were analysed by immunocytochemistry (section 2.6.3) after cell fixation using 50:50, Ethanol:Methanol (section 2.6.3.2) and permeabilisation.

Table 3.2: Antibodies used in immunocytochemistry of cells

Antibody	Dilution	Species	Detection method	Supplier
Tetramethylrhodamine	1:3000	Rabbit	Tyramide	Life Technologies
DDX4	1:300	Rabbit	Streptavidin	Abcam
DAZL	1:800	Mouse	Streptavidin	AbDSerotec
C-KIT	1:100	Rabbit	Streptavidin	DAKO
LIN28	1:500	Rabbit	Streptavidin	Abcam
OCT4	1:250	Mouse	Streptavidin	Santa Cruz
IFITM3	1:500	Rabbit	Streptavidin	Abcam

Fetal bovine somatic cells (FBSCs) labelled with rhodamine dextrans were fixed with NBF (section 2.6.3.2) and immunostained for the presence of rhodamine using a tetramethylrhodamine antibody (details in Table 3.2) to assess the viability of the dextrans to trace cells post fixation (section 2.6.3).

Slides were visualised using a Zeiss LSM 780 confocal microscope and scale bars were embedded in the images using Zeiss software.

Labelling of cells

bOSCs were labelled with either fluorescent lentivirus (section 2.6.2.1), cell tracker dye (section 2.6.2.2) or fluorescent dextrans (section 2.6.2.3) for further assessment. The viability of these methods for long term assessment of bOSCs were analysed by visual assessment of the cells and their fluorescent label using live cell imaging (section 2.9.2), cell growth was monitored following labelling and compared to unlabelled cells. FBSCs were also labelled with Rhodamines dextrans in culture as described in section 2.6.2.3.

To assess the amount of fluorescence in cells, corrected total cell fluorescence (CTCF) was calculated using the equation below. Analysis was conducted using ImageJ and Graphpad Prism 6 software.

$$CTCF = Integrated\ Density - (Cell\ area\ x\ Mean\ background\ fluorescence\ )$$

Mean background fluorescence was calculated based on 5 random background readings within each image.

Data are presented as Mean ± SEM throughout.

3.3 Results

3.3.1 Isolation and *in vitro* culture of putative bovine oogonial stem cells from adult bovine ovary using FACS against DDX4

Putative bovine oogonial stem cells were consistently isolated from pooled adult bovine ovaries (15 ovarian cortical pieces per experiment) using FACS against the epitope DDX4. A representative sort is shown in Figure 3.1. The parameters for the isolation of bOSCs were established using two control populations of disaggregated bovine ovarian cells; unstained control sample and secondary antibody only control (primary antibody was omitted). Single cells were assessed for their uptake of DAPI to determine viability and APC for DDX4 expression. Control samples (unstained and secondary antibody only) contained only viable and non-viable APC negative cells, thus omission of the primary antibody resulted in no cells identified as DDX4 positive (Figure 2.1. G, H, J and K).

The addition of the DDX4 antibody to samples identified DDX4 positive cells within ovarian bovine cell populations. DDX4 positive cells were further sub-divided into two populations based on size. The first population (Q4, outlined in red in Figure 3.1.I) of cells were smaller in size but greater in number than the second (Q4.1, outlined in red in Figure 3.1.L) population which were larger in size and fewer in number. DDX4 positive cells constituted a small proportion of the total ovarian cortical cell population assessed, 3.6% ± 1.64% and 2.4% ± 1.41% for Q4 and Q4.1 respectively.

Both DDX4 positive cell populations established in culture and no differences were observed between the two populations. Both populations were used in subsequent experiments.

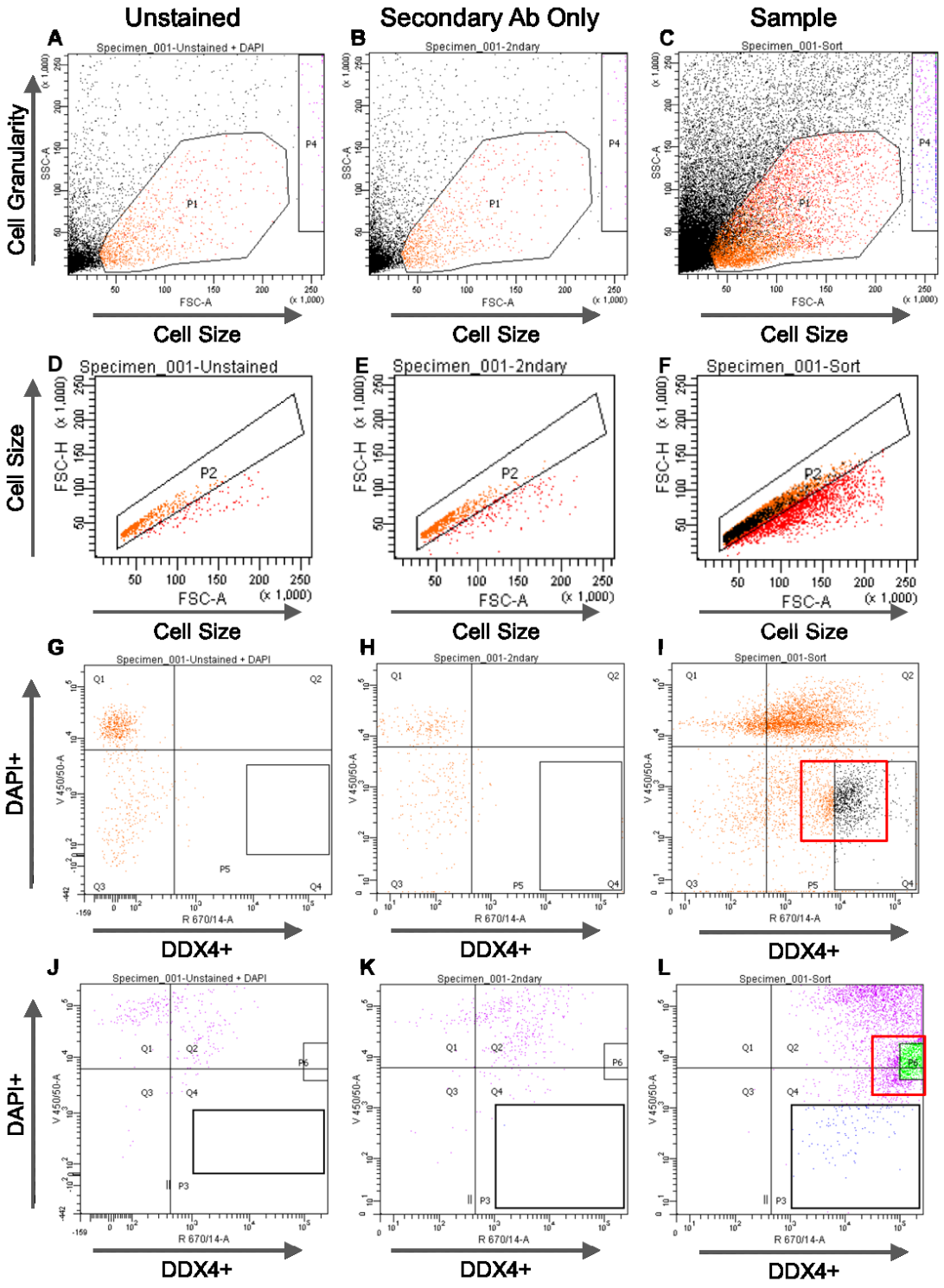

Figure 3.1: Fluorescently activated cell sorting of putative bovine oogonial stem cells. A representative plot of the isolation of bOSCs from adult bovine ovarian cortex. Left hand panels (unstained, **A, D, G** and **J**) represent an unstained sample, where both the primary and secondary antibodies are omitted. Centre panels (secondary antibody only, **B, E, H** and **K**) represent a negative control where the primary antibody is omitted and the right hand panels (**C, F, I** and **L**) are

representative of a complete sort. All events (**A, B** and **C**) are shown as dots and cells selected based on size and granularity (P1 and P4), and are then sorted as single cells (P2) based on cell size on forward and side scatter (**D, E** and **F**). Cells are then determined as live/dead based on DAPI uptake (y-axis) and DDX4 negative or positive based on APC detection (x-axis) shown in panels G, H and I. A larger cell population (P4) was also identified during the initial sort and were also sorted (**J, K** and **L**). The red boxes identify putative bOSC populations determined by FACS isolation against DDX4.

Following isolation, DDX4 positive cells were cultured long term and were visually assessed to detect any visual phenotypical changes. Figure 3.2 shows putative bOSCs across a range of passages (5-20); no phenotypical changes were observed in these cells during culture. Putative bOSCs were maintained in culture long term (> 6months) and underwent several passages (>20).

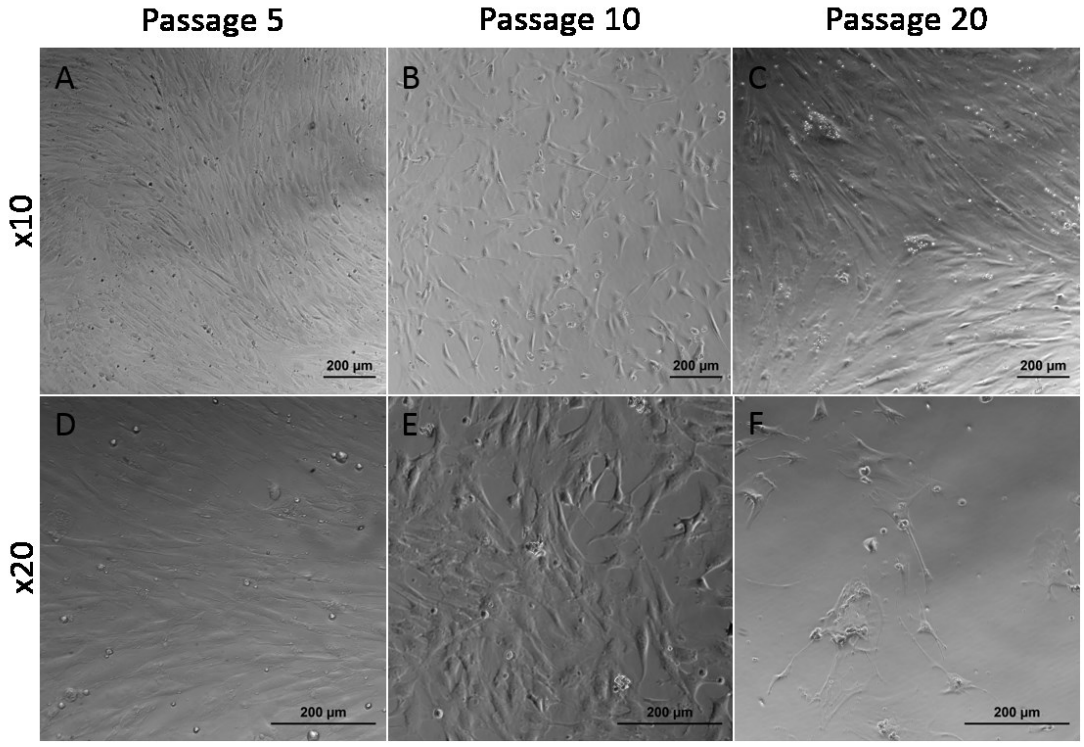

Figure 3.2: Bovine Oogonial Stem Cells visualised live in culture. bOSCs were cultured long term in OSC media following isolation and were maintained at 37ºC in humidified air with 5% CO_2. bOSCs are shown here at passage 5 (**A** & **D**), 10 (**B** & **E**) and 20 (**C** & **F**) at two different magnifications (Top panels imaged at x10 magnification and bottom panels imaged at x20 magnification.). Scale bars represent 200µm.

3.3.2 Putative bOSCs express pluripotency and germ cell markers

RT-PCR was performed on putative bOSCs in culture across different passages to determine the presence and maintenance of mRNA transcripts associated with pluripotency and germ cell lineage, throughout culture. Attempts were made to analyse the expression of genes in putative bOSCs immediately after isolation, however, low cell numbers and total RNA failed to detect housekeeping genes within these samples therefore gene expression analysis was not possible.

Transcripts encoding pluripotency and germ cell associated genes were present in fetal bovine ovary, which served as a positive control (Figure 3.3.A). Pluripotency genes, *LIN28* and *OCT4* were consistently observed to be expressed in putative bOSCs throughout culture. Furthermore, genes restricted to the germ line were also expressed. *IFITM3* and *PRDM1*, markers of early primordial germ cells (PGCs) during mammalian embryogenesis were consistently detected in cultured putative bOSCs (Figure 3.3.A). Expression of *C-KIT*, a PGC marker associated with migration was also detected in bOSCs (Figure 3.3.A). However, the post-migratory PGC markers *DAZL* and *DDX4*, showed little or no expression in putative bOSCs respectively (Figure 3.3.A). *DAZL* expression is established in PGCs upon colonization of the developing gonads and is essential for germ cell competence. Its expression precedes *DDX4* in developing PGCs. Therefore, these results suggest that putative bOSCs maintain gene expression profiles similar to late migratory and/or early post-migratory PGCs. Housekeeping gene, *β-ACTIN*, was expressed in all samples assessed.

Putative bOSCs were isolated from adult bovine ovaries based on the cell surface expression of DDX4. However, it was not possible to examine *DDX4* expression in isolated cells due to low numbers. The absence of *DDX4* expression from cultured putative bOSCs, may suggest loss of expression from during *in vitro* culture or may indicate the absence of *DDX4* expression in putative bOSCs entirely. Negative controls (samples with reverse transcriptase omitted samples and water controls), showed no detectable transcripts.

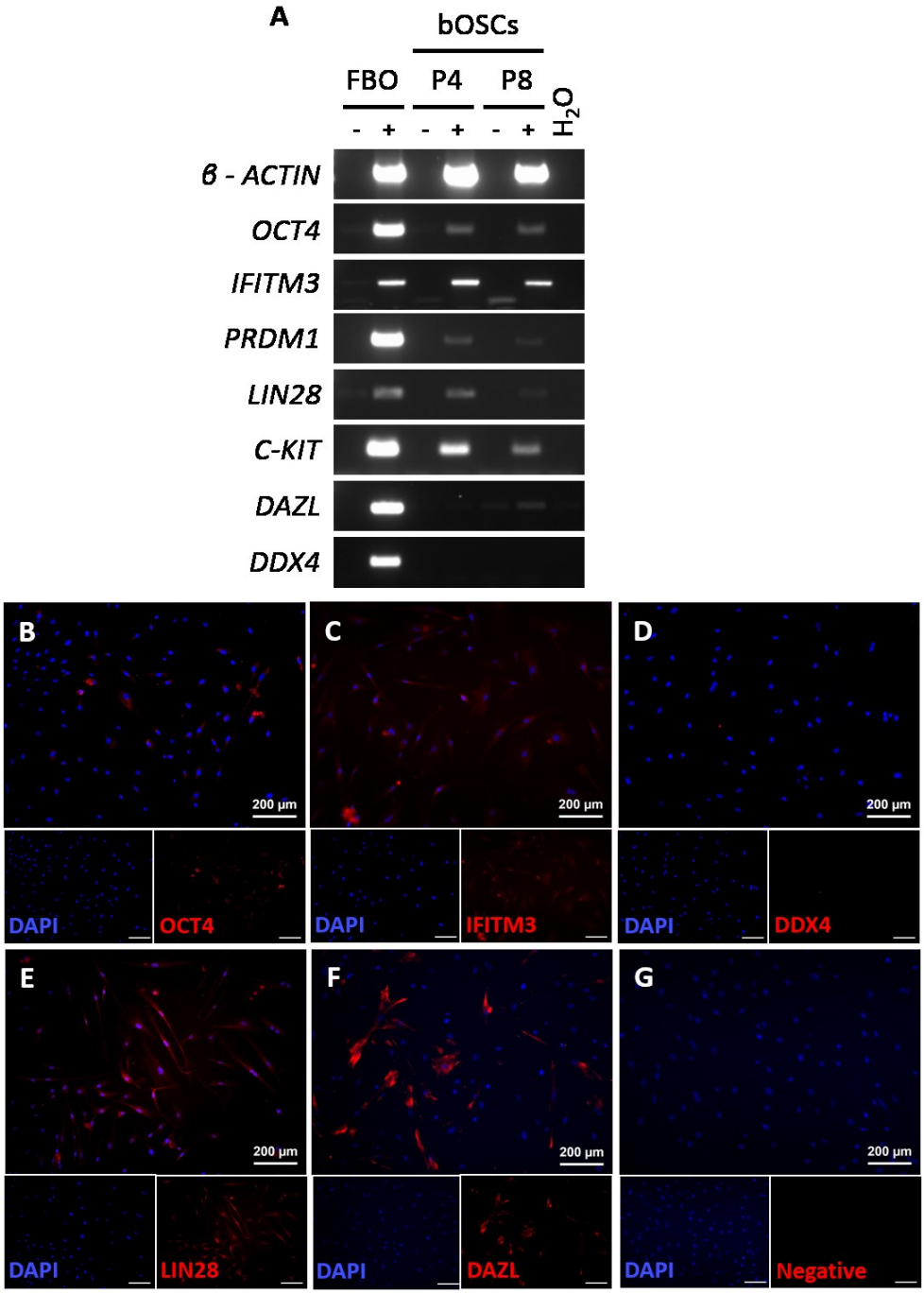

Figure 3.3: Putative bOSCs express markers associated with pluripotency and germ cell lineage. Cultured bovine OSCs (passage 4 and 8 shown) were characterised by RT-PCR (**A**). *OCT4*, *IFITM3*, *PRDM1*, *LIN28*, *C-KIT*, *DAZL* and *DDX4* transcripts were analysed in addition to house-keeping gene *β-ACTIN*. Fetal bovine ovary (FBO) RNA was a positive control, reverse transcriptase omitted (-) and water controls were negative controls. Pluripotency markers OCT4 (B) and LIN28 (E) were expressed in bOSCs, as were germ cell markers IFITM3 (C) and DAZL (F). DDX4 expression was not observed in bOSCs (D). Primary antibody omitted sample was used as a negative control (**E**). Cells were passage 6 and imaged at x10 magnification, scale bars represent 200µm.

Immunocytochemical analysis was used to investigate protein expression in cultured bOSCs. OCT4 a transcription factor associated with cell pluripotency and LIN28, an RNA binding protein known to regulate the self-renewal of stem cells were expressed in cultured putative bovine oogonial stem cells (Figure 3.3.B and Figure 3.3.E, respectively). OCT4 expression was consistently observed in close proximity to or co-localised to cell nuclei (Figure 3.3.B), suggesting that OCT4 may be actively regulating gene transcription within these bovine cells. The early germ cell marker IFITM3 (Figure 3.3.C) associated with germ cell specification and the germ cell marker DAZL (Figure 3.3.F) which is first expressed in germ cells after migration to the genital ridges in fetal life, were both expressed by cultured bovine cells which were DDX4 positive by FACS isolation. However, DDX4 was not identified in cultured bOSCs (Figure 3.3.D). Absence of DDX4 from putative bOSCs in culture suggests that bOSCs do not express DDX4 at isolation or DDX4 expression is lost in bOSCs in culture. Further characterisation of putative bOSCs at isolation is essential to determine if the use of DDX4 as an epitope for OSC isolation is appropriate. The protein expression profile of putative bOSCs appears to be similar to early post-migratory PGCs which maintain pluripotency but acquire germ cell competence through the expression of DAZL. However, protein expression of these pluripotency and germ cell associated markers was variable in cells and not all cells expressed them. This suggests that the population of bovine ovarian cells isolated by FACS and cultured is heterogeneous. Primary antibody omitted negative control samples showed no staining (Figure 3.3.E).

Taken together the mRNA and protein expression data of these bovine ovarian cells isolated based upon the assumed cell surface expression of DDX4, suggests that the cells share both pluripotent and germ lineage characteristics. Furthermore, the cells appear to share gene and protein expression characteristics with late migratory and/or early post-migratory primordial germ cells. These cells also share many characteristics with putative OSCs of other species. Therefore, these cells have been characterised as adult bovine oogonial stem cells.

3.3.3 Labelling of bOSCs

Once established in culture, bOSCs were fluorescently labelled using different methods to allow tracking of this cell population in subsequent experiments. Successful labelling of bOSCs would allow testing of the functional capabilities of these cells and importantly not impede their potential.

An mCherry tagged lentivirus was used to label a population of bOSCs. The fluorescent mCherry protein would be expressed under the stem cell promoter SFFV in bOSCs. Cells were transfected with Lv-cppt-SFFV-IRES-mCherry-opre at different ratios; 1, 5 or 10 lentiviral particles to bOSCs, to identify the optimal transfection rate. Uptake of the lentivirus was confirmed by visualisation of the fluorescent mCherry protein in live cells within 72 hours of transfection as shown in Figure 3.4.A-C. To assess and quantify transfection rates, cells were analysed by FACS for the presence of mCherry protein, 7 days after transfection. 18.1%, 88.8% and 82.8% of bOSCs were found to express mCherry protein following transfection with 1, 5 or 10 particles of lentivirus to bOSCs, respectively (Figure 3.4.D-F). These data indicate that the 5:1 ratio yielded the most efficient transfection ratio.

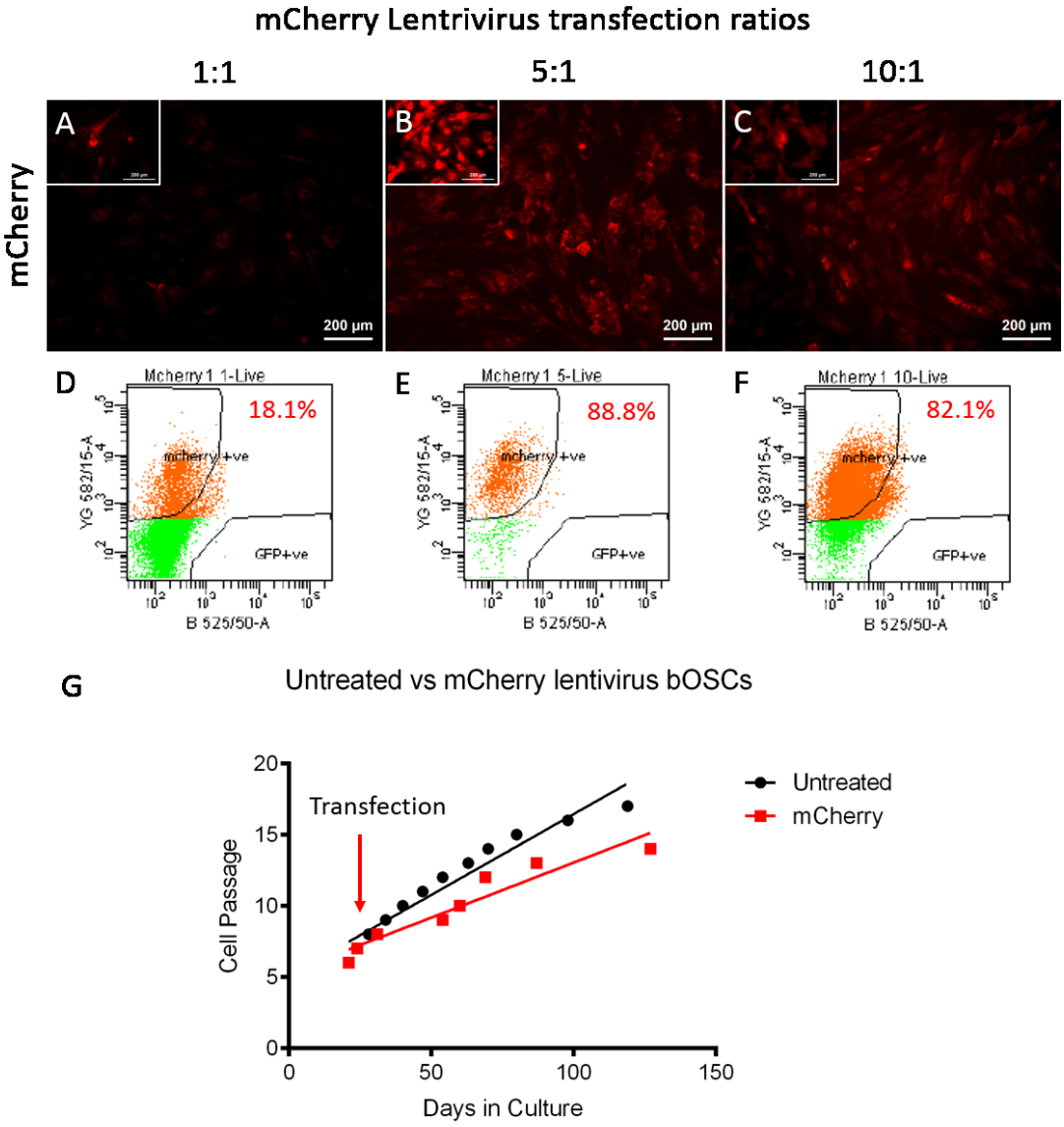

Figure 3.4: mCherry Lentiviral Labelling of bOSCs. bOSCs were transfected Lv-cppt-SFFV-IRES-mCherry-opre for future tracking of the cells. Initially three different ratios were used 1:1, 5:1 and 10:1, lentivirus to bOSCs respectively. The expression of mCherry protein could be detected in live cells (A, B, C) at all three ratios, although expression appeared stronger at 5:1 and 10:1. Cells were imaged at x10 magnification and insets imaged at x20 magnification, scale bars represent 200µm. Cells were then analysed by FACS for the expression of mCherry to determine the level of lentiviral uptake and expression (D, E, F). mCherry positive cells are represented in orange, cells negative for mCherry expression are shown in green. The percentage of total cells expressing mCherry is shown in red. The growth of cells transfected with 5:1 lentivirus: bOSCs was monitored to assess the effect of lentiviral transfection (G). Cells were passaged at a ratio of 1:2 once confluent. Growth of cells transfected with lentivirus appeared to decrease compared to non-transfected controls.

Cells were further propagated in culture, but a decline in growth rate was observed compared to untreated control cells (Figure 3.4.G). Corrected total cell fluorescence was calculated to assess the stability of the fluorescent label in cells successfully transfected. Figure 3.5 shows that bOSCs successfully labelled with Lv-cppt-SFFV-IRES-mChery-opre at a ratio of 5:1 maintained stable mCherry fluorescence 4 weeks post labelling. However, 12 weeks post transfection, bOSCs treated with 5:1 mCherry lentivirus and maintained in culture were reanalysed by FACS for mCherry expression, at which point only 1.07% of cells were mCherry positive. Although the mCherry fluorophore signal remained strong, these results taken together indicate that mCherry lentivirus was detrimental to the growth and health of bOSCs and over long term culture the mCherry positive bOSC population was not stable.

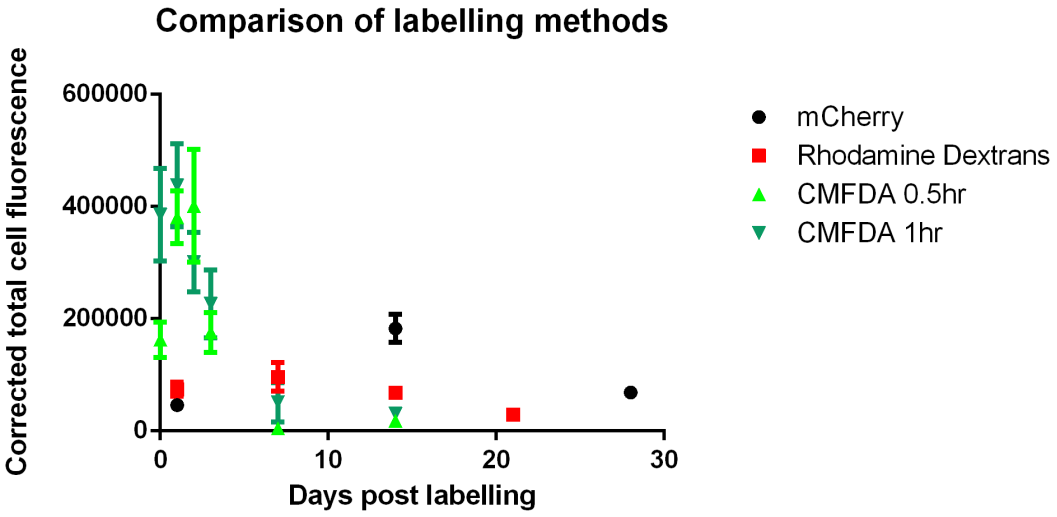

Figure 3.5: Corrected total cell fluorescence (CTCF) of fluorophores used to label bovine Oogonial Stem Cells. Average CTCF of 5 cells for each label and time point are plotted +/- SEM. Fluorescence was measured in each cell using ImageJ and corrected for cell area and background fluorescence.

To avoid cellular toxicity of bOSCs, alternative methods of fluorescent labelling were sought out. CMFDA (5-chloromethylfluorescein diacetate) cell tracker dye, a fluorescent dye able to freely pass through cell membranes into cells, where it transforms into a cell-impermanent fluorescent product, was used to label bOSCs. The dye was applied to bOSCs in culture for 30mins or 1hour when 50% confluent. Following treatment with CMFDA, cells were visualised live to assess CMFDA

presence over 14 days. Figure 3.6 illustrates the presence of CMFDA in bOSCs after both exposure lengths alongside untreated control bOSCs. CMFDA could be visualised in live bOSCs for 72hours post labelling, however CMFDA label was restricted to unhealthy or dead cells by 7 and 14 days post labelling. Quantification of CMFDA fluorescence by corrected total cell fluorescence (CTCF) shown in Figure 3.5, revealed a decrease in fluorescence from 48hours post labelling for both exposure groups. The decline in cell health as a result of CMFDA labelling (Figure 3.6) and the poor long term stability of the label (Figure 3.5) suggest that CMFDA would not be an appropriate method for long term labelling of bOSCs.

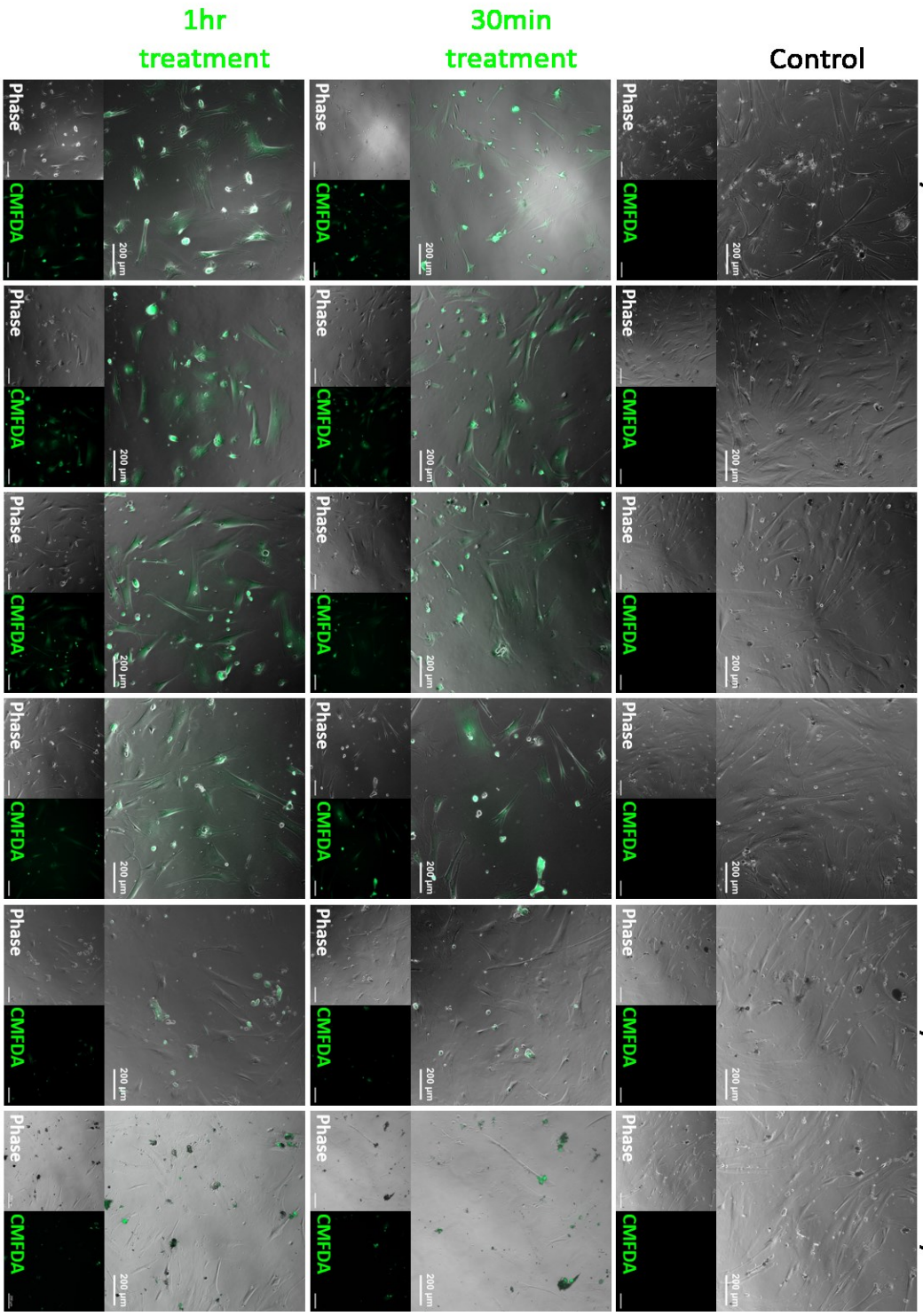

Figure 3.6: Labelling of bOSCs with CMFDA. bOSCs were labelled with green cell tracker, 5-chloromethylfluorescein diacetate (CMFDA), as a possible method to track bOSCs in subsequent experiments. Cells were treated with 3.33ug/ml of CMFDA in DMEM for 30 minutes (middle panels) or 1 hour (bottom panels) before washing and visualisation. Control samples were untreated (top panels). Cells were imaged at x20 magnification, scale bars represent 200µm.

Dextrans are complex polysaccharides which are actively transported into cells by endocytosis. Fluorescently (rhodamine) labelled dextrans (10,000 MW) were used as an alternative labelling method to track bOSCs. bOSCs were labelled with 100μg/ml of rhodamine dextrans overnight to allow sufficient uptake of the molecules into the cells, which had previously been determined in the laboratory as an optimum concentration and exposure time through titration. bOSCs were then visualised live to assess the potential of the fluorescent dextrans as a labelling tool. Control untreated cells showed no rhodamine fluorescence as seen in Figure 3.7.E-H, whereas bOSCs treated with rhodamine dextrans illustrated rhodamine detection over a period of 21 days (Figure 3.7.A-D). Figure 3.7 shows that rhodamine dextrans were maintained within live healthy bOSCs, which underwent several passages and showed no difference in growth rate compared to control unlabelled bOSCs. Corrected total cell fluorescence did illustrate a decrease in average cell fluorescence after 14 days of culture (Figure 3.5), thus long term (>14 days) labelling of bOSCs using rhodamine dextrans may not be a viable option.

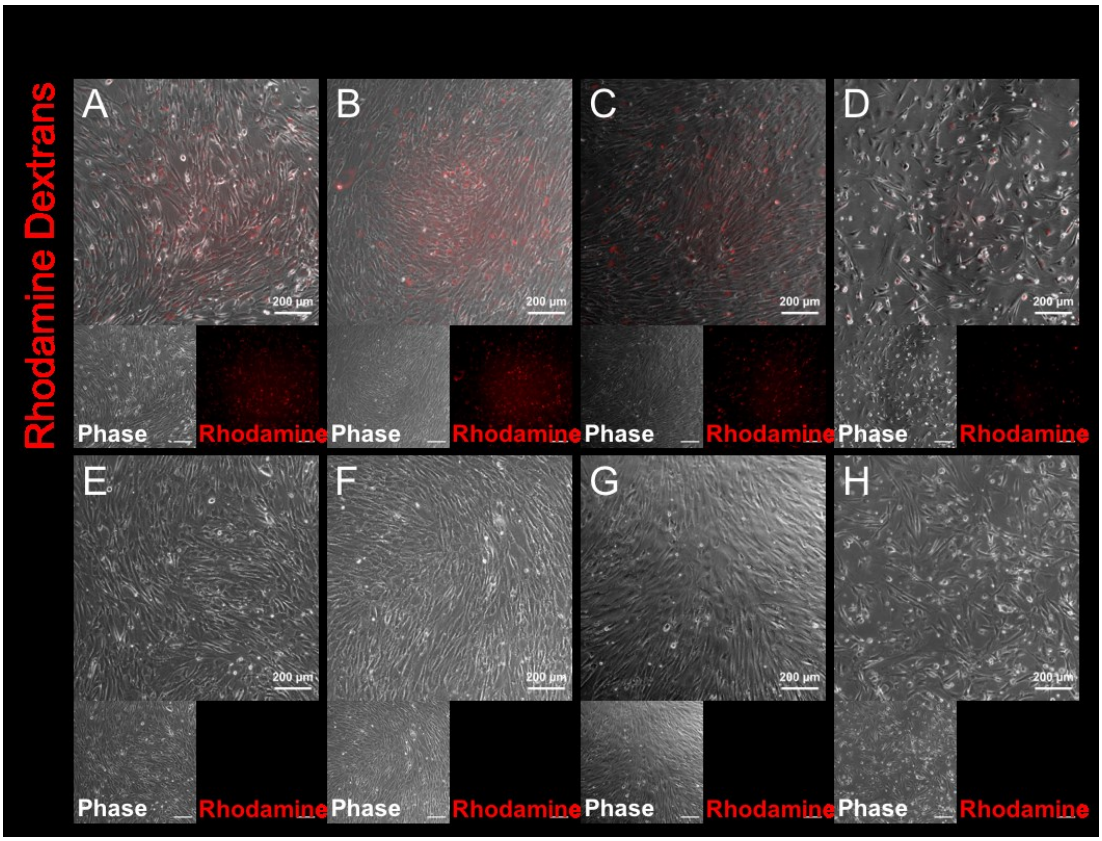

Figure 3.7: Labelling of bOSCs with Rhodamine Dextrans. To assess the viability of rhodamine dextrans as a method to label and track bOSCs, cells treated overnight with 100µg/ml rhodamine dextrans in OSC media were visualised live over a time course of 21 days. Control untreated cells were also visualised and showed no rhodamine fluorescence (E, F, G and H). Following labelling, rhodamine could be detected within healthy live bOSCs continuously for 21 days (A, B, C and D) and through several passages. Cells were imaged at x10 magnification, scale bars represent 200µm.

A suitable fluorescent label would also need to be detectable following fixation. To investigate the detection of dextrans following fixation, fetal bovine somatic cells (FBSCs) were labelled overnight with 100µg/ml Rhodamine Dextrans in FSC media and cultured for a further 7 days. Cells were then fixed with NBF and subjected to immunocytochemistry to detect rhodamine presence. Figure 3.8 shows FBSCs with (Figure 3.8.E, F, G and H) and without (Figure 3.8.A, B, C and D) rhodamine dextrans. Rhodamine dextrans were easily visible in live (Figure 3.8.E) and NBF fixed (Figure 3.8.F) FBSCs. Anti-rhodamine antibody co-localised to rhodamine fluorescence following immunocytochemistry (Figure 3.8.G; blue staining) and no

staining was observed in the primary antibody omitted control (Figure 3.8.H). Unlabelled FBSCs also showed no staining for rhodamine (Figure 3.8.C). Thus, rhodamine dextrans maintain their fluorescence following fixation and allow tracking of bOSCs in future experiments without further intervention.

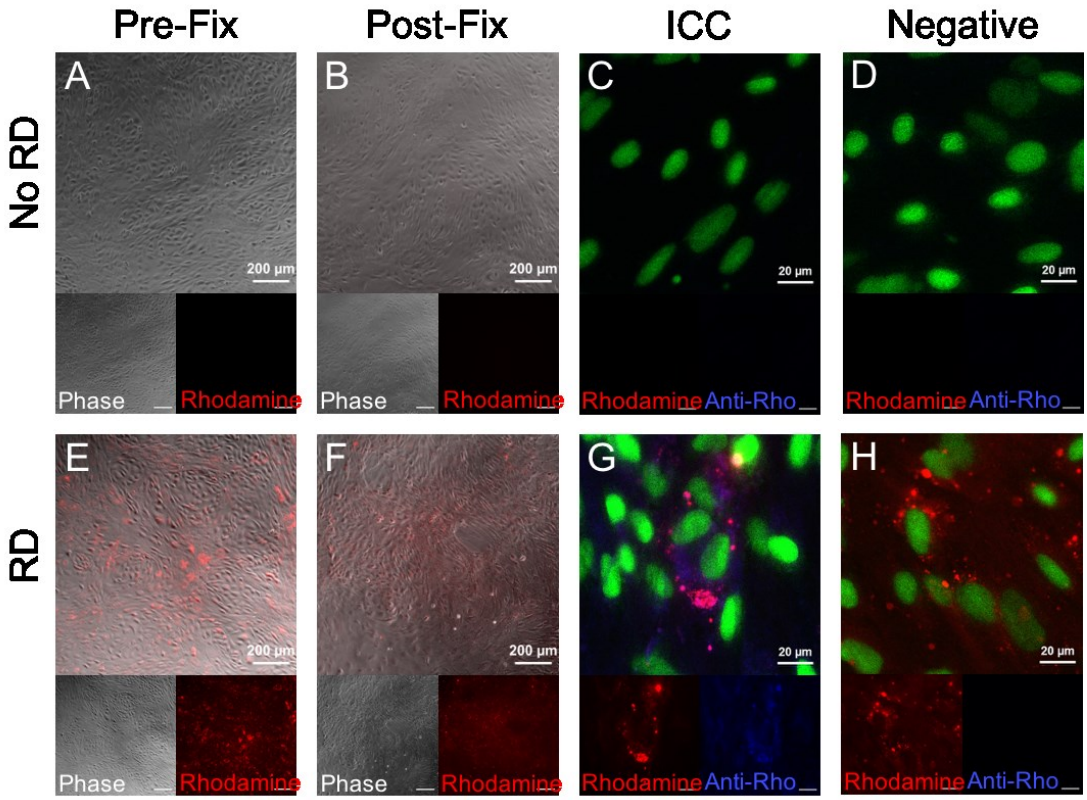

Figure 3.8: Maintenance of rhodamine dextran fluorescence following fixation. Fetal bovine somatic cells -/+ rhodamine dextrans (100ug/ml) visualised prior to fixation (A and E, respectively). Cells were then fixed with NBF for 10 minutes and re-visualised (B and F). Rhodamine fluorescence was maintained in fetal bovine somatic cells containing rhodamine dextrans following fixation with NBF. Immunocytochemistry was carried out against rhodamine, no signal was observed in FBSC's without rhodamine dextrans (C), whereas anti-rhodamine signal (marked by blue fluorescence) was found to co-localise to the cytoplasm of FBSC's containing rhodamine dextrans (G). Negative controls where primary antibody was omitted show no anti-rhodamine signal (D and H). Sytox green was used as counterstain for immunocytochemistry. Cells were imaged at x10 magnification pre- (A and E) and post- (B and F) fixation, and scale bars represent 200µm in images A, B, E and F. Cells were imaged at x63 following immunocytochemistry and scale bars represent 10µm in images C, D, G and H.

3.4 Discussion

The ovary is a highly dynamic organ capable of dramatic cyclical remodelling to generate a pre-ovulatory follicle containing a functional oocyte, followed by the formation, maintenance and degradation of a corpus luteum in the absence of a pregnancy. Yet the mammalian ovary was believed to be incapable of generating new oocytes in adult life, with the exception of a few prosimian primates (*Loris tardigradus lydekkerianus* and *Nycecticebus coucang*) (David et al., 1974; Duke, 1967) and bat species (*Artibeus jamaicensis, Glossophaga soricina* and *Sturnira lilium*) (Antonio-Rubio et al., 2013). The apparent identification of a population of mitotically active germ cells in the adult murine ovary by Johnson and colleagues (2004) has opened a new avenue of research in ovarian biology.

Isolation of mitotically active cells which co-express markers associated with pluripotency and germ lineage, termed oogonial stem cells, from adult ovaries has been reported in several different mammalian species, including humans (Hernandez et al., 2015; Pacchiarotti et al., 2010; White et al., 2012; Woods and Tilly, 2015; Zhou et al., 2014; Zou et al., 2009). The data presented here show the isolation of cells from adult bovine ovaries with characteristics similar to those reported in other species.

Putative bovine OSCs were FACS isolated following tissue dissociation, using the germ cell marker DDX4. DDX4 is an RNA helicase, with restricted expression in the germline in mammalian species (Castrillon et al., 2000; Toyooka et al., 2000). The use of Ddx4/DDX4 as an external cellular epitope for FACS isolation of OSCs (Imudia et al., 2013; Park et al., 2013; White et al., 2012; Zou et al., 2009) has provoked controversy (Albertini and Gleicher, 2015). Computational analysis has provided conflicting reports as to whether Ddx4/DDX4 contains a transmembrane domain (White et al., 2012; Zarate-Garcia et al., 2016). The successful isolation of putative OSCs based on Ddx4/DDX4 cell surface expression suggest that Ddx4/DDX4 can be expressed on the cell surface (Imudia et al., 2013; Park et al., 2013; White et al., 2012; Zou et al., 2009). Analysis using N- and C- terminus antibodies suggested that these protein terminuses are located intracellularly and extracellularly, respectively (White et al., 2012). However, it has been speculated

that the DDX4 antibody utilised for FACS isolation may cross-react to an alternative epitope expressed in putative OSCs (Hernandez et al 2015). Cells within the adult porcine testis were found to express DDX4 at the cell surface (Kakiuchi et al., 2014), suggesting that DDX4 can be located at the cell surface. Expression of DDX4 through transfection of human OSCs with a tagged DDX4 lentivirus showed no cell surface DDX4 expression (Hernandez et al., 2015). In contrast DDX4 plasmids induced DDX4 cell surface expression within porcine testicular cells (Kakiuchi et al., 2014). These results suggest that the cellular location of Ddx4/DDX4 may be cell specific. Furthermore, it has been hypothesised that Ddx4 may internalise in putative murine OSCs as the progress through germ cell development (Imudia et al., 2013; White et al., 2012). This thesis has not focused on the structure or cellular location of Ddx4/DDX4. However, the use of DDX4 to identify and isolate putative bOSCs shown here, and the absence of a DDX4 positive cell population with omission of the primary antibody, suggests that these cells are being isolated based on DDX4 expression.

The putative OSC population in the adult bovine ovary was determined to make up a small proportion, no more than 5% of the total live intact cells from the disaggregated ovarian cell population. Isolated cells were successfully established and maintained in culture, as described in other species (Hernandez et al., 2015; Park et al., 2013; White et al., 2012; Zhou et al., 2014; Zou et al., 2009). However, to fully determine whether putative bOSCs were isolated based on the expression of DDX4 or cross-reaction of the antibody to another epitope analysis of freshly isolated cells would be essential. However due to low cell numbers it was not possible to determine the expression of *DDX4* within the cell population at the time of isolation. Thus, we cannot determine whether putative bOSCs were isolated based on DDX4 cell surface expression. Expression of *Ddx4*/*DDX4* in freshly isolated putative murine and human OSCs has been detected in some samples (White et al., 2012) and not in others (Hernandez et al., 2015) despite use of the same protocol. Even in the absence of *Ddx4*/*DDX4* expression at isolation murine, rhesus macaque monkeys and humans FACS sorted based on Ddx4/DDX4 expression were characterised as putative OSCs (Hernandez et al., 2015). This data provided the basis of the hypothesis that the DDX4 antibody cross-reacts with an alternative epitope on the

cell surface of putative OSCs. In contrast, Ddx4/DDX4 protein expression has been observed in freshly isolated and cultured mouse and baboon OSCs (Woods and Tilly, 2015). Although the issues surrounding the use of DDX4 as the epitope of choice to isolate putative OSCs are not addressed in this thesis, characterisation of DDX4 positive cells isolated from adult bovine ovaries has revealed a gene signature similar to those reported in other species.

Two populations of cells, differentiated by size, were identified as DDX4 positive and isolated as putative bovine OSCs. Both populations could establish in culture and previous characterisation in the laboratory showed that both populations shared characteristics. Putative bOSCs were found to express pluripotency markers *LIN28* and *OCT4*, early germ cell markers *IFITM3* and *PRDM1* and marker of germ cell competence *DAZL*, consistent with other reports of OSCs in the literature (Hernandez et al., 2015; Park et al., 2013; White et al., 2012; Zhou et al., 2014; Zou et al., 2009). However, the DDX4 gene and protein was not found to be expressed in cultured putative bOSCs. These results indicate that either putative bOSCs lose expression of DDX in culture, or lack DDX4 expression entirely and are selected based on a cross-reaction of the antibody during isolation. The gene expression pattern observed in bOSCs is similar to PGCs described at late migratory and/or early post-migratory stages and is indicative of an undifferentiated germ cell in adult bovine ovaries.

The variable protein expression identified in putative bOSCs suggests that the cultured population is heterogeneous. Analysis of freshly isolated cells would reveal whether this is a consequence of *in vitro* culture or a characteristic of the isolated population.

Putative bOSCs could be passaged in excess of 20 times and cultured continuously for 6 months, a characteristic consistently reported in murine OSCs (White et al., 2012; Zou et al., 2009). These data are indicative of a distinct population of germ cells with pluripotent hallmarks within the adult bovine ovary and are consistent with previous findings in our laboratory and reports of OSCs from other mammalian species (Hernandez et al., 2015; Pacchiarotti et al., 2010; White et al., 2012; Woods and Tilly, 2015; Zhou et al., 2014; Zou et al., 2009).

Successful labelling of bOSCs is essential to be able to investigate the function of the cells in subsequent experiments. Several labelling methods were investigated to deduce the most appropriate. Viral labelling has previously been used to label OSCs in the literature and has allowed the function of rodent and human OSCs to be tested when combined with ovarian tissue (Grieve et al., 2015; White et al., 2012; Zhou et al., 2014; Zou et al., 2009). Labelling of bOSCs with a fluorescent lentivirus caused a decrease in growth rate compared to un-transfected controls, suggesting that the virus may impede the function of these cells. To facilitate the transfection of the lentivirus into cells, Polybrene a cationic polymer was utilised. By neutralising the electrostatic repulsion between the cell surface and viral particles, polybrene facilitates the absorption of viral particles into the cell. At concentrations similar to those used here, polybrene was found to reduce cell proliferation in human mesenchymal stem cells which could not be overcome with treatments to increase cell proliferation (Lin et al., 2011). Polybrene did not increase cell death but decreased the number of cells entering the S phase of the cell cycle in a dose dependent manner. This suggests polybrene acts to reduce cell proliferation through prevention of cells replicating DNA in preparation for cell division and proliferation, although the underlying mechanism for this has not been determined (Lin et al., 2011). The reduction in bOSC growth rate may be associated with the effects of exposure to polybrene rather than the direct effects of the lentivirus. Use of alternative non-toxic transfection reagents may provide better outcomes for bOSC viral transfection in future experiments.

In an attempt to avoid cell toxicity, non-genomic labelling methods were utilised for bOSC labelling. CMFDA cell tracker dye, a fluorescent dye which passes into cells where it transforms into cell-impermanent fluorescent product successfully for 72 hours, but was not well maintained in bOSCs after this time. CMFDA has been utilised in cell migration assays (Beem and Segal, 2013) and also as a intracellular marker during cell events such as meiosis (Tarin and Cano, 1998). CMFDA is a temporary cell marker which can label cells for more than 6 generations, however it has also been suggested that cytoplasmic cell tracker dyes may be treated like toxins by certain cells (Beem and Segal, 2013). Over time CMFDA expression became restricted to unhealthy or dead cells, suggesting that bOSCs may have responded to

CMFDA as a toxin resulting in expulsion of the dye from cells or cell toxicity leading to death. Due to its limited labelling capacity in bOSCs, CMFDA was not utilised in subsequent experiments.

Rhodamine dextrans are fluorescently labelled complex polysaccharides which can be endocytosed into live cells and offer a gene-transfer-free rapid labelling method for bOSCs. Fluorescently labelled dextrans have previously been used in *in vivo* and *in vitro* tracing of cells from various tissue types including the brain, kidney, lungs and also in xenografts (Weigert et al., 2013). Rhodamine dextrans were clearly visible within live bOSCs up to 14 days. Although expression was detected in bOSCs after this point, it reduced over time. No negative effects were observed in bOSCs following dextran labelling and cell growth was not impacted. Rhodamine fluorescent dextrans persisted in cells following fixation and could be identified by immunocytochemistry with co-localisation of staining for anti-rhodamine antibody. Thus, rhodamine dextrans can be utilised to identify bOSCs after fixation. As dextrans are maintained within cell vesicles the decline in fluorescence observed in labelled bOSCs may be associated with endosomal recycling and this may limit the longevity of this label. The data presented here suggest that rhodamine dextrans are non-toxic to bOSCs and can label bOSCs for medium term tracing *in vitro*. Thus, rhodamine dextrans were utilised to label bOSCs for further investigation into their functional potential.

4 Development of an *in vitro* ovarian aggregation culture model

4.1 Introduction

Oogonial stem cells have been observed to spontaneously differentiate into oocyte-like cells (OLCs) *in vitro*, in rodents (Pacchiarotti et al., 2010; White et al., 2012; Zhou et al., 2014), pigs (Bui et al., 2014) and humans (White et al., 2012), with peak oogenesis observed following cell passage (White et al., 2012). These differentiated OSCs show an increase in cell size, to form large (35-60μm diameter) spherical cells expressing germ cell specific markers (*Ddx4/DDX4*, *Kit*/*KIT* and *Oct4*/*OCT4*) and oocyte specific genes (*Gdf9/GDF9*, *Zp1/ZP1*, *Zp2*/*ZP2* and *Zp3*/*ZP3*), which are absent from OSCs. OLCs derived from OSCs also exhibited large nuclei with diffuse chromatin (Pacchiarotti et al., 2010), characteristic of oocytes, in conjunction with the expression of meiotic proteins (Sycp3/SYCP3, YBX2 and LHX8) (Bui et al., 2014; White et al., 2012). Many also had zona pellucida structures surrounding the cell (White et al., 2012; Zhou et al., 2014), although these were not always observed (Zhou et al., 2014). Thus, OSCs may have the potential to undergo differentiation to form oocytes and enter meiosis in an *in vitro* culture. However further characterisation of *in vitro* OSC derived OLCs has revealed concerns over their meiotic and developmental competence. Ploidy analysis of OLCs revealed a population of haploid cells (White et al., 2012), a karyotype rarely reached in oocytes *in vivo* as fertilisation triggers the resumption of meiosis, although spontaneous resumption of meiosis has been reported in oocytes *in vivo* (Xu et al., 1997). Inconsistency in the presence of zona pellucida in OLCs derived from OSCs (Zhou et al., 2014) and concerns over the ploidy of the cells (White et al., 2012), suggest that while OSCs may harbour the potential to generate new oocytes, spontaneous differentiation of these cells *in vitro*, unsupported and unregulated by somatic cells has generated OLCs with abnormal development. Furthermore the potential of *in vitro* OSC derived OLCs to undergo successful fertilisation, meiosis and subsequent embryonic development has not been established and these are essential requirements for successful oogenesis (Handel et al., 2014).

Oocyte growth and development is a tightly regulated process *in vivo* to marry the development of the oocyte with the timing of ovulation. Somatic cells, in particular granulosa cells, are known to play a crucial role in regulating oocyte growth, development, health (Kidder and Vanderhyden, 2010) and the repression of meiotic resumption (Sun et al., 2009). The absence of granulosa cells in the differentiation of OSCs into OLCs in *in vitro* culture may be responsible for the aberrant nature of the cells. In cultures without any other cell type present, OSCs which undergo differentiation to form an OLC also appear to associate with undifferentiated OSCs to form follicle like structures (Bui et al., 2014; Pacchiarotti et al., 2010) suggesting that interaction with supporting cells is an element desired by OLCs to support this process. When co-cultured with ovarian somatic cells, OSCs been observed to form follicle like structures with somatic cells surrounding the OSC derived OLCs (Bui et al., 2014; Pacchiarotti et al., 2010). Upon re-introduction to the ovarian microenvironment *in vitro*, human OSCs transfected with GFP adenovirus formed new GFP positive oocytes encapsulated within host (GFP negative) somatic cells following a 7 day culture (Grieve et al., 2015). Thus, there is a strong argument that the ovarian somatic cell environment is crucial to support OSC differentiation into oocytes, and this may be necessary for meiotic and developmental competence, although these aspects have not been yet demonstrated. Development of a model including somatic cell support, replicating the ovarian niche, for OSCs is required to fully determine their potential to produce oocytes and understand the requirements of this process.

A chimeric ovarian aggregate model has previously been developed to investigate species differences in germ-somatic cell interactions (Eppig and Wigglesworth, 2000). Pairing rat oocytes with mouse somatic cells from neonatal ovaries and vice versa, the authors showed that oocytes and somatic cells from different species could interact to form follicles comprising of an oocyte with somatic cells which were exclusively of the alternative species, capable of initiating growth within a xeno-transplant model. These oocytes were also capable of meiotic resumption in both the mouse and rat and capable of fertilisation and embryo development using pseudo-pregnant foster mothers in the mouse. This study shows that germ-somatic cell interactions appear to be conserved across species. Due to limited fetal or neonatal

bovine tissue to generate a somatic cell niche for bOSCs, this chimeric ovarian aggregation model was utilised to investigate the differentiation potential of bovine oogonial stem cells. The development of an *in vitro* system will allow better control of the environment to elucidate the potential mechanisms by which OSCs undergo differentiation to OLCs.

4.2 Materials and Methods

Ovarian aggregation model

To investigate the potential of putative bovine oogonial stem cells (bOSCS), we developed a previously described ovarian aggregation model (Eppig and Wigglesworth, 2000) for use in *in vitro* culture systems. We utilised the somatic cells of neonatal murine ovaries to provide an ovarian niche for bOSCs. Negative (murine ovarian somatic cells only) and positive (murine germ and somatic cells) controls were also generated for comparison.

Bovine oogonial stem cells

bOSCs were FACS isolated (section 2.2) from adult bovine ovaries collected from the local abattoir (section 2.1). Following isolation bOSCs were cultured (section 2.6.1.1) in OSC media (section 2.12). Cells were also frozen and stored long term in liquid nitrogen (section 2.6.1.3) until required.

Disaggregation of neonatal ovaries

Ovaries were collected from neonatal (postnatal day 0-5) CD-1 female mice following cervical dislocation and placed in pre-warmed PBS supplemented with 1mg/ml BSA, then removed from their bursae. Ovaries were disaggregated (described in section 2.5.1) with pre-warmed trypsin/EDTA/DNAse and gentle agitation over a 25 minute period. The enzymatic digestion was neutralised with equal volumes with sterile supplemented M199 media (see section 2.12) and the cell suspension centrifuged at 450 RCF for 5 minutes. The cell pellet was then re-suspended in sterile supplemented M199 media (section 2.12) and placed into 35mm culture dishes for culture overnight 37^{o}C with humidified air and 5% CO_2.

Separation of germ and somatic cells

Germ and somatic cells from neonatal mice were separated based on cell adhesion characteristics as previously described (section 2.5.2), such that floating germ cells could be aspirated off the somatic cell monolayer. Germ cells were incubated in M199 with supplements at 37^{o}C, with humidified air and 5% CO_2 until required for aggregation. Somatic cells were washed twice with pre-warmed PBS supplemented

with 1mg/ml BSA, then lifted from the culture plate with 2ml of pre-warmed trypsin/EDTA/DNAse. The enzymes were neutralized with equal volumes of M199 with supplements and the somatic cell suspension was either filtered (size 30μm, 20μm or 10μm, CellTrics Partec) or not filtered then centrifuged at 450 RCFfor 5 minutes. The supernatant was then discarded and cells were re-suspended in M199 media with supplements, placed in a new culture dish and returned to 37^{o}C, with humidified air and 5% CO_2 for 5-6 hours.

Following a second incubation, the murine neonatal ovarian somatic cells were washed with 2 ml pre-warmed PBS, twice, lifted from the culture plate a 2nd time with pre-warmed trypsin/EDTA/DNAse, which was then neutralized with equal volumes of M199 with supplements and the somatic cell suspension was either filtered (size 30μm, 20μm or 10μm) or not filtered then centrifuged at 450 RCF for 5minutes. The supernatant was then discarded and cells re-suspended in an appropriate volume of Waymouths media with supplements (section 2.12) for cell counting, prior to aggregation.

Aggregation of ovarian cells

All cell populations used for aggregations (murine neonatal somatic cells, murine neonatal germ cells and bOSCs) were centrifuged at 2000rpm for 5 minutes and re-suspended in an appropriate volume of Waymouths media with supplements (section 2.12) for counting. Cell populations were manually counted using a haemocytometer and cells were then combined and placed into 0.5ml Eppendorf tubes with 35μg Phytohaemagluttanin (PHA) at the desired ratio/concentration to create different aggregates (Figure 2.4). Cells were mixed by brief vortex and centrifuged in a microcentrifuge at 11,200 RCF for 30 seconds, the 0.5ml eppendorfs were then rotated 180^{o} and cells were centrifuged at 11,200 RCF for 30 seconds a second time. Cell pellets (aggregates) were then transferred with 30μl of Waymouths media with supplements to a hanging drop culture overnight at 37^{o}C with humidified air and 5% CO_2 to encourage cell interaction and adhesion.

Positive control ovarian aggregate

Positive control aggregates recombined neonatal murine somatic cell and germ cell populations at varying ratios (Figure 2.4). Positive control aggregates were then cultured as described in section 2.6.4.

Negative control ovarian aggregate

To investigate the quality of our separation technique, negative control aggregates were generated, aggregating together mouse neonatal ovarian somatic cells only (Figure 2.4). Negative control aggregates were generated alongside every chimeric aggregate. Negative control aggregates were then cultured as described in section 2.6.4.

Chimeric ovarian aggregate

bOSCs were isolated (section 2.2), cultured (section2.6.1.1) and labelled with rhodamine dextrans (section 2.6.2.3) then aggregated together with neonatal mouse ovarian somatic cells at a ratio of 1:10 respectively (Figure 2.4). Chimeric aggregates were then cultured as described in section 2.6.4.

In vitro culture of ovarian aggregates

Ovarian aggregates generated as described previously (section 2.5.4) were cultured in either 1% alginate gel or a hanging drop as described below, after an initial overnight hanging drop culture to promote cell interaction.

Ovarian aggregates were cultured within a 1% alginate gel, cross-linked with pre-warmed $CaCl_2$ for 10 minutes, in Waymouths media with supplements (section 2.12) at 37^{o}C with humidified and 5% CO_2 as described in section 2.6.4.1. 50% of the volume of the medium was replaced with fresh medium on alternate days of culture.

Alternatively, ovarian aggregates were cultured in a hanging drop with sterile supplemented Waymouths medium (Section 2.12) continuously for the whole culture period and incubated at 37^{o}C with humidified air and 5% CO_2 as described in section 2.6.4.2. Aggregates were transferred to fresh medium on alternate days of culture and incubated at 37^{o}C with humidified air and 5% CO_2.

Xeno-transplant of ovarian aggregates

Positive ovarian aggregates (murine germ and somatic cells) following an overnight hanging drop culture in supplemented Waymouths media (section 2.12) were xeno-transplanted to the kidney capsule of SCID (severe combined immunodeficiency) mice for 7 days for comparison with the *in vitro* culture models.

All animal experiments were conducted under a UK Home Office licence in line with the Animals Scientific Procedure Act (1986). SCID (C.B-17/IcrHan Hsd-Prkdc^{scid}) mice from Envigo laboratories were housed as described in section 2.7 and given a minimum of 6 days to acclimatise to their new environment prior to the start of any experimental work.

Briefly, SCID mice were anaesthetised with isoflourane (section 2.7.1), shaved and skin sterilised. Subcutaneous injection of saline around the hind leg and a subcutaneous injection of vetergesic (at a dose of 0.03mg/ml in 100µl) around the neck were given. A longitudinal incision in the skin was made in the middle of the back, followed by a small incision in the body wall directly above the ovary, allowing the ovary and ovarian fat pad to be removed from the body cavity, and the ovary to be excised. Using the ovarian fat pad as a guide the kidney was pulled out of the body cavity with forceps. Sterile PBS kept the kidney moist and a tiny incision was made in the kidney capsule with a sterile needle. Using a pulled glass pipette, aggregates were transferred through the hole in the capsule to the surface of the kidney and moved from the incision site to ensure their security. The kidney and associated tissue was then returned to the body cavity, and the body wall sutured using number 5 polyglactin sutures. The ovary was then removed on the other side following the same protocol and the skin incision closed using wound clips. Mice were then transferred to individual cages which were maintained at 30ºC while they recovered and then housed as described in section 2.7 for 7 days until tissue collection.

7 days after xeno-transplantation, mice were culled by lethal exposure to CO_2 and tissues were collected, inspected and fixed as described below.

Histological Techniques

Aggregate ovarian tissue was fixed in natural buffered formalin (NBF) for 6 hours, then transferred to 70% ethanol and embedded in wax using an automated Leica TP1050 processor. Tissue was sectioned at 5μM and mounted onto electrostatically charged glass slides and maintained at 50^{o}C overnight in a slide oven to ensure tissue adherence to the slide surface.

Haematoxylin and eosin staining

Every third section of each ovarian aggregate was stained with haematoxylin and eosin for histological evaluation to detect the presence of oocytes and follicles. Slides were de-waxed and rehydrated (section 2.8.3) and washed briefly in running tap water, then stained with haematoxylin and eosin (section 2.8.4) before dehydration and mounting (section 2.8.5).

DAPI Counterstain

To identify the location of bOSCs based on the presence of rhodamine dextrans, tissue was counterstained with DAPI to view the fluorescence. Adjacent sections to previously stained H&E sections were counterstained with DAPI. Slides were de-waxed and rehydrated (section 2.8.3), then washed in running tap water, then washed twice in PBS. Slides were then incubated with DAPI, diluted 1:1000 in PBS, for 10 minutes in a humidity chamber at room temperature. Slides were then washed in PBS twice and mounted with coverslips (section 2.8.6.5).

Immunofluorescence

To assess tissue antigens, slides were dewaxed and rehydrated (section 2.8.3) prior to antigen retrieval (section 2.8.6). Slides were then washed and cooled in water 3 times. Non-specific binding of antibodies was prevented by using a peroxidase block followed by a serum block (section 2.8.6.1). Slides were then exposed to the primary antibody (listed in Table 4.1) diluted in NS/PBS/BSA and incubated overnight at 4^{o}C. Negative controls (primary antibody omitted) were always used and positive controls were used where applicable and appropriate.

Table 4.1: Primary antibodies used in Immunofluorescence in Chapter 4

Antibody	Dilution	Species	Supplier
Cleaved Caspase 3	1:100	Rabbit	Cell Signalling Technology
Dazl	1:100	Mouse	AbDSerotec
Tetramethylrhodamine	1:3000	Rabbit	Life Technologies

Primary antibodies were washed off with PBS for 5minutes, twice, and the appropriate secondary antibodies (listed in Table 4.2) were diluted 1:200 in blocking serum (NS/PBS/BSA) and applied to slides for 30minutes at room temperature in a humidity chamber.

Table 4.2: Secondary antibodies used in Immunofluorescence in Chapter 4

Antibody	Supplier
Chicken anti Rabbit	Santa Cruz
Chicken anti Mouse	Santa Cruz

Slides were then washed twice with PBS and incubated in tyramide in accordance with the manufacturer's instructions, for 10 minutes. Slides were then washed in PBS to remove the tyramide, in an opaque chamber to prevent bleaching of the fluorescence before counterstaining and mounting (section 2.8.6.5). Slides were then stored in the dark at 4^{o}C until visualisation (section 2.9.4).

Microscopy

Tissue histology was imaged with a Provis AX70 (Olympus) or a Zeiss Imager Z1 both fitted with a AxioCam HRc camera (Zeiss) using Zeiss software.

Live cell and tissue imaging was conducted using an Axiovert 200 fitted with a AxioCam HRc camera and a Hamamatsu camera for collection of images including fluorescent images. Cells and tissue were maintained at 37^{o}C with 5% CO_2 throughout live imaging.

Sections were visualised using a Zeiss LSM 780 confocal microscope using Zeiss software.

All scale bars were generated and embedded in image files using Zeiss software.

Tissue Analysis

All image analysis, measurements and cell counting was carried out using ImageJ software.

Every third section of all ovarian aggregates were stained with haematoxylin and eosin for histological assessment. For chimeric ovarian aggregates the subsequent sections were all DAPI counterstained to localise bOSCs within the tissue. The remaining unstained sections were used in immunofluorescent analysis.

Cells were counted using cell counter software on ImageJ per section and cell sizes and section areas were also measured using ImageJ following scale calibration.

Oocytes were counted when the nucleolus was present, and follicles classified based on their stage (primordial, a single layer of flattened granulosa cells; transitory, a mixture of flattened and cuboidal granulosa cells; primary, a single layer of cuboidal granulosa cells). Follicles were also classified as healthy (round oocyte containing a nucleus, even cytoplasmic staining with eosin and no pyknotic granulosa cells) or unhealthy (contraction of the oocyte from the granulosa cells, uneven or dark cytoplasmic staining of the oocyte, nuclear contraction and/or pyknotic granulosa cells).

Two measurements were taken for bOSC cell sizes, the first at the widest point of the cell and the second perpendicular to the first. The average of these two measurements was taken to establish the size of bOSCs.

Statistical Analysis

Statistical analysis was conducted using Graphpad Prism 6 software. One-way ANOVA analysis with post-hoc Tukeys multiple comparisons testing was used where three or more groups were compared when only one variable was present. Where only two groups were present a t-test was used to determine differences between groups.

4.3 Results

4.3.1 bOSCs do not spontaneously differentiate into oocyte-like cells in vitro

bOSC cultures were monitored for the presence of detached large spherical oocyte-like cells (OLCs) throughout culture. bOSCs did not appear to undergo spontaneous differentiation *in vitro*; no large cells were observed throughout their culture and across several different populations (different isolation dates) of bOSCs. As no oocyte-like cells were observed in bOSC cultures, further investigation of this process independently of extrinsic factors could not be undertaken and alternative techniques were utilised to investigate the differentiation potential of bOSCs.

4.3.2 Separation of germ and somatic cell populations following disaggregation of neonatal murine ovaries

To establish whether the germ and somatic cell populations were successfully separated following disaggregation of neonatal murine ovaries, somatic cell only aggregates were generated. When described previously, authors (Eppig and Wigglesworth, 2000) separated these two cell populations based entirely on their adhesive characteristics (illustrated in Figure 2.4) such that germ cells are aspirated off the somatic cell monolayer, which is then washed to remove any remaining germ cells. When this original separation technique was used, oocytes were consistently seen in negative aggregates 7 days after creation as seen in Figure 4.1.C (21.5 ± 5.5, n=4). Thus, a more rigorous separation protocol was developed to establish an uncontaminated somatic cell population. Somatic cells were filtered twice through cell filters following both trypsinisation in the original protocol, to remove contaminating oocytes. Significantly fewer oocytes were seen in aggregates following somatic cell filtration through 30μm (Figure 4.1.D; 11.0 ± 6.1, n=3, $P \leq 0.05$), 20μm (Figure 4.1.E; 4.0 ± 6.1, n=4, $P \leq 0.0001$) and 10μm (Figure 4.1.F; 0 ± 0, n=27, $P \leq 0.0001$) cell filtration. Oocytes were consistently eliminated from aggregates following somatic cell filtration with 10μm cell filters, thus to achieve complete separation of germ and somatic cell populations following disaggregation

of neonatal murine ovaries, somatic cells required filtration through a 10μm cell filter. This protocol was utilised in all subsequent *in vitro* ovarian aggregation experiments.

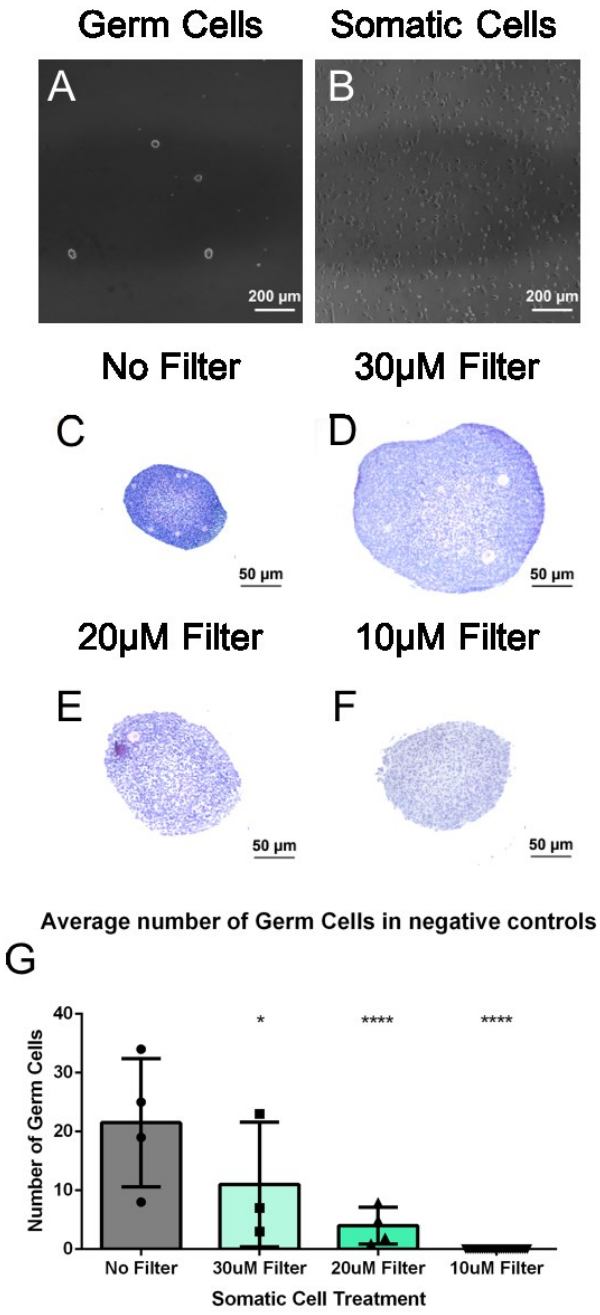

Figure 4.1: Successful disaggregation of neonatal ovaries and separation of germ and somatic cell populations. Neonatal murine germ cells (A) and somatic cells (B) in culture following disaggregation. Cells were imaged at x10 magnification and scale bars represent 200µm. Somatic cells were aggregated together with PHA and cultured for 7 days and analysed for the presence of germ cells. Germ cells were observed in aggregates where somatic cells were unfiltered (C; n=4), filtered through a 30µm (D; n=3) or 20µm (E; n=4) cell filters, but not when filtered through a 10µm filter (F; n=27). Tissue sections imaged at x10 magnification and scale bars represent 50µm. (G) A significant decrease was observed between the number of germ cells in aggregates filtered through 20µm and 10µm cell filters compared to unfiltered samples (Mean ± SEM plotted, One-Way ANOVA with Tukey post-hoc multiple comparisons, * P≤0.05 and ****P≤0.0001)

4.3.3 Aggregation of neonatal murine germ and somatic cells results in follicle formation after 7 days of culture

Aggregates containing both neonatal mouse germ and somatic cells were used to identify and develop a suitable *in vitro* culture model to support follicle formation and subsequent growth. Two culture methodologies were investigated following an overnight hanging drop culture; continuation of the hanging drop culture or a 1% alginate gel matrix culture.

Following an overnight culture in a hanging drop with Waymouths medium plus supplements, oocytes were clearly visible in aggregates, although no clear interactions with the surrounding ovarian somatic cells were observed (Figure 4.2.A). In contrast, Figure 4.2.B & C show that after 7 days of culture in both systems mouse oocytes appear to have established interactions with surrounding somatic cells and have formed follicles. A proportion of these follicles appear to have initiated follicular development, with a single layer of cuboidal granulosa cells observed, characteristic of a primary follicle. The absence of interactions between the germ cells and somatic cells at day 0 further reflects that complete disaggregation of the neonatal ovaries and separation of the two cell populations was been achieved. Aggregates clearly show extensive reorganisation from Day 0 (Figure 4.2.A) to Day 7 (Figure 4.2.B & C) generating ovary-like aggregates with a clear surface epithelium surrounding the whole tissue in both culture systems. This reorganisation and establishment of follicles in these aggregates reflects cell-cell interactions and suggests that cells within the aggregates are communicating to co-ordinate follicle formation and growth initiation. Analysis of tissue volume in uncultured day 0 ($0.10mm^3 \pm 0.08mm^3$, n=3) and day 7 alginate ($0.13mm^3 \pm 0.02\ mm^3$, n=9) cultured positive control ovarian aggregates showed no difference, suggesting that aggregates cultured within alginate undergo tissue remodelling but do not increase in size. Whereas hanging drop ($0.28mm^3 \pm 0.08\ mm^3$, n=5) cultured positive control ovarian aggregates were significantly larger than uncultured ($p \leq 0.05$) and alginate cultured ($p \leq 0.01$), suggesting that these aggregates had undergone proliferation in conjunction with remodelling. These results also suggest that the hanging drop model may better support the development of ovarian aggregates.

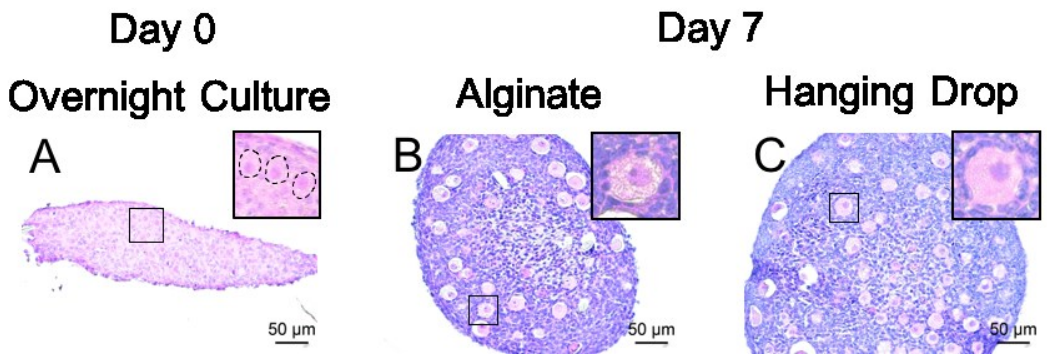

Figure 4.2: Aggregation of neonatal mouse germ and ovarian somatic cells supports follicle establishment within 7 days of culture. (A) Oocytes are visible (outlined in dashed lines) in germ and somatic cell aggregates following an overnight culture. After 7 days of culture oocytes were observed encapsulated in somatic cells to form follicles in both the alginate culture **(B)** and the hanging drop culture **(C)**. Tissue sections were imaged at x20 magnification and scale bars represent 50µm.

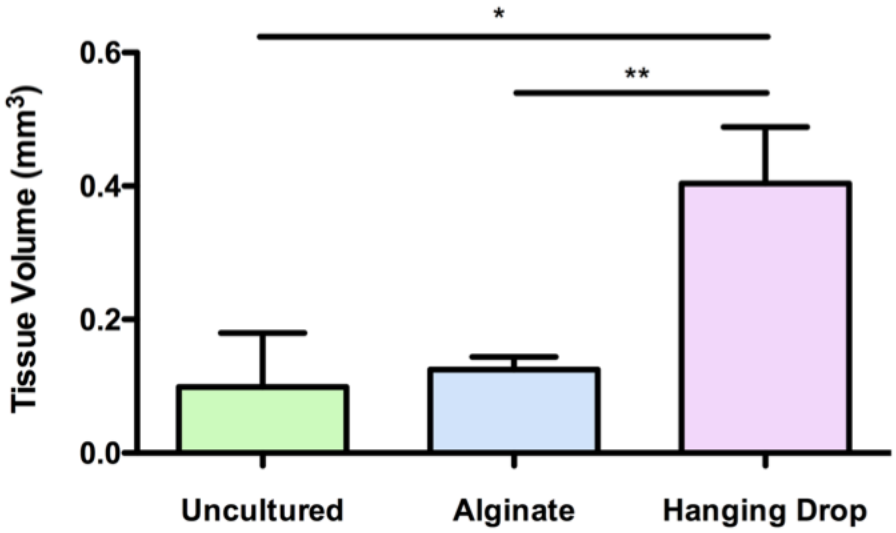

Figure 4.3: Estimated tissue volume of uncultured (day 0), alginate and hanging drop cultured (7 days) ovarian aggregates. Estimated tissue volume of alginate cultured positive control ovarian aggregates (0.13mm^3 ± 0.02 mm^3, n=9) were not significantly different in size to uncultured ovarian aggregates (0.10mm^3 ± 0.08mm^3, n=3). However, hanging drop cultured ovarian aggregates (0.28mm^3 ± 0.08 mm^3, n=5) were significantly larger than uncultured and alginate cultured ovarian aggregates. Mean ± SEM. One-way ANOVA with post hoc Tukeys multiple comparison tests, * $P<0.05$ and ** $P<0.01$.

4.3.4 Hanging drop culture better supports germ cell survival than alginate gel culture system

Both the alginate gel culture system and the hanging drop culture model utilised Waymouths media with supplements for culture (section 2.12) with either 50% replacement of media or complete replacement of media on alternate days, respectively. Although the aggregates from each system can be compared to one another, a further positive control for comparison was needed to determine the success of the culture systems. The ovarian aggregate model had previously been used in a xeno-transplant system which successfully supported follicle formation and growth to generate antral follicles (Eppig and Wigglesworth, 2000) after 21 days. Thus a 7 day xeno-transplant model was used as a comparison to investigate the success of the ovarian aggregate culture systems to support healthy follicle formation and growth.

All germ cells observed at the end of the culture or xeno-transplant period were seen in association with somatic cells, for both healthy and unhealthy oocytes. Example images from cultured aggregates are shown in Figure 4.4.A. Oocytes were counted where the nucleolus was present and classified based on their follicle stage (primordial, a single layer of flattened granulosa cells; transitory, a mixture of flattened and cuboidal granulosa cells; primary, a single layer of cuboidal granulosa cells) and health (healthy follicles consisted of a round oocyte containing a nucleus, even cytoplasmic staining with eosin and no pyknotic granulosa cells; follicles were considered unhealthy if the follicle showed contraction of the oocyte from the granulosa cells, uneven or dark cytoplasmic staining of the oocyte, nuclear contraction and/or pyknotic granulosa cells; Figure 4.4.A). No follicles were observed with a healthy oocyte and pyknotic granulosa cells, suggesting that follicular atresia is driven by apoptosis of the germ cell rather than the somatic cells in ovarian aggregates. This may be a consequence of the initial disaggregation process or as a result of germ cells failing to establish sufficient somatic cell support within a timeframe necessary for germ cell survival resulting in poor cell health and death.

The hanging drop system retained significantly ($P \leq 0.01$) more germ cells in ovarian aggregates throughout the culture than those cultured in alginate (Figure 4.4.B), although neither group were significantly different to xeno-transplanted ovarian aggregates. The percentage distribution of follicles by developmental stage was not significantly different between groups (Figure 4.4.C), however, the xeno-transplant model did show a trend for a higher proportion of follicles to reach the primary stages of development, suggesting that the culture models are potentially deficient in the support system necessary to facilitate the transition of follicles from primordial through transitory to primary, or the *in vitro* model facilitates this process at a slower rate compared to the xeno-transplant system.On average a larger number of healthy follicles, irrespective of developmental stage, were identified in the hanging drop aggregates than in both alginate and xeno-transplanted ovarian aggregates, although this difference is not statistically significant (Figure 4.4.D). The wider distribution of results observed in both culture systems, shows that there was greater variability within each culture system than that observed in the xeno-transplant model. The cause of this variability is unclear, but may be a result of differences between the initial ovaries used, variation between enzyme aliquots used for disaggregation, sizes of aggregates and variation in media aliquots.

The percentage of healthy follicles did not differ between experimental groups at the primordial and transitory stages of development, but the xeno-transplant model had a higher proportion of healthy primary follicles than both culture systems (Figure 4.4.E). Although not statistically significant, these data suggest that while both culture systems can support the reformation of follicles when neonatal murine germ and somatic cells are aggregated together, and can facilitate the early stages of follicular development, they appear to be less efficient than the xeno-transplant model at supporting healthy follicle development to the primary stages of development. This also suggests that the culture systems and/or media would need adapting for long term culture of the aggregates to support full follicle development *in vitro*.

The expression of cleaved caspase 3 (CC3), a marker of active cellular apoptosis was assessed in aggregates after a 7 day culture or xeno-transplant to explore the health of the ovarian aggregates. At this time point very few germ cells were identified as

apoptotic (Figure 4.5.A-C, arrowheads). As cleaved caspase 3 is a marker of active early apoptosis, this time point may be too late to detect oocyte death as previously assessed by tissue histology in these aggregates. In contrast a number of somatic cells not associated with follicles were identified as actively apoptotic in the centre of the aggregates, suggesting that the nutrient supply to the centre of the aggregate is insufficient resulting in cellular death (Figure 4.5.A-C). There were significantly fewer CC3 positive cells per area of tissue in ovarian aggregates cultured by hanging drop than those cultured in alginate (Figure 4.5.D), furthermore, very few cells were observed to be cleaved caspase 3 positive in aggregates following xeno-transplantation. These results illustrate that the health of aggregates cultured in alginate is poorer than those cultured in a hanging drop and those xeno-transplanted. Xeno-transplanted aggregates were observed to have developed a blood supply at the time of tissue collection, thus establishing a nutritional supply facilitating survival and promoting tissue health. Cultured aggregates in contrast relied upon media at the tissue surface either passing through the tissue or nutrients being delivered via cell/cell interactions. The localisation of CC3 expression (Figure 4.5.A & B) and histological visualisation of necrotic tissue located centrally in cultured aggregates (Figure 4.2.B & C), suggests poor nutrition supply at the centre of these aggregates. However, the differences in CC3 expression between culture groups suggests that the hanging drop model supports better nutrient supply in the tissue than the alginate system.

Although there were very little differences between the two techniques for culturing positive control aggregates, the hanging drop methodology was observed to have significantly better germ cell survival than the alginate gel culture system and had less active apoptosis in aggregates after 7 days. Given these results the hanging drop culture system was used in subsequent experiments to further investigate the potential of bovine OSCs.

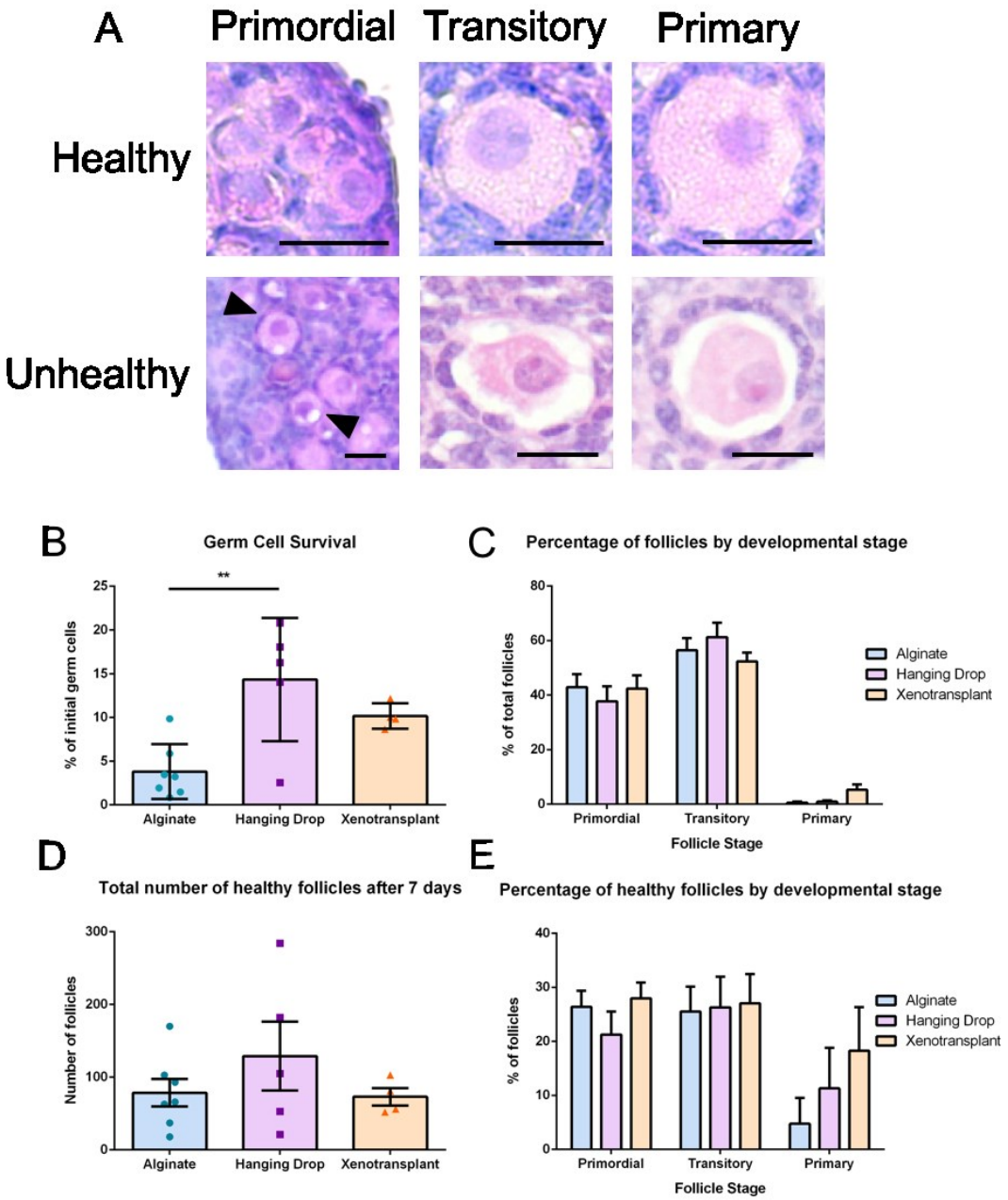

Figure 4.4: Follicle establishment, initiation of growth and health in ovarian aggregates in two *in vitro* culture systems compared to a xeno-transplant model. (A) Healthy (top panels) and unhealthy (bottom panels) follicles by developmental stage. Arrowheads mark unhealthy primordial follicles and scale bars represent 20µm. **(B)** Percentage of initial germ cells remaining in aggregates after 7 days of culture in an alginate gel (n=9), hanging drop (n=5) or xeno-transplant (n=4). **(C)** Percentage of total follicles by developmental stage. **(D)** Total number of healthy follicles in aggregates after 7 days. **(E)** Percentage of healthy follicles by developmental stage. Mean ± SEM. One-way ANOVA with post hoc Tukeys multiple comparison tests, **P<0.01.

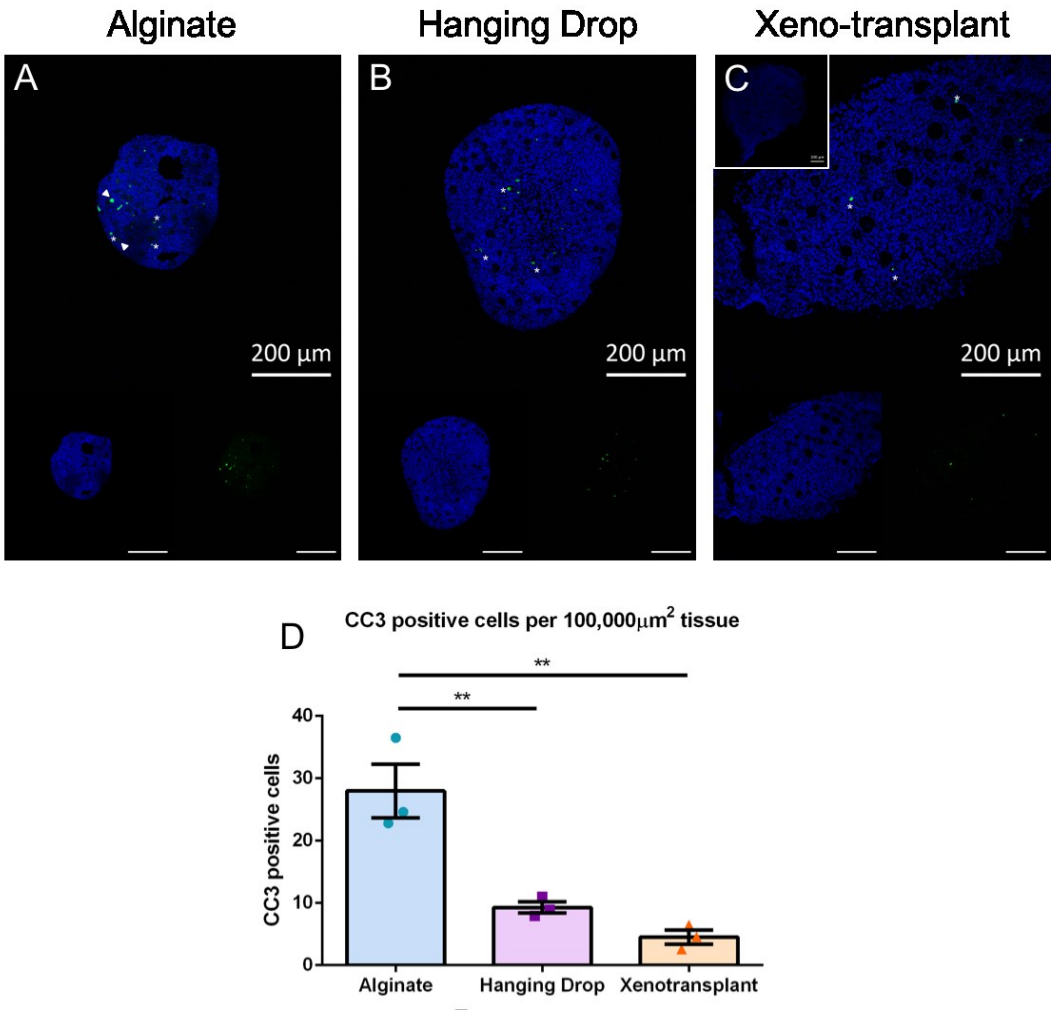

Figure 4.5: Immunofluorescent detection of the apoptotic marker cleaved caspase 3 (CC3) in cultured ovarian aggregates. Representative sections from an ovarian aggregates cultured in alginate (A), hanging drop system (B) or xeno-transplanted to the kidney capsule of an immune deficient mouse (C) for 7 days immunostained for the presence of the active apoptotic marker cleaved caspase 3 (green). CC3 expression was found in both somatic cells (*) and germ cells (arrow heads) and appeared to be distributed across tissue cultured within an alginate gel, but was observed to be centrally located in those cultured in a hanging drop. Inset shows a negative control section where the primary antibody has been omitted. (D) Significantly fewer cleaved caspase 3 cells (per 100,000µm^2 area of tissue) were observed in ovarian aggregates cultured in a hanging drop (n=3) or xeno-transplanted (n=3) than those cultured within an alginate gel (n=3) after 7 days. One-way ANOVA with post hoc Tukeys multiple comparison tests, **P<0.01. Tissue sections were imaged at x10 magnification and scale bars represent 200µm.

4.3.5 Bovine Oogonial Stem Cells in the ovarian aggregate culture model

bOSCs isolated from adult bovine ovaries, cultured (passage 5-18) and labelled with rhodamine dextrans, were combined with neonatal murine ovarian somatic cells at a ratio of 1:10 cells respectively to generate chimeric ovarian aggregates for the investigation of bOSC potential. A total of 26 chimeric ovarian aggregates were generated. Rhodamine dextrans are endocytosed by bOSCs at the time of labelling and reside within vesicles in the cell cytoplasm. Rhodamine dextrans in vesicles within bOSCs could be visualised in all aggregates throughout 7 days in a hanging drop culture (Figure 4.6.A & B). Histology of aggregates at day 0 (Figure 4.6.C) and day 7 (Figure 4.6.D) shows that chimeric aggregates undergo structural reorganisation to create a spherical aggregate with a surface epithelium similar to that seen in negative (Figure 4.1) and positive (Figure 4.2) ovarian aggregates.

When counterstained with DAPI and visualised by confocal microscopy, rhodamine labelled bOSCs could be visualised throughout the chimeric aggregates (Figure 4.7). No patterns or consistent observations were made about bOSC localization in the aggregates, they appeared randomly distributed throughout all chimeric ovarian aggregates.

Although rhodamine was easily visible in chimeric ovarian aggregates and was absent from negative and positive ovarian aggregates (data not shown), to confirm that the rhodamine detected by confocal microscopy in chimeric aggregates was true rhodamine expression, immunofluorescence was performed on the tissue. Anti-tetramethylrhodamine antibody staining was absent from neonatal mouse ovary controls (Figure 4.8.A) lacking rhodamine, whereas staining was seen corresponding to rhodamine location in chimeric aggregates (Figure 4.8.B). These data confirm and expand on results from Chapter 3, such that rhodamine dextrans are maintained within bOSCs over medium term culture periods (< 3 weeks), can be fixed and visualized in bOSCs after processing and furthermore can be identified within chimeric ovarian aggregates both directly and by immunofluorescence following these processes. Thus, bOSCs can be successfully traced when labelled with

rhodamine dextrans. All subsequent *in vitro* experiments utilized this methodology to identify bOSCs in chimeric ovarian aggregates.

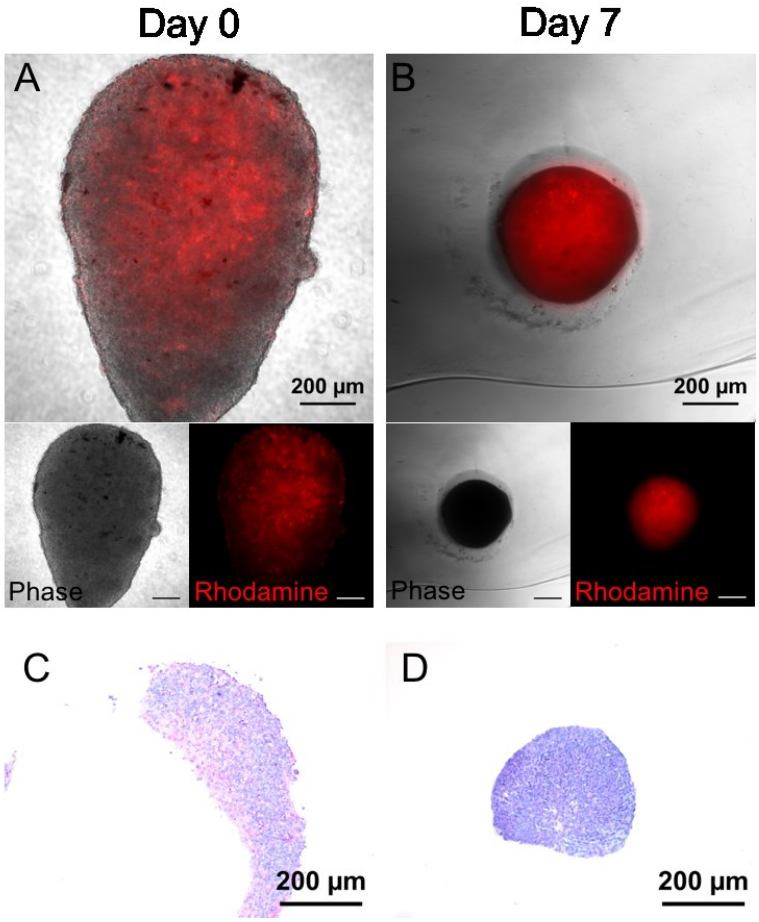

Figure 4.6: bOSCs in the *in vitro* ovarian chimeric aggregate. bOSCs labelled with rhodamine dextrans can be identified and traced live in chimeric aggregates throughout a hanging drop culture, shown at day 0 (A) and day 7 (B). Haematoxylin and eosin staining of chimeric aggregate sections at day 0 (C) and day 7 (D). Live tissue and tissue sections were imaged at x10 magnification and scale bars represents 200µm.

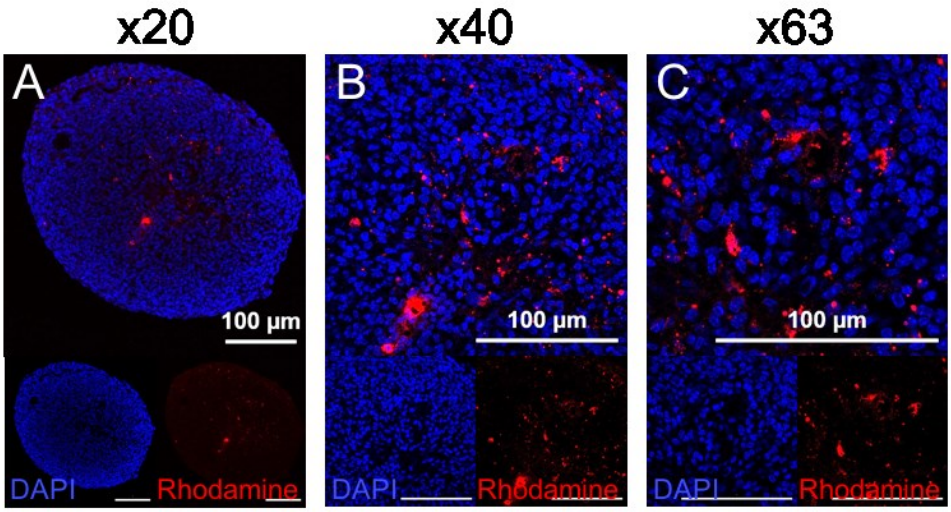

Figure 4.7: bOSCs visualised using rhodamine dextran labelling following fixation in a chimeric ovarian aggregate cultured in a hanging drop for 7 days. bOSCs could be identified in sections of chimeric aggregate tissue counterstained with DAPI by the location of fluorescent rhodamine dextrans. A representative section is shown here at x20 (A), x40 (B) and x63 (C) magnification and scale bars represent 100µm in all images.

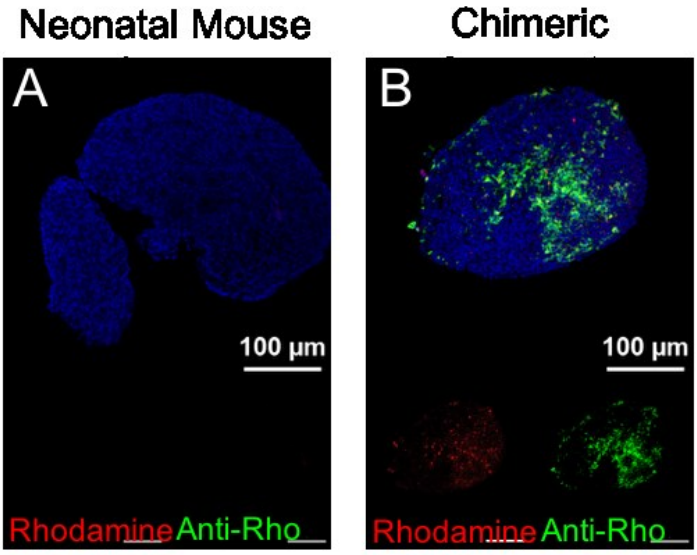

Figure 4.8: Immunofluorescent analysis of rhodamine expression in chimeric aggregate containing bOSCs labelled with rhodamine dextrans. Chimeric aggregates containing bOSCs labelled with rhodamine dextrans and control neonatal murine ovaries lacking rhodamine expression were assessed for the presence of rhodamine. Anti-tetramethylrhodamine (Anti-Rho; green) staining was absent from the neonatal mouse ovary (A) and showed staining co-localised to rhodamine fluorescence in chimeric ovarian aggregates (B). Tissue sections were imaged at x20 magnification and scale bars represent 100µm.

4.3.6 Health of chimeric ovarian aggregates cultured *in vitro*

To assess the health of the chimeric ovarian aggregates following culture, apoptosis was measured by the expression of cleaved caspase 3 (CC3). 15.6 ± 1.9 CC3 positive cells (mean ± SEM, n=3) per 100,000μm^2 area were identified in chimeric ovarian aggregates, which was significantly higher (P=0.04) than the number of CC3 positive cells per 100,000μm^2 area of positive ovarian aggregates (9.3 ± 0.9; mean ± SEM, n=3, Figure 5.4). This suggests that the culture system previously developed using positive control ovarian aggregates (consisting of murine germ and somatic cells) may be less efficient at supporting aggregate health in chimeric ovarian aggregates. The pattern of CC3 expression in the chimeric ovarian aggregates (Figure 4.9) was randomly distributed throughout the tissue, a pattern similar to xeno-transplanted positive ovarian aggregates, whereas CC3 expression was restricted to the center of the positive ovarian aggregates. This expression pattern does not suggest consistent failure of the nutrition supply to reach the center of the aggregates. Although CC3 expression was greater in chimeric ovarian aggregates it still reflected a small proportion of the overall tissue. Furthermore, very few (3.64% ± 1.58%, mean ± SEM, n=3) bOSCs were CC3 positive in the chimeric ovarian aggregates, suggesting that culture system supports bOSC survival in the aggregates.

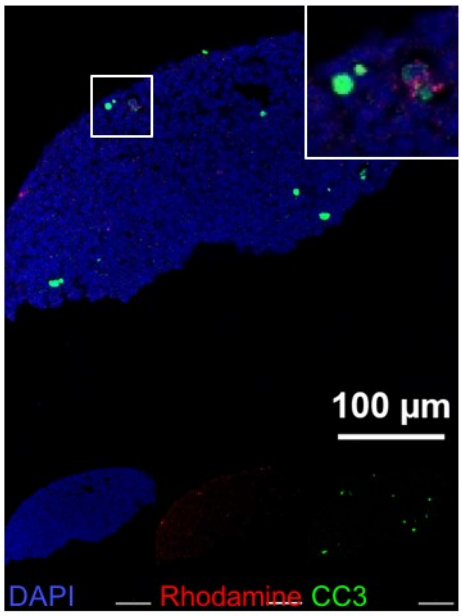

Figure 4.9: Cleaved Caspase 3 (CC3) expression in chimeric ovarian aggregates. Apoptotic cells in chimeric ovarian aggregates were identified by CC3 expression following a 7 day hanging drop culture period. 9.46% of all CC3 positive cells identified co-localised to rhodamine labelled bOSCs. Overall very little active apoptosis was identified in chimeric ovarian aggregates. Inset shows a CC3 positive bOSC adjacent to a CC3 positive somatic cell. Tissue section was imaged at x20 magnification and the scale bar represents 100µm.

4.3.7 bOSCs maintain DAZL expression in chimeric aggregates

One of the main features used to characterise and define oogonial stem cells is their co-expression of germ and pluripotency markers. DAZL is a germ cell specific RNA-binding protein which was expressed in bOSCs during cell culture (Section 3.3.2). Here DAZL has been used to assess whether bOSCs maintain their germline phenotype when aggregated with neonatal murine ovarian somatic cells.

DAZL expression was restricted to oocytes in control neonatal mouse ovaries (Figure 4.10.A) and staining was absent when the primary antibody was omitted (Figure 4.10.B), confirming antibody specificity to germ cells. DAZL expression was observed to co-localise with bOSCs in chimeric ovarian aggregates (Figure 4.10.C&D). All DAZL staining in chimeric ovarian aggregates was observed in conjunction with rhodamine signal from bOSCs. Thus, all germ cells, as confirmed by the presence of DAZL staining, in the chimeric ovarian aggregate system are bOSCs.

However not all bOSCs (determined by rhodamine signal) were observed to express DAZL in the aggregates (Figure 4.10.C&D). DAZL expression in bOSCs in culture was variable and likely a result of heterogeneity in the isolated population, thus resulting in variable DAZL expression in bOSCs in the chimeric aggregate model. Alternatively, bOSCs may have lost their DAZL expression as a result of aggregation with neonatal murine somatic cells or as a consequence of the culture.

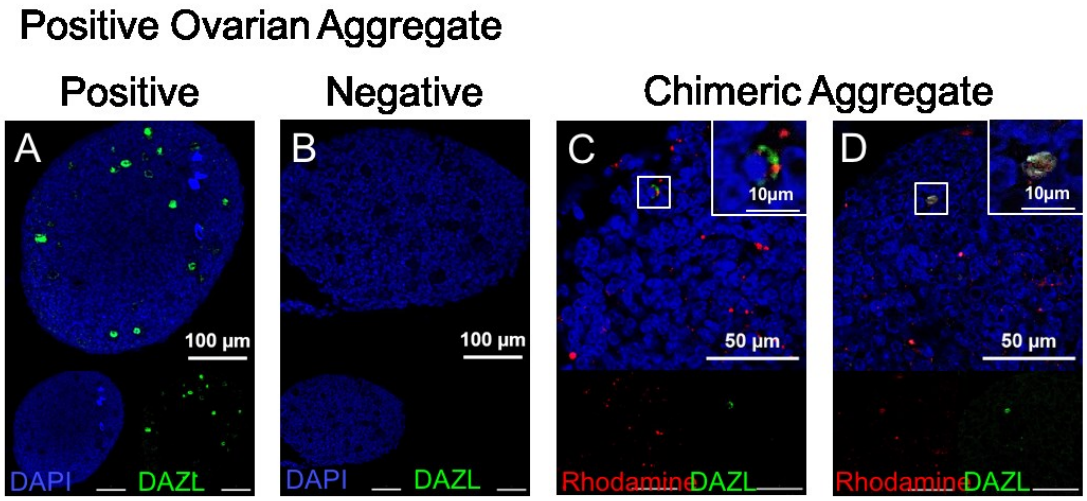

Figure 4.10: DAZL expression in chimeric ovarian aggregates cultured *in vitro* is restricted to bOSCs. (A) Neonatal mouse ovaries demonstrate DAZL (green) expression restricted to the oocytes. (**B**) Staining was absent from the tissue when the primary antibody was omitted. (**C** & **D**) Dazl expression (green) was identified in chimeric ovarian aggregates co-localised to bOSCs (red). Tissue sections were imaged at x20 magnification (**A** & **B**) and x63 magnification (**C** & **D**), **s**cale bars represent 100µm in **A** and **B**, 50µm in **C** and **D** and 10 µm in inset images.

4.3.8 A subpopulation of bOSCs undergoes morphological changes in chimeric ovarian aggregates within 7 days of culture.

Further characterisation of chimeric ovarian aggregates containing rhodamine dextran labelled bOSCs showed a proportion of bOSCs appeared to have an altered morphology compared to other bOSCs. bOSCs identified within 24 hours of aggregate creation were small (<10μm) and demonstrated irregular shape. Following 7 days in a hanging drop culture, the large majority of bOSCs identified in chimeric ovarian aggregates retained this size (Figure 4.11.A & B) and have been termed undifferentiated. However, a small population of bOSCs (n=11) were significantly ($P \leq 0.0001$; Figure 4.11.E) larger in size with a more spherical morphology and are referred to as differentiated bOSCs. The differentiated bOSCs (Figure 4.11.C & D) appear to be a distinct population of cells when compared to undifferentiated bOSCs in the same aggregates (Figure 4.11.F). Sections adjacent to those which had been DAPI counterstained had previously been stained with haematoxylin and eosin to evaluate the histology of chimeric ovarian aggregates. When sections adjacent to those with differentiated bOSCs identified were analysed, the cells corresponding to the differentiated bOSCs appeared to have larger cytoplasm area consistent with the size of the bOSCs measured in Figure 4.11.E. Furthermore, these cells appeared to have a more spherical morphology and show association with neighbouring cells (Figure 4.12), which were rhodamine negative neonatal mouse somatic cells. These features are similar to the characteristics of ovarian follicles.

Due to the limited amount of this tissue and the low frequency with which differentiation of bOSCs occurred within this system, it has not been possible to investigate the expression of oocyte specific factors such as GDF9 or BMP15 to determine if these bOSCs have undergone oogenesis to produce oocytes. However it is clear that a subpopulation of bOSCs have undergone morphological changes, including an increase in cell size, when combined with neonatal murine ovarian somatic cells and cultured in a hanging drop system.

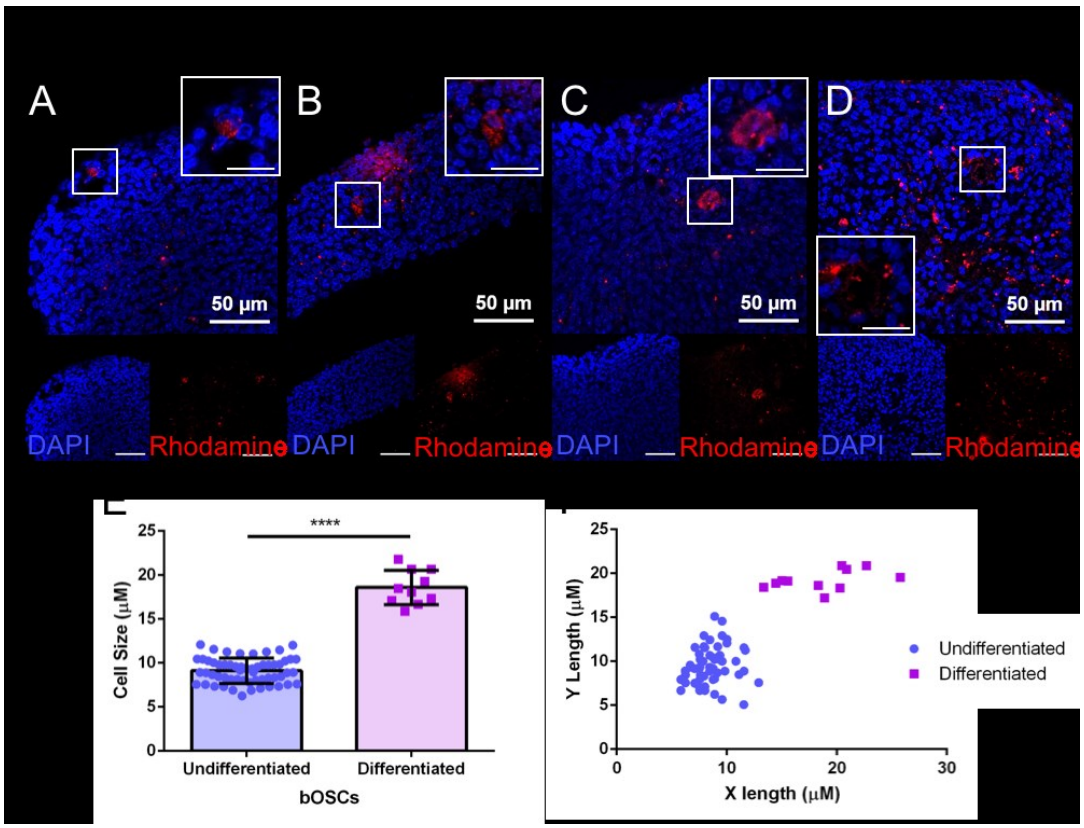

Figure 4.11: A subpopulation of bOSCs undergo morphological changes in chimeric ovarian hanging drop cultures within 7 days. bOSCs in chimeric ovarian aggregates were identified by the expression of rhodamine dextrans following counterstaining with DAPI. Two distinct populations of bOSCs were identified. Undifferentiated bOSCs (A&B) were small in size (9.11µm ± 0.189µm; Mean ± SEM, n=57) and varied in shape. Differentiated bOSCs (C&D) were significantly larger (18.96 ± 0.705; Mean ± SEM, n=11. P≤0.0001, un-paired t-test) than undifferentiated bOSCs (E &F) and demonstrated a more spherical shape. Tissue sections were imaged at x40 magnification and all scale bars represent 50µm and 20µm in insets.

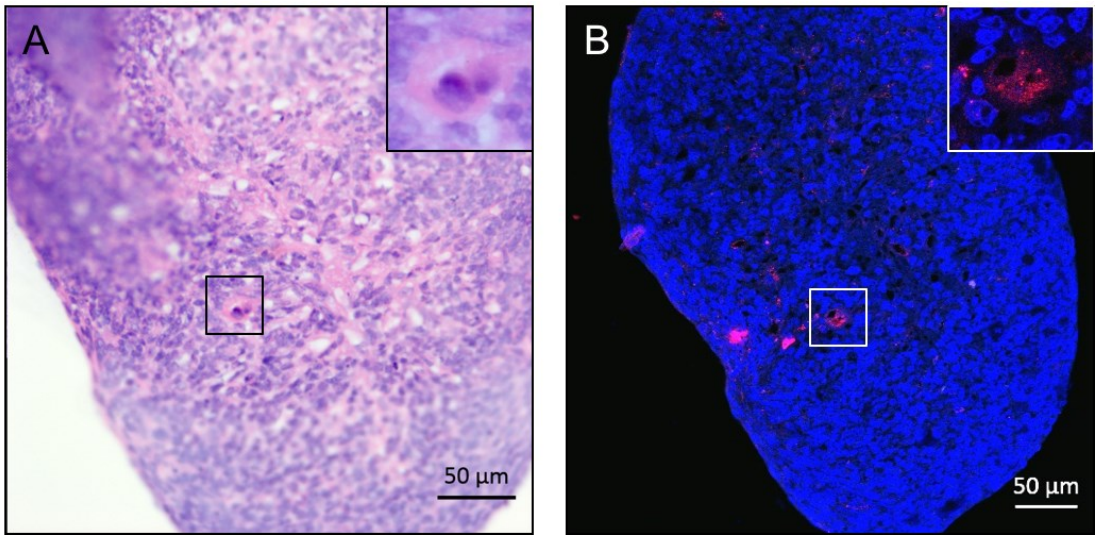

Figure 4.12: Adjacent H&E and DAPI counterstained sections from chimeric ovarian aggregates. H&E (A) section of a chimeric ovarian aggregate appears to contain a larger cell with a spherical morphology which co-localises with a rhodamine labelled differentiated bOSC in the DAPI counterstained adjacent section (B). Differentiated bOSCs appears to have a larger cytoplasm than undifferentiated bOSCs, they also appear to associate with surrounding rhodamine negative murine somatic cells. Tissue sections were imaged at x20 magnification and scale bars represent 50µm.

4.4 Discussion

The production of an oocyte *in vivo* is a tightly regulated process, influenced and controlled by the surrounding somatic cells to ensure meiotic and developmental competence is achieved in tandem with the timing of ovulation. Disruption of this relationship is known to interfere with the ability of the oocyte to undergo meiosis and fertilisation successfully (reviewed by Eppig (1991), Kidder and Vanderhyden (2010)). Early research showed that oocyte growth is hindered when removed from its follicle (Eppig, 1979) and the rate of oocyte growth *in vitro* is correlated with the number of granulosa cells in the follicle (Brower and Schultz, 1982). Genetic manipulation has further illustrated the importance of this relationship. Mice lacking connexin 43 (Cx43) had disrupted folliculogenesis with noticeable reduction in oocyte growth, resulting in abnormal, developmentally incompetent oocytes (Ackert et al., 2001; Tong et al., 2006). The interactions between somatic cells and germ cells are thus pivotal for reproductive success.

Prior to isolation from mammalian ovaries, it is likely that OSCs will interact with surrounding somatic cells and have a relationship with their microenvironment. This may either play a role in their maintenance or could influence their differentiation, should they contribute to the follicular pool in the adult ovary *in vivo* which is still unclear. Therefore, ovarian somatic cells may have an important role in determining the oogenic potential of oogonial stem cells.

Large spherical cells similar to oocytes were not observed in bOSC cultures, possibly due to a lack of extrinsic signals to co-ordinate their differentiation. The observation of spontaneous differentiation of OSCs into oocyte-like cells (OLCs) in culture without the support of somatic cells in other species, reported in the literature, generated abnormal OLCs (Bui et al., 2014; Ding et al., 2016; Hernandez et al., 2015; White et al., 2012; Zhou et al., 2014). Single cell RT-PCR showed heterogeneous expression of oocyte and meiotic markers in these OSC derived OLCs (Ding et al., 2016), suggesting variation in the differentiation of oogonial stem cells, likely a result of the uncontrolled nature of the differentiation in contrast to the *in vivo* process. Spontaneous differentiation of OSCs is also a rare event with only 0.1% of porcine OSCs producing OLCs in culture (Bui et al., 2014). Thus, the absence of

spontaneous differentiation of bOSCs in culture is reflective of the rare nature of the event, as previously reported by others. Extrinsic factors have been shown to increase the rate of OSC differentiation *in vitro*. Bmp4, a growth factor expressed in ovarian somatic cells known to have several roles in regulating germ cell development within the ovary (Pangas, 2012), significantly increased the rate at which mouse OSCs spontaneously differentiate into OLCs and induced expression of meiotic genes (*Stra8*, *Msx1* and *Msx2*) in a dose dependent manner when added to cultures (Park et al., 2013). These effects could be inhibited by the administration of Noggin, a Bmp4 antagonist, to cultures, confirming the effects were as a result of Bmp4 signalling. Granulosa cells and retinoic acid (RA) significantly increased differentiation of human OSCs into oocyte-like cells with meiotic spreads revealing SYCP3 staining associated with the leptotene stage of meiosis (Ding et al., 2016). Mouse granulosa cells were also observed to interact with human OSC derived OLCs via filopodia like structures with gap junctions (GJA4 positive) identified between the two cell types despite originating from different species (Ding et al., 2016). Considering these data collectively, while OSC differentiation can occur spontaneously, it appears to be controlled by extrinsic factors primarily originating from the ovarian somatic cell niche. Thus bOSC differentiation was investigated using a model which promotes somatic cell interaction.

The ovarian aggregation model has previously been used in conjunction with a xeno-transplant model to support follicle development (Eppig and Wigglesworth, 2000). The use of this model *in vitro* described in this thesis, is a novel approach and required optimisation to fully explore its potential to support follicle formation and growth. Two different culture techniques were explored using a control ovarian aggregate (neonatal mouse germ and somatic cells) to assess their viability for this process. The use of pre-formed germ cells enabled analysis of the techniques abilities to support follicle formation and growth, without concerns regarding oogenesis. Three-dimensional organ culture techniques were utilised as these better represent the architecture of the tissue (reviewed in Edmondson et al. (2014)).

Alginate gel matrices have been used to support follicle growth *in vitro* successfully in both individual follicle cultures (Amorim et al., 2009; Camboni et al., 2013; Hornick et al., 2013) and whole tissue cultures (Laronda et al., 2014). Pieces of

human ovarian cortex have successfully been cultured for 6 weeks in an alginate gel and supported the transition of primordial follicles to secondary follicles within 14 days of culture (Laronda et al., 2014). That study found that there were no obvious differences in the extracellular matrices, stroma or follicle morphology of ovarian tissue pieces cultured in different concentrations of alginate gel (0.25%, 0.5%, 1% or 2%). The ovarian aggregates described here were cultured in a 1% alginate gel as it has previously been shown that rigid alginate gels (1% or 2%) better supported early follicle development (Hornick et al., 2013). We hypothesised that the ovarian aggregates would also require a more rigid environment to facilitate establishment of tissue structure. In contrast the hanging drop methodology is a scaffold free three-dimensional culture technique previously used to culture gonadal tissue fragments successfully generating metaphase II oocytes from murine secondary follicles (Choi et al., 2013) and supporting human spermatogenesis for up to 14 days in culture (Jorgensen et al., 2014), as well as being widely used in stem cell culture. Thus both the three-dimensional systems investigated here, have previous success at supporting germ cell growth and development.

Ovarian aggregates containing murine germ cells consistently showed formation of follicles following 7 days in culture in both systems, illustrating that germ and somatic cells can re-establish interactions following disruption *in vitro*, similar to the current and previous xeno-transplant models (Eppig and Wigglesworth, 2000). Aggregates also developed a surface epithelium in the culture systems, similar to reports in the literature for tissue cut or previously damaged prior to culture (Jackson et al., 2009; Laronda et al., 2014). No differences were observed in the distribution of follicles or the total number of healthy follicles between culture groups, however significantly greater proportions of the initial number of germ cells in the aggregates were counted at the end of the 7 day culture in the hanging drop system. These results were also comparable with a xeno-transplant model for the same duration. Degenerate follicles were observed with an unhealthy oocyte in all groups (alginate, hanging drop and xeno-transplant). Enzymatic digestion of neonatal murine ovaries was essential to achieve a single cell suspension and to separate fully the somatic and germ cell populations. Cellular damage as a result of enzymatic digestion of the tissue would therefore be expected. Oocytes are highly susceptible to this damage;

isolation of early stage follicles by enzymatic digestion has previously been identified to be detrimental to the subsequent success of cultured oocytes compared to mechanically isolated follicles (Choi et al., 2013). Thus high levels of poor oocyte health and quality observed in these ovarian aggregates are likely to be a consequence of the methodology used to separate them from their somatic cells.

The effect of enzymatic damage to oocytes may be compounded in an aggregation model by the length of time taken to re-establish germ and somatic cell interactions, such that oocytes which failed to establish communication with somatic cells swiftly could not be salvaged. Alternatively, oocytes which suffered the greatest enzymatic damage during tissue digestion may have lost the ability to form effective interactions with somatic cells, ultimately leading to the death of the oocyte. It is unclear which of these possibilities accurately describes the scenario in these aggregates, but it is important to note that no 'loose' germ cells with no interactions with their surrounding somatic cells were observed, thus all oocytes appeared to strive to re-establish cell-cell interactions with the somatic niche, some more successfully than others. The effect of enzymatic digestion on the somatic cell population was not investigated, although analysis of apoptosis in the tissue at earlier time points may identify somatic cells affected by the process.

Histological evaluation of the cultured aggregates showed the development of necrotic tissue in the centre of the aggregates. The outer layers of the ovarian aggregates are exposed to the medium, allowing for good oxygen, nutrient and growth factor supply. In contrast the centre of the aggregate relies upon diffusion of these factors through the tissue, thus receiving less, and in addition is exposed to a greater concentration of carbon dioxide waste. Necrosis in the centre of the tissue or cell aggregate in three-dimensional culture systems is well documented in the literature (reviewed by Edmondson et al. (2014)). Active apoptosis was observed centrally in the cultured ovarian aggregates, whereas xeno-transplanted aggregates showed very little sporadic cleaved caspase 3 staining. Xeno-transplant systems reduce the problems described above through the development of vasculature to and throughout the transplanted tissue (Edmondson et al., 2014) facilitating nutrient supply and waste removal, although establishment of vasculature takes approximately 48 hours to establish (Dissen et al., 1994). Smaller aggregate sizes

may have reduced the level of necrosis observed and should be investigated further. Cell viability in three-dimensional cultures declines after 5 days of culture (Edmondson et al., 2014), and it is possible that the systems used here may not be appropriate for long term culture, although ovarian cortical fragments have been successfully cultured within alginate hydrogels for up to 6 weeks (Laronda et al., 2014). Apoptosis was significantly lower per section area in aggregates cultured in hanging drops compared to those cultured within an alginate gel and apoptosis was more widespread in the centre of alginate cultured aggregates. Heise et al. (2005) found that a 1% alginate gel hindered the transport of FSH from the medium to cultured rat follicles hampering their growth. The same concentration of alginate gel was used to culture ovarian aggregates here and may have resulted in poorer aggregate quality as a consequence of the failure of nutrients to pass through alginate. The hanging drop model allows for direct access of the tissue to the surrounding medium and this may have improved the outcome for ovarian aggregates cultured in this way.

The complete separation of germ and somatic cells was essential to produce a pure population of somatic cells that could be used to investigate the differentiation potential of bOSCs. Separation of oocytes from somatic cells has previously been conducted based solely on the adherent characteristics of these two cell types, allowing oocytes to be removed from a somatic cell monolayer following culture of the cells after disaggregation (Eppig and Wigglesworth, 2000). Somatic cell only ovarian aggregates have not been reported in the literature, thus full assessment of separation of the two cell types has never been described. Germ cells were only consistently removed from the somatic cell population following two filtrations of the somatic cells through a 10μm filter. It is possible that this technique in the hands of others does not require somatic cells to be filtered for complete removal of all germ cells. In somatic cell only ovarian aggregates, any oocytes which had not been removed by washing or filtration, might have a greater chance of survival due to the increased somatic cell to germ cell ration present in these aggregates compared to aggregates where oocytes are introduced. Furthermore, xeno-transplanted ovarian aggregates have previously been assessed after 21 days, by which time the tissues have established a vasculature, which is likely to facilitate the elimination of the

large majority of germ cells damaged by the disaggregation process, or those which fail to establish the appropriate somatic cell support. Thus any residual germ cells within the somatic cell population may be overlooked if they had not persisted through the whole process. The identification of germ cells in negative ovarian aggregates allowed the development of a more robust methodology to ensure a pure population of neonatal somatic cells was used for aggregation with bOSCs to generate chimeric ovarian aggregates.

bOSCs could be clearly identified by rhodamine fluorescence in the chimeric ovarian aggregates during culture with live tissue microscopy and also following processing, counterstaining with DAPI and visualisation by confocal microscopy. Chimeric ovarian aggregates underwent tissue remodelling throughout culture like the negative and positive control ovarian aggregates to produce a clear surface epithelium, as previously seen with tissue cultured *in vitro* (Jackson et al., 2009; Laronda et al., 2014). Most bOSCs remained undifferentiated in the chimeric ovarian aggregates and maintained their small size and irregular shapes. Additionally, many bOSCs retained their germline phenotype marked by the expression of DAZL. However, not all bOSCs were observed to show DAZL expression. One possible explanation for this is that bOSCs may have lost expression of DAZL when combined with somatic cells, losing their germ cell phenotype. Although this is a possible explanation for the absence of the germ cell marker DAZL in some bOSCs, immunocytochemistry of bOSCs in culture revealed a heterogeneous pattern of DAZL expression in these cells prior to aggregation with neonatal murine somatic cells, thus variation in DAZL staining of bOSCs in chimeric ovarian aggregates is likely to be a reflection of the heterogeneity within the cell population from isolation.

As discussed above, the frequency with which oogonial stem cells appear to differentiate *in vitro* is very low in all mammalian species investigated (Bui et al., 2014; Pacchiarotti et al., 2010; White et al., 2012; Zhou et al., 2014). This novel *in vitro* chimeric ovarian aggregate model revealed a small subpopulation of bOSCs which showed characteristics of differentiation comparable to previously characterised oocyte-like cells. The bOSCs increased significantly in size, became spherical in shape and appeared to show some association with surrounding somatic cells. Only 11 of these cells were identified in chimeric ovarian aggregates,

representing a very small proportion of all bOSCs aggregated with neonatal somatic cells, but all shared these characteristics. Due to the labelling method of the bOSCs, identification of them within the tissue was conducted fluorescently, sections were also stained with haematoxylin and eosin for histological assessment to identify any abnormal structures or points of interest i.e. to identify any oocyte or follicle like structures. H&E sections adjacent to differentiated bOSCs identified by rhodamine expression showed cells with a larger cytoplasm than other cells which appeared in association with the surrounding cells. Further investigation into these differentiated bOSCs and the chimeric ovarian aggregates was not possible due to the limited number of cells observed, tissue generated and the nature of identifying bOSCs within the tissue. Previous investigations into OLCs derived from OSCs have identified the expression of oocyte specific markers in combination with meiotic markers. Unfortunately, it has not been possible to explore the expression of these markers in the differentiated bOSCs, and without this evidence it is not possible to say whether these cells have indeed initiated oogenesis within this system despite their shared morphological characteristics with oocytes. Thus, extensive investigation into the nature of differentiated bOSCs, including assessment of gene and protein expression is still necessary.

The absence of spontaneous bOSCs differentiation in culture suggests that extrinsic factors, supplied in this model by the neonatal mouse somatic cells, increased the rate of bOSC differentiation. Somatic cell derived extrinsic factors have been shown to increase the rate of OSC differentiation previously (Ding et al., 2016; Park et al., 2013) and co-culture with granulosa cells also increased differentiation of OSCs (Ding et al., 2016), furthermore cell-cell interactions between granulosa cells and mouse embryonic stem cells are essential in the differentiation of these pluripotent cells into oocyte-like cells (Qing et al., 2007), which could not be replicated with granulosa cell conditioned media. bOSC differentiation observed within the chimeric ovarian aggregates *in vitro* was limited and the model developed here may not perfectly simulate the full requirements for bOSC differentiation, such that very few cells were capable of undergoing the process. Significantly more apoptotic cells were identified in chimeric ovarian aggregates than in positive control ovarian aggregates. Suggesting that the system previously developed using ovarian aggregates containing

mouse oocytes may be less efficient at supporting the development of the chimeric aggregates. The model developed could support the establishment of interactions between oocytes but may not be suited to support the differentiation of OSCs. Research into mammalian OSCs has been limited, therefore the requirements of OSC differentiation are poorly understood. To utilise an *in vitro* aggregation model a multi-step approach may be more suitable

The low incidence of bOSC differentiation may also result from the heterogeneity observed in the cultured cell population, such that some cells possess the potential to differentiate more than others given their expression profiles. Single cell RT-PCR would reveal the extent of cellular heterogeneity in isolated and cultured populations of oogonial stem cells and shed light on the distinct gene pattern of the cell type, thus should be considered as a tool in future investigations into these cells.

The process of generating oocytes *in vivo* is a complicated process and has only recently been recapitulated *in vitro* in full, from bi-potential primordial germ cells to functional metaphase II oocytes capable of fertilisation and full embryonic development following embryo transfer to a psuedopregnant foster mother (Morohaku et al., 2016). The development of an *in vitro* system to fully support this entire process has revealed the essential role of somatic cells at all stages of germ cell development. The differentiation of pluripotent stem cells such as embryonic stem cells (ESCs) and induced pluripotent stem cells (iPSCs) into oocytes has thus far only been achieved when combined with ovarian somatic cells (Eguizabal et al., 2009; Hayashi et al., 2012; Qing et al., 2007), and cell-cell interactions appear essential for this process (Qing et al., 2007). The use of neonatal murine somatic cells to provide an ovarian niche for bovine oogonial stem cells was a novel approach to investigate their potential to differentiate into oocytes. It is unclear whether the tools of communication between germ and somatic cells is evolutionarily conserved between species, thus murine somatic cells may not fully support the development and differentiation of bOSCs. However, there is evidence to suggest conservation between species allowing for communication between somatic and germ cells of different species. Eppig and Wigglesworth (2000) showed that mouse oocytes could undergo full maturation and development supported entirely by rat somatic cells in a xeno-transplant model. Electron micrographs of these chimeric

follicles also showed cytoplasmic processes from rat cumulus granulosa cells traversing the mouse zona pellucida, to allow communication between the cell types. Furthermore, mouse granulosa cells co-cultured with human OSCs increased the rate of differentiation to OLCs and also generated projections towards the OSC derived OLCs culminating in gap junctions (Ding et al., 2016). This evidence suggests methods of communication between germ cells and somatic cells are conserved between species sufficiently to support interaction between the two cell types and may allow for somatic cell support of an oocyte originating from a different species and illustrated the potential of somatic cells to increase the rate of OSC differentiation to OLCs in a different species. Mouse somatic cells similarly increased the differentiation of bOSCs in the chimeric ovarian aggregation model. Differentiated bOSCs were observed in association with rhodamine negative somatic cells, further indicating that mouse neonatal somatic cells have interacted with bOSCs within the chimeric ovarian aggregation model. Although this model has not robustly recapitulated OSC differentiation, the data presented here demonstrates the potential of this model, which with further refinement could provide the support for full differentiation and subsequent development of any resulting oocyte-like cells and also allow for greater investigation of the mechanisms responsible for this process which cannot be elucidated using an *in vivo* xeno-transplant model. This model also offers potential to investigate OSCs in species where a lack of same species somatic cells is a methodological hindrance.

Due to the novel use of this methodology *in vitro* and its development there are several limitations to its use. A short time point was utilised to ensure survival of the tissue could be established (Edmondson et al., 2014). Longer culture periods may have revealed further development of reformed follicles within positive control ovarian aggregates and also further differentiation of bOSCs. The 7 day culture of the ovarian aggregates revealed some central apoptosis within the aggregates. The use of smaller aggregates may reduce this problem in the future and allow for successful healthy development of the tissue for longer term culture. A basic medium with minimal supplements was utilised to investigate the ability of follicles to form and grow following aggregation of the germ and somatic cells of neonatal murine ovaries. The data presented here shows that this medium supported the reformation

of follicles when somatic cells and oocytes were combined and also supported the differentiation of a subpopulation of bOSCs. However, the requirements for OSC differentiation and establishment of communication between oocytes and somatic cells are likely to be dissimilar thus use of different media may have supported these two different processes better. Furthermore, to develop follicles to advanced pre-ovulatory stages *in vitro* (Eppig and O'Brien, 1996; Eppig and Schroeder, 1989; McLaughlin and Telfer, 2010; Morohaku et al., 2016; Spears et al., 1994; Telfer et al., 2008), follicles need to be cultured individually, to remove any presumed inhibitory factors in the ovarian microenvironment, and this has generated oocytes capable of fertilisation in murine models. Supplements, including FSH and Activin A are also required to support follicular development (McLaughlin and Telfer, 2010; Telfer et al., 2008), thus alternative media should be investigated for longer term use of this methodology to be able to support full OSC differentiation and subsequent follicle growth *in vitro*.

Unfortunately, due to time restraints within this project it was not possible to fully develop this *in vitro* ovarian aggregation model or investigate its full potential to support bOSC differentiation. Given recent developments in the field, recapitulating the full process of oogenesis from murine primordial germ cells *in vitro*, it is likely that a multistep approach, with alterations in media content, would be required to induce OSC differentiation and nurture any resulting oocyte-like and follicle-like structures to maturity.

To date, functional oocytes capable of fertilisation and production of viable offspring in rodents, derived from pluripotent cells including ESCs, iPSCs and OSCs have only been generated with the use of xeno-transplant models (Hayashi et al., 2012; White et al., 2012; Zhou et al., 2014; Zou et al., 2009). This reflects a lack of understanding of the intricacies and complexities of oogenesis to be able to replicate the process in its entirety from pluripotent stem cell to oocyte *in vitro*. The use of an *in vivo* model may eliminate many of the limitations of the chimeric ovarian aggregate model detailed here to fully investigate the potential of bOSCs to undergo oogenesis.

The data presented here show that murine oocytes can reform follicles with ovarian somatic cells during an *in vitro* culture following aggregation. Furthermore, ovarian aggregates were healthier when cultured within a hanging drop suspension. Robust measures must be taken to ensure complete separation of oocytes from somatic cells following ovarian disaggregation. The use of this chimeric ovarian aggregate gave an innovative insight into the differentiation potential of bOSCs and provided novel evidence for the use of a chimeric ovarian aggregation system to investigate the potential of oogonial stem cells, although further development of this model is necessary.

5 Use of a xeno-transplant model to investigate the oogenic potential of bOSCs *in vivo*

5.1 Introduction

The previous chapter reported data demonstrating the potential of putative bovine oogonial stem cells to undergo differentiation *in vitro* within a chimeric ovarian aggregation model. As chimeric ovarian aggregates have previously generated functional rodent oocytes following a 21 day xeno-transplant to the kidney capsule of immune deficient mice (Eppig and Wigglesworth, 2000), that approach seemed likely to have value in the exploration of the oogenic potential of bOSCs.

Until recently support of full germ cell differentiation from primordial germ cells to functional mature oocytes could not be recapitulated *in vitro* without a period *in vivo* (Morohaku et al., 2016). Thus, transplantation models have been utilised to further our understanding of oogenesis and folliculogenesis. Transplantation of reconstituted fetal ovaries to the kidney capsule of recipient mice have produced oocytes capable of fertilisation and generation of offspring following *in vitro* maturation (Hashimoto et al., 1992; Matoba and Ogura, 2011; Qing et al., 2008). Additionally, functional oocytes derived from mouse embryonic stem cells and induced pluripotent stem cells have been made following transplantation of ovarian aggregates containing primordial germ cell-like-cells derived from the precursor cells to recipients (Hayashi et al., 2012). Similar results have been observed with mouse skin cells (Dyce et al., 2011).

To date successful oogenesis from oogonial stem cells in rodent species has also utilised *in vivo* models. Injection of fluorescently labelled OSCs into intact of follicle depleted ovaries in both mice and rats has generated oocytes capable of successful fertilisation, subsequent embryonic development (White et al., 2012) and produced healthy offspring (Zhou et al., 2014; Zou et al., 2009).

The development of immune deficient rodents has allowed the investigation of oogenesis and folliculogenesis in different species, such that ovarian tissue several species, including bovine, has been successfully transplanted to the kidney capsule of immune deficient mice. Bovine follicles have been successfully retrieved following

ovarian tissue transplantation and have been shown to support oocyte development capable of fertilisation and early embryonic development up to blastocyst stages (Campos-Junior et al., 2016; Senbon et al., 2005). Despite species differences, the recipient's hormone environment appears to support ovarian functions and follicular development. Re-vascularisation of ovarian grafts is estimated to occur within 48 hours (Dissen et al., 1994), establishing a nutrient supply and waste disposal system, negating many of the limitations associated with long term tissue culture (Aubard, 2003; Edmondson et al., 2014; Gook et al., 2001). Bilaterally ovariectomised rodents are typically used as recipients of xeno-transplants, however orchidectomised male mice have also been utilised as recipients. Juvenile and adult bovine ovarian tissues transplanted to the kidney capsule of male immune-deficient mice were observed to undergo successful follicular development (Hernandez-Fonseca et al., 2005) despite gender differences, suggesting that the GnRH/pituitary/gonadal feedback loop in rodents can support bovine follicular development in spite of species and gender differences. Elevated circulating levels of gonadotropins in these models is believed to be beneficial for follicular development (reviewed by Paris et al. (2004)) however the optimal hormonal profile of recipient individuals may be species specific and/or related to the age of the donor tissue as conflicting evidence has been reported.

To further investigate the potential of bOSCs and try to better understand this process, an *in vivo* xeno-transplant model using the chimeric ovarian aggregate model was utilised.

5.2 Materials and Methods

Ovarian aggregation model

Somatic cells from neonatal murine ovaries (freshly separated and cultured) were used to provide an ovarian niche for bOSCs. Negative (murine ovarian somatic cells only) and positive (murine germ and murine somatic cells) controls were also generated for comparison.

These experiments were initially conducted at the University of Oxford with the assistance of Anna Deleva and Sairah Sheikh who demonstrated the generation of ovarian aggregates and carried out the xeno-transplant surgeries, subsequently all experiments were carried out by Kelsey Grieve at the University of Edinburgh. RNA Scope analysis was carried out by Aquila HistoPlex, University of Edinburgh, all other analyses were carried out by Kelsey Grieve.

Bovine oogonial stem cells

bOSCs were FACS isolated (section 2.2) from adult bovine ovaries collected from the local abattoir (section 2.1). Following isolation bOSCs were either cryopreserved for future use (section 2.6.1.3) or cultured (section 2.6.1.1) in OSC media (section 2.12). Cultured cells were also cryopreserved and stored long term in liquid nitrogen (section 2.6.1.3) until required.

bOSCs were fluorescently labelled with Rhodamine Dextrans (section 2.6.2.3) prior to aggregation with somatic cells.

To store bOSCs long term and for transport, cells were cryopreserved as described in section 2.6.1.3.

Disaggregation of neonatal ovaries

Ovaries were collected from neonatal (postnatal day 0-5) female mice (CD-1, B6SJLF1 or B6;129-Gt(ROSA)26) following cervical dislocation and placed in pre-warmed PBS supplemented with 1mg/ml BSA then removed from their bursa. Ovaries were disaggregated (described in section 2.5.1) with pre-warmed trypsin/EDTA/DNAse and gentle agitation over a 25 minute period. The enzymatic digestion was neutralised with equal volumes with sterile supplemented M199 media

(see section 2.12) and the cell suspension centrifuged at 450 RCF for 5minutes. The cell pellet was then re-suspended in sterile supplemented M199 media (section 2.12) and placed into 35mm culture dishes for culture overnight 37ºC with humidified air and 5% CO_2.

Separation of germ and somatic cells

Germ and somatic cells from neonatal mice were separated based on cell adhesion characteristics as previously described (section 2.5.2), such that floating germ cells could be aspirated off the somatic cell monolayer. Somatic cells were then washed with pre-warmed PBS supplemented with 1mg/ml BSA, twice then lifted from the culture plate with 2ml of pre-warmed trypsin/EDTA/DNAse. The enzymes were neutralized with equal volumes of M199 with supplements and the somatic cell suspension was either filtered (size 30μm, 20μm or 10μm) or not filtered then centrifuged at 450 RCF for 5minutes. The supernatant was then discarded and cells were re-suspended in M199 media with supplements, placed in a new culture dish and returned to 37ºC, with humidified air and 5% CO_2 for 5-6 hours.

Following a second incubation, the murine neonatal ovarian somatic cells were washed with 2 ml pre-warmed PBS, twice, lifted from the culture plate a 2nd time with pre-warmed trypsin/EDTA/DNAse, which was then neutralized with equal volumes of M199 with supplements and the somatic cell suspension was either filtered (size 30μm, 20μm or 10μm) or not filtered then centrifuged at 450 RCFfor 5minutes. The supernatant was then discarded and cells re-suspended in an appropriate volume of Waymouths media with supplements (section 2.12) for cell counting, prior to aggregation.

Some populations of neonatal murine somatic cells were cultured longer term (section 2.5.3). Briefly, once separated from germ cells somatic cells were cultured in ovarian fetal somatic cell medium (section 2.12) and passaged using Trypsin (0.05%) with EDTA (Life Technologies), when confluent. Cells were also cryopreserved (section 2.6.1.3) if necessary.

Aggregation of ovarian cells

All cell populations used for aggregations (murine neonatal somatic cells, murine neonatal germ cells and bOSCs) were centrifuged at 450 RCF for 5 minutes and re-suspended in an appropriate volume of Waymouths media with supplements (section 2.12) for counting. Cell populations were manually counted using a haemocytometer. Freshly isolated bOSCs were also assessed using trypan blue for cell viability once thawed. Cells were then combined and placed into 0.5ml eppendorfs with 35µg Phytohaemagluttanin (PHA) at the desired ratio/concentration to create different aggregates (Figure 2.4). Cells were mixed by brief vortex and centrifuged in a microcentrifuge at 11,200 RCF for 30 seconds, the 0.5ml eppendorfs were then rotated 180^{o} and cells were centrifuged at 11,200 RCF for 30 seconds a second time. Cell pellets (aggregates) were then transferred with 30µl of Waymouths media with supplements to a hanging drop culture overnight at 37^{o}C with humidified air and 5% CO_2 to encourage cell interaction and adhesion.

Positive control ovarian aggregate

Positive control aggregates recombined neonatal murine somatic cell and germ cell populations at varying ratios (Figure 2.4). Positive control aggregates were then xeno-transplanted as described in section 2.7.1.

Negative control ovarian aggregate

To investigate the quality of the separation technique, negative control aggregates were generated, aggregating together mouse neonatal ovarian somatic cells only (Figure 2.4). Negative control aggregates were generated alongside every chimeric aggregate. Negative control aggregates were then xeno-transplanted as described in section 2.7.1.

Chimeric ovarian aggregate

Rhodamine dextran labelled cultured bOSCs were aggregated together with neonatal mouse ovarian somatic cells at a ratio of 1:10 respectively (Figure 2.4). Chimeric aggregates were then xeno-transplanted as described in section 2.7.1.

Xeno-transplant of ovarian aggregates

Ovarian aggregates, following an overnight hanging drop culture in supplemented

Waymouths media (section 2.12) were xeno-transplanted to the kidney capsule of SCID (C.B.17/IcrHan Hsd-Prkdc) mice for 21 days for comparison with the *in vitro* culture models.

All animal experiments were conducted under a UK Home Office licence in line with the Animals Scientific Procedure Act (1986). SCID Mice were housed as described in section 2.7 and obtained from Envigo laboratories and provided a minimum of 6 days to acclimatise to their new environment prior to the start of any experimental work.

Briefly, SCID mice were anaesthetised with isoflourane (section 2.7.1), shaved and skin sterilised. Subcutaneous injection of saline around the hind leg and a subcutaneous injection of vetergesic (at a dose of 0.03mg/ml in 100µl) around the neck were given. A vertical incision along the skin was made in the middle of the back, followed by a small incision in the body wall directly above the ovary, allowing the ovary and ovarian fat pad to be removed from the body cavity, and the ovary to be excised. Using the ovarian fat pad as a guide the kidney was pulled out of the body cavity with forceps. Sterile PBS kept the kidney hydrated and a tiny incision was made in the kidney capsule with a sterile needle. Using a pulled glass pipette, aggregates were transferred through the hole in the capsule to the surface of the kidney and moved from the incision site to ensure their security. 1, 2 or 4 ovarian aggregates were transplanted to recipient mice, all ovarian aggregates transplanted to any individual recipient were of the same description. The kidney and associated tissue was then returned to the body cavity, and the body wall sutured using number 5 sutures. The ovary was then removed on the other side following the same protocol and the skin incision closed using wound clips. Mice were then transferred to individual cages which were maintained at 30ºC while they recovered and then housed as described in section 2.7 for 21 days until tissue collection.

21 days after xeno-transplantation, mice were culled by lethal exposure to CO_2 or cervical dislocation of the neck and tissues were collected and fixed as described below.

Histological Techniques

Ovarian aggregate tissue was fixed in natural buffered formalin (NBF) for 6 hours, then transferred to 70% ethanol and embedded in wax using an automated Leica TP1050 processor. Tissue was sectioned at 5μM and mounted onto electrostatically charged glass slides and maintained at 50^{o}C overnight in a slide oven to ensure tissue adherence to the slide surface.

Haematoxylin and eosin staining

Every third section of each ovarian aggregate was stained with haematoxylin and eosin for histological evaluation to detect the presence of oocytes and follicles. Slides were de-waxed and rehydrated (section 2.8.3) and washed briefly in running tap water, then stained with haematoxylin and eosin (section 2.8.4) before dehydration and mounting (section 2.8.5).

Immunofluorescence

To assess tissue antigens, slides were dewaxed and rehydrated (section 2.8.3) prior to antigen retrieval (section 2.8.6). Slides were then washed and cooled in water 3 times. Non-specific binding of antibodies was prevented by using a peroxidase block followed by a serum block (section 2.8.6.1). Slides were then exposed to the primary antibody (listed in Table 5.1) diluted in NS/PBS/BSA and incubated overnight at 4^{o}C. Negative controls (primary antibody omitted) were always used and positive controls were used where applicable and appropriate.

Table 5.1: Primary antibodies used in Immunofluorescence in Chapter 5

Antibody	Dilution	Species	Supplier
β-Galactosidase	1:800	Mouse	Promega

Primary antibodies were washed off with PBS for 5minutes, twice, and the appropriate secondary antibodies (listed in Table 5.2) were diluted 1:200 in blocking serum (NS/PBS/BSA) and applied to slides for 30minutes at room temperature in a humidity chamber.

Table 5.2: Secondary antibodies used in Immunofluorescence in Chapter 5

Antibody	Supplier
Chicken anti Mouse	Santa Cruz

Slides were then washed twice with PBS and incubated in tyramide in accordance with the manufacturer's instructions, for 10 minutes. Slides were then washed in PBS to remove the tyramide, in an opaque chamber to prevent bleaching of the fluorescence before DAPI counterstaining and mounting (section 2.8.6.5). Slides were then stored in the dark at 4^{o}C until visualisation (section 2.9.4).

RNA Scope

RNA Scope analysis was carried out by Aquila HistoPlex, University of Edinburgh. Briefly, tissue sections were dewaxed and rehydrated (section 2.8.3) and allowed to air dry for 5 minutes at room temperature. Tissues were then treated with hydrogen peroxidase block for 10 minutes at room temperature and washed in deionised water. Target RNA's were then retrieved by exposure of slides to changes in pH (retrieval buffer, used according to manufacturer's instructions Advanced Cell Diagnostics) and high temperatures (100^{o}C) for 8minutes. Tissue was permeabilised using protease digestion (Protease Plus, Advanced Cell Diagnostics) at 40^{o}C for 15 minutes. Slides were then washed in deionised water and incubated with pre-warmed (40^{o}C) probe (Bt-ATP5b or Mm-UBC) for 30 minutes at 40^{o}C, then washed with buffer for 2 minutes at room temperature. The signal was then amplified using amplification solutions (Advanced Cell Diagnostics); amplification solution 1 was applied for 30 minutes at 40^{o}C, amplification solution 2 for 15 minutes at 40^{o}C, amplification solution 3 for 30 minutes at 40^{o}C, amplification solution 4 for 15 minutes at 40^{o}C, amplification solution 5 for 30 minutes at room temperature and amplification solution 6 for 15 minutes at room temperature. Slides were washed between each amplification with wash buffer twice for 2 minutes at room temperature. DAB was then applied to slides at room temperature for 10 minutes, to detect the signal. Slides were then washed in deionised water and tissue counterstained with Harris haematoxylin for two minutes followed by acid alcohol for 5 seconds, and Scott's tap water for 10 seconds. Slides were then dehydrated and

mounted (section 2.8.5). All reagents were sourced from Advanced Cell Diagnostics by Aquila HistoPlex, University of Edinburgh.

Microscopy

Tissue histology was imaged with a Provis AX70 (Olympus) or a Zeiss Imager Z1 both fitted with a AxioCam HRc camera (Zeiss) using Zeiss software. Whole tissue images were captured using a Leica MZF III with a RS Photometrics camera. Sections were visualised using a Zeiss LSM 780 confocal microscope using Zeiss software.

All scale bars were generated and embedded in image files using Zeiss software.

Tissue analysis

Every third section of all xeno-grafted ovarian aggregates were stained with either X-Gal and eosin staining or haematoxylin and eosin staining, and visualised and assessed for the presence of follicles in the tissue.

Oocytes were counted when the nucleolus was present and follicles classified based on their stage (primordial, a single layer of flattened granulosa cells; transitory, a mixture of flattened and cuboidal granulosa cells; primary, a single layer of cuboidal granulosa cells). Follicles and oocytes were also measured when the nucleolus was present, if this was not possible the section with the largest oocyte size was used. ImageJ software was used to take oocyte and follicle measurements following image scale calibration. Two perpendicular measurements were taken for oocyte and follicle size at the widest point, the average of was used.

Total tissue volumes analysed histologically was estimated using the sum of areas for all sections analysed (measured using ImageJ software) multiplied by the section depth (5μm).

Statistical Analysis

Statistical analysis was conducted using Graphpad Prism 6 software. One-way ANOVA analysis with post-hoc Tukeys multiple comparisons testing was used to compare oocyte sizes between ovarian aggregate groups where three or more groups were compared. Data are presented as Mean ± SEM throughout.

5.3 Results

5.3.1 Chimeric ovarian aggregates generate follicles following xeno-transplantation

Table 5.3 summarises the total number of chimeric, negative control and positive control ovarian aggregates generated, xeno-grafted and successfully retrieved from immune deficient recipient mice after 21 days. Positive control ovarian aggregates demonstrated the highest retrieval rates (100%) and negative control and chimeric ovarian aggregates showed lower retrieval rates (81% and 75%, respectively).

Table 5.3: Tabular summary of all ovarian aggregates generated, xeno-grafted and successfully retrieved following 21 days.

Ovarian Aggregates	Xeno-grafted	Retrieved	Retrieval Rate
Chimeric	48	36	75%
Negative control	42	34	81%
Positive control	21	21	100%

Three chimeric ovarian aggregates showed the presence of growing, multi-laminar follicles upon macroscopic visualisation at the time of retrieval (Figure 5.1. A, C & E), however growing follicles were not detected in the other chimeric ovarian aggregates (n=32; Figure 5.1.G, I & K). Histological analysis was carried out on 30 chimeric ovarian aggregates (estimated total tissue volume of $124.3x10^6$ μm^3), 3 of which appeared to contain growing follicles at retrieval. All chimeric ovarian aggregates retrieved showed good overall tissue health, developed vasculature and few pyknotic cells observed.

Histology confirmed a total of 9 follicles in the 3 ovarian aggregates identified as containing growing follicles by macroscopic visualisation (Figure 5.1.B, D & F). Follicles observed within chimeric ovarian aggregates showed healthy morphology with round oocytes containing a single nuclei, with even cytoplasmic eosin staining and no pyknotic granulosa cells. Eight of these follicles were multi-laminar, containing more than 1 layer of cuboidal granulosa cells and 1 contained a single

layer of cuboidal granulosa cells, illustrating that these follicles had successfully initiated growth in this system.

Histology was conducted on 27 chimeric ovarian aggregates which did not appear to contain growing follicles upon retrieval and confirmed the absence of multi-laminar follicles by H&E staining (Figure 5.1.H, J & K). However, several of these aggregates (n=11) contained small structures formed by groups of cells. These structures showed interactions between a central larger cell and surrounding cells forming a spherical shape. These structures share similarities with primordial follicles (Figure 5.1.H & J) and may represent precursors to primordial follicles in this system, thus have been termed pre-primordial follicle-like structures. A total of 16 pre-primordial follicle-like structures were identified in all chimeric ovarian aggregates and may indicate the initial formation of oocyte-like cells within this model. No distinguishable structures could be identified by histological analysis of any of the other chimeric ovarian aggregates (n=16, Figure 5.2), in these tissues cells shared similar morphology (Figure 5.1.L). Thus, growing follicles were identified in 10% of chimeric ovarian aggregates and pre-primordial follicle-like structures in 36.6% (Figure 5.2) of analysed chimeric ovarian aggregates.

A further 12 chimeric ovarian aggregates were also generated using cultured neonatal murine ovarian somatic cells and successfully retrieved from recipient mice. Histological analysis showed that these aggregates did not contain multi-laminar follicles or pre-primordial follicle-like structures (Figure 5.3).

For each experimental chimeric ovarian aggregate a complimentary negative control ovarian aggregate was generated consisting only of the same ovarian somatic cell population. None of the corresponding negative controls contained oocytes or follicles, confirmed by histological assessment of the tissue (see Section 5.3.4, Figure 5.9).

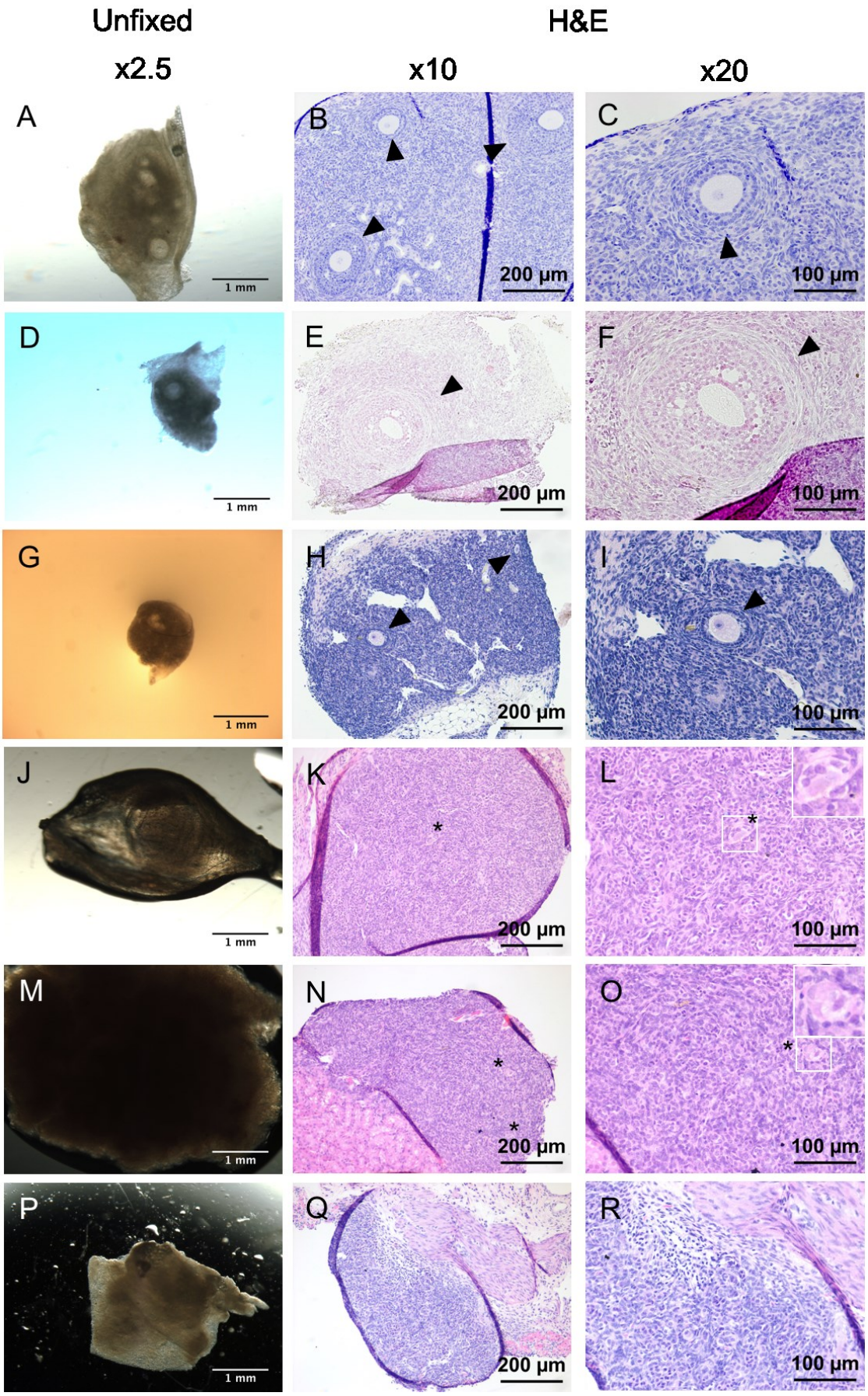
Unfixed
H&E
x2.5
x10
x20
A
B
C
D
E
F
G
H
I
J
K
L
M
N
O
P
Q
R
1 mm
200 µm
100 µm

Figure 5.1: Chimeric ovarian aggregates generate follicles following xenotransplantation. 48 chimeric ovarian aggregates were xeno-grafted for 21 days, and 36 were successfully retrieved. Tissues were visualised upon collection (A, D, G, J, M and P), 3 chimeric ovarian aggregates appeared to contain follicles (A, D and G), confirmed by histological analysis and indicated by arrowheads (B, C, E, F, H and I). 32 Chimeric ovarian aggregates did not appear to contain follicles macroscopically (J, M and P), histological analysis did not show oocytes or follicles (K, L, N, O, Q and R), however structures were observed showing interaction between morphologically different cell types with a central cell and adjacent surrounding cells forming a follicle-like structure, indicated by asterisks. Unfixed tissue was imaged at x2.5 magnification and scale bars represent 1mm. H&E tissue sections were imaged at x10 magnification (scale bars represent 200µm) and x20 magnification (scale bars represent 100µm).

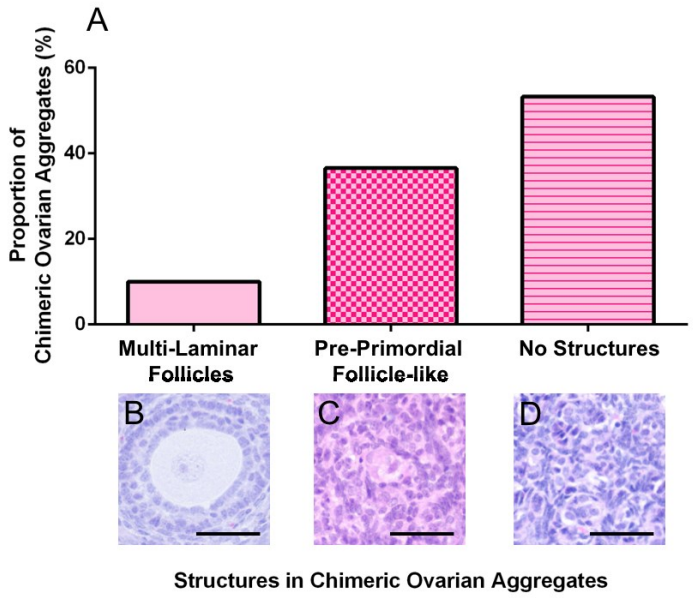

Figure 5.2: Distribution of chimeric ovarian aggregates based on structures identified within aggregates, represented by proportion of total ovarian aggregates analysed. Of 48 chimeric ovarian aggregates transplanted, 12 were not retrieved and 36 were successfully retrieved following 21 days. Haematoxylin and eosin staining was conducted on 30 retrieved chimeric ovarian aggregates. Three types of ovarian aggregates were identified based on structures observed within the aggregates (**A**). Multi-laminar follicles (**B**) with oocytes surrounded by more than 1 layer of cuboidal granulosa cells were identified in 10% (n=3) of chimeric ovarian aggregates analysed. Pre-primordial follicle-like structures (**C**), with a larger spherical-like central cell associated with adjacent cells to form a spherical-like structure with morphological similarities to primordial follicles and were found in 36.6% (n=11) of chimeric ovarian aggregates. All other chimeric ovarian aggregates (53.3%; n=16) did not contain multi-laminar follicles or pre-primordial follicle-like structures and have been described as having 'no structures' (**D**). Tissue sections were imaged at x20 magnification and scale bars represent 50µm.

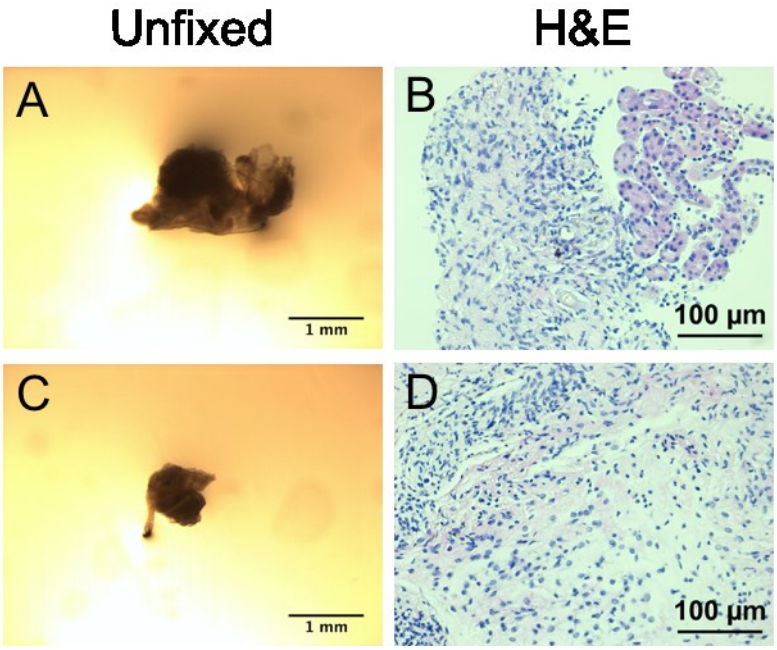

Figure 5.3: Cultured neonatal somatic cells do not support follicle formation in xeno-transplanted chimeric ovarian aggregates. Somatic cells isolated from neonatal cd-1 mice were cultured then aggregated with bovine oogonial stem cells to from chimeric ovarian aggregates (n=12). Ovarian aggregates were transplanted to the kidney capsule of immune-deficient mice for 21 days. All chimeric ovarian aggregates were collected (example aggregates shown in A and C). Histological analysis showed that no follicles had been generated in chimeric ovarian aggregates with cultured neonatal mouse ovarian somatic cells with (B and D). Unfixed tissue was imaged at x2.5 magnification and scale bars represent 1mm. H&E tissue sections were imaged at x20 magnification and scale bars represent 100µm.

5.3.2 Oocytes in chimeric ovarian aggregates are significantly larger than oocytes in positive control ovarian aggregates

A total of 9 oocytes encapsulated within well organised somatic cells forming follicles were identified in chimeric ovarian aggregates. These follicles ranged in developmental stage from transitory (n=1; oocyte with flattened and cuboidal granulosa cells), pre-antral (n=6; oocyte in multi-laminar follicle without an antral cavity) and incipient antral (n=2, multi-laminar follicle with initial separation of granulosa cells to form antral cavities). No large antral follicles were observed in chimeric ovarian aggregates.

Oocytes within pre-antral follicles in chimeric ovarian aggregates (n=6; 60.9±3.6μm) were significantly larger ($P<0.0001$) than murine oocytes in positive control ovarian aggregates (n=38; 34.5±1μm; Figure 5.4.E). Endogenous pre-antral oocytes from murine (n=14; 44.5±3.3μm) and bovine (n=6; 67.9±7.8μm) adult ovarian tissues were also measured as controls. Bovine oocytes were significantly ($P<0.0001$) larger than their murine counterparts. Oocytes in chimeric ovarian aggregates were also significantly ($P<0.01$) larger than native murine pre-antral oocytes, but were not different in size to native bovine pre-antral oocytes.

These data also revealed that murine oocytes within positive ovarian aggregates were significantly ($P<0.01$; Figure 5.4.E) smaller in size than native murine oocytes within pre-antral follicles in adult ovarian tissue. All oocytes observed in positive control ovarian aggregates were observed within a follicle structure suggesting successful re-establishment of cell-cell interactions between oocytes and somatic cells. Furthermore, follicles demonstrated extensive development with no non-growing follicles observed and many follicles containing developed antral cavities (Figure 5.4.A). Differences between oocytes from positive control ovarian aggregates and native oocytes suggests that the ovarian aggregate xeno-transplant model does not directly replicate *in situ* follicle growth. This may indicate that cell-cell interactions between oocytes and somatic cells are insufficiently established to support coordinated oocyte and follicle growth in positive control ovarian aggregates.

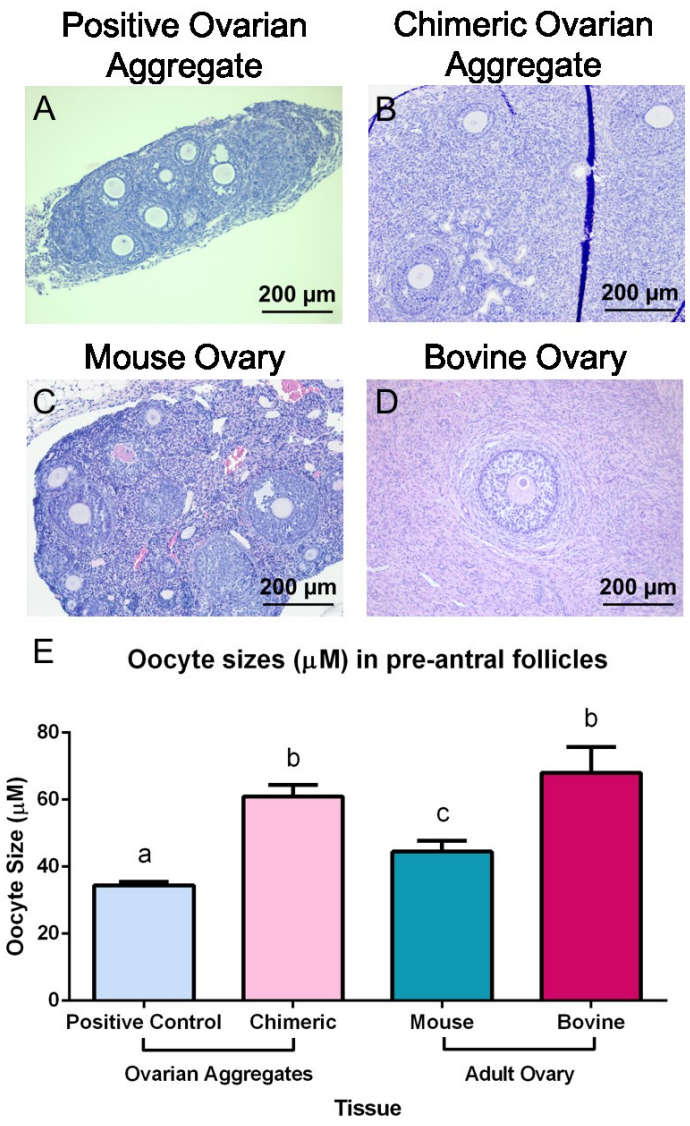

Figure 5.4: Oocyte Sizes in pre-antral follicles of chimeric and positive ovarian aggregates compared to control murine and bovine adult ovarian tissue. H&E sections of positive ovarian aggregates (A), chimeric ovarian aggregate (B), adult mouse ovary (C) and adult bovine ovary (D). Oocyte sizes within pre-antral follicles were measured and compared between groups by One-Way ANOVA with Tukeys Post Hoc testing for multiple comparisons (E; mean ± SEM). Oocytes with in chimeric ovarian aggregates (n=6; 60.9±3.6µm) were significantly ($P<0.0001$) larger than positive control ovarian aggregates (n=38; 32.9±1µm) and endogenous murine pre-antral oocytes (n=14; 42.8±3µm) but not significantly different from endogenous bovine pre-antral oocytes (n=6; 65.9±6.8µm). Native murine oocytes were significantly larger than oocytes in positive control ovarian aggregates ($P<0.01$) and bovine oocytes significantly ($P<0.0001$) larger than murine counterparts endogenously and wihin ovarian aggregates. Tissue sections were imaged at x10 magnification and scale bars represent 200µm. Different letters denote significant difference between variables, no statistical difference was observed between variables with the same letter.

Oocyte sizes were compared to pre-antral follicle sizes to investigate whether oocytes were disproportionate in size to their follicle (Figure 5.5). Pearson's correlational analyses showed significant correlation between oocyte and follicle size in positive control ovarian aggregates (r^2=0.14, p=0.02), chimeric ovarian aggregates (r^2=0.69, p=0.04) and mouse (r^2=0.66, p=0.0004) and bovine adult ovarian tissue (r^2=0.98, p=0.0001). Thus, ovarian aggregates, both chimeric and positive controls, showed oocyte growth associated with follicle growth.

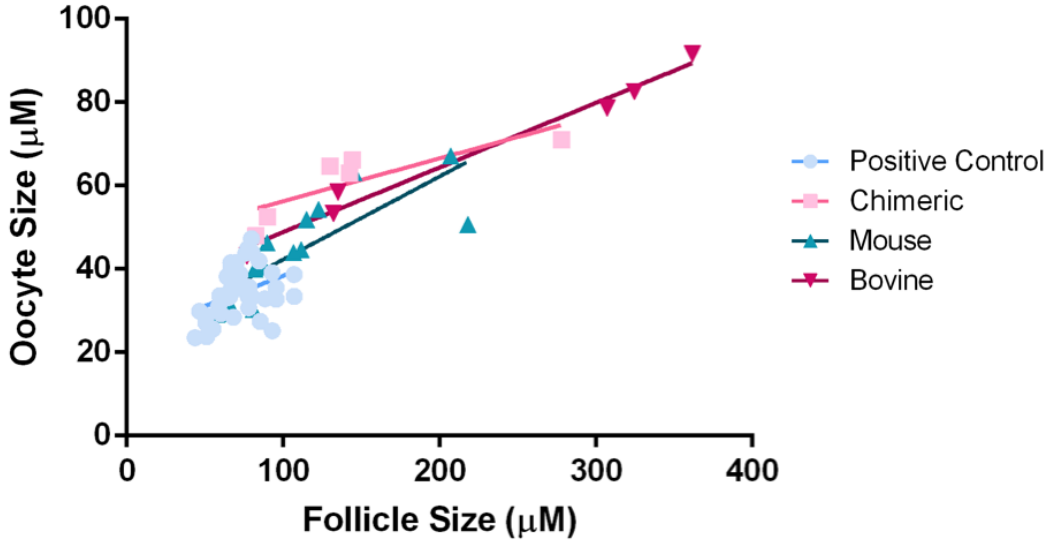

Figure 5.5: Pre-antral oocyte and follicle sizes of ovarian aggregates and control ovarian tissues. Pearson's correlation analyses revealed that oocyte size was correlated to follicle size within each experimental group (Positive control ovarian aggregate, n=38, r^2=0.14, p=0.02; Chimeric ovarian aggregate, n=6, r^2=0.68, p=0.04; Mouse adult ovarian tissue, n=14, r^2=0.66, p=0.0004 and Bovine adult ovarian tissue, n=6, r^2=0.98, p=0.0001).

Two incipient antral follicles were observed within chimeric ovarian aggregates. These follicles demonstrated very early antral cavity development, with the initial separation of granulosa cells within the follicle structure (Figure 5.4.B). These follicles contained several layers of granulosa cells (>5). Pre-antral follicles within chimeric ovarian aggregates also contained many layers of granulosa cells without evidence of antral cavity formation. In contrast, positive control ovarian aggregates showed antral cavity formation in follicles with fewer layers of granulosa cells (>2; Figure 5.4.A). Differences in antral cavity formation and the number of granulosa cell layers between positive control and chimeric ovarian aggregates could not be

statistically analysed due to low follicle numbers in chimeric ovarian aggregates, however, these observations suggest differences in follicle growth dynamics between follicles within chimeric bOSC ovarian aggregates and positive control ovarian aggregates.

Follicles in adult murine ovarian tissue showed antral development in follicles with significantly more granulosa cell layers (5.7 ± 0.5 cell layers; P<0.0001, Figure 5.6) than follicles in positive control ovarian aggregates (2.9 ± 0.2 cell layers). This suggests that follicles in positive control ovarian aggregates are undergoing altered follicle development compared to *in situ* control follicles.

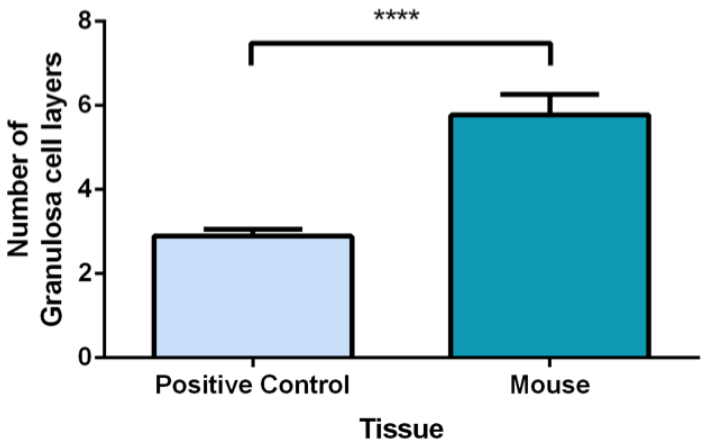

Figure 5.6: Number of granulosa cell layers in murine incipient antral follicles of positive control ovarian aggregates and adult ovarian tissue. The number of granulosa cell layers was counted in follicles with early antral development and compared by Student's t-test. Significantly more layers of granulosa cells were observed in early antral follicles with initial cavity formation in adult mouse ovarian tissue (5.7 ± 0.5 cell layers, mean ± SEM) than follicles in positive control ovarian aggregates (2.9 ± 0.2 cell layers, mean ± SEM). **** P<0.0001.

5.3.3 Chimeric ovarian aggregates containing freshly isolated bOSCs form pre-primordial follicle-like structures *in vivo*

The oogenic potential of bOSCs was also investigated by using freshly isolated cells. FACS isolated bOSCs were immediately frozen and thawed just prior to aggregation with somatic cells. bOSCs were counted prior to aggregation and cell viability was 55%, using trypan blue as a marker of dead cells. Thus, almost half of freshly isolated bOSCs did not maintain membrane integrity when frozen and thawed, in contrast, bOSCs previously established in culture demonstrated 90% cell viability following freeze/thaw. This suggests the combined effect of isolation and cryopreservation was detrimental to cell integrity and health of bOSCs.

Four chimeric ovarian aggregates containing uncultured bOSCs were generated and successfully retrieved following xeno-transplantation. Histological analysis of 3 ovarian aggregates was conducted. Overall tissue health was good and very few pyknotic cells were observed, suggesting that the aggregates had established a good nutrient and waste disposal supply through host vasculature. However, chimeric ovarian aggregates containing uncultured bOSCs did not contain oocytes or follicles when analysed histologically (Figure 5.7). On further inspection, aggregates appeared morphologically similar to chimeric ovarian aggregates containing cultured bOSCs. Pre-primordial follicle-like structures were also observed (Figure 5.7.B inset), suggesting that the early stages of oogenesis may be occurring in these ovarian aggregates. No complementary negative controls were retrieved for this study.

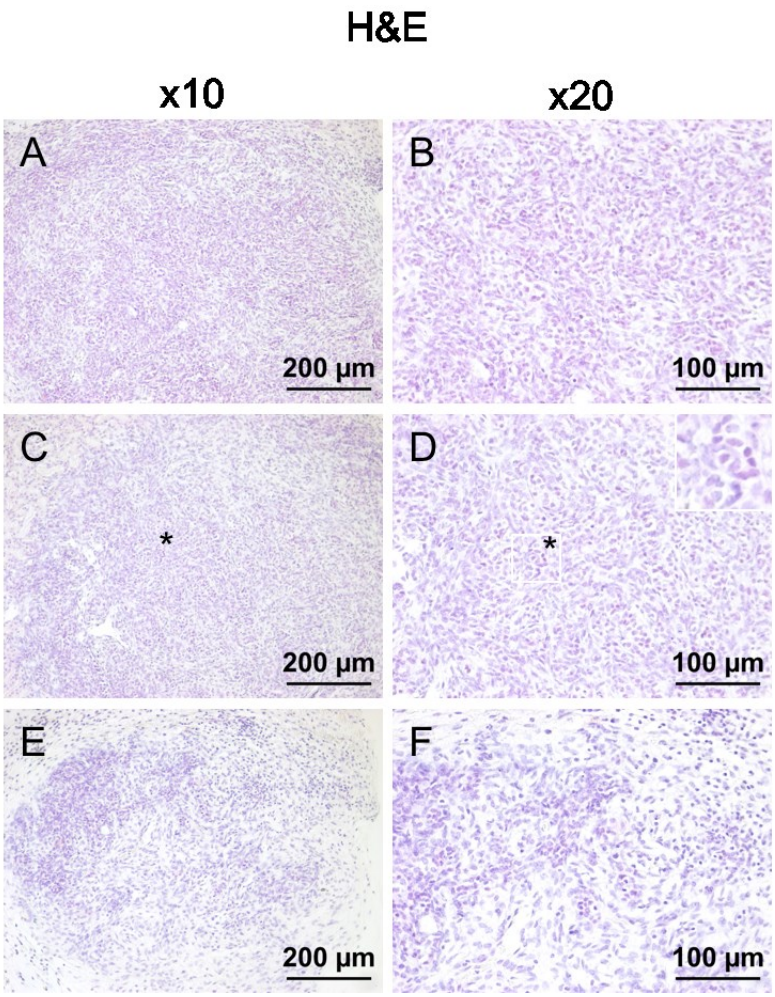

Figure 5.7: Freshly isolated bOSCs form pre-primordial follicle-like structures in xeno-transplanted chimeric ovarian aggregates. bOSCs frozen immediately after FACS isolation were thawed prior to aggregation with murine somatic ovarian cells and then xeno-grafted to the kidney capsule of immune deficient recipient mice for 21 days (n=4). Histological assessment of 3 chimeric ovarian aggregates (A-F) showed that no multi-laminar follicles were formed during transplantation, however, pre-primordial follicle-like structures were observed (C and D; indicated by asterisks), like those in chimeric ovarian aggregates with cultured bOSCs. Tissue sections were imaged at x10 magnification (scale bars represent 200µm) and x20 magnification (scale bars represent 100µm).

5.3.4 Early stage follicles observed in negative control ovarian aggregates

To determine the full role of bOSCs when combined with neonatal murine ovarian somatic cells, somatic cell only aggregates were utilised as negative controls. 11 negative control ovarian aggregates were fixed prior to xeno-graft as day 0 controls. These had been exposed to the same processes as xeno-grafted negative control ovarian aggregates (n=42). No oocytes were observed in day 0 negative control ovarian aggregates (Figure 5.8), suggesting successful separation of germ and somatic cells following ovarian disaggregation, was achieved, consistent with results from *in vitro* cultured negative control ovarian aggregates (see section 4.3.2).

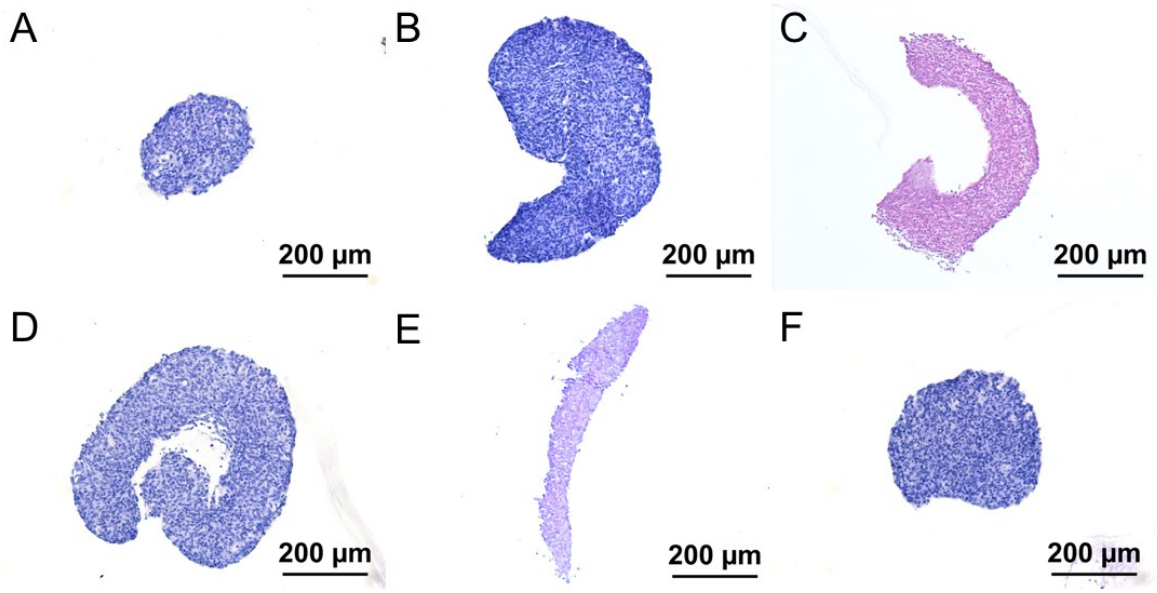

Figure 5.8: Day 0 controls of negative control ovarian aggregates do not contain oocytes. Neonatal murine ovarian somatic cells were separated from oocytes following ovarian disaggregation based on cell adhesion characteristics and filtration of somatic cells (10µm). Ovarian somatic cells were aggregates to form negative control ovarian aggregates. Day 0 controls (n=11) were fixed for histological assessment prior to xeno-transplantation. Haematoxylin and eosin staining of these tissues showed no oocytes or follicles were present throughout day 0 negative control ovarian aggregates (A-F). Tissue sections were imaged at x10 magnification and scale bars represent 200µm.

Thirty-four negative control ovarian aggregates were successfully retrieved following xeno-transplantation. Thirty aggregates (estimated total tissue volume of 132.7 x10^6 μm^3) showed no visible signs of oocyte or follicle development upon retrieval, which was confirmed by histological analysis (Figure 5.9.B-C, E-F, H-I, K-L, N-O). Further suggesting that oocytes have been successfully removed from neonatal murine ovarian somatic cell populations prior to ovarian aggregate generation. Additionally, negative control ovarian aggregates (n=10, 2 collected) were also made using cultured neonatal murine ovarian somatic cells, and did not contain oocytes or follicles following xenotransplantation.

However, 4 negative control ovarian aggregates recovered after xeno-grafting, contained early stage follicles (Figure 5.10.G). A total of 6 follicles were identified in negative control ovarian aggregates (Figure 5.10.A-F). 3 follicles were non-growing (Figure 5.10.A-C) and 3 were multi-laminar and had initiated growth (Figure 5.10.D-F) A single follicle showed separation of granulosa cell layers indicating the initial formation of an antral cavity (Figure 5.10.F). Oocytes from growing follicles in negative control ovarian aggregates (n=3, 53.3 ± 2.4μm) were significantly ($P<0.05$) larger than murine oocytes in positive control ovarian aggregates (n=38; 34.5±1μm) but not statistically different in size to oocytes from chimeric ovarian aggregates (n=6; 60.9±3.6μm) and endogenous oocytes from murine (n=14; 44.5±3.3μm) and bovine (n=6; 67.9±7.8μm) adult ovarian tissue. Although follicles were observed the incidence of this was low for xeno-transplanted negative control ovarian aggregates. Multi-laminar follicles and non-growing follicles were observed in a total of 11.8% of negative control ovarian aggregates, compared to 100% of positive control ovarian aggregates and 46.6% of chimeric ovarian aggregates which also contained pre-primordial follicle-like structures, which were not observed in negative control ovarian aggregates or positive control ovarian aggregates.

These results suggest that murine neonatal ovarian somatic cells can support oogenesis and folliculogenesis when placed in an *in vivo* environment. However, the source of the oocytes within growing follicles in the chimeric ovarian aggregates is unclear. Although there are differences in the follicle and follicle-like structures

observed in negative control and chimeric ovarian aggregates, results presented here may indicate that oocytes observed in chimeric ovarian aggregates may be derived from cells other than bovine oogonial stem cells. Thus, methods to determine the source of oocytes in chimeric ovarian aggregates must be established.

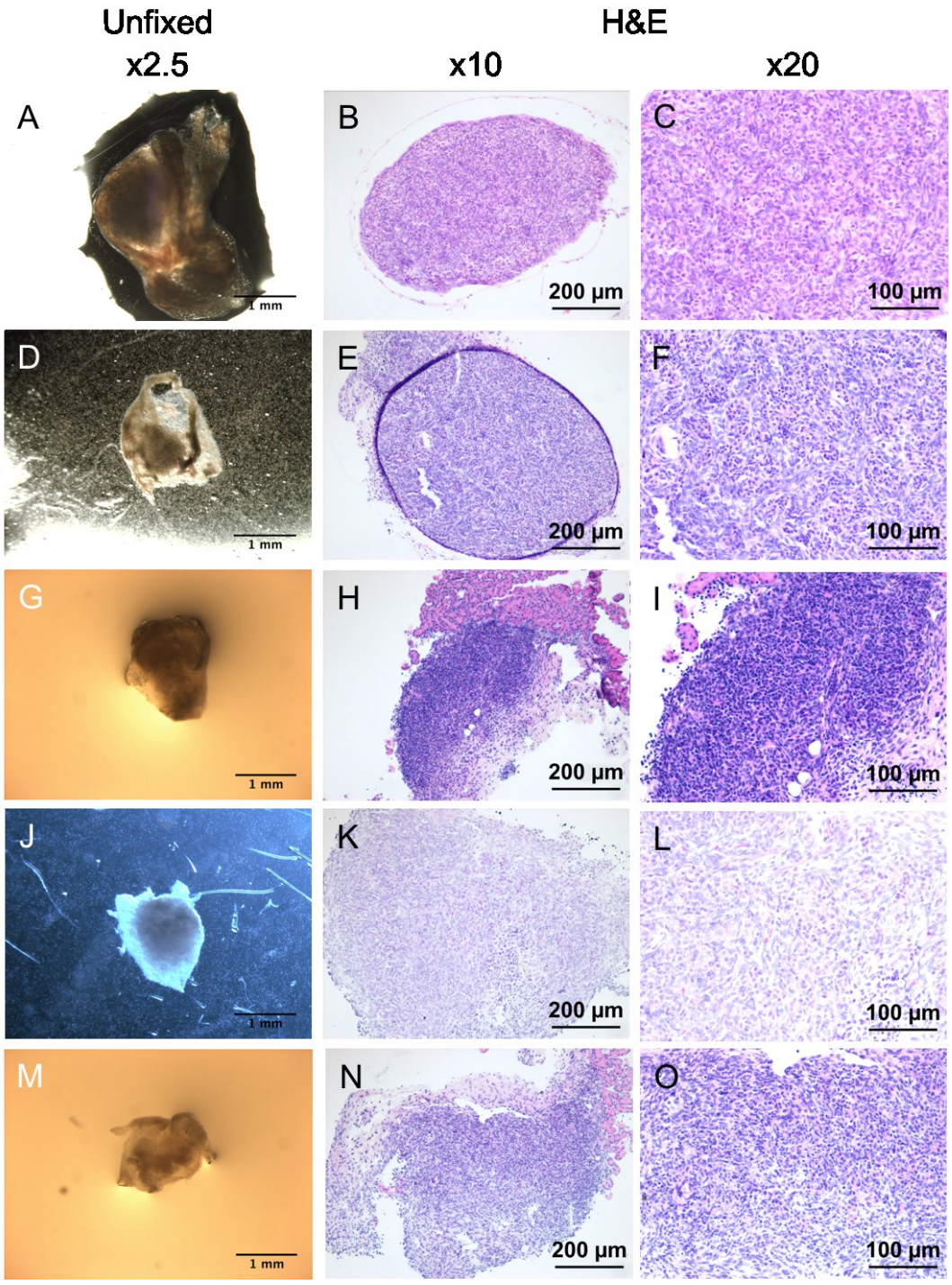

Figure 5.9: Negative control ovarian aggregates lack follicles following xeno-transplantation. 30 negative control ovarian aggregates did not appear to contain oocytes and follicles upon retrieval (A, D, G, J & M), confirmed by histological analysis (B, C, E, F, H, I, K, L, N & O). Unfixed tissue was imaged at x2.5 magnification and scale bars represent 1mm. H&E tissue sections were imaged at x10 magnification (scale bars represent 200µm) and x20 magnification (scale bars represent 100µm).

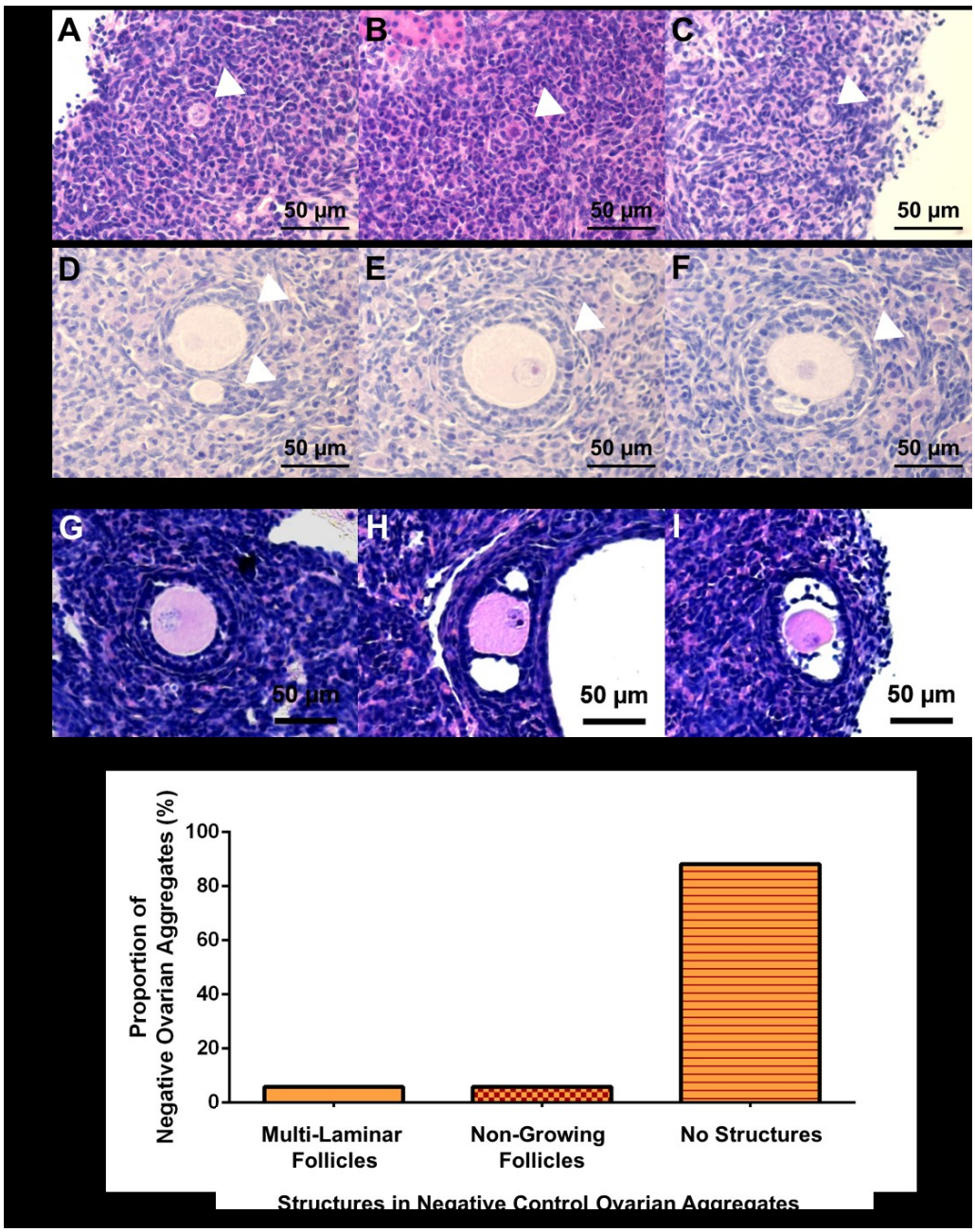

Figure 5.10: Early stage follicles were observed within negative control ovarian aggregates. Of 42 negative control ovarian aggregates, 34 were successfully retrieved. Histological analysis of all aggregates revealed the presence of follicles within 4 negative control ovarian aggregates. A total of 6 Follicles were observed (A-F). These follicles ranged in developmental stage from non-growing (A, B and C) to multi-laminar follicles (D and E). The initial separation of granulosa cells to form an antral cavity was observed in one follicle (F). G-I illustrate early stage follicles within positive control ovarian aggregates. (J) Summary of the proportion of negative ovarian aggregates where no structures were observed (n=30, 88.2%) or multi-laminar follicles (n=2, 5.9%) and non-growing follicles (n=2, 5.9%) were identified. Follicles are indicated by white arrowheads. Tissue sections were imaged at x40 magnification and scale bars represent 50µm.

5.3.5 Cell labelling methods in chimeric ovarian aggregates

The presence of follicles within negative control ovarian aggregates highlights the necessity to determine the origin of oocytes within chimeric ovarian aggregates. Thus, methods to identify bovine and murine cells within chimeric ovarian aggregates were utilised.

To determine the contribution of bOSCs to oogenesis in chimeric ovarian aggregates, rhodamine dextrans were utilised to track bOSCs. Rhodamine fluorescence could be detected within chimeric ovarian aggregates prior to xeno-transplantation (Figure 5.11.A), however rhodamine fluorescence was almost undetectable in these tissues following collection (Figure 5.11.B). Histological analysis of chimeric ovarian aggregates also showed no rhodamine expression within the tissues when counterstained with DAPI (Figure 5.11.C). These results suggest that fluorescence from rhodamine dextrans is not sufficiently maintained in bOSCs following xeno-transplantation and is not an appropriate labelling method to trace bOSCs in this system.

Negative control ovarian aggregates did not show rhodamine fluorescence prior to (Figure 5.11.D) or following (Figure 5.11.E) xenotransplantation, which was confirmed by histological analysis (Figure 5.11.F).

Alternative labelling methods were also used to identify murine cells within chimeric ovarian aggregates. Cells from B6;129-Gt(ROSA)26) mice were utilised as they ubiquitously express β-Galactosidase, which can be detected by XGal staining. However, both XGal staining (Figure 5.12.A & B) and immunofluorescence for β-Galactosidase were unsuccessful (Figure 5.12.C).

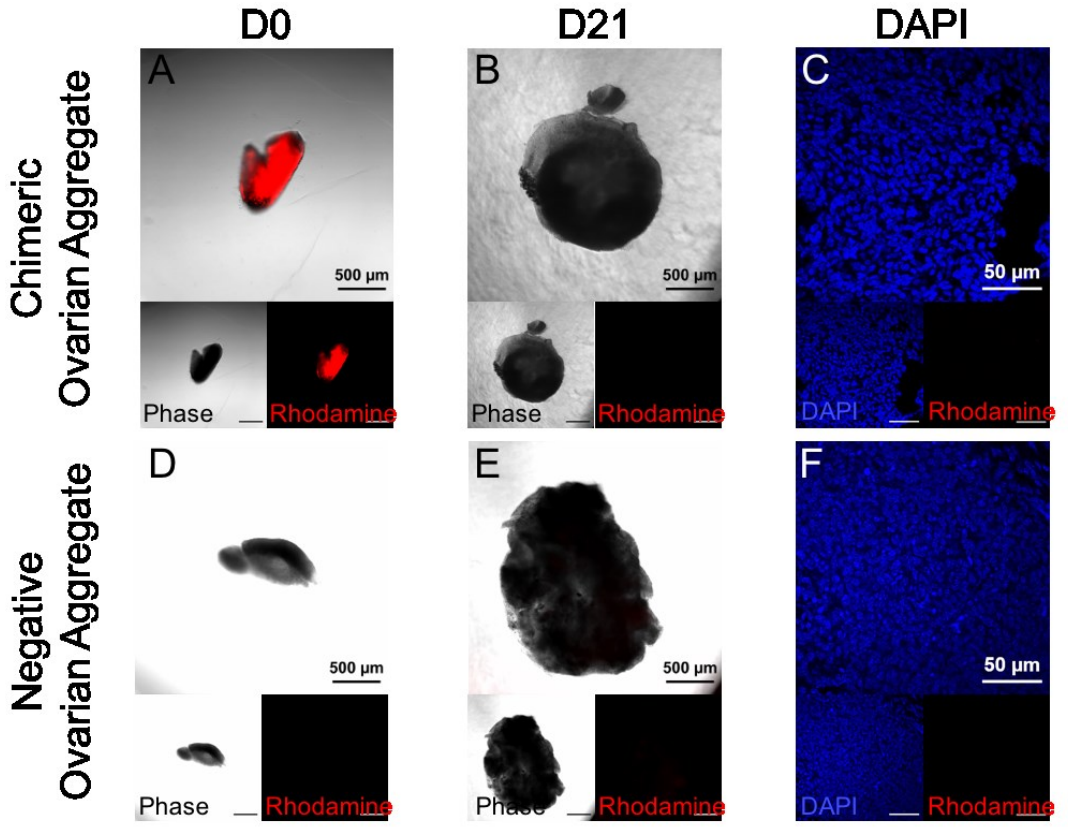

Figure 5.11: Xeno-transplanted chimeric ovarian aggregates do not maintain rhodamine dextran expression in bOSCs. bOSCs fluorescently labelled with rhodamine dextrans were aggregated with neonatal mouse somatic cells. Rhodamine dextrans were identified within chimeric ovarian aggregates prior to xenotransplantation (A), however could not be detected in tissues following collection (B) and were absent from chimeric ovarian aggregate sections when DAPI counterstained and visualised by confocal microscopy (C). Negative ovarian aggregates containing only neonatal mouse somatic cells showed no rhodamine fluorescence at any time point (D-F). Whole ovarian aggregates were imaged at x10 magnification and scale bars represent 500µm (A, B, D & E). Tissue sections were imaged at x40 magnification and scale bars represent 50µm (C & F).

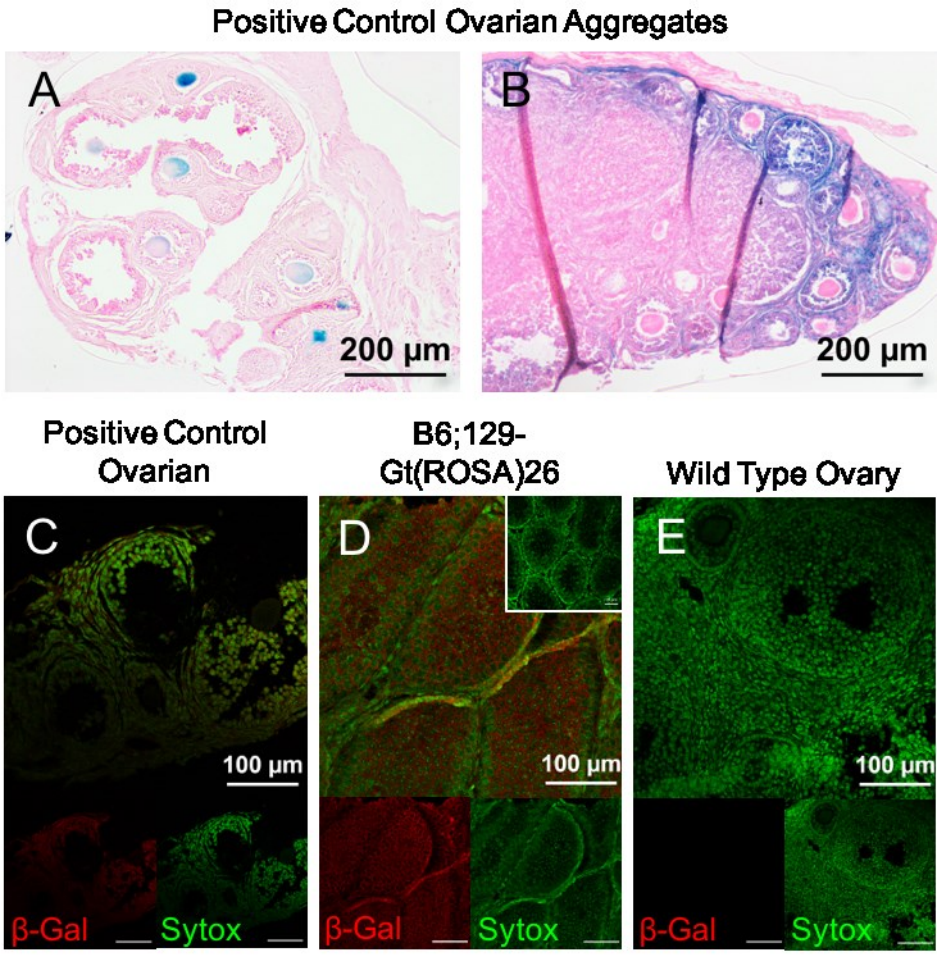

Figure 5.12: Inconsistent XGal staining and β-Galactosidase immunofluorescence in control ovarian aggregates. XGal is used to detect β-Galactosidase activity found in cells of B6;129-Gt(ROSA)26 mice and is observed as a blue pigment. Following glutaraldehyde fixation, ovarian aggregates containing B6;129-Gt(ROSA)26) cells, were transferred to an XGal solution for staining. Positive control ovarian aggregates (A; B6;129-Gt(ROSA)26 germ cells and B; B6;129-Gt(ROSA)26 somatic cells), show inconsistent XGal staining within individual oocytes and only peripheral aggregate staining. β-Galactosidase immunofluorescence was used to further investigate these observations. (C) Positive ovarian aggregate with B6;129-Gt(ROSA)26 germ cells and wild type somatic cells shows non-specific staining of β-Galactosidase throughout the tissue. Positive (D) control, B6;129-Gt(ROSA)26 testis, show expected staining patterns and staining is eliminated when the primary antibody is omitted (inset). No staining is observed in negative control tissue (E), wild type ovary. H&E tissue sections were imaged at x10 magnification (scale bars represent 200µm) and immunofluorescent sections were imaged at x20 magnification (scale bars represent 100µm).

5.3.6 RNA Scope to determine species of oocytes in chimeric ovarian aggregates

To determine the species of origin of the oocytes observed in chimeric ovarian aggregates and the location of bOSCs, we utilised RNA Scope. Mouse Ubiquitin C (m-UBC) and bovine adenosine triphosphate (ATP) synthase subunit 5β (b-ATP5B) probes were used as markers of bovine and mouse cells within ovarian aggregates. Control adult ovarian tissues were utilised to determine the specificity of the probes to target cells and tissues. Due to the time required for development of this protocol, RNA degradation within the tissue appeared to be a significant confounder in many chimeric tissues.

m-UBC staining was observed in cells within chimeric ovarian aggregates throughout the tissue (Figure 5.13.A), although not all cells stained positive. Oocytes present within this tissue showed chromogenic staining of m-UBC (Figure 5.13.A). m-UBC staining was consistent throughout positive control ovarian aggregates (Figure 5.13.C) and adult murine ovarian tissue (Figure 5.13.G) and staining was observed within all ovarian cell types within control mouse tissues as expected. However, m-UBC staining was also observed in oocytes and follicles of adult bovine ovarian tissue (Figure 5.13.E), although staining was not observed in the surrounding stromal tissue. These results suggest that the m-UBC probe is non-specifically binding to RNAs within bovine oocytes and follicles and thus the findings in chimeric aggregates cannot be interpreted.

b-ATP5B showed little or no staining in xeno-transplanted chimeric ovarian aggregates (Figure 5.13.B), although some cells appeared to be positive for b-ATP5B. However almost no staining for the presence of b-ATP5B was observed within adult bovine ovarian tissue (Figure 5.13.F). Furthermore, weak staining was observed in some sporadic cells within murine tissue (Figure 5.13.D and Figure 5.13.H).

Thus, we cannot determine the species of oocytes in chimeric ovarian aggregates with these probes or this protocol without further optimisation and validation.

Figure 5.13: RNA Scope analysis of the ovarian aggregates. Probes against mouse Ubiquitin C (m-UBC) and bovine ATP5B (b-ATP5B) were used to determine the location of mouse and bovine cells within chimeric ovarian aggregates (A and B, respectively). Positive control ovarian aggregates (C and D), bovine (E and F) and mouse (G and H) adult ovarian tissues were stained for the presence of mouse UBC and bovine ATP5B to ensure probe specificity. m-UBC staining was observed throughout chimeric ovarian aggregates and showed staining within the oocyte present (A). Control mouse tissues (positive control ovarian aggregate (C) and adult ovarian tissue (G)) showed staining in all ovarian cell types, however m-UBC also showed non-specific staining of bovine oocytes and follicles (E). b-ATP5B showed little staining within chimeric ovarian aggregate tissue (B), furthermore almost no staining was observed in control bovine tissues (F) and some non-specific staining was observed in mouse control tissues (positive control ovarian aggregate (D) and adult ovarian tissue (H)). Tissue sections were imaged at x20 magnification and scale bars represent 50µm.

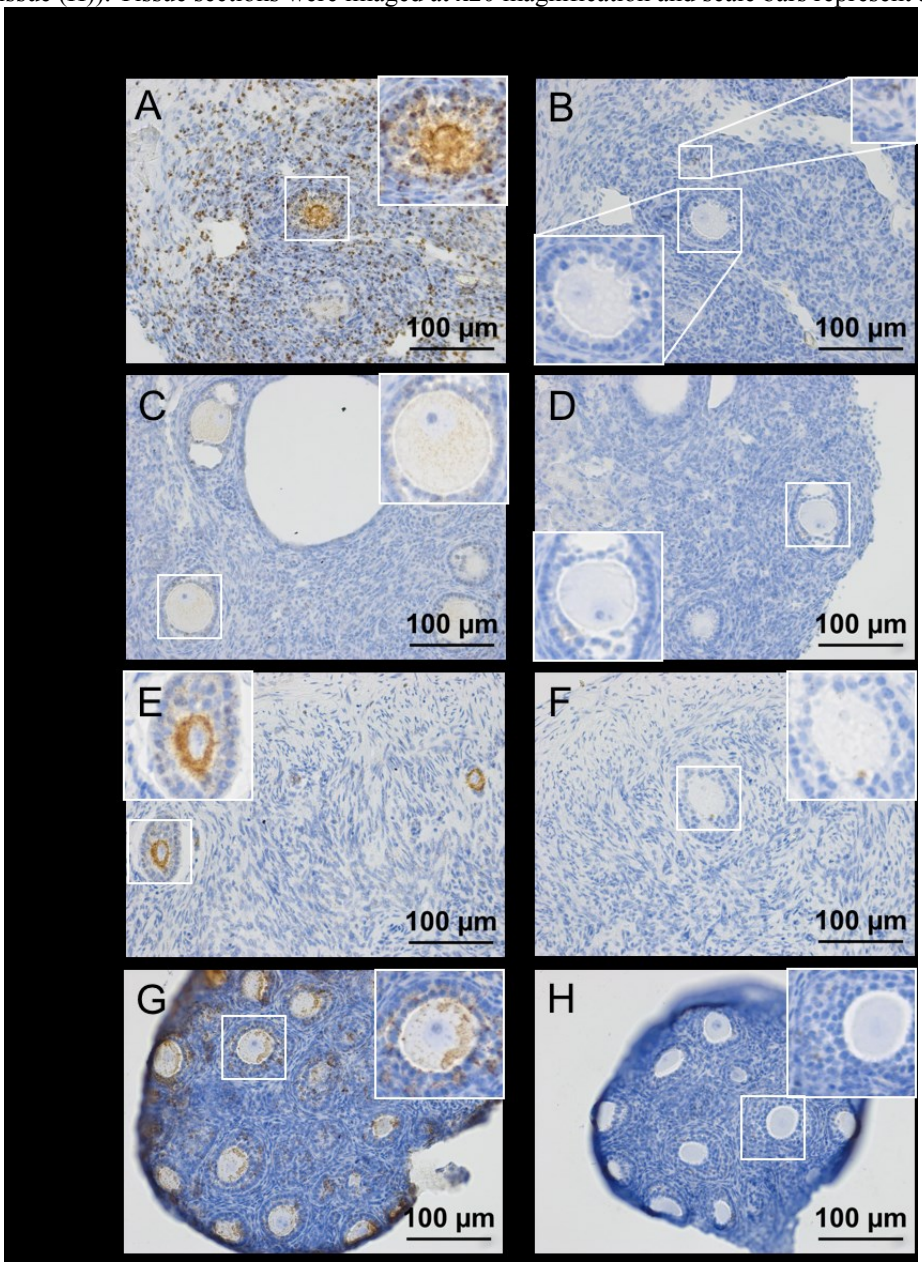

5.4 Discussion

Rodent labelled OSCs introduced into oocyte depleted (Zhou et al., 2014; Zou et al., 2009) and healthy adult recipient ovaries (White et al., 2012) have demonstrated the successful population of recipient ovaries with OSC derived oocytes. Furthermore, OSC derived oocytes have undergone successful ovulation and fertilisation, by both natural conception (Zhou et al., 2014; Zou et al., 2009) and *in vitro* fertilisation (IVF) (White et al., 2012), to generate embryos (White et al., 2012) and fully fertile offspring (Zhou et al., 2014; Zou et al., 2009). In contrast, *in vitro* techniques have been unable to recapitulate these results, thus *in vivo* modelling may provide a more supportive environment for the differentiation of OSCs.

Immune compromised rodents also allow the *in vivo* investigation of tissues from other species. White et al. (2012), showed that human OSCs could produce oocyte like cells after re-introduction into human ovarian cortical tissue following a 7 day xeno-transplant into immune-deficient recipient mice. Thus, illustrating the potential of xeno-graft models in exploring the function and potential of mammalian OSCs from larger animals and primates including humans.

We hypothesised that using an *in* vivo xeno-graft model, bOSCs would have the capabilities to undergo oogenesis within chimeric ovarian aggregates. This study showed that chimeric ovarian aggregates containing bOSCs were capable of folliculogenesis within a 21 day xenograft model, although we were unable to validate the source of oocytes.

Multi-laminar and primary follicles were observed in 10% of chimeric ovarian aggregates, demonstrating round healthy oocytes with a clear nucleolus present and at least one layer of cuboidal granulosa cells. Although follicles are observed in chimeric ovarian aggregates, it is unclear from the current experimental data presented here whether bOSCs have undergone differentiation and contributed oocytes to these follicles. Thus, these results indicate that chimeric ovarian aggregates have the capability to support folliculogenesis and may have the ability to support oogenesis.

Differentiation of mitotically active stem cells into meiotically arrested oocytes would require a series of changes which would likely be associated with observable

morphological alterations, such as an increase in cell size and change in cell shape. In addition to cellular changes, transitioning cells would also need to establish interactions with supporting cells to form follicles. While the differentiation of OSCs into oocytes within established ovarian niches has previously been reported (White et al., 2012; Zhou et al., 2014; Zou et al., 2009), the transition of OSCs into oocytes and the intermediary stages between these two cell types has not been documented in the literature. Pre-primordial follicle-like structures, described in approximately a third of xeno-grafted ovarian aggregates, demonstrated a larger spherical-like central cell observed in association with adjacent cells. Thus, pre-primordial follicle-like structures may illustrate OSCs transitioning in to oocytes and may represent precursors to follicles, although further characterisation of these structures is required to establish their roles in ovarian aggregates. Furthermore, due to current cell labelling limitations it is unclear if bOSCs contribute to these structures in chimeric ovarian aggregates. However, similar structures were not observed in ovarian aggregates containing only murine cells, suggesting that these structures were a unique feature of chimeric ovarian aggregates. Pre-primordial follicle-like structures were also similar to the subpopulation of bOSCs which underwent morphological changes associated with increased cell size, spherical shape and association with adjacent cells within cultured chimeric ovarian aggregates (section 4.3.5), thus suggesting that cultured bOSCs may initiate differentiation characterised by changes in cell morphology when combined with neonatal murine ovarian somatic cells.

bOSCs contributed approximately 10% of cells in chimeric ovarian aggregates, however low numbers of follicles (n=9) and pre-primordial follicle-like structures (n=16) were identified. These results suggest that the generation of these structures within chimeric ovarian aggregates was a rare event. In contrast, chimeric ovarian aggregates containing uncultured bOSCs did not contain follicles or pre-primordial follicle-like structures. Thus, suggesting that the ability of bOSCs to contribute to oogenesis, although currently not fully determined, may be acquired through *in vitro* culture. Concerns have previously been raised over the potential *in vitro* transformation of OSCs to generate a more ‘stem-cell’ like cell (Dunlop et al., 2013). Several small molecule ligands have been identified as essential to maintain pluripotency of cells *in vitro*, including LIF (leukaemia inhibitory factor, reviewed

by Onishi and Zandstra (2015)), EGF (epidermal growth factor), bFGF (basic fibroblast growth factor, (Burton et al., 2010)), and GDNF (glial cell line-derived neurotrophic factor, GDNF in spermatogonial stem cell (SSC) self-renewal (reviewed by Kanatsu-Shinohara and Shinohara (2013)). These small molecules activate pathways within cells to maintain their self-renewal capacities *in vitro* and were all used in the *in vitro* culture of bOSCs. Reports of successful differentiation of putative OSCs into oocytes have consistently utilised an initial period of *in vitro* culture (White et al., 2012; Zhou et al., 2014; Zou et al., 2009). Thus, Ddx4/DDX4 positive cells, isolated from adult mammalian ovaries may not naturally possess pluripotent characteristics, but through *in vitro* exposure to a pluripotency promoting environment may inherit these characteristics. Although uncultured bOSCs have not formed oocytes or oocyte-like cells within this system, which may suggest the potential of putative OSCs to differentiate may be inherited through *in* vitro culture, there were also several compounding factors which may have inhibited the potential of freshly isolated putative bOSCs within this system.

Due to licence restrictions in place at the University of Edinburgh, all xeno-grafts of chimeric ovarian aggregates containing uncultured bOSCs were conducted at the University of Oxford. To conduct these experiments, bOSCs were frozen for transportation and thawed immediately prior to aggregation with somatic cells. Cell freezing is known to cause cell injury, however the addition of cryoprotective agents, such as DMSO and glycerol which passively cross the cell membrane, have been shown to reduce cell apoptosis following freeze-thawing (Chatterjee et al., 2017). Yet, new evidence suggests that the freeze-thaw process has detrimental effects on the genetic and epigenetic qualities of cells and stem cells have demonstrated reduced pluripotency gene expression, and altered capacity to differentiate following cryopreservation (reviewed by Chatterjee et al. (2017) and Diaferia et al. (2008)). Post-thaw survival assessments, which are currently used to measure the success of cryoprotection protocols, do not provide insight into the cellular effects of cryopreservation on cells and the effects of cryopreservation on the cell phenotype of OSCs is uncharacterised. Effects of cryopreservation on stem cells including embryonic stem cells have been identified and reported loss of pluripotency, possibly due to epigenetic alterations within the cells (reviewed by Chatterjee et al. (2017)).

Almost half of bOSCs did not maintain cell membrane integrity following isolation, immediate freezing, storage and thawing. Thus, suggesting that cryopreservation had a negative effect on bOSCs and may have hindered their true potential in this model. The detrimental effects of cryopreservation on bOSCs may have been further exacerbated by their exposure to enzymes for tissue disaggregation and subsequent FACS isolation, both with potential to disrupt cell integrity, immediately prior to cryopreservation. To fully test the capabilities of freshly isolated putative OSCs, cells should be introduced into an ovarian niche immediately, without further intervention.

Although we were unable to fully explore the potential of uncultured bOSCs in this study, chimeric ovarian aggregates containing cultured bOSCs did show evidence of folliculogenesis and possibly evidence of the early stages of oogenesis. Oocytes from pre-antral follicles in chimeric ovarian aggregates were not different in size to pre-antral oocytes in adult bovine tissue but were significantly larger than oocytes from pre-antral follicles in positive control ovarian aggregates and those in the adult mouse ovary. It is well established that follicle sizes vary significantly between species. This difference has been observed in primordial follicles (Gosden and Telfer, 1987), but is particularly prominent during the latter stages of follicular development with variations in antral cavity sizes correlating with body weight (Gosden and Telfer, 1987). Oocytes show less variability in size between species, however significant differences in oocyte size between mouse, hamster and pig were identified at all stages of follicle development (Griffin et al., 2006), and the present data show differences between endogenous mouse and bovine oocytes at the pre-antral stage. Thus, differences observed in oocyte size between chimeric and positive control ovarian aggregates may be due to species differences. However, a population of follicles were also observed in some negative control ovarian aggregates. Oocytes within negative control ovarian aggregates were also significantly larger than murine oocytes in positive control ovarian aggregates, but were not different in size from pre-antral oocytes in chimeric ovarian aggregates and endogenous murine and bovine adult tissues. This suggests similarities between oocytes found in chimeric ovarian aggregates and negative control ovarian aggregates and indicates the need to identify daughter cells of bOSCs and/or murine cells to determine the origin of oocytes in all ovarian aggregates.

Viral labelling methods have previously been used to successfully trace OSCs and their daughter cells in other species (Bui et al., 2014; Ding et al., 2016; White et al., 2012; Zhou et al., 2014; Zou et al., 2009). Use of lentiviruses to fluorescently label bOSCs hindered their growth and health *in vitro*, such that alternative non-genomic labelling of putative bOSCs was utilised. Rhodamine dextrans were successfully used within the chimeric ovarian aggregate model *in vitro*. However, rhodamine fluorescence from dextrans could not be identified in chimeric ovarian aggregates a 21 day xeno-graft period. It is unclear whether rhodamine dextrans in bOSCs were metabolised or diluted through cell proliferation to undetectable levels. The dilution of fluorescent dextrans through cell proliferation is widely used and exploited in cell lineage analysis studies to track daughter cells (Progatzky et al., 2013). *In vitro* labelling of bOSCs in culture with rhodamine dextrans showed a decrease in corrected total cell fluorescence from day 7 to day 21, reflecting the dilution of fluorescent dextrans in individual cells over time through proliferation. Definitive comparative studies of cell proliferation *in vitro* and *in vivo* are absent from the literature. However, the rate of cell proliferation is higher in 3D culture systems compared to 2D monolayer cultures (Edmondson et al., 2014). Thus, it is possible that bOSCs in a 3D ovarian aggregate *in vivo* model could proliferate faster and dilution of rhodamine dextrans occur at a higher rate, resulting in a signal too weak to detect following xeno-grafting. While fluorescent dextrans offer a gene-transfer-free rapid labelling method for bOSCs and are suitable for their study *in vitro*, evidence presented here shows that their use for labelling OSCs in an *in vivo* model is limited. A shorter transplant period may reduce the dilution of the rhodamine signal to maintain detectable fluorescence following retrieval. Alternatively, increased uptake resulting in higher concentrations of rhodamine dextrans in bOSCs prior to aggregation may promote longevity of the fluorescent signal within this system. Amendments to the protocol for labelling bOSCs with rhodamine dextrans may negate the limitations identified here and allow their use in future investigations, however, their potential applications in the chimeric ovarian aggregate need further examination.

We also utilised genetically labelled mouse cells (B6;129-Gt(ROSA)26) in chimeric ovarian aggregates. β-Galactosidase is ubiquitously expressed in the cells of these

mice and X-Gal staining identifies these cells by visualisation of blue pigmentation. Inconsistent XGal staining was observed throughout ovarian aggregates and within individual oocytes in positive control ovarian aggregates, suggesting that X-Gal staining was insufficient to identify the B6;129-Gt(ROSA)26 murine cells within chimeric ovarian aggregates, and consequently putative bOSCs could not be identified. Immunofluorescent detection of β-galactosidase also failed in these tissues, suggesting that epitopes were insufficiently preserved within these tissues for effective histological analysis. It was subsequently identified that the glutaraldehyde fixative utilised was not sufficient for the tissues and prevented the appropriate staining with X-Gal and disrupted epitope preservation. Use of appropriate fixatives may ensure that all B6;129-Gt(ROSA)26 cells can be identified in chimeric ovarian aggregates allowing bovine and murine cells to be distinguished. However reduced retrieval rates were observed in ovarian aggregates containing B6;129-Gt(ROSA)26 cells, suggesting that these cells were not adequate for this model. Alternative labelling of murine cells, for example fluorescently labelled cells using mice strains with ubiquitously expressed fluorescent proteins, may provide a more suitable model. The use of such cells may allow live fluorescent imaging immediately after collection and histological assessment of tissues for fluorescent epitopes to determine the species of origin for any oocytes within chimeric ovarian aggregates.

To further investigate the contribution of putative bOSCs to undergo oogenesis within chimeric ovarian aggregates, histological techniques to characterize cells of each species were considered. Structures and sequences of essential proteins are highly conserved among species, such that many antibodies against antigens of interest will react with multiple species in immunohistological techniques. Many antibodies have also been shown to bind to epitopes other than their targets (Bradbury and Pluckthun, 2015; Saper, 2009). While monoclonal antibodies are more reliable than the batch variability observed in polyclonal antibodies, the specificity of antibodies to epitopes of individual species is poor. A greater level of species variance is present in the RNAs responsible for coding proteins. RNA Scope is a recently developed *in situ* RNA analysis, capable of single RNA molecule detection within cell lines, illustrated by a punctate staining pattern (Wang et al., 2012). Species specific probes (m-UBC and b-ATP5B) were utilised on chimeric

ovarian aggregate tissue sections to determine the location of murine and bovine cells within the tissue. These two probes were selected as the corresponding RNAs are ubiquitously expressed in all cell types of the respective species and have previously been used as reference genes in gene expression analysis (Connor et al., 2005; Wang et al., 2012). The RNA Scope results presented here do not determine whether the oocytes identified in chimeric ovarian aggregates are murine or bovine. Failure of b-ATP5B probe to bind to bovine ovarian tissue, suggests that either the probe is not functioning or the detection process has been insufficient to generate a reaction. In contrast, the m-UBC probe successfully bound to murine cells in chimeric ovarian aggregates and murine control tissue, however non-specific staining was observed with this probe in bovine oocytes and follicles. These results suggest that the m-UBC probe may be cross-reacting with bovine RNAs. The m-UBC staining pattern in bovine tissue was restricted to oocytes and follicles, thus the probe is not consistently cross-reacting across all bovine cell types. Oocyte 'stickiness' is a common problem associated with immuno-detection in ovarian tissue sections. These RNA Scope results indicate that current protocols with these probes are insufficient to differentiate between bovine and murine cells within chimeric ovarian aggregates. It is unclear whether RNA Scope could provide insight into the location of the different cell types from each species, and their contributions to the follicles observed within chimeric ovarian aggregates with improved protocols or alternative probes and/or target RNAs. Further validation of this methodology would be necessary to use in analysis of future chimeric ovarian aggregates.

All methodologies described in this thesis failed to differentiate murine and bovine cells in xeno-transplanted chimeric ovarian aggregates. Without successful identification of cells from each species, the origin of oocytes within chimeric ovarian aggregates could not be determined. Thus, it is unclear whether bOSCs have successfully undergone oogenesis and contributed to the folliculogenesis observed in this model. For future use of this model, alternative experimental approaches may identify the origin of oocytes in chimeric ovarian aggregates. Meiotic spreads of isolated oocytes would identify the species by the number of chromosome pairs present (20 chromosome pairs in murine oocytes and 30 chromosome pairs in bovine oocytes). This technique would also provide insight into the meiotic progression of

any OSC derived oocytes and potentially reveal in more detail the ability of OSCs to successfully undergo oogenesis. Furthermore, meiotic spreads are able to determine chromosome content and organisation, two factors previously identified as essential gold standards for assessment of artificial gametogenesis (Handel et al., 2014). However meiotic spreads are technically very difficult and often require many oocytes, and given the low numbers of oocytes generated in chimeric ovarian aggregates, this may not be feasible. Meiotic spreads also provide no insight into the histology and morphology of ovarian aggregates. All methodologies have benefits and limitations and given the difficulties encountered when analysing chimeric ovarian aggregates, a multi-technique approach may provide contingency measures to ensure oocyte origin can be determined.

Negative control ovarian aggregates were generated to ensure a pure population of neonatal ovarian somatic cells was established prior to ovarian aggregate creation, and no oocytes contaminated this population. This control was essential to determine the contribution of bOSCs within chimeric ovarian aggregates, however, 4 (11.8%) negative control ovarian aggregates contained early stage non-growing and growing follicles. Thus, suggesting that a germ cell population has contaminated the ovarian somatic cells within these experiments. Negative control ovarian aggregates, as described here, consisting of somatic cells only, have not previously been described in the literature, however, complete exchange of rodent germ and somatic cells has been reported based solely on cell adhesion characteristics (Eppig and Wigglesworth, 2000). We reported that separation of ovarian somatic cells from oocytes based solely on cell adhesion characteristics was insufficient and additional cell filtration steps were developed to ensure complete separation (shown in section 4.3.2). Negative control ovarian aggregates consistently showed no oocytes after 7 days in culture, following extra filtration of somatic cells. Furthermore, no oocytes were observed in day 0 negative control ovarian aggregates, suggesting that oocytes had been successfully removed from disaggregated ovarian cell cultures prior to ovarian aggregate formation. These results further suggest that the presence of oocytes in a small proportion of negative control ovarian aggregates following xeno-grafting is not a consequence of oocyte contamination of the somatic cell population, but possibly as a result of spontaneous formation from an alternative cell source. While

the current experimental data cannot conclusively determine that oocytes in negative control ovarian aggregates were not a consequence of contamination in the somatic cell population prior to aggregation, there are several lines of evidence that indicate these oocytes are different from those mixed with somatic cells at aggregate formation as seen in positive control ovarian aggregates, which would constitute contamination in negative control and chimeric ovarian aggregates.

Within positive control ovarian aggregates, neonatal oocytes were re-aggregated with their supporting somatic cells. Within a 21 day xeno-graft, all follicles identified had initiated growth, many reaching late stages of follicle development with large antral cavities present. No non-growing or primordial follicles were identified within these ovarian aggregates. Similar results have previously been reported when rat and mouse oocytes were aggregated with supporting somatic cells of the opposing species (Eppig and Wigglesworth, 2000). Within 21 days of transplantation, mouse oocytes were encapsulated in large antral follicles and vice versa. Furthermore, xeno-grafted reconstituted murine embryonic (E12.5) ovaries consisted of large antral follicles 28 days after transplantation and contained haemorrhagic sites indicative of ovulation 35 days after transplantation (Matoba and Ogura, 2011). No further follicle development was observed in reconstituted embryonic ovaries past these time points, and the authors suggested that a single wave of oogenesis and folliculogenesis had occurred within these reconstituted ovaries. The absence of non-growing follicles in positive control ovarian aggregates indicates that all surviving oocytes re-introduced to an ovarian somatic niche initiate growth in this system and suggests that a single wave of folliculogenesis may have occurred within these ovarian aggregates, resulting in a population of follicles which have all initiated growth. The systemic environment to which ovarian aggregates or reconstituted ovaries are introduced to may influence the growth of re-established follicles within these model. At the time of transplantation, ovarian aggregates do not have established cell-cell interactions and are exposed to high circulating gonadotropins following ovariectomy of the adult recipient. Thus, newly formed follicles are exposed to a growth conductive environment, which appears to cause initiation of all follicles simultaneously. Continual folliculogenesis over several months post transplantation was achieved in reconstituted embryonic ovaries when a proportion of the recipients ovaries were left

intact (Hashimoto et al., 1992). These results suggest that the growth promoting environment ovarian aggregates were exposed to in this study were further exacerbated by the absence of growth inhibiting factors secreted by growing follicles, such as AMH (Durlinger et al., 2002; Durlinger et al., 1999). Thus, oocytes introduced to an ovarian niche and subsequently xeno-grafted to a growth promoting and non-inhibitory systemic environment, appear to form follicles and initiate growth immediately, as seen in positive control ovarian aggregates in this system. In contrast follicles identified in negative control ovarian aggregates were all early stage follicles and several appeared to be non-growing. Data previously described would suggest that contaminating oocytes in negative control ovarian aggregates would be unhindered to grow. Thus, the observation that all follicles in negative control ovarian aggregates are early stage may suggest that these oocytes do not originate from oocyte contamination of the somatic cell population at the time of cell aggregation.

Although very few growing follicles (n=3) were observed in negative control ovarian aggregates, the oocytes within these were significantly larger than pre-antral oocytes in positive control ovarian aggregates. Oocytes in negative control ovarian aggregates were also not significantly different in size to endogenous murine oocytes in pre-antral follicles, whereas oocytes in positive control ovarian aggregates were significantly smaller in size than their endogenous counterparts. These results show differences between pre-antral oocytes in positive control and negative control ovarian aggregates, and suggest that oocytes and follicles within positive control ovarian aggregates have a perturbed growth trajectory compared to endogenous controls. Follicles within positive control ovarian aggregates showed development of antral cavities with significantly fewer layers of granulosa cells than endogenous follicles, suggesting that these follicles are initiating antral cavity formation earlier than *in situ* follicles. Although the cause of this is unclear, it is possible that a mismatch between oocyte growth and somatic cell development has occurred in positive control ovarian aggregates. A single follicle in a negative control ovarian aggregate also showed early incipient antral cavity formation. This follicle had very few granulosa cell layers, similar to those seen in positive control ovarian aggregates, however the size of the oocyte within this follicle was larger than similar staged

follicles in positive ovarian aggregates. Thus, somatic cells in murine follicles are initiating antral cavity formation earlier in follicle development in xeno-transplanted ovarian aggregates than *in situ* controls. Although the size of oocytes in incipient antral follicles could not be analysed between positive and negative control ovarian aggregates due to low numbers, increased size of oocytes in pre-antral growing follicles in negative control ovarian aggregates would predict that oocytes in incipient antral and antral follicles of negative controls would be larger than those in positive controls. Thus, oocytes in negative ovarian aggregates appear to be undergoing different growth dynamics than those in positive control ovarian aggregates.

The results presented here do not exclude oocyte contamination as the source of oocytes in negative control ovarian aggregates, however they do indicate that this is an unlikely source of these cells. The differences observed in both oocyte and follicle developmental stage and size identified between negative control and positive control ovarian aggregates suggest that the oocytes in these different ovarian aggregates are on different growth trajectories and may originate from different sources. Oogonial stem cells have been identified within juvenile and adult murine ovaries (Pacchiarotti et al., 2010; White et al., 2012; Zou et al., 2009) and have shown their ability to generate functional oocytes within *in vivo* models (White et al., 2012; Zou et al., 2009). Methods used in this study did not actively remove potential OSCs from murine ovarian cell populations. Thus, murine OSCs may be present within neonatal murine ovarian somatic cell populations, and may have contributed to oogenesis, forming new oocytes in negative control ovarian aggregates. Characterisation of neonatal murine ovarian somatic cells would identify any putative oogonial stem cells within this population.

Populations of neonatal murine ovarian somatic cells were cultured for a minimum of 7 days and underwent at least 1 passage, then utilised to create ovarian aggregates. Culture of somatic cells would eliminate any potential contaminating oocytes, creating a population of mitotically active viable ovarian cells which may or may not contain murine OSCs. No oocytes were observed within negative control ovarian aggregates with cultured somatic cells, as expected. These results may suggest that oocytes previously observed within negative control ovarian aggregates were a

consequence of oocyte contamination following ovary disaggregation. However, culture of somatic cells caused a decrease in the retrieval rates of negative ovarian aggregates and histology of these ovarian aggregates also revealed morphological differences in the somatic cells when compared to aggregates using uncultured ovarian somatic cells. These observations suggest that the culture of murine ovarian somatic cells may have altered this population of cells, such that they behave differently in xeno-transplanted ovarian aggregates. *In vitro* culture of cells has been shown to alter and transform differentiated somatic cells without possibly present in the murine ovarian cell populations, may have also undergone transformation in this culture system. Characterisation of neonatal murine ovarian somatic cells was not undertaken prior to or during culture. Thus, the different cell types within this population were not elucidated. Gene and/or protein expression analysis would determine whether cells in this population maintained or altered their phenotype during *in vitro* culture. The current culture conditions utilised were developed for fetal human ovarian somatic cells (Bayne et al., 2016) and may not fully support the growth of all neonatal murine ovarian somatic cell types (e.g. granulosa, stroma). Furthermore, lack of factors to support pluripotency (e.g. LIF, EGF, bFGF and GDNF) in this culture may result in putative OSCs losing their differentiation capabilities. Culture of mouse embryonic stem cells without LIF caused the loss of self-renewal capabilities and induced cell differentiation (Williams et al., 1988). Thus, the absence of oocytes in negative control ovarian aggregates generated from cultured ovarian somatic cells may reflect the elimination of oocytes from this cell population following ovary disaggregation and/or the loss of function in putative OSCs within this cell population. The results could also suggest that the somatic cells have lost the ability to support folliculogenesis through *in vitro* culture. Incorporation of oocytes into ovarian aggregates containing cultured neonatal murine ovarian somatic cells would provide information into whether these cells maintain their functional ability to support folliculogenesis. As previously discussed the source of oocytes within negative control ovarian aggregates is undetermined and the use of cultured somatic cells to generate ovarian aggregates has provided little further insight into the origin of these oocytes.

The observation of oocytes in negative control ovarian aggregates suggest that oocytes in chimeric ovarian aggregates may not be derived from bOSCs or associated with their presence in the ovarian aggregates. Oocytes within pre-antral follicles in both negative control and chimeric ovarian aggregates were not statistically different from each other, however oocytes in chimeric ovarian aggregates were significantly larger than endogenous murine oocytes, whereas oocytes in negative control ovarian aggregates were not. Furthermore, follicles in chimeric ovarian aggregates showed antral cavity formation later in development with several layers of granulosa cells present, whereas murine follicles in ovarian aggregates developed antral cavities early in follicle development. These results illustrate differences in oocyte and follicle dynamics between chimeric and murine control ovarian aggregates. Furthermore, negative control ovarian aggregates did not contain pre-primordial follicle-like structures as described in chimeric ovarian aggregates. In contrast, they contained small non-growing primordial/transitory follicles with archetypal characteristics of endogenous primordial and transitory follicles. Putative OSCs are a poorly characterised ovarian cell type and although their physiological contribution to oogenesis in mammalian ovaries is undetermined, their physiological niche also remains undescribed. Despite their known ability to produce functional oocytes in rodents (Zhou et al., 2014; Zou et al., 2009) the extrinsic factors and underlying mechanisms controlling their differentiation into oocytes is not known. Thus, it is difficult to predict whether murine somatic cells provide a suitable environment to support bOSC differentiation. Should bOSCs contribute to oogenesis in chimeric ovarian aggregates, they would be interacting and communicating with cells from an alien source. Although healthy oocytes are observed in chimeric ovarian aggregates, the larger cells within pre-primordial follicle-like structures, which are speculated to be the precursors to primordial follicles, may illustrate that the communication between the cell types of the different species is not perfect, resulting in a structure similar to a primordial follicle but not identical to an archetypal primordial follicle. Failure to identify bOSCs within chimeric ovarian aggregates has prevented this from being investigated further. However, it is possible that the potential differentiation of bOSCs to oocytes within this system may be aberrant. Whereas murine OSCs (mOSCs) which may be present

in the somatic cell population would be surrounded by familiar cells and it is possible that within this system mOSCs can establish themselves within the appropriate niche to coordinate oocyte formation with the correct cell types. This may explain why non-growing follicles are observed in negative control ovarian aggregates whereas pre-primordial follicle-like structures are seen in chimeric ovarian aggregates.

Follicles and pre-primordial follicle-like structures were observed in almost half (46.6%) of chimeric ovarian aggregates, whereas follicles (growing and non-growing) were observed in only 11.8% of negative control ovarian aggregates. If putative OSCs or contaminating murine oocytes were contributing to follicles in chimeric ovarian aggregates, we would expect a similar proportion of negative control ovarian aggregates to contain follicles, however, this is not the case. As previously discussed the somatic cell population utilised in ovarian aggregates was not characterised, thus it is unclear whether putative mOSCs are present in this population of cells and if so what proportion of cells are mOSCs. White et al. (2012) estimated that in the adult murine ovary mOSCs make up a very small proportion of total ovarian cells (0.014% ± 0.002%). Thus, mOSCs in ovarian aggregates may only contribute a very small proportion of cells. In contrast, bOSCs were enriched in chimeric ovarian aggregates, making up 10% of the total number of cells, which may reveal why a higher proportion of chimeric ovarian aggregates contained follicles and/or pre-primordial follicle-like structures.

Together these data suggest that bOSCs may have contributed to oogenesis in chimeric ovarian aggregates, however due to limitations of the model outlined here we were unable to determine conclusively the species of oocytes in chimeric ovarian aggregates. They also suggest that mOSCs may have contributed to oogenesis within negative control ovarian aggregates. As previously discussed the optimum niche to maintain OSCs and support their differentiation is not known. Further characterisation of these cells and their requirements for differentiation into oocytes is essential. While this study aimed to investigate the potential of bOSCs to undergo oogenesis in a chimeric ovarian aggregate model, murine ovarian somatic cells may not provide the optimum support for this cell type, thus conspecific ovarian somatic cells may provide a more physiologically relevant model.

6 Aggregation of bOSCs with fetal bovine ovarian somatic cells

6.1 Introduction

The extent to which mechanisms underlying folliculogenesis are conserved across species is poorly understood. Differences in follicle kinetics, suggest that regulation of folliculogenesis may be different between species. Work by Eppig and Wigglesworth (2000), showed that mechanisms were conserved sufficiently between rodent species to support the production of meiotically competent oocytes of rats and mice when supported by somatic cells of the other species. However, conservation between more genetically distant species is unknown. Chimeric ovarian aggregates, described in previous chapters, suggests that ovarian niches of different species may be able to support oogenesis, however, the ability of bOSCs to differentiate within a murine ovarian microenvironment could not be definitively evaluated with the current methodologies. Species differences may prevent murine ovarian somatic cells from fully supporting the generation of a meiotically and developmentally competent bovine oocyte.

Experimental evidence of successful recapitulation of oogenesis from progenitor cells (ESCs, iPSCs and OSCs) has utilised the ovarian somatic cell environment of the same species (Hayashi et al., 2012; Hayashi and Saitou, 2013; White et al., 2012; Zhou et al., 2014; Zou et al., 2009). Rodent and human OSCs have formed oocytes, confirmed by protein expression analysis, when placed in young adult ovarian tissue (White et al., 2012; Zhou et al., 2014; Zou et al., 2009), furthermore rodent OSC derived oocytes have demonstrated meiotic and developmental competence through successful fertilisation and production of healthy offspring (Zhou et al., 2014; Zou et al., 2009). Differentiation of murine ESCs and iPSCs has utilised an initial *in vitro* culture to induce germ lineage differentiation of these cells followed by aggregation with murine ovarian somatic cells (Hayashi et al., 2012; Hayashi and Saitou, 2013). In this model, Hayashi and colleagues have used temporally appropriate ovarian somatic cells to support the continued development of differentiating pluripotent cells. Mismatch of ovarian somatic cells and developing germ cells has resulted in failure to produce functional oocytes in re-aggregated embryonic mouse ovaries

(Qing et al., 2008). Whereas co-ordination of germ cell and somatic cell developmental stage results in successful oogenesis and folliculogenesis in xeno-grafted re-aggregated embryonic ovaries as early as E12.5 (Hashimoto et al., 1992; Matoba and Ogura, 2011; Qing et al., 2008). These data suggest that the somatic environment influences the success of oogenesis, and that temporal alignment of germ and somatic cells may be essential to maximise germ cell success.

It is well established that the somatic cells of fetal ovaries support and help to co-ordinate the differentiation of primordial germ cells to mitotically active oogonia to meiotically arrested oocytes (Sarraj and Drummond, 2012). Different ovarian somatic cells (vascular epithelial cells, vasculature-associated cells, general somatic cells and pre-granulosa cells) have been identified in fetal mammalian ovaries, characterised by gene expression patterns (Maatouk et al., 2012). Gonadal ridge epithelial-like (GREL) cells which form the genital ridge in the developing bovine ovary give rise to the ovarian epithelium and are proposed to be precursors for all pre-granulosa cells (Hummitzsch et al., 2013). Two sub-populations of pre-granulosa cells have been identified in the fetal murine ovary and can be distinguished by the expression of two markers, Foxl2 (Forkhead box L2, a transcription factor) and Lgr5 (Leucine-rich repeat-containing G-protein coupled receptor 5) (Mork et al., 2012; Rastetter et al., 2014). *Lgr5*$^{-/-}$ ovaries have demonstrated a delay in germ cell differentiation (Rastetter et al., 2014) and *Foxl2*$^{-/-}$ ovaries show aberrant follicle activation (Uda et al., 2004), suggesting that these two ovarian somatic cell populations are important to support germ cell differentiation and follicle growth in mammalian ovaries. Thus, fetal ovarian somatic cells have known potential to support oogenesis and may provide an appropriate niche to support the differentiation of OSCs.

The lineage of putative oogonial stem cells is unknown and it is unclear whether they are precursor cells to oogonia, which are active in fetal mammalian ovaries, or of a separate developmental lineage. The optimum niche to support differentiation of putative bOSCs is not known, however fetal bovine ovarian somatic cells support the differentiation of precursor germ cells *in situ*, therefore may possess the requirements to support and facilitate the differentiation of oocytes from precursor cells. Thus,

fetal bovine ovarian somatic cells were utilised as a niche to investigate the oogenic potential of bOSCs in a conspecific ovarian aggregate model.

6.2 Materials and Methods

Ovarian aggregation model

To further investigate the potential of putative bovine oogonial stem cells (bOSCS) the ovarian aggregation model was utilised *in vivo* in a xeno-transplant model with fetal bovine ovarian somatic cells as an ovarian niche. bOSCs and fetal bovine ovarian somatic cells were aggregated together with various amounts of PHA (35μg, 50μg) at a ratio of 1:10, respectively (further details in section 2.5). A higher concentration of phytohaemagglutinin (PHA) was required to adhere bOSCs with fetal bovine ovarian somatic cells. When using the standard 35μg PHA, which had previously been used to generate chimeric ovarian aggregates, cells within bovine ovarian aggregates with or without bOSCs did not adhere well. Bovine ovarian aggregates were fragile, and broke upon handling, resulting in unsuccessful hanging drop culture and failed xeno-grafting.

To accommodate the difference in cell adhesion observed in bovine ovarian aggregates, 50μg PHA was utilised. This successfully facilitated the adhesion of bovine ovarian cells to form ovarian aggregates.

Negative controls containing bovine fetal somatic cells only were also generated for comparison.

All experiments were carried out at the University of Edinburgh by Kelsey Grieve.

Bovine oogonial stem cells

bOSCs were isolated by FACS (section 2.2) from adult bovine ovaries collected from the local abattoir, as described previously (section 2.1). Following isolation bOSCs were either cryopreserved for future use (section 2.6.1.3) or cultured (section 2.6.1.1) in OSC media (section 2.12). Cultured cells were also cryopreserved and stored long term in liquid nitrogen (section 2.6.1.3) until required.

bOSCs were fluorescently labelled with Rhodamine Dextrans (section 2.6.2.3) prior to aggregation with somatic cells.

Fetal bovine ovarian somatic cells

Fetal bovine ovaries (gestational age 163.5 days, determined by crown-rump length) were received from the local abattoir (see section 2.1.1). Each ovary was disaggregated using enzymatic and mechanical dissociation (further details in section 2.3). Once disaggregated, ovarian cells were cultured overnight in fetal somatic cell medium (section 2.12). The following day, cells were washed twice with pre-warmed PBS and new fetal somatic cell media was added (section 2.12). Cells were maintained and passaged as described in section 2.6.1.2.

RNA extraction, cDNA synthesis and RT-PCR

To determine the expression of mRNA transcripts in fetal bovine ovarian somatic cells, RT-PCR was performed. RNA extraction, cDNA synthesis and RT-PCR protocols are outlined in section 2.10 and primer pairs detailed in Table 6.1.

Table 6.1: PCR primer pairs used to characterise FBSCs

Gene Target	Forward Primer	Reverse Primer
β-ACTIN	CTCTTCCAGCCTTCCTTCCT	GGGCAGTGATCTCTTTCTGC
DDX4	TATATGGGGGAACCCAGTTG	CATATCCAGCATGCGATC
DAZL	GAAGGCAAAATCATGCCAAACAC	CTTCTGCACATCCACGTCATTA
FOXL2	CCGGCATCTACCAGTACATTATAGC	GCACTCGTTGAGGCTGAGGT
LGR5	AGTTGTTCAGCCTCCGATCT	TGGAAAATGCATTAGGGTCA
NR2F2	CGGATCTTCCAAGAGCAAGTG	CACAGGCATCTGAGGTGAACA

Xenotransplant of ovarian aggregates

Bovine ovarian aggregates following an overnight hanging drop culture in supplemented Waymouths media (section 2.12) were xenotransplanted to the kidney capsule of SCID (C.B.17/IcrHan Hsd-Prkdc) mice for 21 days for comparison with the *in vitro* culture models.

All animal experiments were conducted under a UK Home Office licence in line with the Animals Scientific Procedure Act (1986). SCID Mice were housed as described in section 2.7 and obtained from Envigo laboratories and provided a minimum of 6 days to acclimatise to their new environment prior to the start of any experimental

work.

Briefly, SCID mice were anaesthetised with isoflourane (section 2.7.1), shaved and skin sterilised. Subcutaneous injection of saline around the hind leg and a subcutaneous injection of vetergesic (at a dose of 0.03mg/ml in 100µl) around the neck were given. A vertical incision along the skin was made in the middle of the back, followed by a small incision in the body wall directly above the ovary, allowing the ovary and ovarian fat pad to be removed from the body cavity, and the ovary to be excised. Using the ovarian fat pad as a guide the kidney was pulled out of the body cavity with forceps. Sterile PBS kept the kidney hydrated and a tiny incision was made in the kidney capsule with a sterile needle. Using a pulled glass pipette, aggregates were transferred through the hole in the capsule to the surface of the kidney and moved from the incision site to ensure their security. The kidney and associated tissue was then returned to the body cavity, and the body wall sutured using number 5 sutures. The ovary was then removed on the other side following the same protocol and the skin incision closed using wound clips. Mice were then transferred to individual cages which were maintained at 30ºC while they recovered and then housed as described in section 2.7 for 7 or 21 days until tissue collection.

7 or 21 days after xeno-transplantation, recipient mice were culled by lethal exposure to CO_2 or cervical dislocation of the neck and tissues were collected and fixed as described below.

In vitro culture of bovine ovarian aggregates

Ovarian aggregates generated as described previously (section 2.5.4) were cultured in a hanging drop with sterile supplemented Waymouths medium (Section 2.12) continuously for the whole culture period and incubated at 37ºC with humidified air and 5% CO_2 as described in section 2.6.4.2. Aggregates were transferred to fresh medium on alternate days of culture and incubated at 37ºC with humidified air and 5% CO_2.

Histological Techniques

Bovine ovarian aggregate tissue was fixed in natural buffered formalin (NBF) for 6 hours, then transferred to 70% ethanol and embedded in wax using an automated

Leica TP1050 processor. Tissue was sectioned at 5μM and mounted onto electrostatically charged glass slides and maintained at 50ºC overnight in a slide oven to ensure tissue adherence to the slide surface.

Haematoxylin and eosin staining

Every third section of each ovarian aggregate was stained with haematoxylin and eosin for histological evaluation to detect the presence of oocytes and follicles. Slides were de-waxed and rehydrated (section 2.8.3) and washed briefly in running tap water, then stained with haematoxylin and eosin (section 2.8.4) before dehydration and mounting (section 2.8.5).

Microscopy

Live cell and tissue imaging was conducted using an Axiovert 200 fitted with a AxioCam HRc camera and a Hamamatsu camera for collection of images including fluorescent images. Cells and tissue were maintained at 37ºC with 5% CO_2 throughout live imaging. Epithelial-like and fibroblast-like cells were counted to establish cell proportions throughout culture using ImageJ cell counter software.

Tissue histology was imaged with a Provis AX70 (Olympus) or a Zeiss Imager Z1 both fitted with a AxioCam HRc camera (Zeiss) using Zeiss software. All scale bars were generated and embedded in image files using Zeiss software. Tissue was analysed for overall health (pyknotic nuclei were used as a marker of cell death), and the presence of follicle or follicle-like structures.

6.3 Results

6.3.1 *In vitro* culture and characterisation of fetal bovine ovarian somatic cells

Fetal bovine ovarian somatic cells were established in culture following ovary disaggregation. Mixed cell morphology was observed in cultures, suggesting cells of different phenotypes are present. A proportion of cells showed an epithelial cell-like morphology defined by their polygonal shape, indicative of gonadal-ridge epithelial-like cells (GREL; Figure 6.1). Spindle shaped fibroblast-like cells were also observed interspersed in cultures. Epithelial-like and fibroblast-like cells were consistently observed together in fetal bovine ovarian somatic cell cultures and were maintained over several passages as shown in Figure 6.1. Epithelial-like cells constituted 64.8±1.0%, 66.8±2.8% and 65.3±4.5%, across P0, P1 and P2, respectively (Table 6.2), whereas fibroblast like cells contributed 35.2±1.0%, 33.2±2.8% and 34.7±4.5% through culture (Table 6.2). No statistical differences were observed in cell composition based on morphology throughout culture, suggesting that the culture conditions maintained cell proportions. These cells were successfully cryopreserved and thawed, maintaining morphological characteristics throughout. No large spherical cells resembling oocytes were observed throughout culture.

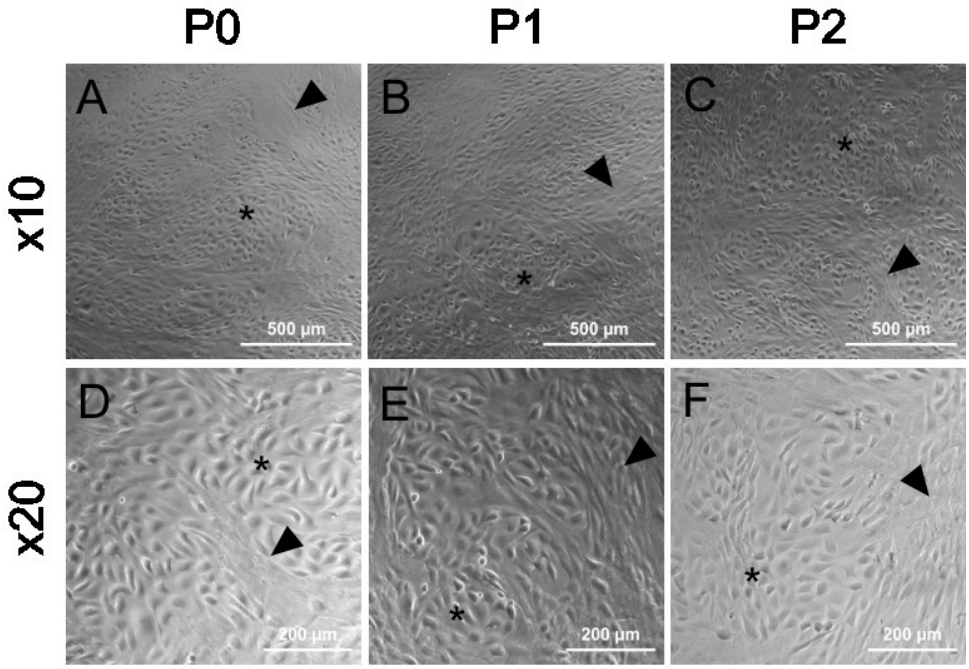

Figure 6.1: Fetal bovine ovarian somatic cells maintain morphology in culture. Fetal bovine ovarian somatic cells exhibit different cell morphology. Polygonal shaped epithelial-like cells (indicated by asterisks) and spindle shaped fibroblast-like cells (marked by arrowheads). Mixed cell morphology was consistently observed in cultures. Top panels imaged at x10 magnification (scale bars represent 500µm) and bottom panels imaged at x20 magnification (scale bars represent 200µm).

Table 6.2: Average proportion of epithelial-like and fibroblast-like cells per mm^2 in fetal bovine ovarian somatic cell cultures across several passages.

Cell Type	P0	P1	P2
Epithelial-like	64.8±1.0%	66.8±2.8%	65.3±4.5%
Fibroblast-like	35.2±1.0%	33.2±2.8%	34.7±4.5%

Gene expression analysis was carried out by PCR. RNA from whole fetal bovine ovary was used as a positive control and reverse transcriptase omitted (-) and a water substitute were used as negative controls. In the presence of reverse transcriptase, fetal bovine ovary was shown to express all genes analysed, however *LGR5* was inconsistently observed (Figure 6.2). As fetal bovine germ and somatic cells were separated based on cell adhesion characteristics and were not actively separated, both cell types were expected to be present in cell suspensions following disaggregation (T0) and overnight culture (S0). Disaggregated bovine ovary cell suspension (T0) expressed all transcripts analysed, illustrating that all ovarian cell types were present within this sample. A similar expression pattern was observed in cells collected from the supernatant (S0) after overnight culture following ovary disaggregation, suggesting both germ cells and unattached somatic cells were present (Figure 6.2).

Housekeeping gene β-Action was observed to be stably expressed in fetal bovine ovarian somatic cell cultures across several early passages (P0-P2). Similarly, ovarian somatic cell specific genes (*FOXL2*, *LGR5* and *NR2F2*) were also consistently expressed by fetal bovine ovarian somatic cells (Figure 6.2).

In contrast, oocyte marker *DDX4* was not observed to be expressed in cultured fetal bovine ovarian somatic cells (Figure 6.2), illustrating that oocytes did not survive the culture process, consistent with observations that large spherical cells were not observed throughout culture. However, germ cell marker *DAZL* was expressed in early cultured fetal bovine ovarian somatic cells (Figure 6.2). *DAZL* has previously been utilised as a marker of bovine oogonial stem cells, it's continued presence in these samples may suggest bovine OSCs are also present in the cell population. A reduction in *DAZL* expression is observed throughout culture (Figure 6.2), suggesting that any bOSCs present in this population are reducing in number.

Water and reverse transcriptase omitted negative controls showed no detectable transcripts.

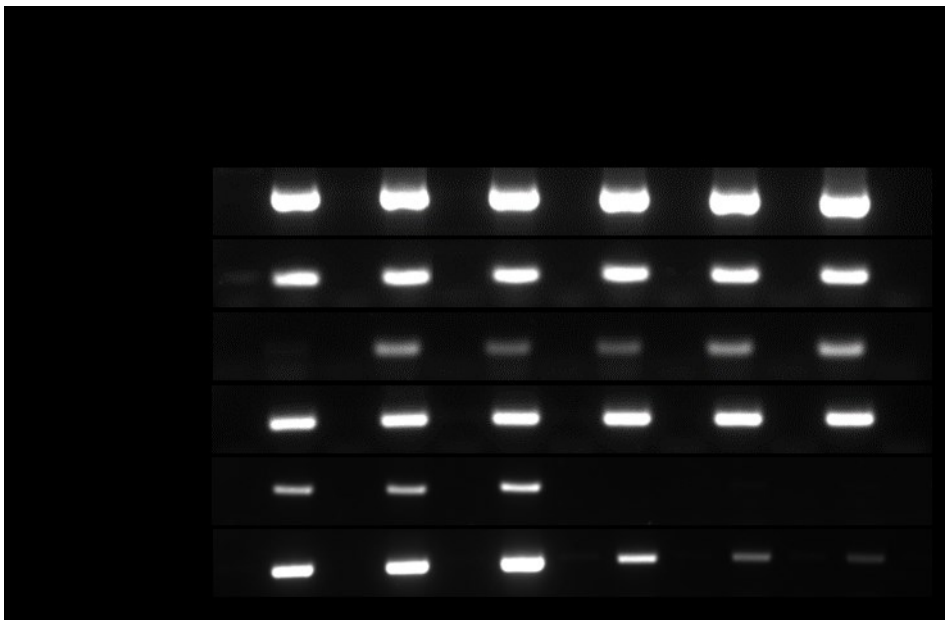

Figure 6.2: Fetal bovine ovarian somatic cells express ovarian somatic cell associated genes in culture. RNA was collected from cells at different time points, immediately after fetal bovine ovary disaggregation (T0), the cell supernatant following overnight culture after disaggregation (S0) and at different cell passages (P0, P1, P2). Several ovarian somatic cell genes (*FOXL2*, *LGR5* and Nr2F2) and germ cell genes (*DDX4* and *DAZL*) were analysed by PCR, *β-ACTIN* was used as a house-keeping control gene. RNA from fetal bovine ovary (FBO) was used as a positive control, reverse transcriptase omitted controls (-) and a water control were used as negative controls. Fetal bovine ovary expressed all genes with the exception of *LGR5*, which demonstrated variable expression (not demonstrated in figure). Germ cell markers were observed in T0 and S0 samples and decreased throughout culture. Somatic cell markers were consistently expressed throughout culture of fetal bovine ovarian somatic cells.

6.3.2 Bovine ovarian aggregates do not survive a 21 day xeno-graft model

A total 12 negative bovine ovarian aggregates and 12 bovine ovarian aggregates containing labelled bOSCs were xeno-transplanted. No ovarian aggregates could be observed on the kidney surface at collection 21 days later. Kidneys were retrieved for visual assessment under a dissecting microscope, no aggregates or anomalies were observed.

Bovine ovarian aggregates (+/- bOSCs) were also xeno-grafted for 7 days (n=4, for both groups). All ovarian aggregates were retrieved and analysed histologically. Morphological assessment of 7 day xeno-grafted bovine ovarian aggregates showed good overall tissue health and few pyknotic nuclei were observed. No follicles or pre-primordial follicle-like structures were observed within bovine ovarian with or without bOSCs (Figure 6.3) following a 7 day transplant period. Cells in bovine ovarian aggregates (+/- bOSCs) appeared less dense than uncultured murine neonatal ovarian somatic cells in murine negative control and chimeric ovarian aggregates. However cultured murine ovarian somatic cells also appeared to be less dense in xeno-grafted ovarian aggregates (Figure 5.3), suggesting that this is a feature of cultured ovarian somatic cells. Bovine ovarian aggregates with bOSCs did show areas within the tissue with increased cell density (Figure 6.3.B & C), however no clear structures could be identified in these areas.

Bovine ovarian aggregates were also cultured within a hanging drop for 7 days for comparison (Figure 6.3. G-L), and also showed dispersity between cells. Cell morphology in cultured bovine ovarian aggregates, showed high numbers of pyknotic nuclei, illustrating high levels of cell death, suggesting that the hanging drop culture system does not support survival of cells within bovine ovarian aggregates.

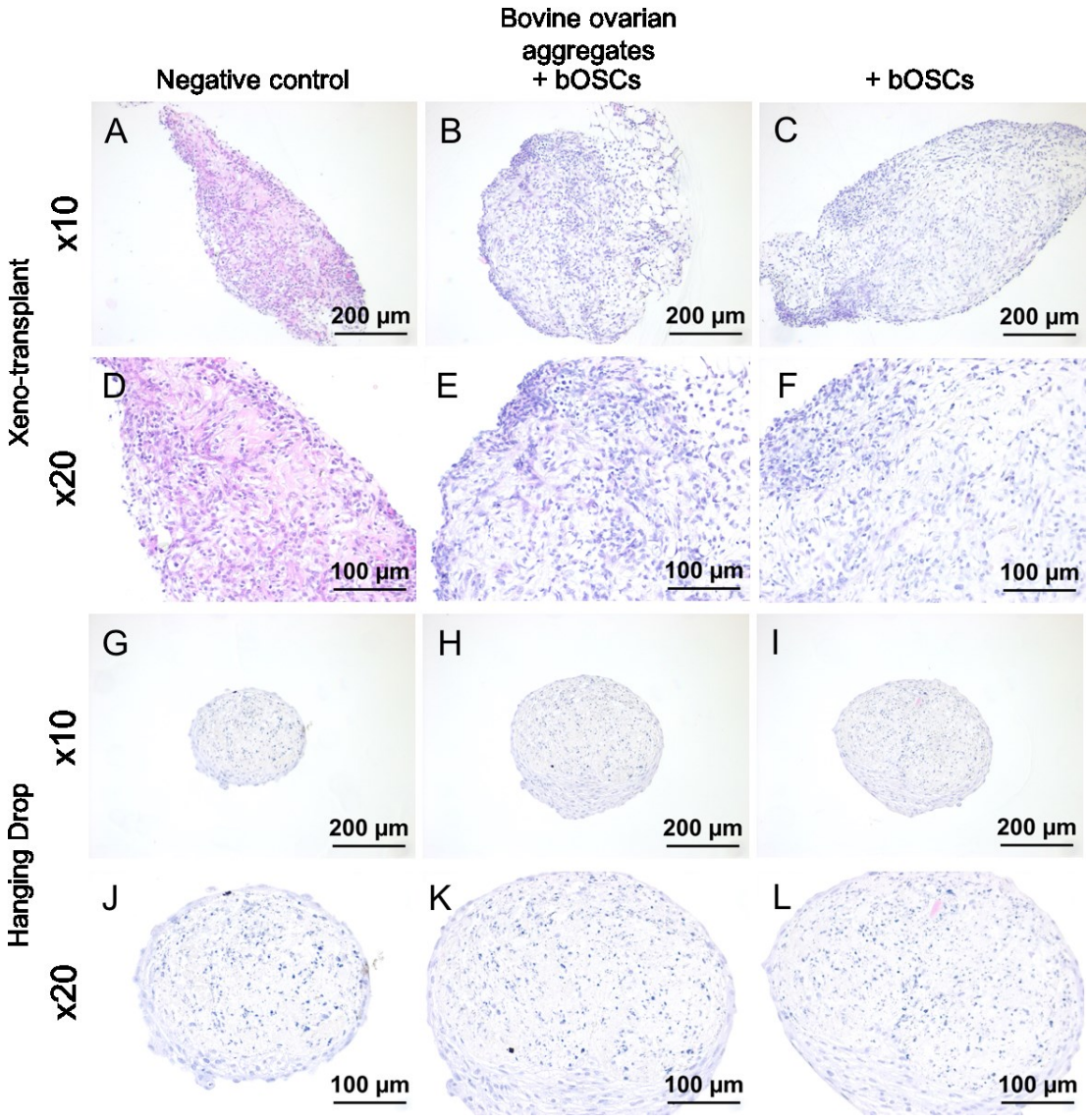

Figure 6.3: Histological analysis of bovine ovarian aggregates following a 7 day xeno-transplantation or hanging drop culture. Negative control bovine ovarian aggregates (A and D, n=4) and bovine ovarian aggregates containing bOSCs (B, C, E and F, n=4) were retrieved 7 days after xeno-transplantation. No oocytes or follicles were observed in any bovine ovarian aggregates retrieved. As a comparison bovine ovarian aggregates with (H, I, K and L, n=4) and without bOSCs (G and J, n=4) were culture for 7 days in a hanging drop system. Cultured bovine ovarian aggregates did not contain oocytes or follicles when analysed by haematoxylin and eosin staining, these aggregates also contained large numbers of cells with pyknotic, fragmented nuclei. Sections imaged at x10 and x20 magnification, scale bars represent 200µm and 100 µm respectively.

6.4 Discussion

Successful differentiation of rodent OSCs to functional oocytes (Zhou et al., 2014; Zou et al., 2009) and human OSCs to meiotic oocytes within primordial follicles (White et al., 2012) has utilised young adult ovarian tissues of the same species by injection of labelled OSCs into these tissues to help co-ordinate and support the differentiation process. In contrast, differentiation of pluripotent rodent stem cells such as ESCs and iPSCs into functional oocytes have been aggregated with fetal ovarian somatic cells of the same species to facilitate oogenesis (Hayashi et al., 2012; Hayashi and Saitou, 2013). *In vitro* cultured and *in vivo* xeno-transplanted chimeric ovarian aggregates suggested that bOSCs may have the potential to initiate differentiation and undergo oogenesis in an unfamiliar ovarian niche. Alternative ovarian niches, in particular a bovine ovarian niche, may better support bOSCs than a murine ovarian environment. We hypothesised that a fetal bovine ovarian niche would facilitate bOSC differentiation in an ovarian aggregation model.

In the developing fetal bovine ovary germ cell mitosis ceases at approximately 150 days gestation and meiosis initiates between 75-80 days post conception (Erickson, 1966). Gradual follicle formation extends from the medulla to the ovarian surface from 130 days gestation and gonadal ridge epithelial-like (GREL) cells interact with germ cells and transition to pre-granulosa cells (Hummitzsch et al., 2013). This study reports the culture of fetal bovine ovarian somatic cells following disaggregation of fetal ovary, gestational age 163.5 days (determined by crown-rump measurement). Thus, germ cells within this ovary are likely to be meiotic and undergoing germ cell nest breakdown to form primordial follicles with surrounding GREL cells. Fetal bovine ovarian somatic cells were established in culture to adhere to licence restrictions.

Fetal bovine ovarian somatic cells were established in a viable monolayer culture, revealing two morphologically distinct cell types. Polygonal-shaped cells characteristic of GREL cells and were identified alongside spindle-shaped cells like fibroblast cells, these represented approximately two-thirds and a third of fetal bovine ovarian somatic cells respectively. No large spherical cells were observed in

cultures suggesting that oocytes had successfully been eliminated following ovary disaggregation and culture.

Intact and disaggregated fetal bovine ovary showed consistent gene expression of both germ and somatic cell markers as expected. In contrast, *DDX4* expression was not observed and *DAZL* expression was lost during culture fetal bovine ovarian somatic cells. These results further suggest that ooctyes are not present in fetal bovine ovarian cell cultures. However, the expression of *DAZL* in these cultures suggests that germ cells may be present, although the source is unclear and requires further investigation. The expression decreased with increasing passage which is indicative that cells expressing *DAZL* are becoming less prominent within the cultures. DAZL expression has been observed to be restricted to oogonia in the developing fetal bovine ovary (Hummitzsch et al., 2013) and in the developing human ovary is temporally expressed in mitotic germ cells and then again in oocytes within primordial follicles (He et al., 2013). Dazl/DAZL has been observed in OSCs of several different species (Bui et al., 2014; Ding et al., 2016; White et al., 2012; Zhou et al., 2014; Zou et al., 2009) and was observed to be expressed in bovine OSCs (Section 3.3.2). Thus, *DAZL* expression is associated with several different germ cell types and the source in fetal bovine ovarian somatic cells is unknown. The absence of large spherical cells and *DDX4* expression from fetal bovine ovarian somatic cells, suggests that *DAZL* expression in these samples is not associated with the presence of oocytes. Mitosis of oogonia ceases around 150 days post conception in the bovine (Erickson, 1966), the gestational age of these somatic cells was determined to be 163.5 days post conception, determined by crown-rump length, which provides an estimate rather than an accurate age. Thus, *DAZL* expression in fetal bovine ovarian cells from fetal ovaries 163.5 days post conception is unlikely to be due to the presence of oogonia, however it is possible that oogonia are still present in this population. It is unknown if OSCs are present in fetal bovine ovaries or if this is a population of cells specific to postnatal tissues. Due to Home Office regulations, bovine fetal tissue is incredibly scarce and we were unable to investigate whether bOSCs could be isolated by FACS from fetal ovarian tissue. Thus, it is unclear which cell population is responsible for *DAZL* expression in fetal bovine ovarian somatic

cell cultures. Further characterisation, such as immunocytochemical analysis of these cells may elucidate the source of *DAZL* expression.

Morphological characterisation of fetal bovine ovarian somatic cell cultures indicated the presence of two distinct cell populations; epithelial-like cells and fibroblast-like cells. Gene expression analysis showed the consistent expression of three ovarian somatic cell markers; *FOXL2* (Forkhead box L2), *LGR5* (Leucine-rich repeat-containing G-protein coupled receptor 5) and *NR2F2* (nuclear receptor subfamily 2, group F, member 2 also known as COUP-TFII, COUP transcription factor 2).

Folx2/FOXL2 is a well described marker of both adult granulosa cells (Cocquet et al., 2002; Pisarska et al., 2004) and fetal pre-granulosa cells in several mammalian species (Cocquet et al., 2002; Mork et al., 2012; Rastetter et al., 2014; Zheng et al., 2014). GREL cells in the developing bovine ovary express high levels of FOXL2 (Hummitzsch et al., 2013), and it has been hypothesised that all pre-granulosa cells are derived from GREL cells. However, *Foxl2* expression was not present in all pre-granulosa cells in the fetal murine ovary (Zheng et al., 2014). FOXL2 expressing fetal pre-granulosa cells contribute to follicles located in the ovarian medulla (Mork et al., 2012; Rastetter et al., 2014; Zheng et al., 2014). In contrast, Lgr5 expression is restricted to the ovarian cortex in the developing and adult mammalian ovary (Ng et al., 2014; Rastetter et al., 2014). Ng et al. (2014) found that a collection of GFP positive cells, driven by *Lgr5* expression in the subsurface of neonatal rodent ovaries co-express Foxl2, suggesting that *Lgr5* expression also marks a population of pre-granulosa cells. Analysis of *Lgr5* expression in embryonic ovaries, confirmed that a distinct population of pre-granulosa cells are marked by the expression of *Lgr5*. These cells form follicles with germ cells in the ovarian cortex (Rastetter et al., 2014). Expression of *LGR5* and *FOXL2* in fetal bovine ovarian somatic cells indicates the presence of pre-granulosa cells in the population, although it's unclear if this reflects one or multiple pre-granulosa cell populations.

Consistent expression of *NR2F2* in fetal bovine ovarian somatic cells was also observed. Nr2f2 positive cells have been found in close proximity to vascular endothelial cells, marked by Pecam1 expression, in the embryonic murine ovary (Rastetter et al., 2014). Nr2f2 positive cells in the developing murine ovary do not

co-localise with pre-granulosa cell markers (Lgr5 and Foxl2), suggesting that these cells are an additional population of cells that do not contribute to the adult granulosa cell population (Rastetter et al., 2014). In the human ovary, NR2F2 is expressed in theca cells of growing follicles (Sato et al., 2003). Theca cells are steroidogenic follicular cells, responsible for the production of androgens in the ovary (Fortune and Armstrong, 1977; Liu and Hsueh, 1986). *Nr2f2* heterozygous mouse ovaries have shown reduced capabilities to produce sex steroids (Takamoto et al., 2005), thus it has been speculated that Nr2f2 may mark precursor cells for steroidogenic theca cells in the fetal murine ovary (Rastetter et al., 2014). Consistent gene expression of *NR2F2* in fetal bovine ovarian somatic cell cultures, may suggest the presence of steroidogenic precursor cells.

From the current study it is unclear if distinct populations of fetal bovine ovarian somatic cells express each of these markers, similar to that described in the embryonic mouse ovary (Rastetter et al., 2014). Preliminary characterisation of fetal bovine ovarian somatic cells, suggest that GREL cells as previously described by Hummitzsch et al. (2013), are present based on cell morphology and gene expression of *FOXL2*. GREL cells have been characterised by the expression of FOXL2, and proteins associated with cell adhesion (Plakophilin-2, Desmoglein, Cytokeratin 18 and 19) and absence of germ cell markers (DAZL, DDX4 and OCT3/4) and NR2F2 (Hummitzsch et al., 2013). Thus, expression of *FOXL2* and *NR2F2* reported here indicates at least two separate populations of somatic cells as described in other mammalian ovaries (Rastetter et al., 2014). To confirm the identity of polygonal-shaped and spindle-shaped cells in fetal bovine ovarian somatic cell cultures requires more extensive characterisation of the cells, including protein expression analysis. However, morphological characterisation and gene expression analysis suggest that several cell populations are found within fetal bovine ovarian cell cultures, including pre-granulosa cells and possibly precursor steroidogenic cells and potential bOSCs or oogonia.

This mixed population of fetal bovine ovarian somatic cells was utilised as a niche to investigate the oogenic potential of bOSCs. The optimum environment to support OSCs is unknown and very little work has investigated this. GREL cells are known to be the somatic cells which interact with fetal germ cells (Hummitzsch et al., 2013),

thus it is plausible that these cells may also possess the ability to support bOSCs in an ovarian aggregation model. Since the isolation of OSCs from adult mammalian ovaries, questions over the mechanism of ovarian quiescence reached with increasing age have been raised (Dunlop et al., 2014). Two potential mechanisms have been put forward: failure of OSCs to form new oocytes or failure of the ovarian niche to support the mechanisms underlying this process, or both. Currently no experimental evidence to substantiate either of these theories has been presented and given that the optimum niche for OSCs remains unknown, it is difficult to understand which may be responsible. The use of different ovarian niches may elucidate the optimum niche for putative OSC differentiation and also provide insight into the underlying causes of age related ovarian quiescence.

In cultured ovarian aggregates of fetal ovarian bovine somatic cells +/- putative bOSCs, poor tissue health was observed throughout aggregates after 7 days. High levels of pyknotic cells were observed in all aggregates, suggesting that cells within these aggregates were undergoing cell death. Pyknotic cells were not restricted to the core of the ovarian aggregates, suggesting that the cell death observed was not solely due to hypoxia and lack of nutrients often associated with 3D cell cultures (Edmondson et al., 2014). The extensive cell death observed in bovine ovarian aggregates suggest that the hanging drop model previously used to support chimeric ovarian aggregates is not sufficient to support ovarian aggregates containing fetal bovine ovarian somatic cells. Alternative media with more appropriate supplements to support fetal bovine somatic cells rather than neonatal murine somatic cells may yield better tissue survival. No follicles or follicle-like structures were observed within cultured bovine ovarian aggregates; this is possibly a consequence of poor tissue health or may illustrate that the somatic cells used here are not appropriate to support putative bOSC differentiation.

Bovine ovarian aggregates with or without bOSCs were also xeno-grafted to immune deficient mice to investigate the potential of fetal bovine ovarian somatic cells to support bOSC differentiation within an *in vivo* environment. All bovine ovarian aggregates transplanted for 21 days were not successfully retrieved. Upon collection, no observable aggregates could be seen on the surface of the kidney. The cause of poor tissue retrieval rates for this length of xeno-graft is unknown. Due to licence

restrictions, fetal bovine ovarian somatic cells were cultured prior to aggregate formation and transplant. Culture of neonatal murine ovarian somatic cells prior to aggregate formation and transplantation resulted in a decreased retrieval rate (Appendix II), suggesting that culture of mammalian ovarian somatic cells may alter their phenotype. *In vitro* transformation of fetal bovine ovarian somatic cells may explain the failure of bovine ovarian aggregates to survive a 21 day xeno-graft model, however comparison with aggregates made with uncultured fetal bovine ovarian somatic cells would be needed. Due to limited tissue availability and licence restrictions, this was not possible in the current study, but is a possible avenue for further research. Alternatively, the host environment may not be adequate to support bovine ovarian aggregates. The immune deficient recipient mice used, lack functional T and B immune cells through an inherited recessive gene mutation (Bosma et al., 1983), which contributes to their ability to accept allogeneic or xenogeneic grafts (Zhang et al., 2009). However, the mice retain residual immunity including functional macrophages, natural killer cells and granulocytes (Dorshkind et al., 1984; Dorshkind et al., 1985). This residual immunity may allow the hosts immune system to detect the ovarian aggregates as foreign and cause degeneration of the grafts resulting in poor retrieval rates.

To further investigate the *in vivo* potential of bOSCs within a fetal bovine ovarian niche, bovine ovarian aggregates were xeno-grafted for a total of 7 days. All bovine ovarian aggregates with or without bOSCs were successfully retrieved. No follicles or pre-primordial follicle like structures were identified following histological analysis of bovine ovarian aggregates. These results suggest that under the current conditions, cultured fetal bovine ovarian somatic cells cannot support the differentiation of putative bOSCs. As previously discussed the effect of culture on fetal bovine ovarian somatic cells and bOSCs has not been fully established. Thus, it is unclear if this has contributed to the failure of this model to initiate oogenesis. Use of freshly isolated fetal bovine ovarian somatic cells and/or freshly isolated bOSCs within bovine ovarian aggregates would allow full investigation of the potential of these cells without possible *in vitro* transformation of cells. Successful differentiation of pluripotent cells using a fetal or juvenile ovarian niche to support the underlying process have utilised uncultured somatic cells (Hayashi et al., 2012; Hayashi and

Saitou, 2013). Thus, uncultured ovarian somatic cells may better replicate the ovarian niche essential for oogenesis.

Characterisation of fetal bovine ovarian somatic cells, illustrates multiple cell types, which supported data in the literature (Hummitzsch et al., 2013). GREL cells have been identified as the pre-cursor cells to pre-granulosa cells within the developing bovine ovary. While these cells were present in the cultures in this study, defined by their expression of *FOXL2* and classic polygonal shape, they were not the only abundant cell type. Foxl2/FOXL2 expressing cells have been identified as precursor granulosa cells in a number of mammalian species (Cocquet et al., 2002; Hummitzsch et al., 2013; Mork et al., 2012; Rastetter et al., 2014; Zheng et al., 2014), suggesting that these cells are essential in supporting the production of oocytes. Current evidence suggests that membrane enclosed clusters of germ and somatic cells feature during ovarian development in all mammalian fetal ovaries (reviewed by Smith et al. (2014)). In bovine ovaries, GREL cells have been identified as the only somatic cells within these membrane bound clusters (Hummitzsch et al., 2013), thus, GREL cells appear to be the only cells interacting with germ cells providing the essential support to complete oogenesis. The aggregation of putative bOSCs with fetal bovine ovarian somatic cells, randomly places bOSCs within this cell population, which could result in bOSCs in an unsupportive environment. The use of a GREL cell enhanced somatic cell population may better support putative bOSCs within an ovarian aggregate model. Enhancement of the GREL cells within the bovine ovarian aggregates, may increase the chance of bOSCs finding an appropriate niche. Further characterisation of GREL cells may reveal potential cell specific, membrane epitopes, which could be utilised in cell sorting techniques to isolate only GREL cells for use in future ovarian aggregate models.

Oocyte formation *in situ* requires complement co-ordination of many intrinsic and extrinsic factors and pathways. Alignment of these mechanisms between the germ cell, supporting somatic cells and the systemic environment of the developing gonad is essential to generate meiotically and developmentally competent oocytes. Recapitulation of this process from a putative precursor cell, requires all of these components to contribute and co-ordinate successfully to support differentiation to

oocytes. Putative OSCs are a recently described ovarian cell type and as such, very limited research has investigated them. Research into OSCs has largely focused on their ability to produce functional oocytes, while this is a key question, it has resulted in other essential questions being overlooked. The niche of putative OSCs has not been described, furthermore their cell lineage is unknown. Putative OSCs may be precursor cells to oogonia, which persist beyond fetal life and are maintained in the postnatal mammalian ovary, however they could also be of a different cell lineage with no relation to oogonia. The use of fetal bovine ovarian somatic cells in an ovarian aggregation model with putative bOSCs as described here may illustrate that this somatic cell environment is inadequate to support the differentiation of bOSCs into oocytes. However, several limitations have been identified in this current study which may have all contributed and perhaps compounded each other resulting in bovine ovarian aggregates which did not form oocytes or oocyte-like cells.

Understanding the *in situ* niche for putative OSCs may identify the optimum niche for these cells to support their maintenance and/or differentiation. The niche for OSC maintenance may be altered to induce their differentiation into oocytes, should they initiate oogenesis under normal physiological conditions, which is currently unknown. Answers to these key questions will help us to understand the requirements to be able to recapitulate differentiation of putative OSCs artificially, and will ultimately help us to unlock the full potential of these cells.

The evidence presented here suggests that at least one of the components essential to replicate oogenesis from putative bOSCs is either missing or unable to support the process fully. Further optimisation and investigations are essential to identify the problems within this model and amendments to the protocol required to fully explore the potential of this model to support the differentiation of putative bOSCs.

7 General Discussion

7.1 Summary of main findings

Putative bovine oogonial stem cells have been successfully isolated from adult ovarian tissue and may contribute to folliculogenesis in a chimeric ovarian aggregate model. Furthermore, the results presented here also demonstrate a crucial role for ovarian somatic cells in supporting bOSC differentiation.

In this study, putative bOSCs were successfully established in long term culture, following their isolation using a FACS based protocol exploiting the controversial cell surface expression of germ cell marker DDX4. DDX4 positive cells were a small proportion of all bovine ovarian cortical cells (approximately 5%) analysed. Gene and protein expression could not be analysed in putative bOSCs immediately after FACS isolation. Characterisation of this cell population during cell culture revealed expression of germ and pluripotency associated genes which were maintained across several generations, thus these cells have a gene expression profile characteristics of putative OSCs. However, DDX4 was not found to be expressed in putative bOSCs assessed in this study, which may indicate that bOSCs have lost expression of DDX4 or lacked DDX4 expression entirely. Immunocytochemical analysis also revealed that the bOSC population was heterogenous, which may reflect cells at different stages of development (Anderson and Telfer, 2016).

bOSCs were not observed to spontaneously differentiate into oocyte-like cells (OLCs) *in vitro*, suggesting that differentiation of putative bOSCs may require extrinsic support. This thesis describes the use of a novel chimeric ovarian aggregate model to investigate the oogenic potential of putative bOSCs. Within cultured chimeric ovarian aggregates many bOSCs maintained their size and irregular shapes and were also observed to retain their germline phenotype, identified by the expression of DAZL. However, expression was variable and likely represents the heterogeneous nature of the cell population, or the limited potential of this model to provide an adequate niche. A small proportion of bOSCs however appeared to undergo differentiation, demonstrating an increase in cell size and a change in cell morphology to form a more spherical shape. These morphological changes were also observed in conjunction with cell association with surrounding murine somatic cells.

These bOSCs share many characteristics of previously described OLCs. Similar structures were also observed in xeno-transplanted chimeric ovarian aggregates, described here as pre-primordial follicle-like structures. These structures may represent an intermittent stage between putative OSCs and newly formed oocytes within follicles however due to technical problems and time constraint it was not possible to fully characterise these structures and determine their role and purpose.

Growing follicles were also observed within xeno-grafted chimeric ovarian aggregates after 21 days. It was not possible to determine the cellular origin of the oocytes within these follicles but differences in oocyte size and follicle growth dynamics suggest an alternative cellular origin for these chimeric oocytes compared to oocytes observed in both positive and negative control ovarian aggregates. Follicles showed healthy and normal morphology suggesting oocytes and somatic cells had established good communication and were co-ordinating growth and development. Although the oocytes within these follicles appeared morphologically healthy, no analysis on their meiotic or developmental competence was undertaken. These analyses are essential to determine whether putative bOSCs have contributed to functional oocytes within this model.

Evidence presented here also demonstrate that putative OSCs require an optimum niche to initiate differentiation as described within this thesis. Culture of somatic cells prior to aggregation with putative bOSCs could not support follicle formation. This was observed for both neonatal murine ovarian somatic cells and fetal bovine ovarian somatic cells. Uncultured bOSCs, previously frozen and thawed, also did not contribute to folliculogenesis in chimeric ovarian aggregates although pre-primordial follicle-like structures were observed. Taken together these results suggest that the optimum niche and healthy functional putative OSCs are both essential to facilitate differentiation and co-ordination of both elements is needed for successful oogenesis. The frequency of pre-primordial follicle-like structures and follicles within chimeric ovarian aggregates was low and possibly reflects inappropriate coordination of putative OSCs and the ovarian niche.

The data presented here supports findings of others and suggests that a population of putative oogonial stem cells can be isolated from adult mammalian ovaries.

Furthermore, putative bovine OSCs maintain a gene expression profile similar to putative OSCs of other species (Hernandez et al., 2015; Imudia et al., 2013; Park et al., 2013; White et al., 2012; Zhou et al., 2014; Zou et al., 2009) expressing germ and pluripotency associated genes throughout long-term culture. However, unlike putative OSCs of other species (Bui et al., 2014; Ding et al., 2016; Hernandez et al., 2015; White et al., 2012; Zhou et al., 2014), bOSCs were not observed to spontaneously differentiate into what have been described as oocyte-like cells (OLCs) *in vitro*. When aggregated with neonatal murine somatic cells in a chimeric ovarian aggregate model, putative bOSCs appeared to undergo morphological differentiation to form pre-primordial follicle-like structures with murine somatic cells when cultured *in vitro* and may have contributed to oogenesis in xeno-transplanted chimeric ovarian aggregates as previously described by others (White et al., 2012; Zhou et al., 2014; Zou et al., 2009).

Although this thesis has answered a number of questions relating to the controversial existence of putative mammalian OSCs, a number of questions remain unanswered. Furthermore, the data presented here has also generated new questions which offer potential avenues for further research.

7.2 Future research avenues

A growing body of evidence now suggests that mammalian ovaries contain a population of putative oogonial stem cells (Bui et al., 2014; Hernandez et al., 2015; Imudia et al., 2013; Pacchiarotti et al., 2010; Park et al., 2013; Virant-Klun et al., 2009; Virant-Klun et al., 2008; White et al., 2012; Zhou et al., 2014; Zou et al., 2009). However this area of research continues to be mired in controversy as its reproducibility has been difficult and several groups have failed to isolate putative OSCs and have been unable to replicate results (Zarate-Garcia et al., 2016; Zhang et al., 2015). Given this, it is important that research into putative OSCs and there oogenic potential is investigated further. This thesis has identified a number of research questions yet to be answered and investigation into these areas may provide more insight into the biology of the mammalian ovary and the function of putative OSCs.

7.2.1 Alternative techniques for the isolation of putative OSCs

There is currently contradictory evidence for the use of Ddx4/DDX4 as a cell surface epitope to isolate putative OSCs (Hernandez et al., 2015; White et al., 2012; Woods and Tilly, 2015; Zou et al., 2009). Ddx4/DDX4 based FACS of ovarian cells has isolated putative OSCs with Ddx4/DDX4 expression (White et al., 2012; Woods and Tilly, 2015; Zou et al., 2009), without Ddx4/DDX4 expression (Hernandez et al., 2015) and cells without characteristics of putative OSCs (Zarate-Garcia et al., 2016; Zhang et al., 2015). Gene and protein expression could not be analysed in putative bOSCs immediately after FACS isolation, thus it is not possible to determine whether they were selected based upon the expression of DDX4 or selected due to antibody cross-reactivity (Hernandez et al., 2015). In fetal germ cell development *Ddx4* expression is associated with post-migratory PGCs with germ cell competence established by the expression of *Dazl* (Gill et al., 2011). It has also been suggested that Ddx4 expression is associated with later stages of murine OSC differentiation (Anderson and Telfer, 2016; Guo et al., 2016). Furthermore, the internalisation of Ddx4 from the cell surface to the cytoplasm has been suggested to mark the progression through differentiation in putative murine OSCs (Imudia et al., 2013). Thus, it is possible that the absence of DDX4 in bOSCs identified in this study is indicative of a less differentiated population of putative OSCs.

Identification of and use of an alternative cell surface epitope to isolate putative OSCs may provide more consistent isolation of an uncontaminated OSC population. Rodent OSCs have also been isolated from adult ovaries using Ifitm3 (Zhou et al., 2014), which is well established as a transmembrane protein. Stage-specific embryonic antigens (SSEA) are a family of cell surface proteins associated with pluripotency. The expression of members of this family of proteins has been identified in putative OSCs (Bui et al., 2014; Pacchiarotti et al., 2010; Parte et al., 2011; Virant-Klun et al., 2008). Furthermore, the cell surface epitope Ssea-1 has been utilised in FACS isolation of artificial germ cells differentiated from murine embryonic and induced pluripotent stem cells (Hayashi et al., 2012). Therefore, Ssea/SSEA proteins and/or Ifitm3/IFITM3 are alternative cell surface antigens that may offer better isolation strategies for putative OSCs and provide more consistent and reproducible results.

7.2.2 Characterisation of putative OSCs *in vivo*

It has been speculated that putative OSCs gain these characteristics as a consequence of *in vitro* culture (Dunlop et al., 2013). It is not possible to comment on whether bOSCs have undergone an *in vitro* transformation to gain the characteristics observed due to a lack of analysis of freshly isolated cells. However, putative OSCs of other species immediately after isolation share similar expression profiles to cultured cells (Hernandez et al., 2015; Woods and Tilly, 2015), suggesting that current culture conditions utilised maintain the phenotype of OSCs.

Characterisation of putative OSCs within their physiological *in vivo* environment would allow investigations into whether putative OSCs were indeed bona fide stem cells within mammalian ovaries. Furthermore, this would aid identification of the somatic cell niche and requirements to support putative OSCs. Genetic murine models could also be utilised to disrupt putative OSCs and the somatic niche to identify molecular pathways and mechanisms underlying potential neo-oogenesis.

The physiological and pathophysiological role of putative OSCs in mammalian ovaries is yet to be fully determined, however several recent reports suggest that putative OSCs function *in situ* and support neo-oogenesis in mammalian ovaries. Murine oocytes ovulated later in life showed increased oocyte depth compared to oocytes ovulated earlier, thus oocytes ovulated later in life had undergone more mitotic divisions than their younger counterparts. Oocyte depth increased following unilateral ovariectomy, suggesting post-natal renewal of oocytes in murine ovaries (Reizel et al., 2012). Small germ cells have also been identified at the ovarian surface in mouse ovaries by expression of DDX4 (Johnson et al., 2004) and OCT4 (Guo et al., 2016). Tamoxifen induced expression of eYFP under the *Oct4* promoter identified a population of eYFP and Sycp3 positive cells 1 day and 2 months after tamoxifen exposure suggesting continued germ cell entry into meiosis within these mouse ovaries (Guo et al., 2016). Single cell RT-PCR of eYFP positive cells showed cells expressed *Dazl*, *Stra8* and *Sycp3*, further evidence of continued entry into meiosis. Consistent with this theory, some cells also expressed *Sohlh1*, a marker of oocytes within primordial follicles, in addition to *Sycp3* and *Stra8* at all time points investigated after tamoxifen exposure. Other eYFP positive cells were identified in

clusters and demonstrated chromosome morphology associated with metaphase or anaphase, BrdU exposure also identified eYFP expressing cells that were also BrdU and Stra8 positive, suggesting that these eYFP expressing cells are actively undergoing mitosis and pre-meiotic DNA replication respectively (Guo et al., 2016). Thus a population of germ cells in the postnatal murine ovary actively undergo mitosis and undergo neo-oogenesis to form new oocytes. In humans, a greater follicle density was observed in patients treated with adriamycin, bleomycin, vinblastine and dacarbazine (ABVD) combined chemotherapy treatment compared to age matched control healthy women (McLaughlin et al., 2017). Although the underlying cause for this observation is unknown, one explanation is that ABVD treatment caused the formation of new oocytes/follicles in that patient group, which was not seen with other chemotherapy regimens. These results suggest that putative OSCs may function to contribute to the ovarian follicle population in postnatal mammalian ovaries under some circumstances. However, the physiological and/or pathophysiological conditions under which putative OSCs may contribute to oogenesis is yet to be elucidated.

7.2.3 Origins of the menopause

Should putative OSCs function to facilitate neo-oogenesis *in vivo*, how and why does ovarian quiescence occur with increasing age in mammals? In lower vertebrate and invertebrate species, the stem cell niche is essential in determining germline stem cell fate (Kimble and White, 1981; Lin, 1997). Thus, failure of the OSC niche may cause depletion of ovarian follicles through reduction in neo-oogenesis. Data presented in this thesis suggest that putative bOSCs require a specific niche to form pre-primordial follicle-like structures, which is potentially conserved between species, allowing murine ovarian somatic cells to support the process, however culture of ovarian somatic cells disrupted their capabilities to support putative bOSCs. These results suggest that ovarian somatic cells harbour unique characteristics to support the differentiation of putative OSCs.

To date successful differentiation of murine pluripotent stem cells and putative OSCs into functional oocytes has utilised an ovarian niche both *in vitro* and *in vivo* to support and facilitate the process of oogenesis and folliculogenesis (Hayashi et al.,

2012; Hayashi and Saitou, 2013; Hikabe et al., 2016; Zhou et al., 2014; Zou et al., 2009). Rodent OSCs introduced into healthy and damaged ovarian environments have successfully contributed functional oocytes to the growing and ovulatory population (White et al., 2012; Zhou et al., 2014; Zou et al., 2009). These data suggest that the ovarian somatic environment facilitates oogenesis from putative OSCs, but does not provide insight into the somatic requirements to facilitate putative OSC differentiation. The chimeric ovarian aggregate model may illustrate that germ and somatic cell interactions are evolutionarily conserved to support oocyte development, previously known to be maintained between rodent species (Eppig and Wigglesworth, 2000). It has previously been shown that temporal matching of germ and somatic cells is necessary for folliculogenesis, with age mismatched fetal murine germ and somatic cells failing to form follicles (Qing et al., 2008). Furthermore, complete differentiation of murine embryonic and induced pluripotent stem cells into functional oocytes utilised embryonic ovarian somatic cells developmentally matched to the stage of oogenesis (Hayashi et al., 2012; Hayashi and Saitou, 2013; Hikabe et al., 2016). Thus, the ovarian aggregate model developed here may be used with aged somatic cell populations and individual cell populations such as GREL cells and may have valuable potential in determining the somatic requirements for OSC differentiation.

Systemic factors have also been implicated in the maintenance of neo-oogenesis in mammals (Johnson et al., 2005; Niikura et al., 2009) and use of xeno-transplant models may further elucidate the role of systemic and paracrine factors in putative OSC maintenance and/or differentiation. Continued investigations into mammalian neo-oogenesis supported by putative OSCs may identify key regulators of OSC function and consequently identify the underlying cause of the menopause.

7.2.4 Clinical applications

The evidence presented in this thesis shows that cells can be isolated from adult bovine ovaries which once established in culture express germ and pluripotency associated markers. Similar cells have been isolated from human ovaries (White et al., 2012). OSCs have wide ranging potential clinical applications and their use may lead to new assisted reproductive technologies. Bovine ovaries, follicles and oocytes

are often used as a model for human ovarian development due to similarities between the two species, furthermore the same ethical concerns do not apply to the study of bovine germ cells.

Further investigation into the niche of putative OSCs *in situ* and better understanding of oogenic regulators in normal follicle formation in the developing ovary would allow development of improved methods to support OSC oogenesis. Recently replication of the full female germ line from PGCs (Morohaku et al., 2016), embryonic and induced pluripotent stem cells (Hikabe et al., 2016) *in vitro*, utilised multi-step models and supporting ovarian somatic cells to facilitate the production of functional oocytes. Multi-step models may provide a better system for the study of putative OSCs and may provide potential clinical technologies to support the differentiation of putative human OSCs into healthy oocytes for fertility treatment. Thus further characterisation of putative OSCs and development of further investigative models may identify potential clinical uses for human OSCs.

8 Conclusions

In summary, putative bovine oogonial stem cells characterised by the expression of germ and pluripotency associated markers have successfully been isolated and established in culture from adult ovaries, based upon the cell surface expression of DDX4 using a FACS based protocol. A subpopulation of putative bOSCs demonstrated morphological changes including increase in size, spherical shape and association with neighbouring somatic cells, similar to primordial follicles (termed pre-primordial follicle-like structures) were identified following aggregation with neonatal murine ovarian somatic cells in an ovarian aggregation model in both *in vitro* culture and *in vivo* xeno-transplant models. Multi-laminar follicles were also observed in chimeric ovarian aggregates following xeno-transplantation for 21 days. The origin of the oocytes in chimeric ovarian aggregates could not be definitively determined due to technical difficulties, however oocyte size and follicle growth dynamics suggest that oocytes in chimeric ovarian aggregates are derived from different cells to those in murine control ovarian aggregates. Therefore, these results suggest that putative bOSCs may have the potential to undergo oogenesis and illustrate the potential of these cells as a tool to investigate germ cell differentiation and further demonstrated the capabilities of an ovarian aggregate model to determine the oogenic potential of putative OSCs.

Appendix I

Manufacturers Details

Manufacturer	Address
Abbot Laboratory Ltd.	Abbott House Vanwall Business Park Vanwell Road Maidenhead SL6 4XE
Abcam	330 Cambridge Science Park Cambridge CB4 0FL UK
AbD Serotec	Endeavour House Langford Lane Kidnlington OX5 1GE
AcuMedic	101-105 Camden High Street London NW1 7JN
AlphaLaboratories	40 Parham Drive Eastleigh Hampshire SO50 4NU
Amazon	410 Terry Ave N Seattle WA 98109 USA
Becton Dickenson	The Danby Building Edmund Halley Road Oxford Science Park Oxford OX4 4DQ
Bioline Reagents Limited	Edge Business Centre Humber Rd London NW2 6EW
Biomolecular Core	SuRF 47 Little France Crescent Queen's Medical Research Institute University of Edinburgh

	EH16 4TJ
Biosera	Labtech International Ltd 2 Birch House Brambleside Bellbrook Industrial Estate UckfieldEast Sussex TN22 1QQ
Cell Signalling Technology	Schuttersveld 2 2316 ZA Leiden Leiden The Netherlands
CellPath Ltd.	80 Mochdre Enterprise Park Newtown Powys SY16 4LE
Corning Incorporated	Elwy House Lakeside Business Village St. David's Park Flintshire CH5 3XD
DAKO	Aligent Technologies Inc 5301 Stevens Creek Blvd Santa Clara CA 95051 United States
Envigo Laboratories	Station Road Blackthorn Bicester Oxfordshire OX25 1TP
Eppendorf UK Ltd.	Eppendorf House Gateway 1000 Whittle Way Arlington Business Park Stevenage SG1 2FP
Greiner Bio-One Ltd.	Brunel Way Stroudwater Business Park Stonehouse
Histolab	Södra Långebergsgatan 36 421 32 Västra Frölunda Sweden

Integrated DNA Technologies	Interleuvenlaan 12A B-3001 Leuven Belgium
Leica	Larch House Woodlands Business Park Breckland Linford Wood Milton Keynes MK14 6FG
Life Technologies	168 Third Avenue Waltham MA 02451 USA
Millipore Ltd.	Suite 21 Building 6 Croxley Green Business Park Watford Hertfordshire WD18 8YH
Miltenyi Biotec Ltd.	Almac House Church Lane Bisley Surrey GU24 9DR
Molecular Probes Inc.	168 Third Avenue Waltham MA 02451 USA
Olympus	KeyMed House Stock Road Southend-on-Sea SS2 5QH
Perkin Elmer Incorporated	Rigaweg 22 9723 TH Groningen Netherlands
Promega	Delta House Southampton Science Park Southampton SO16 7NS
Qiagen Ltd.	Skelton House Lloyd Street North Manchester M15 6SH

R&D Slaughter	Fox Building Pentland Close Cardiff CF14 5DJ
Rockland Inc.	Limerick PA 19468 USA
Santa Cruz	10410 Finnell Street Dallas Texas 75220 USA
Scientific Laboratory Supplies Ltd.	Orchard House The Square Hessle East Riding of Yorkshire HU13 0AE
Sigma-Aldrich	The Old Brickyard New Road Gillingham Dorset SP8 4XT
Stratech Scientific Ltd.	Oaks Drive Newmarket Suffolk CB8 7SY
Swann-Morton Ltd.	Owlerton Green Sheffield S6 2BJ
Sysmex Partec	Am Flugplatz 13 02828 Görlitz Germany
Thermo Fisher Scientific	168 Third Avenue Waltham MA 02451 USA
Vector Laboratories Ltd.	3 Accent Park Bakewell Road Orton Southgate Peterborough PE2 6XS

Animalcare Ltd.	Common Road Dunnington York YO19 5R
VWR	Hunter Boulevard Magna Park Lutterworth Leicestershire LE17 4XN
Carl Zeiss Ltd.	509 Coldhams Lane Cambridge CB1 3JS

Appendix II

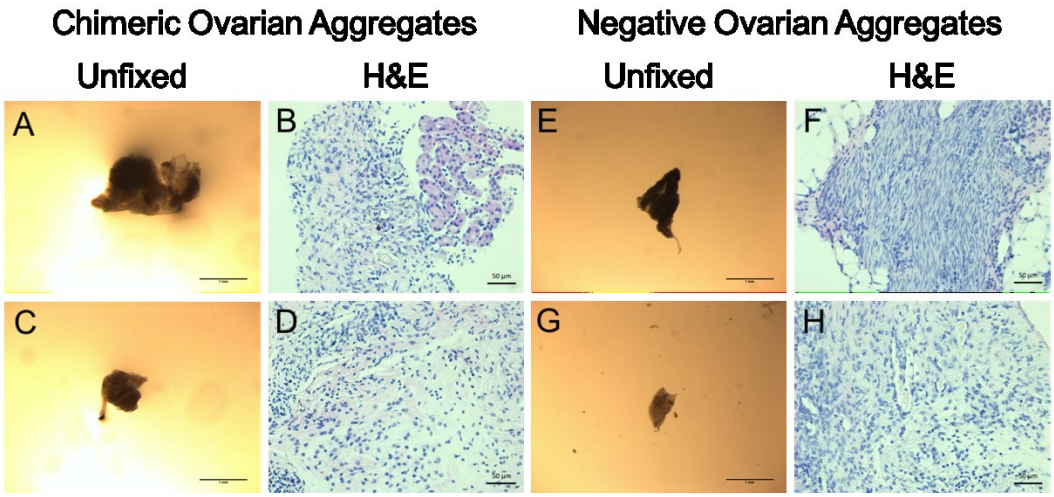

Appendix II Figure 1: Cultured neonatal somatic cells do not support follicle formation in xeno-transplanted chimeric ovarian aggregates. Somatic cells isolated from neonatal cd-1 mice were cultured then aggregated with bovine oogonial stem cells to from chimeric ovarian aggregates (n=12), negative control ovarian aggregates generated with somatic cells only were also generated (n=10). Ovarian aggregates were transplanted to the kidney capsule of immune-deficient mice for 21 days. All chimeric ovarian aggregates were collected (example aggregates shown in A and C), only 2 negative controls were observed and retrieved following transplantation (20% retrieval rate) shown in E and G. Histological analysis confirmed that no follicles had been generated in ovarian aggregates with cultured neonatal mouse ovarian somatic cells with (B and D) or without (F and H) bovine oogonial stem cells. Scale bars for images of unfixed tissue represent 1mm and in H&E images represent 50µm.

References

Ackert, C. L., Gittens, J. E., O'Brien, M. J., Eppig, J. J., and Kidder, G. M. (2001). Intercellular communication via connexin43 gap junctions is required for ovarian folliculogenesis in the mouse. Developmental biology *233*, 258-270.10.1006/dbio.2001.0216.

Adams, G. P., and Pierson, R. A. (1995). Bovine Model for Study of Ovarian Follicular Dynamics in Humans. Theriogenology *43*, 113-120.Doi 10.1016/0093-691x(94)00015-M.

Adams, I. R., and McLaren, A. (2002). Sexually dimorphic development of mouse primordial germ cells: switching from oogenesis to spermatogenesis. Development *129*, 1155-1164

Aflatoonian, B., Ruban, L., Jones, M., Aflatoonian, R., Fazeli, A., and Moore, H. D. (2009). In vitro post-meiotic germ cell development from human embryonic stem cells. Human reproduction *24*, 3150-3159.10.1093/humrep/dep334.

Albertini, D. F. (2004). Micromanagement of the ovarian follicle reserve - do stem cells play into the ledger? Reproduction *127*, 513-514.Doi 10.1530/Rep.1.00247.
Albertini, D. F., and Gleicher, N. (2015). A detour in the quest for oogonial stem cells: methods matter. Nature medicine *21*, 1126-1127.10.1038/nm.3969.

Allen, E. (1923). Ovogenesis during sexual maturity. Am J Anat *31*, 439-481.DOI 10.1002/aja.1000310502.

Amorim, C. A., Van Langendonckt, A., David, A., Dolmans, M. M., and Donnez, J. (2009). Survival of human pre-antral follicles after cryopreservation of ovarian tissue, follicular isolation and in vitro culture in a calcium alginate matrix. Human reproduction *24*, 92-99.10.1093/humrep/den343.

Anderson, E. L., Baltus, A. E., Roepers-Gajadien, H. L., Hassold, T. J., de Rooij, D. G., van Pelt, A. M., and Page, D. C. (2008). Stra8 and its inducer, retinoic acid, regulate meiotic initiation in both spermatogenesis and oogenesis in mice. Proceedings of the National Academy of Sciences of the United States of America *105*, 14976-14980.10.1073/pnas.0807297105.

Anderson, R., Fassler, R., Georges-Labouesse, E., Hynes, R. O., Bader, B. L., Kreidberg, J. A., Schaible, K., Heasman, J., and Wylie, C. (1999). Mouse primordial germ cells lacking beta1 integrins enter the germline but fail to migrate normally to the gonads. Development *126*, 1655-1664

Anderson, R. A., Fulton, N., Cowan, G., Coutts, S., and Saunders, P. T. (2007). Conserved and divergent patterns of expression of DAZL, VASA and OCT4 in the germ cells of the human fetal ovary and testis. BMC developmental biology *7*, 136.10.1186/1471-213X-7-136.

Anderson, R. A., and Telfer, E. E. (2016). Replenishing the adult ovarian follicle population: a fresh look at dogma. Molecular human reproduction *22*, 313-315.10.1093/molehr/gaw017.

Antonio-Rubio, N. R., Porras-Gomez, T. J., and Moreno-Mendoza, N. (2013). Identification of cortical germ cells in adult ovaries from three phyllostomid bats: Artibeus jamaicensis, Glossophaga soricina and Sturnira lilium. Reproduction, fertility, and development *25*, 825-836.10.1071/RD12126.

Ara, T., Nakamura, Y., Egawa, T., Sugiyama, T., Abe, K., Kishimoto, T., Matsui, Y., and Nagasawa, T. (2003). Impaired colonization of the gonads by primordial germ cells in mice lacking a chemokine, stromal cell-derived factor-1 (SDF-1). Proceedings of the National Academy of Sciences of the United States of America *100*, 5319-5323.10.1073/pnas.0730719100.

Aubard, Y. (2003). Ovarian tissue xenografting. European journal of obstetrics, gynecology, and reproductive biology *108*, 14-18

Auersperg, N., Wong, A. S., Choi, K. C., Kang, S. K., and Leung, P. C. (2001). Ovarian surface epithelium: biology, endocrinology, and pathology. Endocrine reviews *22*, 255-288.10.1210/edrv.22.2.0422.

Avilion, A. A., Nicolis, S. K., Pevny, L. H., Perez, L., Vivian, N., and Lovell-Badge, R. (2003). Multipotent cell lineages in early mouse development depend on SOX2 function. Genes & development *17*, 126-140.10.1101/gad.224503.

Bagheri-Fam, S., Sinclair, A. H., Koopman, P., and Harley, V. R. (2010). Conserved regulatory modules in the Sox9 testis-specific enhancer predict roles for SOX, TCF/LEF, Forkhead, DMRT, and GATA proteins in vertebrate sex determination. The international journal of biochemistry & cell biology *42*, 472-477.10.1016/j.biocel.2009.07.001.

Baillet, A., and Mandon-Pepin, B. (2012). Mammalian ovary differentiation - a focus on female meiosis. Molecular and cellular endocrinology *356*, 13-23.10.1016/j.mce.2011.09.029.

Baker, T. G., and Franchi, L. L. (1967). The fine structure of oogonia and oocytes in human ovaries. Journal of cell science *2*, 213-224

Baltus, A. E., Menke, D. B., Hu, Y. C., Goodheart, M. L., Carpenter, A. E., de Rooij, D. G., and Page, D. C. (2006). In germ cells of mouse embryonic ovaries, the decision to enter meiosis precedes premeiotic DNA replication. Nature genetics *38*, 1430-1434.10.1038/ng1919.

Bastock, R., and St Johnston, D. (2008). Drosophila oogenesis. Current biology : CB *18*, R1082-1087.10.1016/j.cub.2008.09.011.

Bayne, R. A., Donnachie, D. J., Kinnell, H. L., Childs, A. J., and Anderson, R. A. (2016). BMP signalling in human fetal ovary somatic cells is modulated in a gene-specific fashion by GREM1 and GREM2. Molecular human reproduction *22*, 622-633.10.1093/molehr/gaw044.

Beem, E., and Segal, M. S. (2013). Evaluation of stability and sensitivity of cell fluorescent labels when used for cell migration. Journal of fluorescence *23*, 975-987.10.1007/s10895-013-1224-8.

Benedict, J. C., Lin, T. M., Loeffler, I. K., Peterson, R. E., and Flaws, J. A. (2000). Physiological role of the aryl hydrocarbon receptor in mouse ovary development. Toxicological sciences : an official journal of the Society of Toxicology *56*, 382-388

Bergeron, L., Perez, G. I., Macdonald, G., Shi, L., Sun, Y., Jurisicova, A., Varmuza, S., Latham, K. E., Flaws, J. A., Salter, J. C.*, et al.* (1998). Defects in regulation of apoptosis in caspase-2-deficient mice. Genes & development *12*, 1304-1314

Bishonga, C., Takahashi, Y., Katagiri, S., Nagano, M., and Ishikawa, A. (2001). In vitro growth of mouse ovarian preantral follicles and the capacity of their oocytes to develop to the blastocyst stage. The Journal of veterinary medical science *63*, 619-624

Boland, M. J., Hazen, J. L., Nazor, K. L., Rodriguez, A. R., Gifford, W., Martin, G., Kupriyanov, S., and Baldwin, K. K. (2009). Adult mice generated from induced pluripotent stem cells. Nature *461*, 91-94.10.1038/nature08310.

Borum, K. (1961). Oogenesis in the mouse. A study of the meiotic prophase. Experimental cell research *24*, 495-507

Bosma, G. C., Custer, R. P., and Bosma, M. J. (1983). A severe combined immunodeficiency mutation in the mouse. Nature *301*, 527-530

Bowles, J., Knight, D., Smith, C., Wilhelm, D., Richman, J., Mamiya, S., Yashiro, K., Chawengsaksophak, K., Wilson, M. J., Rossant, J.*, et al.* (2006). Retinoid signaling determines germ cell fate in mice. Science *312*, 596-600.10.1126/science.1125691.

Bradbury, A., and Pluckthun, A. (2015). Reproducibility: Standardize antibodies used in research. Nature *518*, 27-29.10.1038/518027a.

Brower, P. T., and Schultz, R. M. (1982). Intercellular communication between granulosa cells and mouse oocytes: existence and possible nutritional role during oocyte growth. Developmental biology *90*, 144-153

Bui, H. T., Van Thuan, N., Kwon, D. N., Choi, Y. J., Kang, M. H., Han, J. W., Kim, T., and Kim, J. H. (2014). Identification and characterization of putative stem cells in the adult pig ovary. Development *141*, 2235-2244.10.1242/dev.104554.

Bukovsky, A., Svetlikova, M., and Caudle, M. R. (2005). Oogenesis in cultures derived from adult human ovaries. Reproductive biology and endocrinology : RB&E *3*, 17.10.1186/1477-7827-3-17.

Burton, P., Adams, D. R., Abraham, A., Allcock, R. W., Jiang, Z., McCahill, A., Gilmour, J., McAbney, J., Kane, N. M., Baillie, G. S.*, et al.* (2010). Identification and characterization of small-molecule ligands that maintain pluripotency of human embryonic stem cells. Biochemical Society transactions *38*, 1058-1061.10.1042/BST0381058.

Butcher, J. T., and Nerem, R. M. (2004). Porcine aortic valve interstitial cells in three-dimensional culture: comparison of phenotype with aortic smooth muscle cells. The Journal of heart valve disease *13*, 478-485; discussion 485-476

Byskov, A. G. (1986). Differentiation of mammalian embryonic gonad. Physiological reviews *66*, 71-117

Byskov, A. G., Hoyer, P. E., Yding Andersen, C., Kristensen, S. G., Jespersen, A., and Mollgard, K. (2011). No evidence for the presence of oogonia in the human ovary after their final clearance during the first two years of life. Human reproduction *26*, 2129-2139.10.1093/humrep/der145.

Camboni, A., Van Langendonckt, A., Donnez, J., Vanacker, J., Dolmans, M. M., and Amorim, C. A. (2013). Alginate beads as a tool to handle, cryopreserve and culture isolated human primordial/primary follicles. Cryobiology *67*, 64-69.10.1016/j.cryobiol.2013.05.002.

Campbell, B. K., Souza, C., Gong, J., Webb, R., Kendall, N., Marsters, P., Robinson, G., Mitchell, A., Telfer, E. E., and Baird, D. T. (2003). Domestic ruminants as models for the elucidation of the mechanisms controlling ovarian follicle development in humans. Reproduction, 429-443

Campos-Junior, P. H., Alves, T. J., Dias, M. T., Assuncao, C. M., Munk, M., Mattos, M. S., Kraemer, L. R., Almeida, B. G., Russo, R. C., Barcelos, L.*, et al.* (2016). Ovarian Grafts 10 Days after Xenotransplantation: Folliculogenesis and Recovery of Viable Oocytes. PloS one *11*, e0158109.10.1371/journal.pone.0158109.

Candy, C. J., Wood, M. J., and Whittingham, D. G. (1995). Follicular development in cryopreserved marmoset ovarian tissue after transplantation. Human reproduction *10*, 2334-2338

Castrillon, D. H., Quade, B. J., Wang, T. Y., Quigley, C., and Crum, C. P. (2000). The human VASA gene is specifically expressed in the germ cell lineage. Proceedings of the National Academy of Sciences of the United States of America *97*, 9585-9590.10.1073/pnas.160274797.

Chambers, I., Silva, J., Colby, D., Nichols, J., Nijmeijer, B., Robertson, M., Vrana, J., Jones, K., Grotewold, L., and Smith, A. (2007). Nanog safeguards pluripotency and mediates germline development. Nature *450*, 1230-1234.10.1038/nature06403.

Chassot, A. A., Ranc, F., Gregoire, E. P., Roepers-Gajadien, H. L., Taketo, M. M., Camerino, G., de Rooij, D. G., Schedl, A., and Chaboissier, M. C. (2008). Activation of beta-catenin signaling by Rspo1 controls differentiation of the mammalian ovary. Human molecular genetics *17*, 1264-1277.10.1093/hmg/ddn016.

Chatterjee, A., Saha, D., Niemann, H., Gryshkov, O., Glasmacher, B., and Hofmann, N. (2017). Effects of cryopreservation on the epigenetic profile of cells. Cryobiology *74*, 1-7.10.1016/j.cryobiol.2016.12.002.

Chen, Y., Breen, K., and Pepling, M. E. (2009). Estrogen can signal through multiple pathways to regulate oocyte cyst breakdown and primordial follicle assembly in the neonatal mouse ovary. The Journal of endocrinology *202*, 407-417.10.1677/JOE-09-0109.

Chen, Y., Jefferson, W. N., Newbold, R. R., Padilla-Banks, E., and Pepling, M. E. (2007). Estradiol, progesterone, and genistein inhibit oocyte nest breakdown and primordial follicle assembly in the neonatal mouse ovary in vitro and in vivo. Endocrinology *148*, 3580-3590.10.1210/en.2007-0088.

Cheng, X., Chen, S., Yu, X., Zheng, P., and Wang, H. (2012). BMP15 gene is activated during human amniotic fluid stem cell differentiation into oocyte-like cells. DNA and cell biology *31*, 1198-1204.10.1089/dna.2011.1396.

Childs, A. J., Cowan, G., Kinnell, H. L., Anderson, R. A., and Saunders, P. T. (2011). Retinoic Acid signalling and the control of meiotic entry in the human fetal gonad. PloS one *6*, e20249.10.1371/journal.pone.0020249.

Choi, J. K., Agarwal, P., and He, X. (2013). In vitro culture of early secondary preantral follicles in hanging drop of ovarian cell-conditioned medium to obtain MII oocytes from outbred deer mice. Tissue engineering Part A *19*, 2626-2637.10.1089/ten.TEA.2013.0055.

Cocquet, J., Pailhoux, E., Jaubert, F., Servel, N., Xia, X., Pannetier, M., De Baere, E., Messiaen, L., Cotinot, C., Fellous, M., and Veitia, R. A. (2002). Evolution and expression of FOXL2. Journal of medical genetics *39*, 916-921

Coggins, L. W. (1973). An ultrastructural and radioautographic study of early oogenesis in the toad Xenopus laevis. Journal of cell science *12*, 71-93

Connor, E. E., Laiakis, E. C., Fernandes, V. M., Williams, J. L., and Capuco, A. V. (2005). Molecular cloning, expression and radiation hybrid mapping of the bovine deiodinase type II (DIO2) and deiodinase type III (DIO3) genes. Anim Genet *36*, 240-243.10.1111/j.1365-2052.2005.01282.x.

Cortvrindt, R., Smitz, J., and Van Steirteghem, A. C. (1996). In-vitro maturation, fertilization and embryo development of immature oocytes from early preantral follicles from prepuberal mice in a simplified culture system. Human reproduction *11*, 2656-2666

Cory, S., and Adams, J. M. (2002). The Bcl2 family: regulators of the cellular life-or-death switch. Nature reviews Cancer *2*, 647-656.10.1038/nrc883.
Cox, S., Shaw, J., and Jenkin, G. (2000). Follicular development in transplanted fetal and neonatal mouse ovaries is influenced by the gonadal status of the adult recipient. Fertility and sterility *74*, 366-371

Danner, S., Kajahn, J., Geismann, C., Klink, E., and Kruse, C. (2007). Derivation of oocyte-like cells from a clonal pancreatic stem cell line. Molecular human reproduction *13*, 11-20.10.1093/molehr/gal096.

David, G. F., Anand Kumar, T. C., and Baker, T. G. (1974). Uptake of tritiated thymidine by primordial germinal cells in the ovaries of the adult slender loris. Journal of reproduction and fertility *41*, 447-451

De Felici, M., and Dolci, S. (1991). Leukemia inhibitory factor sustains the survival of mouse primordial germ cells cultured on TM4 feeder layers. Developmental biology *147*, 281-284

De Felici, M., Dolci, S., and Pesce, M. (1992). Cellular and molecular aspects of mouse primordial germ cell migration and proliferation in culture. The International journal of developmental biology *36*, 205-213

De Felici, M., Lobascio, A. M., and Klinger, F. G. (2008). Cell death in fetal oocytes: many players for multiple pathways. Autophagy *4*, 240-242

Di Carlo, A. D., Travia, G., and De Felici, M. (2000). The meiotic specific synaptonemal complex protein SCP3 is expressed by female and male primordial germ cells of the mouse embryo. The International journal of developmental biology *44*, 241-244

Diaferia, G. R., Dessi, S. S., Deblasio, P., and Biunno, I. (2008). Is stem cell chromosomes stability affected by cryopreservation conditions? Cytotechnology *58*, 11-16.10.1007/s10616-008-9163-y.

Ding, X., Liu, G., Xu, B., Wu, C., Hui, N., Ni, X., Wang, J., Du, M., Teng, X., and Wu, J. (2016). Human GV oocytes generated by mitotically active germ cells obtained from follicular aspirates. Scientific reports *6*, 28218.10.1038/srep28218.

Dissen, G. A., Lara, H. E., Fahrenbach, W. H., Costa, M. E., and Ojeda, S. R. (1994). Immature rat ovaries become revascularized rapidly after autotransplantation and show a gonadotropin-dependent increase in angiogenic factor gene expression. Endocrinology *134*, 1146-1154.10.1210/endo.134.3.8119153.

Dolci, S., Williams, D. E., Ernst, M. K., Resnick, J. L., Brannan, C. I., Lock, L. F., Lyman, S. D., Boswell, H. S., and Donovan, P. J. (1991). Requirement for mast cell growth factor for primordial germ cell survival in culture. Nature *352*, 809-811.10.1038/352809a0.

Dorshkind, K., Keller, G. M., Phillips, R. A., Miller, R. G., Bosma, G. C., O'Toole, M., and Bosma, M. J. (1984). Functional status of cells from lymphoid and myeloid tissues in mice with severe combined immunodeficiency disease. Journal of immunology *132*, 1804-1808

Dorshkind, K., Pollack, S. B., Bosma, M. J., and Phillips, R. A. (1985). Natural killer (NK) cells are present in mice with severe combined immunodeficiency (scid). Journal of immunology *134*, 3798-3801

Duke, K. L. (1967). Ovogenetic activity of the fetal-type in the ovary of the adult slow loris, Nycticebus coucang. Folia primatologica; international journal of primatology *7*, 150-154

Dunlop, C. E., Telfer, E. E., and Anderson, R. A. (2013). Ovarian stem cells--potential roles in infertility treatment and fertility preservation. Maturitas *76*, 279-283.10.1016/j.maturitas.2013.04.017.

Dunlop, C. E., Telfer, E. E., and Anderson, R. A. (2014). Ovarian germline stem cells. Stem cell research & therapy *5*, 98.10.1186/scrt487.

Durlinger, A. L., Gruijters, M. J., Kramer, P., Karels, B., Ingraham, H. A., Nachtigal, M. W., Uilenbroek, J. T., Grootegoed, J. A., and Themmen, A. P. (2002). Anti-Mullerian hormone inhibits initiation of primordial follicle growth in the mouse ovary. Endocrinology *143*, 1076-1084.10.1210/endo.143.3.8691.

Durlinger, A. L., Kramer, P., Karels, B., de Jong, F. H., Uilenbroek, J. T., Grootegoed, J. A., and Themmen, A. P. (1999). Control of primordial follicle recruitment by anti-Mullerian hormone in the mouse ovary. Endocrinology *140*, 5789-5796.10.1210/endo.140.12.7204.

Dyce, P. W., Liu, J., Tayade, C., Kidder, G. M., Betts, D. H., and Li, J. (2011). In vitro and in vivo germ line potential of stem cells derived from newborn mouse skin. PloS one *6*, e20339.10.1371/journal.pone.0020339.

Dyce, P. W., Wen, L., and Li, J. (2006). In vitro germline potential of stem cells derived from fetal porcine skin. Nature cell biology *8*, 384-390.10.1038/ncb1388.
Edmondson, R., Broglie, J. J., Adcock, A. F., and Yang, L. J. (2014). Three-Dimensional Cell Culture Systems and Their Applications in Drug Discovery and Cell-Based Biosensors. Assay Drug Dev Techn *12*, 207-218.10.1089/adt.2014.573.

Eggan, K., Jurga, S., Gosden, R., Min, I. M., and Wagers, A. J. (2006). Ovulated oocytes in adult mice derive from non-circulating germ cells. Nature *441*, 1109-1114.10.1038/nature04929.

Eggers, S., and Sinclair, A. (2012). Mammalian sex determination-insights from humans and mice. Chromosome research : an international journal on the molecular, supramolecular and evolutionary aspects of chromosome biology *20*, 215-238.10.1007/s10577-012-9274-3.

Eguizabal, C., Shovlin, T. C., Durcova-Hills, G., Surani, A., and McLaren, A. (2009). Generation of primordial germ cells from pluripotent stem cells. Differentiation; research in biological diversity *78*, 116-123.10.1016/j.diff.2009.07.001.

Eozenou, C., Vitorino Carvalho, A., Forde, N., Giraud-Delville, C., Gall, L., Lonergan, P., Auguste, A., Charpigny, G., Richard, C., Pannetier, M., and Sandra, O. (2012). FOXL2 is regulated during the bovine estrous cycle and its expression in the endometrium is independent of conceptus-derived interferon tau. Biology of reproduction *87*, 32.10.1095/biolreprod.112.101584.

Eppig, J. J. (1979). A comparison between oocyte growth in coculture with granulosa cells and oocytes with granulosa cell-oocyte junctional contact maintained in vitro. The Journal of experimental zoology *209*, 345-353.10.1002/jez.1402090216.

Eppig, J. J. (1991). Intercommunication between mammalian oocytes and companion somatic cells. BioEssays : news and reviews in molecular, cellular and developmental biology *13*, 569-574.10.1002/bies.950131105.

Eppig, J. J., and O'Brien, M. J. (1996). Development in vitro of mouse oocytes from primordial follicles. Biology of reproduction *54*, 197-207

Eppig, J. J., and Schroeder, A. C. (1989). Capacity of mouse oocytes from preantral follicles to undergo embryogenesis and development to live young after growth, maturation, and fertilization in vitro. Biology of reproduction *41*, 268-276

Eppig, J. J., and Wigglesworth, K. (2000). Development of mouse and rat oocytes in chimeric reaggregated ovaries after interspecific exchange of somatic and germ cell components. Biology of reproduction *63*, 1014-1023

Erickson, B. H. (1966). Development and Radio-Response of Prenatal Bovine Ovary. Journal of reproduction and fertility *11*, 97

Estrov, Z. (2009). Stem cells and somatic cells: reprogramming and plasticity. Clinical lymphoma & myeloma *9 Suppl 3*, S319-328.10.3816/CLM.2009.s.031.

Evans, H. M., and Swezy, O. (1931). Ovogenesis and the normal follicular cycle in adult Mammalia, (Berkeley, Calif.,: University of California press).

Evans, M. J., and Kaufman, M. H. (1981). Establishment in culture of pluripotential cells from mouse embryos. Nature *292*, 154-156

Eyrich, D., Brandl, F., Appel, B., Wiese, H., Maier, G., Wenzel, M., Staudenmaier, R., Goepferich, A., and Blunk, T. (2007). Long-term stable fibrin gels for cartilage engineering. Biomaterials *28*, 55-65.10.1016/j.biomaterials.2006.08.027.

Fortune, J. E., and Armstrong, D. T. (1977). Androgen production by theca and granulosa isolated from proestrous rat follicles. Endocrinology *100*, 1341-1347.10.1210/endo-100-5-1341.

Fulton, N., Martins da Silva, S. J., Bayne, R. A., and Anderson, R. A. (2005). Germ cell proliferation and apoptosis in the developing human ovary. The Journal of clinical endocrinology and metabolism *90*, 4664-4670.10.1210/jc.2005-0219.

Gawriluk, T. R., Hale, A. N., Flaws, J. A., Dillon, C. P., Green, D. R., and Rucker, E. B., 3rd (2011). Autophagy is a cell survival program for female germ cells in the murine ovary. Reproduction *141*, 759-765.10.1530/REP-10-0489.

Ge, W., Ma, H. G., Cheng, S. F., Sun, Y. C., Sun, L. L., Sun, X. F., Li, L., Dyce, P., Li, J., Shi, Q. H., and Shen, W. (2015). Differentiation of early germ cells from human skin-derived stem cells without exogenous gene integration. Scientific reports *5*, 13822.10.1038/srep13822.

Ghafari, F., Gutierrez, C. G., and Hartshorne, G. M. (2007). Apoptosis in mouse fetal and neonatal oocytes during meiotic prophase one. BMC developmental biology *7*, 87.10.1186/1471-213X-7-87.

Gill, M. E., Hu, Y. C., Lin, Y., and Page, D. C. (2011). Licensing of gametogenesis, dependent on RNA binding protein DAZL, as a gateway to sexual differentiation of fetal germ cells. Proceedings of the National Academy of Sciences of the United States of America *108*, 7443-7448.10.1073/pnas.1104501108.

Gomperts, M., Garcia-Castro, M., Wylie, C., and Heasman, J. (1994). Interactions between primordial germ cells play a role in their migration in mouse embryos. Development *120*, 135-141

Gondos, B., Westergaard, L., and Byskov, A. G. (1986). Initiation of oogenesis in the human fetal ovary: ultrastructural and squash preparation study. American journal of obstetrics and gynecology *155*, 189-195

Gook, D. A., McCully, B. A., Edgar, D. H., and McBain, J. C. (2001). Development of antral follicles in human cryopreserved ovarian tissue following xenografting. Human reproduction *16*, 417-422

Gosden, R. G. (2004). Germline stem cells in the postnatal ovary: is the ovary more like a testis? Human reproduction update *10*, 193-195.10.1093/humupd/dmh023.

Gosden, R. G., Boulton, M. I., Grant, K., and Webb, R. (1994). Follicular development from ovarian xenografts in SCID mice. Journal of reproduction and fertility *101*, 619-623

Gosden, R. G., and Telfer, E. (1987). Scaling of Follicular Sizes in Mammalian Ovaries. J Zool *211*, 157-168

Grieve, K. M., McLaughlin, M., Dunlop, C. E., Telfer, E. E., and Anderson, R. A. (2015). The controversial existence and functional potential of oogonial stem cells. Maturitas *82*, 278-281.10.1016/j.maturitas.2015.07.017.

Griffin, J., Emery, B. R., Huang, I., Peterson, C. M., and Carrell, D. T. (2006). Comparative analysis of follicle morphology and oocyte diameter in four mammalian species (mouse, hamster, pig, and human). Journal of experimental & clinical assisted reproduction *3*, 2.10.1186/1743-1050-3-2.

Gu, Y., Runyan, C., Shoemaker, A., Surani, A., and Wylie, C. (2009). Steel factor controls primordial germ cell survival and motility from the time of their specification in the allantois, and provides a continuous niche throughout their migration. Development *136*, 1295-1303.10.1242/dev.030619.

Gunasena, K. T., Lakey, J. R., Villines, P. M., Bush, M., Raath, C., Critser, E. S., McGann, L. E., and Critser, J. K. (1998). Antral follicles develop in xenografted cryopreserved African elephant (Loxodonta africana) ovarian tissue. Animal reproduction science *53*, 265-275

Guo, K., Li, C. H., Wang, X. Y., He, D. J., and Zheng, P. (2016). Germ stem cells are active in postnatal mouse ovary under physiological conditions. Molecular human reproduction *22*, 316-328.10.1093/molehr/gaw015.

Handel, M. A., Eppig, J. J., and Schimenti, J. C. (2014). Applying "gold standards" to in-vitro-derived germ cells. Cell *157*, 1257-1261.10.1016/j.cell.2014.05.019.
Hashimoto, K., Noguchi, M., and Nakatsuji, N. (1992). Mouse Offspring Derived from Fetal Ovaries or Reaggregates Which Were Cultured and Transplanted into Adult Females. Dev Growth Differ *34*, 233-238

Hayashi, K., Ogushi, S., Kurimoto, K., Shimamoto, S., Ohta, H., and Saitou, M. (2012). Offspring from oocytes derived from in vitro primordial germ cell-like cells in mice. Science *338*, 971-975.10.1126/science.1226889.

Hayashi, K., Ohta, H., Kurimoto, K., Aramaki, S., and Saitou, M. (2011). Reconstitution of the mouse germ cell specification pathway in culture by pluripotent stem cells. Cell *146*, 519-532.10.1016/j.cell.2011.06.052.

Hayashi, K., and Saitou, M. (2013). Generation of eggs from mouse embryonic stem cells and induced pluripotent stem cells. Nature protocols *8*, 1513-1524.10.1038/nprot.2013.090.

He, J., Stewart, K., Kinnell, H. L., Anderson, R. A., and Childs, A. J. (2013). A developmental stage-specific switch from DAZL to BOLL occurs during fetal oogenesis in humans, but not mice. PloS one *8*, e73996.10.1371/journal.pone.0073996.

Heise, M., Koepsel, R., Russell, A. J., and McGee, E. A. (2005). Calcium alginate microencapsulation of ovarian follicles impacts FSH delivery and follicle morphology. Reproductive biology and endocrinology : RB&E *3*, 47.10.1186/1477-7827-3-47.

Hendriks, S., Hessel, M., Mochtar, M. H., Meissner, A., van der Veen, F., Repping, S., and Dancet, E. A. (2016). Couples with non-obstructive azoospermia are interested in future treatments with artificial gametes. Human reproduction *31*, 1738-1748.10.1093/humrep/dew095.

Hernandez-Fonseca, H. J., Bosch, P., Miller, D. M., Wininger, J. D., Massey, J. B., and Brackett, B. G. (2005). Time course of follicular development after bovine ovarian tissue transplantation in male non-obese diabetic severe combined immunodeficient mice. Fertility and sterility *83 Suppl 1*, 1180-1187.10.1016/j.fertnstert.2004.07.985.

Hernandez, S. F., Vahidi, N. A., Park, S., Weitzel, R. P., Tisdale, J., Rueda, B. R., and Wolff, E. F. (2015). Characterization of extracellular DDX4- or Ddx4-positive ovarian cells. Nature medicine *21*, 1114-1116.10.1038/nm.3966.

Hikabe, O., Hamazaki, N., Nagamatsu, G., Obata, Y., Hirao, Y., Hamada, N., Shimamoto, S., Imamura, T., Nakashima, K., Saitou, M., and Hayashi, K. (2016). Reconstitution in vitro of the entire cycle of the mouse female germ line. Nature *539*, 299-303.10.1038/nature20104.

Horan, C. J., and Williams, S. A. (2017). Oocyte stem cells: fact or fantasy? Reproduction *154*, R23-R35.10.1530/REP-17-0008.

Hornick, J. E., Duncan, F. E., Shea, L. D., and Woodruff, T. K. (2013). Multiple follicle culture supports primary follicle growth through paracrine-acting signals. Reproduction *145*, 19-32.10.1530/REP-12-0233.

Hu, Y. C., Nicholls, P. K., Soh, Y. Q., Daniele, J. R., Junker, J. P., van Oudenaarden, A., and Page, D. C. (2015). Licensing of primordial germ cells for gametogenesis depends on genital ridge signaling. PLoS genetics *11*, e1005019.10.1371/journal.pgen.1005019.

Hubner, K., Fuhrmann, G., Christenson, L. K., Kehler, J., Reinbold, R., De La Fuente, R., Wood, J., Strauss, J. F., 3rd, Boiani, M., and Scholer, H. R. (2003). Derivation of oocytes from mouse embryonic stem cells. Science *300*, 1251-1256.10.1126/science.1083452.

Hummitzsch, K., Irving-Rodgers, H. F., Hatzirodos, N., Bonner, W., Sabatier, L., Reinhardt, D. P., Sado, Y., Ninomiya, Y., Wilhelm, D., and Rodgers, R. J. (2013). A new model of development of the mammalian ovary and follicles. PloS one *8*, e55578.10.1371/journal.pone.0055578.

Hutt, K. J. (2015). The role of BH3-only proteins in apoptosis within the ovary. Reproduction *149*, R81-89.10.1530/REP-14-0422.

Iguchi, T., and Takasugi, N. (1986). Polyovular follicles in the ovary of immature mice exposed prenatally to diethylstilbestrol. Anatomy and embryology *175*, 53-55

Imudia, A. N., Wang, N., Tanaka, Y., White, Y. A., Woods, D. C., and Tilly, J. L. (2013). Comparative gene expression profiling of adult mouse ovary-derived oogonial stem cells supports a distinct cellular identity. Fertility and sterility *100*, 1451-1458.10.1016/j.fertnstert.2013.06.036.

Irie, N., Weinberger, L., Tang, W. W., Kobayashi, T., Viukov, S., Manor, Y. S., Dietmann, S., Hanna, J. H., and Surani, M. A. (2015). SOX17 is a critical specifier of human primordial germ cell fate. Cell *160*, 253-268.10.1016/j.cell.2014.12.013.

Jackson, K. S., Inoue, K., Davis, D. A., Hilliard, T. S., and Burdette, J. E. (2009). Three-dimensional ovarian organ culture as a tool to study normal ovarian surface epithelial wound repair. Endocrinology *150*, 3921-3926.10.1210/en.2008-1674.

Jefferson, W., Newbold, R., Padilla-Banks, E., and Pepling, M. (2006). Neonatal genistein treatment alters ovarian differentiation in the mouse: inhibition of oocyte nest breakdown and increased oocyte survival. Biology of reproduction *74*, 161-168.10.1095/biolreprod.105.045724.

Jefferson, W. N., Couse, J. F., Padilla-Banks, E., Korach, K. S., and Newbold, R. R. (2002). Neonatal exposure to genistein induces estrogen receptor (ER)alpha expression and multioocyte follicles in the maturing mouse ovary: evidence for ERbeta-mediated and nonestrogenic actions. Biology of reproduction *67*, 1285-1296

Johnson, J., Bagley, J., Skaznik-Wikiel, M., Lee, H. J., Adams, G. B., Niikura, Y., Tschudy, K. S., Tilly, J. C., Cortes, M. L., Forkert, R*., et al.* (2005). Oocyte generation in adult mammalian ovaries by putative germ cells in bone marrow and peripheral blood. Cell *122*, 303-315.10.1016/j.cell.2005.06.031.

Johnson, J., Canning, J., Kaneko, T., Pru, J. K., and Tilly, J. L. (2004). Germline stem cells and follicular renewal in the postnatal mammalian ovary. Nature *428*, 145-150.10.1038/nature02316.

Jordan, B. K., Shen, J. H., Olaso, R., Ingraham, H. A., and Vilain, E. (2003). Wnt4 overexpression disrupts normal testicular vasculature and inhibits testosterone synthesis by repressing steroidogenic factor 1/beta-catenin synergy. Proceedings of the National Academy of Sciences of the United States of America *100*, 10866-10871.10.1073/pnas.1834480100.

Jorgensen, A., Young, J., Nielsen, J. E., Joensen, U. N., Toft, B. G., Rajpert-De Meyts, E., and Loveland, K. L. (2014). Hanging drop cultures of human testis and testis cancer samples: a model used to investigate activin treatment effects in a preserved niche. Brit J Cancer *110*, 2604-2614.10.1038/bjc.2014.160.

Jost, A. (1947). The age factor in the castration of male rabbit fetuses. Proceedings of the Society for Experimental Biology and Medicine Society for Experimental Biology and Medicine *66*, 302

Kagawa, N., Silber, S., and Kuwayama, M. (2009). Successful vitrification of bovine and human ovarian tissue. Reproductive biomedicine online *18*, 568-577

Kakiuchi, K., Tsuda, A., Goto, Y., Shimada, T., Taniguchi, K., Takagishi, K., and Kubota, H. (2014). Cell-surface DEAD-box polypeptide 4-immunoreactive cells and gonocytes are two distinct populations in postnatal porcine testes. Biology of reproduction *90*, 82.10.1095/biolreprod.113.114405.

Kanai-Azuma, M., Kanai, Y., Gad, J. M., Tajima, Y., Taya, C., Kurohmaru, M., Sanai, Y., Yonekawa, H., Yazaki, K., Tam, P. P., and Hayashi, Y. (2002). Depletion of definitive gut endoderm in Sox17-null mutant mice. Development *129*, 2367-2379

Kanatsu-Shinohara, M., and Shinohara, T. (2013). Spermatogonial stem cell self-renewal and development. Annual review of cell and developmental biology *29*, 163-187.10.1146/annurev-cellbio-101512-122353.

Kashimada, K., Pelosi, E., Chen, H., Schlessinger, D., Wilhelm, D., and Koopman, P. (2011). FOXL2 and BMP2 act cooperatively to regulate follistatin gene expression during ovarian development. Endocrinology *152*, 272-280.10.1210/en.2010-0636.

Kawase, E., Hashimoto, K., and Pedersen, R. A. (2004). Autocrine and paracrine mechanisms regulating primordial germ cell proliferation. Molecular reproduction and development *68*, 5-16.10.1002/mrd.20031.

Keller, G. M. (1995). In vitro differentiation of embryonic stem cells. Current opinion in cell biology *7*, 862-869

Kerr, J. B., Duckett, R., Myers, M., Britt, K. L., Mladenovska, T., and Findlay, J. K. (2006). Quantification of healthy follicles in the neonatal and adult mouse ovary: evidence for maintenance of primordial follicle supply. Reproduction *132*, 95-109.10.1530/rep.1.01128.

Kezele, P., and Skinner, M. K. (2003). Regulation of ovarian primordial follicle assembly and development by estrogen and progesterone: endocrine model of follicle assembly. Endocrinology *144*, 3329-3337.10.1210/en.2002-0131.

Kidder, G. M., and Vanderhyden, B. C. (2010). Bidirectional communication between oocytes and follicle cells: ensuring oocyte developmental competence. Canadian journal of physiology and pharmacology *88*, 399-413.10.1139/y10-009.

Kim, Y., Kobayashi, A., Sekido, R., DiNapoli, L., Brennan, J., Chaboissier, M. C., Poulat, F., Behringer, R. R., Lovell-Badge, R., and Capel, B. (2006). Fgf9 and Wnt4 act as antagonistic signals to regulate mammalian sex determination. PLoS biology *4*, e187.10.1371/journal.pbio.0040187.

Kimble, J. E., and White, J. G. (1981). On the control of germ cell development in Caenorhabditis elegans. Developmental biology *81*, 208-219

Kimura, F., Bonomi, L. M., and Schneyer, A. L. (2011). Follistatin regulates germ cell nest breakdown and primordial follicle formation. Endocrinology *152*, 697-706.10.1210/en.2010-0950.

Kingery, H. M. (1917). Oogenesis in the white mouse. J Morphol *30*, 261-315.DOI 10.1002/jmor.1050300108.

Koubova, J., Hu, Y. C., Bhattacharyya, T., Soh, Y. Q., Gill, M. E., Goodheart, M. L., Hogarth, C. A., Griswold, M. D., and Page, D. C. (2014). Retinoic acid activates two pathways required for meiosis in mice. PLoS genetics *10*, e1004541.10.1371/journal.pgen.1004541.

Koubova, J., Menke, D. B., Zhou, Q., Capel, B., Griswold, M. D., and Page, D. C. (2006). Retinoic acid regulates sex-specific timing of meiotic initiation in mice. Proceedings of the National Academy of Sciences of the United States of America *103*, 2474-2479.10.1073/pnas.0510813103.

Lacham-Kaplan, O., Chy, H., and Trounson, A. (2006). Testicular cell conditioned medium supports differentiation of embryonic stem cells into ovarian structures containing oocytes. Stem cells *24*, 266-273.10.1634/stemcells.2005-0204.

Laronda, M. M., Duncan, F. E., Hornick, J. E., Xu, M., Pahnke, J. E., Whelan, K. A., Shea, L. D., and Woodruff, T. K. (2014). Alginate encapsulation supports the growth and differentiation of human primordial follicles within ovarian cortical tissue. Journal of assisted reproduction and genetics *31*, 1013-1028.10.1007/s10815-014-0252-x.

Lawson, K. A., Dunn, N. R., Roelen, B. A., Zeinstra, L. M., Davis, A. M., Wright, C. V., Korving, J. P., and Hogan, B. L. (1999). Bmp4 is required for the generation of primordial germ cells in the mouse embryo. Genes & development *13*, 424-436

Lawson, K. A., and Hage, W. J. (1994). Clonal analysis of the origin of primordial germ cells in the mouse. Ciba Foundation symposium *182*, 68-84; discussion 84-91

Le Bouffant, R., Guerquin, M. J., Duquenne, C., Frydman, N., Coffigny, H., Rouiller-Fabre, V., Frydman, R., Habert, R., and Livera, G. (2010). Meiosis initiation in the human ovary requires intrinsic retinoic acid synthesis. Human reproduction *25*, 2579-2590.10.1093/humrep/deq195.

Lei, L., and Spradling, A. C. (2013). Female mice lack adult germ-line stem cells but sustain oogenesis using stable primordial follicles. Proceedings of the National Academy of Sciences of the United States of America *110*, 8585-8590.10.1073/pnas.1306189110.

Lenie, S., Cortvrindt, R., Adriaenssens, T., and Smitz, J. (2004). A reproducible two-step culture system for isolated primary mouse ovarian follicles as single functional units. Biology of reproduction *71*, 1730-1738.10.1095/biolreprod.104.028415.

Lin, H. (1997). The tao of stem cells in the germline. Annual review of genetics *31*, 455-491.10.1146/annurev.genet.31.1.455.

Lin, P., Correa, D., Lin, Y., and Caplan, A. I. (2011). Polybrene inhibits human mesenchymal stem cell proliferation during lentiviral transduction. PloS one *6*, e23891.10.1371/journal.pone.0023891.

Lin, Y., Gill, M. E., Koubova, J., and Page, D. C. (2008). Germ cell-intrinsic and -extrinsic factors govern meiotic initiation in mouse embryos. Science *322*, 1685-1687.10.1126/science.1166340.

Liu, Y., Wu, C., Lyu, Q., Yang, D., Albertini, D. F., Keefe, D. L., and Liu, L. (2007). Germline stem cells and neo-oogenesis in the adult human ovary. Developmental biology *306*, 112-120.10.1016/j.ydbio.2007.03.006.

Liu, Y. X., and Hsueh, A. J. (1986). Synergism between granulosa and theca-interstitial cells in estrogen biosynthesis by gonadotropin-treated rat ovaries: studies on the two-cell, two-gonadotropin hypothesis using steroid antisera. Biology of reproduction *35*, 27-36

Lobascio, A. M., Klinger, F. G., Scaldaferri, M. L., Farini, D., and De Felici, M. (2007). Analysis of programmed cell death in mouse fetal oocytes. Reproduction *134*, 241-252.10.1530/REP-07-0141.

Maatouk, D. M., DiNapoli, L., Alvers, A., Parker, K. L., Taketo, M. M., and Capel, B. (2008). Stabilization of beta-catenin in XY gonads causes male-to-female sex-reversal. Human molecular genetics *17*, 2949-2955.10.1093/hmg/ddn193.

Maatouk, D. M., Mork, L., Hinson, A., Kobayashi, A., McMahon, A. P., and Capel, B. (2012). Germ cells are not required to establish the female pathway in mouse fetal gonads. PloS one *7*, e47238.10.1371/journal.pone.0047238.

Magnusdottir, E., Dietmann, S., Murakami, K., Gunesdogan, U., Tang, F., Bao, S., Diamanti, E., Lao, K., Gottgens, B., and Azim Surani, M. (2013). A tripartite transcription factor network regulates primordial germ cell specification in mice. Nature cell biology *15*, 905-915.10.1038/ncb2798.

Marca, J. E. L., and Somers, W. G. (2014). The Drosophila gonads: models for stem cell proliferation, self-renewal, and differentiation. AIMS Genetics *1*, 55-80

Matoba, S., and Ogura, A. (2011). Generation of functional oocytes and spermatids from fetal primordial germ cells after ectopic transplantation in adult mice. Biology of reproduction *84*, 631-638.10.1095/biolreprod.110.087122.

Matsui, Y., Toksoz, D., Nishikawa, S., Nishikawa, S., Williams, D., Zsebo, K., and Hogan, B. L. (1991). Effect of Steel factor and leukaemia inhibitory factor on murine primordial germ cells in culture. Nature *353*, 750-752.10.1038/353750a0.

McLaughlin, M., Kelsey, T. W., Wallace, W. H., Anderson, R. A., and Telfer, E. E. (2017). Non-growing follicle density is increased following adriamycin, bleomycin, vinblastine and dacarbazine (ABVD) chemotherapy in the adult human ovary. Human reproduction *32*, 165-174.10.1093/humrep/dew260.

McLaughlin, M., and Telfer, E. E. (2010). Oocyte development in bovine primordial follicles is promoted by activin and FSH within a two-step serum-free culture system. Reproduction *139*, 971-978.10.1530/REP-10-0025.

Menke, D. B., Koubova, J., and Page, D. C. (2003). Sexual differentiation of germ cells in XX mouse gonads occurs in an anterior-to-posterior wave. Developmental biology *262*, 303-312

Molyneaux, K. A., Stallock, J., Schaible, K., and Wylie, C. (2001). Time-lapse analysis of living mouse germ cell migration. Developmental biology *240*, 488-498.10.1006/dbio.2001.0436.

Morgan, S., Campbell, L., Allison, V., Murray, A., and Spears, N. (2015). Culture and co-culture of mouse ovaries and ovarian follicles. Journal of visualized experiments : JoVE.10.3791/52458.

Mork, L., Maatouk, D. M., McMahon, J. A., Guo, J. J., Zhang, P., McMahon, A. P., and Capel, B. (2012). Temporal differences in granulosa cell specification in the ovary reflect distinct follicle fates in mice. Biology of reproduction *86*, 37.10.1095/biolreprod.111.095208.

Morohaku, K., Tanimoto, R., Sasaki, K., Kawahara-Miki, R., Kono, T., Hayashi, K., Hirao, Y., and Obata, Y. (2016). Complete in vitro generation of fertile oocytes from mouse primordial germ cells. Proceedings of the National Academy of Sciences of the United States of America *113*, 9021-9026.10.1073/pnas.1603817113.

Motta, P. M., and Makabe, S. (1986). Elimination of germ cells during differentiation of the human ovary: an electron microscopic study. European journal of obstetrics, gynecology, and reproductive biology *22*, 271-286

Motta, P. M., Makabe, S., and Nottola, S. A. (1997). The ultrastructure of human reproduction. I. The natural history of the female germ cell: origin, migration and differentiation inside the developing ovary. Human reproduction update *3*, 281-295

Nakamura, T., Liu, Y. J., Nakashima, H., Umehara, H., Inoue, K., Matoba, S., Tachibana, M., Ogura, A., Shinkai, Y., and Nakano, T. (2012). PGC7 binds histone H3K9me2 to protect against conversion of 5mC to 5hmC in early embryos. Nature *486*, 415-419.10.1038/nature11093.

Ng, A., Tan, S., Singh, G., Rizk, P., Swathi, Y., Tan, T. Z., Huang, R. Y., Leushacke, M., and Barker, N. (2014). Lgr5 marks stem/progenitor cells in ovary and tubal epithelia. Nature cell biology *16*, 745-757.10.1038/ncb3000.

Niikura, Y., Niikura, T., and Tilly, J. L. (2009). Aged mouse ovaries possess rare premeiotic germ cells that can generate oocytes following transplantation into a young host environment. Aging *1*, 971-978.10.18632/aging.100105.

Nilsson, E. E., and Skinner, M. K. (2009). Progesterone regulation of primordial follicle assembly in bovine fetal ovaries. Molecular and cellular endocrinology *313*, 9-16.10.1016/j.mce.2009.09.004.

Novak, I., Lightfoot, D. A., Wang, H., Eriksson, A., Mahdy, E., and Hoog, C. (2006). Mouse embryonic stem cells form follicle-like ovarian structures but do not progress through meiosis. Stem cells *24*, 1931-1936.10.1634/stemcells.2005-0520.

O'Brien, M. J., Pendola, J. K., and Eppig, J. J. (2003). A revised protocol for in vitro development of mouse oocytes from primordial follicles dramatically improves their developmental competence. Biology of reproduction *68*, 1682-1686.10.1095/biolreprod.102.013029.

Ohinata, Y., Ohta, H., Shigeta, M., Yamanaka, K., Wakayama, T., and Saitou, M. (2009). A signaling principle for the specification of the germ cell lineage in mice. Cell *137*, 571-584.10.1016/j.cell.2009.03.014.

Ohinata, Y., Payer, B., O'Carroll, D., Ancelin, K., Ono, Y., Sano, M., Barton, S. C., Obukhanych, T., Nussenzweig, M., Tarakhovsky, A.*, et al.* (2005). Blimp1 is a critical determinant of the germ cell lineage in mice. Nature *436*, 207-213.10.1038/nature03813.

Oktay, K., Newton, H., Mullan, J., and Gosden, R. G. (1998). Development of human primordial follicles to antral stages in SCID/hpg mice stimulated with follicle stimulating hormone. Human reproduction *13*, 1133-1138

Onishi, K., and Zandstra, P. W. (2015). LIF signaling in stem cells and development. Development *142*, 2230-2236.10.1242/dev.117598.

Ottolenghi, C., Pelosi, E., Tran, J., Colombino, M., Douglass, E., Nedorezov, T., Cao, A., Forabosco, A., and Schlessinger, D. (2007). Loss of Wnt4 and Foxl2 leads to female-to-male sex reversal extending to germ cells. Human molecular genetics *16*, 2795-2804.10.1093/hmg/ddm235.

Pacchiarotti, J., Maki, C., Ramos, T., Marh, J., Howerton, K., Wong, J., Pham, J., Anorve, S., Chow, Y. C., and Izadyar, F. (2010). Differentiation potential of germ line stem cells derived from the postnatal mouse ovary. Differentiation; research in biological diversity *79*, 159-170.10.1016/j.diff.2010.01.001.

Pangas, S. A. (2012). Regulation of the ovarian reserve by members of the transforming growth factor beta family. Molecular reproduction and development *79*, 666-679.10.1002/mrd.22076.

Paris, M. C., Snow, M., Cox, S. L., and Shaw, J. M. (2004). Xenotransplantation: a tool for reproductive biology and animal conservation? Theriogenology *61*, 277-291

Park, E. S., Woods, D. C., and Tilly, J. L. (2013). Bone morphogenetic protein 4 promotes mammalian oogonial stem cell differentiation via Smad1/5/8 signaling. Fertility and sterility *100*, 1468-1475.10.1016/j.fertnstert.2013.07.1978.

Park, T. S., Galic, Z., Conway, A. E., Lindgren, A., van Handel, B. J., Magnusson, M., Richter, L., Teitell, M. A., Mikkola, H. K., Lowry, W. E.*, et al.* (2009). Derivation of primordial germ cells from human embryonic and induced pluripotent stem cells is significantly improved by coculture with human fetal gonadal cells. Stem cells *27*, 783-795.10.1002/stem.13.

Parma, P., Radi, O., Vidal, V., Chaboissier, M. C., Dellambra, E., Valentini, S., Guerra, L., Schedl, A., and Camerino, G. (2006). R-spondin1 is essential in sex determination, skin differentiation and malignancy. Nature genetics *38*, 1304-1309.10.1038/ng1907.

Parte, S., Bhartiya, D., Telang, J., Daithankar, V., Salvi, V., Zaveri, K., and Hinduja, I. (2011). Detection, characterization, and spontaneous differentiation in vitro of very small embryonic-like putative stem cells in adult mammalian ovary. Stem cells and development *20*, 1451-1464.10.1089/scd.2010.0461.

Pepling, M. E., de Cuevas, M., and Spradling, A. C. (1999). Germline cysts: a conserved phase of germ cell development? Trends in cell biology *9*, 257-262

Pepling, M. E., and Spradling, A. C. (2001). Mouse ovarian germ cell cysts undergo programmed breakdown to form primordial follicles. Developmental biology *234*, 339-351.10.1006/dbio.2001.0269.

Pepling, M. E., Sundman, E. A., Patterson, N. L., Gephardt, G. W., Medico, L., Jr., and Wilson, K. I. (2010). Differences in oocyte development and estradiol sensitivity among mouse strains. Reproduction *139*, 349-357.10.1530/REP-09-0392.

Perez, G. I., Robles, R., Knudson, C. M., Flaws, J. A., Korsmeyer, S. J., and Tilly, J. L. (1999). Prolongation of ovarian lifespan into advanced chronological age by Bax-deficiency. Nature genetics *21*, 200-203.10.1038/5985.

Pesce, M., Farrace, M. G., Piacentini, M., Dolci, S., and De Felici, M. (1993). Stem cell factor and leukemia inhibitory factor promote primordial germ cell survival by suppressing programmed cell death (apoptosis). Development *118*, 1089-1094

Pisarska, M. D., Bae, J., Klein, C., and Hsueh, A. J. (2004). Forkhead l2 is expressed in the ovary and represses the promoter activity of the steroidogenic acute regulatory gene. Endocrinology *145*, 3424-3433.10.1210/en.2003-1141.

Progatzky, F., Dallman, M. J., and Lo Celso, C. (2013). From seeing to believing: labelling strategies for in vivo cell-tracking experiments. Interface focus *3*, 20130001.10.1098/rsfs.2013.0001.

Qing, T., Liu, H., Wei, W., Ye, X., Shen, W., Zhang, D., Song, Z., Yang, W., Ding, M., and Deng, H. (2008). Mature oocytes derived from purified mouse fetal germ cells. Human reproduction *23*, 54-61.10.1093/humrep/dem334.

Qing, T., Shi, Y., Qin, H., Ye, X., Wei, W., Liu, H., Ding, M., and Deng, H. (2007). Induction of oocyte-like cells from mouse embryonic stem cells by co-culture with ovarian granulosa cells. Differentiation; research in biological diversity *75*, 902-911.10.1111/j.1432-0436.2007.00181.x.

Rajah, R., Glaser, E. M., and Hirshfield, A. N. (1992). The changing architecture of the neonatal rat ovary during histogenesis. Developmental dynamics : an official publication of the American Association of Anatomists *194*, 177-192.10.1002/aja.1001940303.

Rastetter, R. H., Bernard, P., Palmer, J. S., Chassot, A. A., Chen, H., Western, P. S., Ramsay, R. G., Chaboissier, M. C., and Wilhelm, D. (2014). Marker genes identify three somatic cell types in the fetal mouse ovary. Developmental biology *394*, 242-252.10.1016/j.ydbio.2014.08.013.

Reijo, R., Lee, T. Y., Salo, P., Alagappan, R., Brown, L. G., Rosenberg, M., Rozen, S., Jaffe, T., Straus, D., Hovatta, O., and et al. (1995). Diverse spermatogenic defects in humans caused by Y chromosome deletions encompassing a novel RNA-binding protein gene. Nature genetics *10*, 383-393.10.1038/ng0895-383.

Reizel, Y., Itzkovitz, S., Adar, R., Elbaz, J., Jinich, A., Chapal-Ilani, N., Maruvka, Y. E., Nevo, N., Marx, Z., Horovitz, I.*, et al.* (2012). Cell lineage analysis of the mammalian female germline. PLoS genetics *8*, e1002477.10.1371/journal.pgen.1002477.

Resnick, J. L., Bixler, L. S., Cheng, L., and Donovan, P. J. (1992). Long-term proliferation of mouse primordial germ cells in culture. Nature *359*, 550-551.10.1038/359550a0.

Richardson, B. E., and Lehmann, R. (2010). Mechanisms guiding primordial germ cell migration: strategies from different organisms. Nature reviews Molecular cell biology *11*, 37-49.10.1038/nrm2815.

Roth, S. (2001). Drosophila oogenesis: coordinating germ line and soma. Current biology : CB *11*, R779-781

Rowghani, N. M., Heise, M. K., McKeel, D., McGee, E. A., Koepsel, R. R., and Russell, A. J. (2004). Maintenance of morphology and growth of ovarian follicles in suspension culture. Tissue engineering *10*, 545-552.10.1089/107632704323061906.

Saitou, M., Barton, S. C., and Surani, M. A. (2002). A molecular programme for the specification of germ cell fate in mice. Nature *418*, 293-300.10.1038/nature00927.

Salvador, L. M., Silva, C. P., Kostetskii, I., Radice, G. L., and Strauss, J. F., 3rd (2008). The promoter of the oocyte-specific gene, Gdf9, is active in population of cultured mouse embryonic stem cells with an oocyte-like phenotype. Methods *45*, 172-181.10.1016/j.ymeth.2008.03.004.

Saper, C. B. (2009). A guide to the perplexed on the specificity of antibodies. The journal of histochemistry and cytochemistry : official journal of the Histochemistry Society *57*, 1-5.10.1369/jhc.2008.952770.

Sarraj, M. A., and Drummond, A. E. (2012). Mammalian foetal ovarian development: consequences for health and disease. Reproduction *143*, 151-163.10.1530/REP-11-0247.

Sato, M., Kimura, T., Kurokawa, K., Fujita, Y., Abe, K., Masuhara, M., Yasunaga, T., Ryo, A., Yamamoto, M., and Nakano, T. (2002). Identification of PGC7, a new gene expressed specifically in preimplantation embryos and germ cells. Mechanisms of development *113*, 91-94

Sato, Y., Suzuki, T., Hidaka, K., Sato, H., Ito, K., Ito, S., and Sasano, H. (2003). Immunolocalization of nuclear transcription factors, DAX-1 and COUP-TF II, in the normal human ovary: correlation with adrenal 4 binding protein/steroidogenic factor-1 immunolocalization during the menstrual cycle. The Journal of clinical endocrinology and metabolism *88*, 3415-3420.10.1210/jc.2002-021723.

Saunders, P. T., Turner, J. M., Ruggiu, M., Taggart, M., Burgoyne, P. S., Elliott, D., and Cooke, H. J. (2003). Absence of mDazl produces a final block on germ cell development at meiosis. Reproduction *126*, 589-597

Scholer, H. R., Ruppert, S., Suzuki, N., Chowdhury, K., and Gruss, P. (1990). New type of POU domain in germ line-specific protein Oct-4. Nature *344*, 435-439.10.1038/344435a0.

Schuh-Huerta, S. M., and Pera, R. A. R. (2011). Making Germ Cells from Human Embryonic Stem Cells. In Male Germline Stem Cells: Developmental and Regenerative Potential, K.E. Orwig, and B.P. Hermann, eds. (Totowa, NJ: Humana Press), pp. 49-86.

Seki, Y., Yamaji, M., Yabuta, Y., Sano, M., Shigeta, M., Matsui, Y., Saga, Y., Tachibana, M., Shinkai, Y., and Saitou, M. (2007). Cellular dynamics associated with the genome-wide epigenetic reprogramming in migrating primordial germ cells in mice. Development *134*, 2627-2638.10.1242/dev.005611.

Senbon, S., Ishii, K., Fukumi, Y., and Miyano, T. (2005). Fertilization and development of bovine oocytes grown in female SCID mice. Zygote *13*, 309-315.10.1017/S0967199405003400.

Shah, S. M., Saini, N., Ashraf, S., Singh, M. K., Manik, R. S., Singla, S. K., Palta, P., and Chauhan, M. S. (2015). RETRACTED: Bone morphogenetic protein 4 (BMP4) induces buffalo (Bubalus bubalis) embryonic stem cell differentiation into germ cells. Biochimie *119*, 113-124.10.1016/j.biochi.2015.10.021.

Simon, A. M., Goodenough, D. A., Li, E., and Paul, D. L. (1997). Female infertility in mice lacking connexin 37. Nature *385*, 525-529.10.1038/385525a0.

Smith, P., Wilhelm, D., and Rodgers, R. J. (2014). Development of mammalian ovary. The Journal of endocrinology *221*, R145-161.10.1530/JOE-14-0062.

Sneider, M. E. (1940). Rhythms of ovogenesis before sexual maturity in the rat and cat. Developmental Dynamics *67*, 471-499.

Spears, N., Boland, N. I., Murray, A. A., and Gosden, R. G. (1994). Mouse oocytes derived from in vitro grown primary ovarian follicles are fertile. Human reproduction *9*, 527-532

Stoop, H., Honecker, F., Cools, M., de Krijger, R., Bokemeyer, C., and Looijenga, L. H. (2005). Differentiation and development of human female germ cells during prenatal gonadogenesis: an immunohistochemical study. Human reproduction *20*, 1466-1476.10.1093/humrep/deh800.

Sun, Q. Y., Miao, Y. L., and Schatten, H. (2009). Towards a new understanding on the regulation of mammalian oocyte meiosis resumption. Cell cycle *8*, 2741-2747.10.4161/cc.8.17.9471.

Sun, R., Sun, Y. C., Ge, W., Tan, H., Cheng, S. F., Yin, S., Sun, X. F., Li, L., Dyce, P., Li, J.*, et al.* (2015). The crucial role of Activin A on the formation of primordial germ cell-like cells from skin-derived stem cells in vitro. Cell cycle *14*, 3016-3029.10.1080/15384101.2015.1078031.

Takahashi, K., Tanabe, K., Ohnuki, M., Narita, M., Ichisaka, T., Tomoda, K., and Yamanaka, S. (2007). Induction of pluripotent stem cells from adult human fibroblasts by defined factors. Cell *131*, 861-872.10.1016/j.cell.2007.11.019.

Takahashi, K., and Yamanaka, S. (2006). Induction of pluripotent stem cells from mouse embryonic and adult fibroblast cultures by defined factors. Cell *126*, 663-676.10.1016/j.cell.2006.07.024.

Takamoto, N., Kurihara, I., Lee, K., DeMayo, F. J., Tsai, M. J., and Tsai, S. Y. (2005). Haploinsufficiency of chicken ovalbumin upstream promoter transcription factor II in female reproduction. Mol Endocrinol *19*, 2299-2308.10.1210/me.2005-0019.

Tam, P. P., and Snow, M. H. (1981). Proliferation and migration of primordial germ cells during compensatory growth in mouse embryos. Journal of embryology and experimental morphology *64*, 133-147

Tam, P. P., and Zhou, S. X. (1996). The allocation of epiblast cells to ectodermal and germ-line lineages is influenced by the position of the cells in the gastrulating mouse embryo. Developmental biology *178*, 124-132.10.1006/dbio.1996.0203.

Tan, O. L., and Fleming, J. S. (2004). Proliferating cell nuclear antigen immunoreactivity in the ovarian surface epithelium of mice of varying ages and total lifetime ovulation number following ovulation. Biology of reproduction *71*, 1501-1507.10.1095/biolreprod.104.030460.

Tanaka, S. S., and Matsui, Y. (2002). Developmentally regulated expression of mil-1 and mil-2, mouse interferon-induced transmembrane protein like genes, during formation and differentiation of primordial germ cells. Gene expression patterns : GEP *2*, 297-303

Tarin, J. J., and Cano, A. (1998). Distribution of 5-chloromethylfluorescein diacetate staining during meiotic maturation and fertilization in vitro of mouse oocytes. Journal of reproduction and fertility *114*, 211-218

Telfer, E. E. (2004). Germline stem cells in the postnatal mammalian ovary: a phenomenon of prosimian primates and mice? Reproductive biology and endocrinology : RB&E *2*, 24.10.1186/1477-7827-2-24.

Telfer, E. E., Gosden, R. G., Byskov, A. G., Spears, N., Albertini, D., Andersen, C. Y., Anderson, R., Braw-Tal, R., Clarke, H., Gougeon, A.*, et al.* (2005). On regenerating the ovary and generating controversy. Cell *122*, 821-822.10.1016/j.cell.2005.09.004.

Telfer, E. E., McLaughlin, M., Ding, C., and Thong, K. J. (2008). A two-step serum-free culture system supports development of human oocytes from primordial follicles in the presence of activin. Human reproduction *23*, 1151-1158.10.1093/humrep/den070.

Tingen, C., Kim, A., and Woodruff, T. K. (2009). The primordial pool of follicles and nest breakdown in mammalian ovaries. Molecular human reproduction *15*, 795-803.10.1093/molehr/gap073.

Tomaselli, S., Megiorni, F., De Bernardo, C., Felici, A., Marrocco, G., Maggiulli, G., Grammatico, B., Remotti, D., Saccucci, P., Valentini, F.*, et al.* (2008). Syndromic true hermaphroditism due to an R-spondin1 (RSPO1) homozygous mutation. Human mutation *29*, 220-226.10.1002/humu.20665.

Tomizuka, K., Horikoshi, K., Kitada, R., Sugawara, Y., Iba, Y., Kojima, A., Yoshitome, A., Yamawaki, K., Amagai, M., Inoue, A.*, et al.* (2008). R-spondin1

plays an essential role in ovarian development through positively regulating Wnt-4 signaling. Human molecular genetics *17*, 1278-1291.10.1093/hmg/ddn036.

Tong, D., Gittens, J. E., Kidder, G. M., and Bai, D. (2006). Patch-clamp study reveals that the importance of connexin43-mediated gap junctional communication for ovarian folliculogenesis is strain specific in the mouse. American journal of physiology Cell physiology *290*, C290-297.10.1152/ajpcell.00297.2005.

Toyooka, Y., Tsunekawa, N., Takahashi, Y., Matsui, Y., Satoh, M., and Noce, T. (2000). Expression and intracellular localization of mouse Vasa-homologue protein during germ cell development. Mechanisms of development *93*, 139-149
Trombly, D. J., Woodruff, T. K., and Mayo, K. E. (2009). Suppression of Notch signaling in the neonatal mouse ovary decreases primordial follicle formation. Endocrinology *150*, 1014-1024.10.1210/en.2008-0213.

Uda, M., Ottolenghi, C., Crisponi, L., Garcia, J. E., Deiana, M., Kimber, W., Forabosco, A., Cao, A., Schlessinger, D., and Pilia, G. (2004). Foxl2 disruption causes mouse ovarian failure by pervasive blockage of follicle development. Human molecular genetics *13*, 1171-1181.10.1093/hmg/ddh124.

Uhlenhaut, N. H., Jakob, S., Anlag, K., Eisenberger, T., Sekido, R., Kress, J., Treier, A. C., Klugmann, C., Klasen, C., Holter, N. I.*, et al.* (2009). Somatic sex reprogramming of adult ovaries to testes by FOXL2 ablation. Cell *139*, 1130-1142.10.1016/j.cell.2009.11.021.

Vainio, S., Heikkila, M., Kispert, A., Chin, N., and McMahon, A. P. (1999). Female development in mammals is regulated by Wnt-4 signalling. Nature *397*, 405-409.10.1038/17068.

Virant-Klun, I., Rozman, P., Cvjeticanin, B., Vrtacnik-Bokal, E., Novakovic, S., Rulicke, T., Dovc, P., and Meden-Vrtovec, H. (2009). Parthenogenetic embryo-like structures in the human ovarian surface epithelium cell culture in postmenopausal women with no naturally present follicles and oocytes. Stem cells and development *18*, 137-149.10.1089/scd.2007.0238.

Virant-Klun, I., Zech, N., Rozman, P., Vogler, A., Cvjeticanin, B., Klemenc, P., Malicev, E., and Meden-Vrtovec, H. (2008). Putative stem cells with an embryonic character isolated from the ovarian surface epithelium of women with no naturally present follicles and oocytes. Differentiation; research in biological diversity *76*, 843-856.10.1111/j.1432-0436.2008.00268.x.

Waldeyer, W. (1870). Eirstock und Ei, (Leipzig, Germany: Engelmann).

Wang, F., Flanagan, J., Su, N., Wang, L. C., Bui, S., Nielson, A., Wu, X. Y., Vo, H. T., Ma, X. J., and Luo, Y. L. (2012). RNAscope A Novel in Situ RNA Analysis Platform for Formalin-Fixed, Paraffin-Embedded Tissues. J Mol Diagn *14*, 22-29.10.1016/j.jmoldx.2011.08.002.

Wear, H. M., McPike, M. J., and Watanabe, K. H. (2016). From primordial germ cells to primordial follicles: a review and visual representation of early ovarian development in mice. Journal of ovarian research *9*, 36.10.1186/s13048-016-0246-7.

Weber, S., Eckert, D., Nettersheim, D., Gillis, A. J., Schafer, S., Kuckenberg, P., Ehlermann, J., Werling, U., Biermann, K., Looijenga, L. H., and Schorle, H. (2010). Critical function of AP-2 gamma/TCFAP2C in mouse embryonic germ cell maintenance. Biology of reproduction *82*, 214-223.10.1095/biolreprod.109.078717.

Wei, M. C., Zong, W. X., Cheng, E. H., Lindsten, T., Panoutsakopoulou, V., Ross, A. J., Roth, K. A., MacGregor, G. R., Thompson, C. B., and Korsmeyer, S. J. (2001). Proapoptotic BAX and BAK: a requisite gateway to mitochondrial dysfunction and death. Science *292*, 727-730.10.1126/science.1059108.

Wei, W., Qing, T., Ye, X., Liu, H., Zhang, D., Yang, W., and Deng, H. (2008). Primordial germ cell specification from embryonic stem cells. PloS one *3*, e4013.10.1371/journal.pone.0004013.

Weigert, R., Porat-Shliom, N., and Amornphimoltham, P. (2013). Imaging cell biology in live animals: ready for prime time. The Journal of cell biology *201*, 969-979.10.1083/jcb.201212130.

White, Y. A., Woods, D. C., Takai, Y., Ishihara, O., Seki, H., and Tilly, J. L. (2012). Oocyte formation by mitotically active germ cells purified from ovaries of reproductive-age women. Nature medicine *18*, 413-421.10.1038/nm.2669.

Williams, R. L., Hilton, D. J., Pease, S., Willson, T. A., Stewart, C. L., Gearing, D. P., Wagner, E. F., Metcalf, D., Nicola, N. A., and Gough, N. M. (1988). Myeloid leukaemia inhibitory factor maintains the developmental potential of embryonic stem cells. Nature *336*, 684-687.10.1038/336684a0.

Woods, D. C., and Tilly, J. L. (2015). Woods and Tilly reply. Nature medicine *21*, 1118-1121.10.1038/nm.3964.

Wycherley, G., Downey, D., Kane, M. T., and Hynes, A. C. (2004). A novel follicle culture system markedly increases follicle volume, cell number and oestradiol secretion. Reproduction *127*, 669-677.10.1530/rep.1.00040.

Xu, H., Beasley, M. D., Warren, W. D., van der Horst, G. T., and McKay, M. J. (2005). Absence of mouse REC8 cohesin promotes synapsis of sister chromatids in meiosis. Developmental cell *8*, 949-961.10.1016/j.devcel.2005.03.018.

Xu, J., and Gridley, T. (2013). Notch2 is required in somatic cells for breakdown of ovarian germ-cell nests and formation of primordial follicles. BMC biology *11*, 13.10.1186/1741-7007-11-13.

Xu, Z., Abbott, A., Kopf, G. S., Schultz, R. M., and Ducibella, T. (1997). Spontaneous activation of ovulated mouse eggs: time-dependent effects on M-phase

exit, cortical granule exocytosis, maternal messenger ribonucleic acid recruitment, and inositol 1,4,5-trisphosphate sensitivity. Biology of reproduction *57*, 743-750

Xuemei, L., Jing, Y., Bei, X., Juan, H., Xinling, R., Qun, L., and Guijin, Z. (2013). Retinoic acid improve germ cell differentiation from human embryonic stem cells. Iranian journal of reproductive medicine *11*, 905-912

Yamaji, M., Seki, Y., Kurimoto, K., Yabuta, Y., Yuasa, M., Shigeta, M., Yamanaka, K., Ohinata, Y., and Saitou, M. (2008). Critical function of Prdm14 for the establishment of the germ cell lineage in mice. Nature genetics *40*, 1016-1022.10.1038/ng.186.

Yang, M. Y., and Fortune, J. E. (2008). The capacity of primordial follicles in fetal bovine ovaries to initiate growth in vitro develops during mid-gestation and is associated with meiotic arrest of oocytes. Biology of reproduction *78*, 1153-1161.10.1095/biolreprod.107.066688.

Yao, H. H., Matzuk, M. M., Jorgez, C. J., Menke, D. B., Page, D. C., Swain, A., and Capel, B. (2004). Follistatin operates downstream of Wnt4 in mammalian ovary organogenesis. Developmental dynamics : an official publication of the American Association of Anatomists *230*, 210-215.10.1002/dvdy.20042.

Yapura, J., Mapletoft, R. J., Pierson, R., Singh, J., Naile, J., Giesy, J. P., and Adams, G. P. (2011). A bovine model for examining the effects of an aromatase inhibitor on ovarian function in women. Fertility and sterility *96*, 434-U507.10.1016/j.fertnstert.2011.05.038.

Ying, Y., Liu, X. M., Marble, A., Lawson, K. A., and Zhao, G. Q. (2000). Requirement of Bmp8b for the generation of primordial germ cells in the mouse. Mol Endocrinol *14*, 1053-1063.10.1210/mend.14.7.0479.

Ying, Y., Qi, X., and Zhao, G. Q. (2001). Induction of primordial germ cells from murine epiblasts by synergistic action of BMP4 and BMP8B signaling pathways. Proceedings of the National Academy of Sciences of the United States of America *98*, 7858-7862.10.1073/pnas.151242798.

Ying, Y., and Zhao, G. Q. (2001). Cooperation of endoderm-derived BMP2 and extraembryonic ectoderm-derived BMP4 in primordial germ cell generation in the mouse. Developmental biology *232*, 484-492.10.1006/dbio.2001.0173.

Yu, X., Wang, N., Qiang, R., Wan, Q., Qin, M., Chen, S., and Wang, H. (2014). Human amniotic fluid stem cells possess the potential to differentiate into primordial follicle oocytes in vitro. Biology of reproduction *90*, 73.10.1095/biolreprod.113.112920.

Yuan, J., Zhang, D., Wang, L., Liu, M., Mao, J., Yin, Y., Ye, X., Liu, N., Han, J., Gao, Y*., et al.* (2013). No evidence for neo-oogenesis may link to ovarian senescence in adult monkey. Stem cells *31*, 2538-2550.10.1002/stem.1480.

Zachos, N. C., Billiar, R. B., Albrecht, E. D., and Pepe, G. J. (2002). Developmental regulation of baboon fetal ovarian maturation by estrogen. Biology of reproduction *67*, 1148-1156

Zarate-Garcia, L., Lane, S. I., Merriman, J. A., and Jones, K. T. (2016). FACS-sorted putative oogonial stem cells from the ovary are neither DDX4-positive nor germ cells. Scientific reports *6*, 27991.10.1038/srep27991.

Zhang, B., Duan, Z., and Zhao, Y. (2009). Mouse models with human immunity and their application in biomedical research. Journal of cellular and molecular medicine *13*, 1043-1058.10.1111/j.1582-4934.2008.00347.x.

Zhang, H., Panula, S., Petropoulos, S., Edsgard, D., Busayavalasa, K., Liu, L., Li, X., Risal, S., Shen, Y., Shao, J.*, et al.* (2015). Adult human and mouse ovaries lack DDX4-expressing functional oogonial stem cells. Nature medicine *21*, 1116-1118.10.1038/nm.3775.

Zhang, H., Zheng, W., Shen, Y., Adhikari, D., Ueno, H., and Liu, K. (2012). Experimental evidence showing that no mitotically active female germline progenitors exist in postnatal mouse ovaries. Proceedings of the National Academy of Sciences of the United States of America *109*, 12580-12585.10.1073/pnas.1206600109.

Zhao, X. Y., Li, W., Lv, Z., Liu, L., Tong, M., Hai, T., Hao, J., Wang, X., Wang, L., Zeng, F., and Zhou, Q. (2010). Viable fertile mice generated from fully pluripotent iPS cells derived from adult somatic cells. Stem cell reviews *6*, 390-397.10.1007/s12015-010-9160-3.

Zheng, W., Zhang, H., Gorre, N., Risal, S., Shen, Y., and Liu, K. (2014). Two classes of ovarian primordial follicles exhibit distinct developmental dynamics and physiological functions. Human molecular genetics *23*, 920-928.10.1093/hmg/ddt486.

Zhou, L., Wang, L., Kang, J. X., Xie, W., Li, X., Wu, C., Xu, B., and Wu, J. (2014). Production of fat-1 transgenic rats using a post-natal female germline stem cell line. Molecular human reproduction *20*, 271-281.10.1093/molehr/gat081.

Zou, K., Yuan, Z., Yang, Z., Luo, H., Sun, K., Zhou, L., Xiang, J., Shi, L., Yu, Q., Zhang, Y.*, et al.* (2009). Production of offspring from a germline stem cell line derived from neonatal ovaries. Nature cell biology *11*, 631-636.10.1038/ncb1869.

Zuckerman, S. (1951). The Number of Oocytes in the Mature Ovary. Recent Prog Horm Res *6*, 63-109